UNIVERSITY OF LONDON THESIS

Degree	Year	Name of Author
PhD	2005	BAILEY, L.M.

The Roles of Annexins 1 and 2 in Receptor Mediated Endocytosis

Lorna Mary Bailey

Division of Cell Biology
Institute of Ophthalmology
University College London

Thesis submitted to the University of London for the degree of Doctorate of Philosophy

November 2004

ProQuest LLC
789 East Eisenhower Parkway
P.O. Box 1346
Ann Arbor, MI 48106-1346

Abstract

Activated EGF receptors (EGFR) are sorted onto internal vesicles of multivesicular endosomes/bodies (MVBs), thus removing receptors from the recycling pathway and targeting them for degradation. The EGFR tyrosine kinase has two major substrates within MVBs, the EGFR itself and annexin 1. Annexins have been proposed to play multiple roles in membrane traffic and both annexins 1 and 2 have been localised to early transferrin positive endosomes and to MVBs. In these studies a combination of gene knockout and RNAi-induced protein depletion was used to investigate the effect of loss of annexins 1 and 2 on the formation of MVBs and on EGFR trafficking. MVBs form constitutively in unstimulated cells but EGF stimulation significantly increased both the number of MVBs formed and the number of internal vesicles per MVB. Neither annexin is required for MVB formation, but EGF-stimulated inward vesiculation, within a sub-population of EGFR-containing MVBs, is mediated through annexin 1. Consistent with a role for annexin 1 in internal vesicle formation, annexin 1 and EGFR were present on the same internal vesicles within MVBs from EGF stimulated cells, but annexin 2 was not. In annexin 1 -/- cells there was no effect on EGF degradation, but a small reduction in EGFR degradation was seen. Prolonged MAPK signalling was observed in annexin 1 -/- cells, which also exhibited enhanced EGF-stimulated cell motility. Additionally, loss of annexin 1 was found to alter the shape of mouse lung fibroblasts. EGF-stimulated phosphorylation of annexin 1 was required for annexin 1-mediated inhibition of cell motility, but not for annexin 1-mediated regulation of cell shape. Therefore, annexin 1 is involved in specific EGF-stimulated effects, including internal vesicle formation, downregulation of EGFR signalling and inhibition of cell motility.

Table of Contents

List of Figures

Chapter 1 – Introduction

Chapter 3 – Annexin 1 and MVB formation

Chapter 4 – Does annexin 2 play a role in MVB formation?

Chapter 5 – Annexins and receptor trafficking

Chapter 6 – Localisation of annexins in the endocytic pathway

Chapter 7 – A role for annexin 1 in regulation of cell shape and motility

Appendix 1 – Supplementary data

Abbreviations

Abbreviation		Full Word
AIP-1	.....	Ask interacting protein
Anx1	.....	Annexin 1
Anx2	.....	Annexin 2
AP-2	.....	Adaptor protein 2
BSA	.....	Bovine Serum Albumin
Ca^{2+}	.....	Calcium
CALM	.....	Clathrin assembly lymphoid myeloid leukaemia protein
CAML	.....	Calcium-modulating cyclophilin ligand
CCPs	.....	Clathrin coated pits
CCVs	.....	Clathrin coated vesicles
CHMP	.....	Charged MVB proteins
CIP	.....	Calf intestinal alkaline phosphatase
Cpm	.....	Counts per minute
DAB	.....	Diaminobenzidine
ds	.....	Double strand
ECM	.....	Extracellular matrix
ECV	.....	Endosomal carrier vesicle
EE	.....	Early endosomes
EEA1	.....	Early endosomal antigen 1
EGF	.....	Epidermal Growth Factor
EGFR	.....	EGF receptor
Eps15	.....	EGFR pathway substrate clone no. 15
Epsin	.....	Eps15-interacting protein
ERK	.....	Extracellular regulated kinase
ESCRT	.....	Endosomal Sorting Complex Required for Transport
FBS	.....	Foetal Bovine Serum
FGF	.....	Fibroblast Growth Factor
GDI	.....	Guanine-nucleotide dissociation inhibitor
GFP	.....	Green fluorescent protein
GGAs	.....	Golgi associated γ-adaptin homologues, Arf binding

GHR	.....	Growth hormone receptor
hEGFR	.....	Human EGFR
HRP	.....	Horse Radish Peroxidase
HRS	.....	Hepatocyte growth factor regulated tyrosine kinase substrate
IR	.....	Insulin receptor
IRS1	.....	Insulin receptor substrate 1
LBPA	.....	Lysobisphosphatidic acid
LDL	.....	Low density lipoprotein
MAPK	.....	Mitogen activated protein kinase
MC	.....	Methylcellulose
MEK	.....	Mitogen activated ERK kinase
MP1	.....	MEK1 partner
MPR	.....	Mannose-6-phosphate receptor
MVB	.....	Multivesicular Body
NSF	.....	*N*-ethylmaleimide sensitive factor
PBS	.....	Phospho buffered saline
PC	.....	Phosphatidylcholine
PFA	.....	Paraformaldehyde
PI	.....	Phosphoinositides
PI3K	.....	Phosphatidylinositol 3-kinase
PI3P	.....	Phosphatidylinositol 3-phosphate
PIP_2	.....	Phosphoinositol (4,5) bisphosphate
PKC	.....	Protein Kinase C
PLCγ	.....	Phospholipase C γ
PMN	.....	Polymorphonuclear leukocyte
PO	.....	Propylene oxide
PX	.....	Phox
RING	.....	Really interesting new gene
RNAi	.....	RNA interference
RSB	.....	Reducing sample buffer
SEM	.....	Standard error margin
SH2	.....	*Src* homology 2
SNAP	.....	Soluble NSF attachment protein

SNX	.....	Sorting nexin
SOS	.....	Son-of-sevenless
TEM	.....	Transmission Electron Microscopy
Tf	.....	Transferrin
TfR	.....	Transferrin receptor
TGN	.....	Trans-Golgi Network
TKB	.....	Tyrosine kinase binding
TSG101	.....	Tumour susceptibility gene 101
Tx100	.....	Triton X-100
UA	.....	Uranyl acetate
UEV	.....	Ubiquitin E2 variant
UIM	.....	Ubiquitin interacting motif
Vps	.....	Vacuolar Protein Sorting

Acknowledgments

Firstly, I would like to thank Clare Futter, both for giving me the opportunity to take on this project and for all the help and advice she has given me over the past three years. She has been a superb supervisor during my PhD, even during her maternity leave.

Special thanks goes to the following people:

Minoo Aghakhani – for being my radiation lab buddy and for her gentle (!) reminders to start writing up and get fit.

Giulia Chan – for being my fellow student and, more importantly, my friend over the past three years, for squash, cocktails, ladies nights, shopping trips and the list goes on…

Ian White – for teaching me Molecular Biology, for endless discussions about MVB counting, and for proof reading (I'll forgive the red pen and remember my commas).

I would also like to thank Steve Moss and the members of Cell Biology, past and present – with particular mention to Chris Loewen and Emma Kavanagh, both for scientific help and trips to the pub.

Thanks to Mum, Dad and Ross for listening to my grumbles and problems. You've all been great, even if you have no idea what an annexin is!

And finally, I would like to dedicate this thesis to Jim Harvey. Thanks for everything, especially the last few months. I couldn't have done it without you.

Chapter 1 - Introduction

1.1 General Introduction to Growth Factor Receptor Trafficking and Annexins

The cell surface is a dynamic structure and is the site where molecules enter into the cell (endocytosis, phagocytosis or pinocytosis) and exit from the cell (exocytosis). On the surface of cells are many types of proteins, including various receptors through which the cell can sense changes in its extracellular environment. Cells are sensitive to small amounts of signalling molecules and as a result receptors must be highly regulated. Misregulation of intracellular signalling can lead to excessive cell growth or cell division and this is often seen in cancer cells.

Growth factor receptors, such as epidermal growth factor (EGF) receptor (EGFR), are found on the surface of many, if not all, mammalian cells. Ligand binding activates the receptor. In the case of the EGFR, this occurs through receptor dimerisation, autophosphorylation and activation of the intracellular tyrosine kinase, which activates several signalling pathways by initiating phosphorylation cascades. Figure 1.1 shows a simplified diagram of EGFR trafficking. Activated EGFR are immediately downregulated and the first step is receptor internalisation, via clathrin coated pits (CCPs) (Haigler *et al.*, 1979; Hanover *et al.*, 1985). The plasma membrane is induced to curve inwards by a complex group of proteins and eventually the invagination pinches off to form a clathrin coated vesicle (CCV). After shedding their clathrin coats, newly formed endosomes can fuse with each other and with pre-existing early endosomes. The term "early endosome" encompasses a range of peripherally located membrane bound tubular-vesicular structures, which stain positive for Rab5 and EEA1 (early endosomal antigen 1) (Mu *et al.*, 1995; Stenmark *et al.*, 1996). In early endosomes, EGFR are present on the membrane with their cytoplasmic domains exposed to the cytoplasm and extracellular domains within the lumen of the vesicle. Non-kinase receptors, such as transferrin receptor (TfR), are also internalised into these early endosomes (Futter and Hopkins, 1989; Wiley *et al.*, 1991). Interestingly, newly formed TfR are also found in endosomes *en route* to the plasma membrane (Futter *et al.*, 1995). Early endosomes mature to form larger endosomes with a more acidic internal pH.

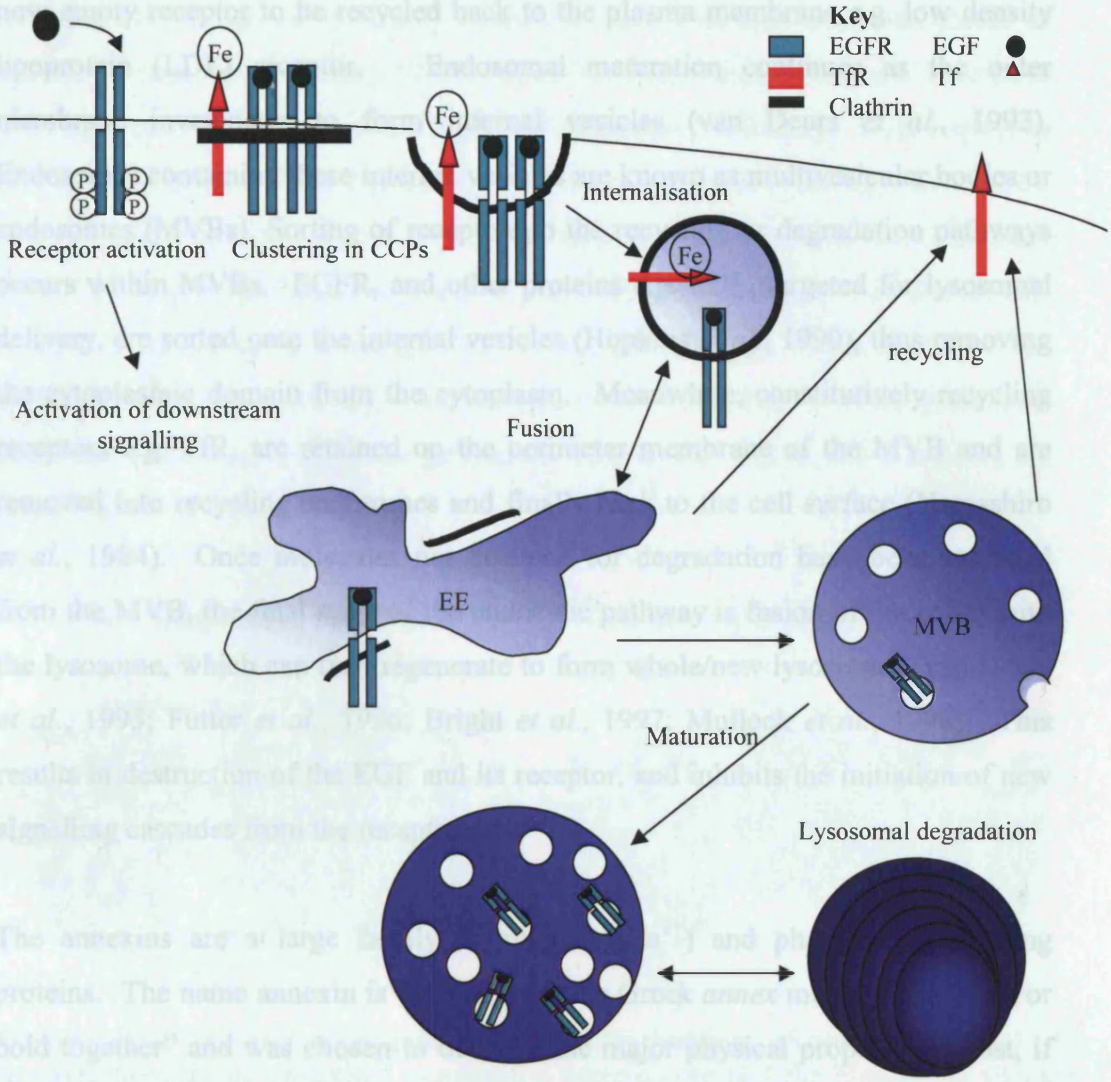

Figure 1.1. *EGFR trafficking through the endocytic pathway.* EGF binds to the extracellular domain of cell surface EGFR, inducing receptor dimerisation and activation of the cytoplasmic tyrosine kinase, which phosphorylates EGFR (autophosphorylation) and downstream molecules, including many signalling pathways. Autophosphorylation allows binding of other proteins to EGFR recruiting it to CCPs. A protein complex, including clathrin, AP-2, epsin and Eps15, induces the formation of CCVs, which are released into the cytoplasm by dynamin-induced fission. The clathrin coat is rapidly removed and vesicles can fuse with each other and pre-existing early endosomes (EE). Endosomes mature to form MVBs, larger vacuoles that contain internal vesicles. Active EGFR are sorted to the degradative pathway here by sequestration onto internal vesicles. MVBs continue to mature and the final stage is fusion with the lysosome and degradation of the contents of the MVB. Recycling of receptors (TfR) not destined for lysosomal degradation can occur from endosomes (fast pathway) or from the perimeter membrane of MVBs (slow pathway through recycling endosomes).

This change in pH causes the ligands of several receptors to dissociate, allowing the now empty receptor to be recycled back to the plasma membrane e.g. low density lipoprotein (LDL) receptor. Endosomal maturation continues as the outer membrane invaginates to form internal vesicles (van Deurs *et al.*, 1993). Endosomes containing these internal vesicles are known as multivesicular bodies or endosomes (MVBs). Sorting of receptors to the recycling or degradation pathways occurs within MVBs. EGFR, and other proteins e.g. LDL, targeted for lysosomal delivery, are sorted onto the internal vesicles (Hopkins *et al.*, 1990), thus removing the cytoplasmic domain from the cytoplasm. Meanwhile, constitutively recycling receptors e.g. TfR, are retained on the perimeter membrane of the MVB and are removed into recycling endosomes and finally back to the cell surface (Yamashiro *et al.*, 1984). Once molecules not destined for degradation have been removed from the MVB, the final stage of the endocytic pathway is fusion of the MVB with the lysosome, which can then regenerate to form whole/new lysosomes (van Deurs *et al.*, 1995; Futter *et al.*, 1996; Bright *et al.*, 1997; Mullock *et al.*, 1998). This results in destruction of the EGF and its receptor, and inhibits the initiation of new signalling cascades from the receptor.

The annexins are a large family of calcium (Ca^{2+}) and phospholipid binding proteins. The name annexin is derived from the Greek *annex* meaning "to bring or hold together" and was chosen to describe the major physical property of most, if not all, annexin family members (for a review see Gerke and Moss, 2002). However, the annexins were not discovered as a complete family. In the late 1970s and early 1980s, several groups were working independently on unidentified proteins, which would later form the annexin family. These proteins were given a range of diverse and unrelated names based on their biochemical properties. These included synexins (Creutz *et al.*, 1978), chromobindins (Creutz *et al.*, 1987), calcimedins (Moore *et al.*, 1984), lipocortins (Flower, 1986) and calpactins (Glenney, 1986b). More detailed work on these proteins revealed that they shared key biochemical properties, as well as gene structure and sequence features. The family name annexin was agreed on in 1990 to solve the nomenclature confusion (Crumpton and Dedman, 1990). From this date onwards, an annexin was defined by two major criteria: (i) it must be capable of binding to negatively charged phospholipids in a Ca^{2+} dependent manner and (ii) it must contain the annexin

repeat, four of which form a highly α-helical disk called the annexin domain, which is conserved throughout the family members. Annexins have been considered of interest to those investigating EGFR endocytosis and sorting because they have been implicated in many aspects of general membrane trafficking. With respect to EGFR-trafficking, annexin 1 (formerly known as lipocortin 1 (Huang *et al.*, 1986), p35 (Brugge, 1986; Isacke *et al.*, 1989) and calpactin II (Glenney, 1986b; Glenney, Jr. *et al.*, 1987)) has been proposed to play a role in sorting within MVBs and annexin 2 (lipocortin II (Huang *et al.*, 1986), p36 (Brugge, 1986; Isacke *et al.*, 1989) or calpactin I (Glenney, 1986b; Glenney, Jr. *et al.*, 1987)) in the generation of MVBs. Annexins 1 and 2 are structurally very similar and Figure 1.2 shows the 3-D structure of annexin 1.

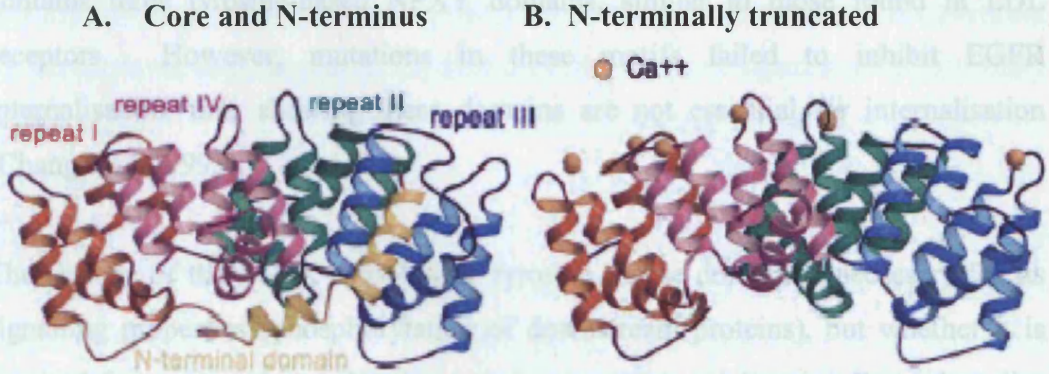

Figure 1.2. *3-D structure of annexin 1.* Ribbon diagrams of one monomer of (A) recombinant porcine annexin 1 comprising protein core and the N-terminal domain and (B) human annexin 1 lacking the first 32 amino acid residues (Δ1 to 32 annexin I. Repeat I is presented in red, repeat II in green, repeat III in blue, repeat IV in purple and the N-terminal domain in yellow. The yellow N-terminal helix in (A) is replacing the two-turn blue helix in (B). Bound calcium ions in Δ1-32 annexin 1 are illustrated as yellow spheres. This figure was obtained from Rosengarth *et al.*, 2001.

1.2 Growth Factor Receptor internalisation

Internalisation of growth factor receptors, especially EGFR, has been widely studied. Efficient internalisation of EGFR requires multiple signals, including active tyrosine kinase function, endocytic signals in the cytoplasmic domain of the receptor, and possibly receptor ubiquitination.

1.2.1 EGFR internalisation signals and tyrosine kinase activity

Several sequences in the EGFR carboxyl terminus have been reported as necessary for efficient EGFR internalisation. These sequences, or internalisation motifs, are short linear arrays of amino acids generally classed as tyrosine-based or dileucine motifs. A region of the EGFR cytoplasmic domain (973-1022) was identified as essential for ligand-induced receptor internalisation and contains FYRAL and QQGFF motifs (Chen *et al.*, 1989; Chang *et al.*, 1991; Chang *et al.*, 1993). These motifs were also shown to efficiently substitute for those found in TfR, indicating that common mechanisms are involved in internalisation of ligand dependent and ligand independent receptors. Another region of the cytoplasmic tail of EGFR contains three tyrosine-based NPXY domains, similar to those found in LDL receptors. However, mutations in these motifs failed to inhibit EGFR internalisation, thus showing these domains are not essential for internalisation (Chang *et al.*, 1993).

The activity of the EGFR cytoplasmic tyrosine kinase domain is necessary for its signalling properties (phosphorylation of downstream proteins), but whether it is required for receptor internalisation remains a controversial topic. Several studies showed that EGF-bound, kinase negative EGFR underwent normal internalisation, but were incorrectly processed within the cell resulting in an inhibition of EGF degradation and an increase in EGFR recycling (Honegger *et al.*, 1987; Felder *et al.*, 1990). In contrast, Glenney *et al.* (1988) reported a tyrosine kinase mutant EGFR that failed to internalise, and also showed that receptor internalisation of EGFR was abrogated by inhibition of tyrosine phosphorylation using anti-phosphotyrosine antibodies (Glenney, Jr. *et al.*, 1988). Wiley *et al.* (1991) showed that there is a constitutive low level rate of EGFR internalisation and that unoccupied EGFR undergo endocytosis at the same rate as receptors lacking the cytoplasmic tyrosine kinase domain (Wiley *et al.*, 1991). Ligand binding to wild type receptors increased the rate of receptor internalisation (up to 10-fold), but had no effect on the internalisation rate of kinase negative receptors (Wiley *et al.*, 1991).

From these and other studies, it became apparent that high and low affinity EGFR differ in the efficiency with which they are endocytosed. Kinase activity is required for an enhanced rate of endocytosis of high affinity receptors and it was shown that this system could be saturated using increased amounts of EGF, which reduced the overall rate of receptor internalisation (Wiley *et al.*, 1991; Felder *et al.*, 1992). Ligand-induced autophosphorylation of EGFR results in a more open conformation, which exposes trafficking domains, and this change in conformation is thought to allow more proteins involved in internalisation to bind to the receptor (Cadena *et al.*, 1994). Much of the controversy over the requirement for kinase activity in internalisation may be explained by differences in the cell type and experimental conditions used. Those favouring high receptor occupancy, through use of high concentrations of EGF, had a tendency to favour measurements of both high and low affinity receptor internalisation. EGFR tyrosine kinase activity is not essential for receptor endocytosis, but is required for efficient internalisation of high affinity receptors.

1.2.2 Clathrin and adaptor proteins

The majority of activated EGFR are internalised via the clathrin-dependent endocytic pathway, which is a rapid process compared to the kinetics of the clathrin-independent pathway. Investigations into the exact role of clathrin in receptor internalisation require low levels of EGF and receptor expression to avoid saturation of the clathrin-dependent pathway (Jiang and Sorkin, 2003). Activated EGFR are recruited to CCPs through specific adaptors proteins, which have the bivalent capacity to interact with clathrin and the cytoplasmic domain of the receptor. The cytoplasmic tails of activated EGFRs interact with adaptor protein 2 (AP-2), which recruits clathrin to the plasma membrane and is involved in the formation of CCPs (Sorkin *et al.*, 1996). Clathrin and AP-2 bind several proteins of the endocytic regulatory machinery, including amphiphysin 1, amphiphysin II, epsin and Eps15, thus creating a complex at the membrane (reviewed in Mousavi *et al.* 2004). The action of this complex, together with several other proteins, including dynamin, synaptojanin, intersectin, endophilin and syndapin, regulates the formation of CCVs (Simpson *et al.*, 1999; Mousavi *et al.*, 2004).

AP-2 was originally thought to be the central protein in, and absolutely necessary for, clathrin-mediated endocytosis. However, deletion of the yeast equivalent of AP-2 had no effect on clathrin-mediated endocytosis or on any other pathway investigated (Yeung *et al.*, 1999). Further work in mammalian cells revealed that several of the accessory proteins that bind AP-2 are also able to bind clathrin and phosphoinositol (4,5) bisphosphate (PIP_2), indicating that they may be adaptors in their own right. Motley *et al.* (2003) used RNA interference (RNAi) to knock down the AP-2 μ2 subunit and clathrin heavy chain and reported that although loss of AP-2 led to a decreased number of CCPs, it is not essential for clathrin-mediated endocytosis of EGFR (Motley *et al.*, 2003). It is proposed that other adaptors play a role in endocytosis of EGFR and, in the absence of AP-2, these are still recruited to the protein complex that forms at the plasma membrane. In contrast, endocytosis of TfR was significantly inhibited by loss of AP-2, expression of a mutant form of AP-2 unable to bind tyrosine based sorting motifs, or overexpression of adaptor-associated kinase that sequestered AP-2, indicating that TfR can only bind AP-2 and not any other adaptor molecules (Nesterov *et al.*, 1999; Motley *et al.*, 2003; Conner and Schmid, 2003). Another potential adaptor protein CALM (clathrin-assembly lymphoid myeloid leukaemia protein, also known as AP180) was recently proposed to be involved in CCP formation. CALM depletion had a partial but specific inhibitory effect on EGFR internalisation. However, there was no effect observed on TfR internalisation, indicating that CALM is not an essential part of the clathrin-associated endocytic complex (Huang *et al.*, 2004).

Fission of the CCV is mediated by the GTPase dynamin, releasing it into the cytoplasm (van der Bliek *et al.*, 1993; Damke *et al.*, 1994; Hill *et al.*, 2001). The clathrin coat is rapidly removed by the lipid phosphatase synaptojanin (Hill *et al.*, 2001; Rusk *et al.*, 2003), and the vesicle is now capable of fusing with other membrane bound structures within the cell. Many groups have used a dominant negative mutant form of dynamin (K44A), which lacks functional GTPase activity, to block endocytosis (van der Bliek *et al.*, 1993; Damke *et al.*, 1994; Ceresa *et al.*, 1998; Hill *et al.*, 2001; Huang *et al.*, 2004).

After EGF stimulation many other proteins are also phosphorylated. One such protein is Eps15 (EGFR pathway substrate clone 15), which is recruited to the plasma membrane where it is involved in receptor recruitment to the AP-2 complex (Benmerah *et al.*, 1995). Interestingly, Eps15 is absent from CCVs but appears to rejoin the endosome after removal of the clathrin coat (Cupers *et al.*, 1998; Torrisi *et al.*, 1999). Eps15 interaction with AP-2 is negatively regulated by its interaction with Hepatocyte growth factor-regulated tyrosine kinase substrate (Hrs, also known as Hgs). Hrs also interacts with the clathrin coat and is involved with later sorting stages of EGFR (Raiborg *et al.*, 2002). Expression of a dominant negative mutant Eps15 inhibits EGFR endocytosis by trapping receptors in coated pits, yet this has no effect on constitutive TfR endocytosis (Confalonieri *et al.*, 2000).

Rab5a, a member of the membrane bound Rab family of small GTPases, is activated by EGF stimulation and has been shown to be essential for endocytosis (Barbieri *et al.*, 2000). Rab5a is present on the cytoplasmic face of the plasma membrane and on early endosomes (Chavrier *et al.*, 1990), and can promote endosomal fusion *in vitro* (Gorvel *et al.*, 1991). These properties made Rab5a an ideal candidate for a role in endocytosis. Interestingly, not only does Rab5a regulate the transport of endocytic cargo from the cell surface into endosomes (Bucci *et al.*, 1992), it is also capable of promoting CCP formation as part of a complex with GDI (guanine-nucleotide dissociation inhibitor) (McLauchlan *et al.*, 1998). Rab5a induces the translocation of its effector protein EEA1 from the cytoplasm to the plasma membrane (Trischler *et al.*, 1999). The importance of Rab5a in endocytosis was highlighted through studies using a dominant negative mutant that blocked both EGF-stimulated receptor mediated endocytosis and fluid phase endocytosis (Barbieri *et al.*, 2000).

1.2.3 Role of ubiquitination in receptor internalisation

After ligand-induced activation, EGFR is not only phosphorylated but is also modified by the addition of ubiquitin, a 76-amino acid protein found in all eukaryotic cells. Ubiquitin is added to proteins as a form of post-translational modification and is one of the key signals for protein sorting within the endocytic

pathway. The cbl protein family are ubiquitin ligases, implicated in the regulation of receptor trafficking. C-Cbl is a substrate of the EGFR tyrosine kinase and phosphorylation on residue 371 activates c-Cbl ubiquitin ligase activity. This allows it to bind to activated (phosphorylated) EGFRs via its tyrosine kinase-binding (TKB) domain, which contains a unique SH2 (src-homology 2) domain (Stang *et al.*, 2000; Longva *et al.*, 2002). A separate domain, the RING finger, recruits the E2 ubiquitin-conjugating enzymes UbcH7 and mediates the transfer of ubiquitin to the receptor (Yokouchi *et al.*, 1999; Waterman *et al.*, 1999). The proline-rich regions of c-Cbl are involved in interactions with SH3 containing adaptor proteins, such as Grb2 and Nck (Meisner *et al.*, 1995; Fukazawa *et al.*, 1996; Donovan *et al.*, 1996; Thien and Langdon, 1997). After EGF stimulation c-Cbl mediates monoubiquitination (the addition of a single ubiquitin moiety) of EGFR at the plasma membrane (de Melker *et al.*, 2001). As EGFR passes along the endocytic pathway more single ubiquitin molecules are added resulting in the desensitisation of the receptor (Mosesson *et al.*, 2003).

Extensive work has been carried out to elucidate whether c-Cbl activity is required for EGFR internalisation. Evidence that c-Cbl is involved in early stages of endocytosis comes from the detection of c-Cbl in CCPs after EGFR activation and the finding that EGFR ubiquitination occurs before endocytosis (Stang *et al.*, 2000; de Melker *et al.*, 2001). In support of a role for c-Cbl in receptor internalisation, a mutant form of c-Cbl, that still binds Grb2 but is unable to ubiquitinate, was shown to inhibit EGFR internalisation (Jiang and Sorkin, 2003). However, contradictory data exists that shows c-Cbl activity is not essential for receptor internalisation and suggests that there are alternative internalisation routes (Levkowitz *et al.*, 1998; Thien *et al.*, 2001; Duan *et al.*, 2003; de Melker *et al.*, 2004). Taken together, these data suggest that c-Cbl facilitates, but is not essential for, efficient EGFR internalisation.

Having established that c-Cbl activity is only required for efficient EGFR internalisation, the exact mechanism of its action was investigated. Monoubiquitination of EGFR could be sufficient to serve as a signal for internalisation, as observed for Growth Hormone Receptor (GHR) in mammalian cells and Ste2p, a surface receptor, in yeast (Hicke and Riezman, 1996; Govers *et*

al., 1999). Alternatively, the RING finger domain could monoubiquitinate proteins associated with EGFR or CCPs. C-Cbl monoubiquitinates CIN85, an adaptor protein (Haglund *et al.*, 2002), which constitutively interacts with endophilins via its proline-rich domain. It is proposed that this recruitment to the activated receptor complex allows endophilins to bind the lipid bilayer and induce membrane curvature. However, while CIN85 would seem to be an important protein in this pathway, mutant forms of CIN85 do not affect EGFR internalisation (Jiang and Sorkin, 2003). Additionally, the ubiquitin ligase activity of c-Cbl may be required for efficient internalisation of EGFR through recruitment of Eps15, via its ubiquitin interacting motif (UIM), either by ubiquitinated receptors or an adaptor protein (de Melker *et al.*, 2004). The final theory is that the RING finger domain may interact with other proteins independently of its role in ubiquitylation. C-Cbl is able to interact with the adaptor protein Grb2, which also binds EGFR, and together this complex is thought to anchor EGFR to the Eps15 complex at the rim of CCPs (Jiang and Sorkin, 2003; Stang *et al.*, 2004). Therefore, it seems likely that c-Cbl mediated ubiquitination of EGFR is required for efficient receptor internalisation via a clathrin/Eps15 dependent route (de Melker *et al.*, 2004).

1.2.4 Role of annexins in internalisation

The internalisation of growth factors has been extensively studied, but so far little work has been carried out to elucidate potential roles for annexins in this process. Annexin 6 (annexin VI) was reported to be involved in the budding of CCPs, after depletion of the protein inhibited the budding of CCPs from membranes *in vitro* (Lin *et al.*, 1992). However, it was later shown that annexin 6 is not essential for CCP formation or budding, as these process occurred efficiently in A431 cells that do not express annexin 6 (Smythe *et al.*, 1994). These findings indicated that there might be more than one type of CCP and Kamal *et al.* (1998) showed that at least one type was dependent on annexin 6 activation of a cysteine protease involved in dissociation of CCP from the spectrin cytoskeleton (Smythe *et al.* 1994;Kamal *et al.*, 1998). To date, no other annexin family members have been identified as having roles in internalisation, although both annexins 1 and 2 have been localised to the plasma membrane (Nakata *et al.*, 1990; Traverso *et al.*, 1998).

1.3 Intracellular sorting of growth factor receptors

While the mechanisms involved in receptor internalisation have been well characterised, the later stages of receptor endocytosis remain less well understood. Internalisation is the first stage of receptor downregulation and signal attenuation. This process continues within MVBs where EGFR and other proteins targeted for lysosomal degradation are sorted onto internal vesicles (Hopkins *et al.*, 1990), while recycling receptors, e.g. TfR, are constitutively recycled back to the cell surface from the MVB perimeter membrane (Jackle *et al.*, 1991). Recently, there has been an increase in published data investigating mechanisms of receptor sorting, and a number of signals and proteins involved in the process of receptor sorting and/or inward vesiculation have been identified.

1.3.1 EGFR lysosomal targeting signals, tyrosine kinase activity and role of ubiquitination

The exact process of receptor sorting and inward vesiculation are not yet fully understood. A number of motifs within the cytoplasmic domain of the EGFR are thought to be necessary for lysosomal targeting. A tyrosine-based sorting signal (YLVI) was identified at the distal border of the tyrosine kinase domain and is similar to those found in lysosomal proteins, such as LAMP-1 and –2 (Opresko *et al.*, 1995; Guarnieri *et al.*, 1995). A dileucine motif in the juxtamembrane domain of EGFR is also important for lysosomal targeting, as mutation of this region reduced degradation efficiency, although had no effect on receptor endocytosis (Kil *et al.*, 1999). Additionally, sorting of EGFR onto the internal vesicles of MVBs requires its actin binding domain, deletion of which results in the relocalisation of EGFR to recycling compartments, rather than lysosomes (Stoorvogel *et al.*, 2004).

Sorting of EGFR onto the internal vesicles of MVBs removes the active receptor tyrosine kinase domain from the cytoplasm, thus limiting the number of downstream target molecules available. In addition to its signalling potential, the

activity of the tyrosine kinase is thought to be necessary for efficient targeting to the lysosome. EGFR lacking tyrosine kinase activity were internalised but were mostly recycled back to the cell surface (Honegger *et al.*, 1987; Felder *et al.*, 1990; Stoorvogel *et al.*, 2004), suggesting that tyrosine kinase activity is required to prevent entry to the recycling pathway by inducing inward vesiculation into MVBs (Felder *et al.*, 1990). In spite of this work, there are reports that the tyrosine kinase activity is not essential for lysosomal targeting of EGFR (Opresko *et al.*, 1995). Taken together, the findings of these studies suggest that distinct cytoplasmic domains regulate endocytosis and lysosomal delivery of EGFR.

Although the role of ubiquitin in receptor internalisation remains unclear, its role in endosomal sorting is less controversial. Several groups have reported that c-Cbl mediated ubiquitination of activated EGFR is required for efficient lysosomal targeting (Levkowitz *et al.*, 1998; Longva *et al.*, 2002; Duan *et al.*, 2003). Further evidence for the role of ubiquitin in receptor sorting comes from the association of c-Cbl with EGFR, from the plasma membrane throughout the endocytic pathway, including colocalisation on the internal vesicles of MVB, until degradation in the lysosome (de Melker *et al.*, 2001).

1.3.2 Role of ESCRTs in receptor sorting

Much of the information on the molecular mechanisms involved in sorting within MVBs has come from the identification of proteins in yeast vps (vacuolar protein sorting) mutants. Class E vps mutants contain characteristic enlarged aberrant endosomal structures and exhibit defects in protein sorting to the MVB. In yeast, the class E vps proteins were first identified as required for MVB formation and sorting of Ste2p into the vacuolar lumen (Odorizzi *et al.*, 1998). Class E vps proteins have been shown to form three protein complexes termed ESCRT (endosomal sorting complex required for transport)-I, ESCRT-II and ESCRT-III, thought to interact sequentially in sorting within the MVB (Katzmann *et al.*, 2001; Babst *et al.*, 2002a; Babst *et al.*, 2002b). A model of vps and ESCRT protein function in receptor sorting and MVB formation is presented in Fig. 1.3. To date over 70 yeast vps genes, and 18 class E vps mutants, have been identified.

Mammalian homologues have now been found for all Class E vps proteins, most recently Vps37p, part of yeast ESCRT-I (von Schwedler *et al.*, 2003; Bache *et al.*, 2004). For several yeast proteins, there are two or more human orthologs, implying that the mammalian system is more complex. However, not all of the mammalian proteins seem to have the same function as their yeast counterparts. Additionally in mammalian cells, tyrosine kinase receptors that are not present in yeast, utilize the endocytic pathway. It is clear that further work needs to be carried out to elucidate the exact properties and functions of these proteins in mammalian cells.

After EGFR internalisation into endosomes, Hrs is believed to be the first of the soluble factors recruited, via the interaction of its FYVE domain with phosphatidylinositol 3-phosphate (PI3P) molecules on the endosomal membrane (Komada *et al.*, 1997). Recruitment of Hrs may also be mediated via interactions between its UIM and ubiquitin on proteins that require sorting (Raiborg *et al.*, 2002). Hrs is concentrated in flat bilayered clathrin coats on the surface of endosomes and is proposed to sort ubiquitinated proteins destined for lysosomal degradation, but not recycling receptors (Sachse *et al.*, 2002; Raiborg *et al.*, 2002; Clague, 2002). This was further confirmed by the retention of ubiquitin tagged TfR within endosomes, as normally TfR is not ubiquitinated and recycles back to the plasma membrane (Raiborg *et al.*, 2002). Once Hrs is recruited to the endosome, it also recruits STAM 1 and 2, which are involved in receptor sorting (Bache *et al.*, 2003b). Additionally, Hrs acts as a docking site for ESCRT-1, which is comprised of three component proteins Vps23, Vps28 and Vps37 (Katzmann *et al.*, 2003; Bache *et al.*, 2003a). Vps23 (Tumour susceptibility gene or Tsg101) binds Hrs via its UIM (Lu *et al.*, 2003) and ESCRT-1 is recruited to the endosome. Reduced Tsg101 protein levels have been shown to impair the efficient downregulation of EGFR and result in prolonged signalling through the MAPK (mitogen activated protein kinase) pathway (Babst *et al.*, 2000). ESCRT-II is a smaller protein complex (155kDa) comprised of Vps22, two Vps25 molecules and the C-terminus of Vps36, which together form a Y shape (Hierro *et al.*, 2004). This complex transiently associates with the endosomal membrane and initiates the formation of ESCRT-III (Babst *et al.*, 2002b). ESCRT-III has two sub complexes: the first, Vps20/Snf 7, binds to the endosomal membrane and recruits the second, Vps2/Vps24, which, in turn, recruits additional factors (Babst *et al.*, 2002a).

ESCRT-III proteins show considerable homology to human CHMP (charged MVB) proteins (Babst *et al.*, 2002a).

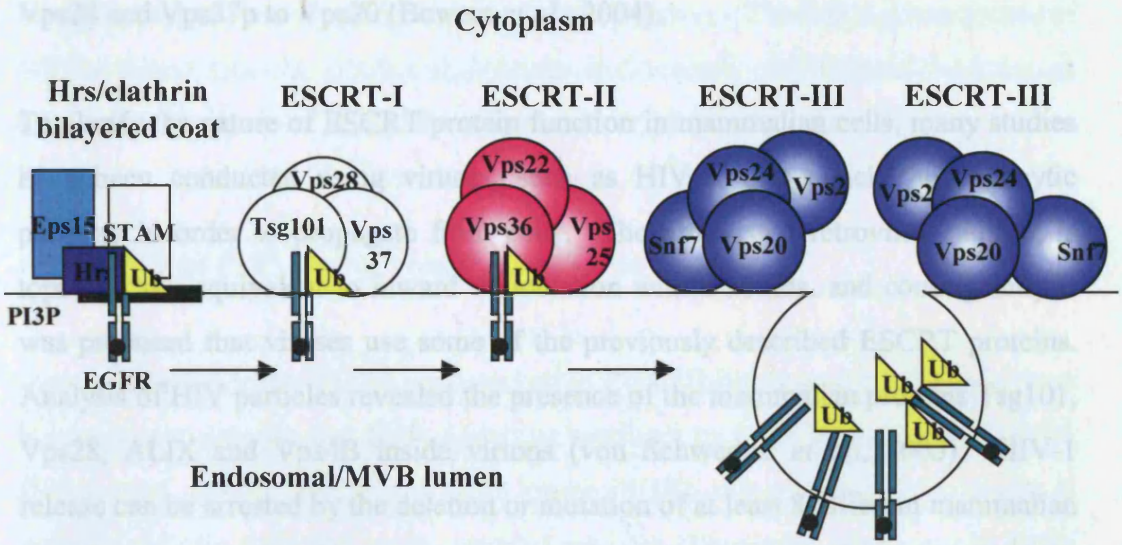

Figure 1.3. *Model of vps and ESCRT protein mediated EGFR sorting and MVB formation.* PI3P mediates the localisation of Hrs and its associated proteins Eps15, STAM and clathrin to endosomal membranes. The complex binds to ubiquitinated EGFR and retains them in the endosome membrane. Ubiquitinated (Ub) EGFR are delivered to ESCRT-I by interacting with Tsg101. EGFR is then relayed to ESCRT-II and transported into an intraluminal vesicle, which is formed through polymerisation of ESCRT-III complexes. The membrane association of several of these proteins is controlled by the AAA ATPase Vps4 (not shown). Before vesicle scission, EGFR is deubiquitinated. Arrows indicate the direction of the sorting process. Diagram modified from Raiborg *et al.*, 2003.

Vps4 is an AAA type ATPase responsible for disassociation and recycling of the ESCRT complex from the endosomal membrane at the same time as inward vesiculation occurs (Babst *et al.*, 1998). Vps4p and Doa4p, a deubiquitinating enzyme, have both been shown to bind directly to components of ESCRT-III (Bowers *et al.*, 2004). Work on yeast Vps4p and mammalian Vps4 suggest that the protein is involved in release of components of the bilayered clathrin coat, from the endosomal membrane and that this release is coupled to the generation of internal vesicles (Sachse *et al.*, 2003).

Another yeast vps protein, Vps31p/Bro1, has been identified on endosomes and this interaction is dependent on Snf7, part of ESCRT-III (Odorizzi *et al.*, 2003). Similarly, the mammalian homologue Ask interacting protein (AIP)-1/ALIX, has been shown to interact with ESCRT proteins, and forms an indirect link between

ESCRT-I and –III complexes (Martin-Serrano *et al.*, 2003). In yeast there is a direct interaction between ESCRT complexes mediated by the direct binding of Vps28 and Vps37p to Vps20 (Bowers *et al.*, 2004).

To clarify the nature of ESCRT protein function in mammalian cells, many studies have been conducted using viruses, such as HIV-1, that hijack the endocytic pathway in order to propagate from cells. The process of retroviral budding is topologically equivalent to inward vesiculation within MVBs, and consequently it was proposed that viruses use some of the previously described ESCRT proteins. Analysis of HIV particles revealed the presence of the mammalian proteins Tsg101, Vps28, ALIX and Vps4B inside virions (von Schwedler *et al.*, 2003). HIV-1 release can be arrested by the deletion or mutation of at least 8 different mammalian Vps proteins. Viral budding requires interaction with Tsg101, a functional ESCRT-III complex and ATPase activity of Vps4. For the release of HIV-1 and several other pathogenic human viruses from the cell, a specific tetrapeptide sequence, P(S/T)AP or "late" domain, is required. This domain recruits Tsg101, via its N-terminal ubiquitin E2 variant (UEV) domain, to facilitate viral budding (Garrus *et al.*, 2001). P(S/T)AP sequences have also been identified in several mammalian proteins involved in endocytosis, including Hrs and ALIX (Pornillos *et al.*, 2003; Bache *et al.*, 2003a). It is therefore suggested that HIV binds Tsg101 in order to recruit the downstream ESCRT proteins that usually catalyse the formation of internal vesicles. Although the UEV domain of Tsg101 has been shown to interact with the P(S/T)AP sequence found in HIV Gag, Tsg101 itself and Hrs, binding to the viral protein occurs with a much higher affinity (Pornillos *et al.*, 2003). The surrounding sequence appears to influence the binding affinity as several proteins containing the P(S/T)AP sequence fail to bind Tsg101. The fact that viral and mammalian proteins interact differently with Tsg101 could be due to the fact that viruses need to exit cells as efficiently as possible, whereas cells need to regulate protein sorting. The viral protein appears to be able to out compete its mammalian counterpart and recruit the protein it requires to initiate budding.

In most mammalian cell lines viruses bud from the plasma membrane, but in macrophages viruses tend to bud into endosomes/MVBs. Deletion of the Vps proteins results in a class E phenotype (as observed in yeast) and accumulation of

viral particles on endosomal membranes (von Schwedler *et al.*, 2003). Interestingly, these viral particles/virions, that bud into intracellular compartments, can still emerge from the cell via the exosome pathway. The limiting membrane of MVBs fuses with the plasma membrane and releases the internal vesicles as exosomes (Denzer *et al.*, 2000; Pornillos *et al.*, 2002; Raposo *et al.*, 2002).

1.3.3 PI3P and PI3P binding proteins involved in sorting

Internal membranes of MVBs are enriched in PI3P (Gillooly *et al.*, 2000) and there is evidence to suggest that PI3P signalling regulates receptor sorting within MVBs (Petiot *et al.*, 2003). Inhibition of PI3 kinase (PI3K), using wortmannin, results in enlarged MVBs with few or no internal vesicles (Fernandez-Borja *et al.*, 1999; Chen and Wang, 2001; Futter *et al.*, 2001). This effect was mimicked using antibodies to hVps34, which was identified as the PI3K required for inward vesiculation (Futter *et al.*, 2001). EGFRs clustered on the limiting membrane of these MVBs. Although delivery to the lysosome was not affected, increased levels of tyrosine phosphorylated proteins were observed, indicating that sorting of EGFR onto internal vesicles serves to attenuate signal transduction, but is not necessary for lysosomal delivery (Futter *et al.*, 2001).

Other groups have reported contrasting results when using wortmannin. Petiot *et al.* (2003) reported that treatment of BHK cells with wortmannin or a double FYVE-domain-containing construct, which specifically binds PI3P, inhibits the transport of EGFR to lysobisphosphatidic acid (LBPA)-containing late endosomes (Petiot *et al.*, 2003). The work of Bright *et al.* (2001) reported that although wortmannin treatment resulted in enlarged late endosomal structures, this did not inhibit formation of internal vesicles within LBPA containing MVBs (Bright *et al.*, 2001). This latter study did not involve EGF stimulation and, taken together with the findings of Futter *et al.* (2001), there is growing evidence for the presence of more than one population of MVB/late endosomes within cells, one that is PI3K dependent and one that is not, but may contain LBPA. However, the discrepancies between the work of Petiot and Futter cannot be due to the investigation of different populations of MVB, as both groups used EGFR as a marker. Instead, the

differences could be due to the timing of PI3K inhibition as Futter *et al.* (2001) pre-loaded cells with EGF at 20°C before treating cells with wortmannin and it is possible that receptor sorting may occur during this incubation period. Further evidence for the heterogeneity of MVBs can be drawn from the work of Kobayashi *et al.* (2002), who found that there were two populations of membranes within MVBs, those containing phosphatidylcholine (PC) and those containing LBPA (Kobayashi *et al.*, 2002).

The PI3P dependent sorting of EGFR is likely mediated by Hrs (Petiot *et al.*, 2003). Hrs contains a FYVE domain that specifically binds PI3P, it is sensitive to wortmannin and is involved in EGFR downregulation (Bishop *et al.*, 2002; Lloyd *et al.*, 2002; Raiborg *et al.*, 2002). Functional and mutational analysis of Hrs has led to the suggestion that the processes of receptor sorting and inward vesiculation are linked through the UIM domain of Hrs (Urbe *et al.*, 2003). The primary role of this domain is to recruit ubiquitinated receptors into clathrin-coated microdomains on endosomes by an active retention mechanism, as a prelude to internalisation into lumenal vesicles (Urbe *et al.*, 2003). Overexpression of Hrs inhibits EGFR downregulation by trapping EGFR within early endosomes (Raiborg *et al.*, 2002; Petiot *et al.*, 2003), indicating that there must be a release step to remove Hrs before inward vesiculation occurs. Internal vesicle formation also requires the Hrs UIM domain and it has been proposed that a component of ESCRT-I, e.g. Tsg101, may compete with Hrs for binding to EGFR (Urbe *et al.*, 2003). The downstream recruitment of other ESCRT complexes would result in formation of internal vesicles. Hrs is phosphorylated by kinases, downstream of EGFR (Bache *et al.*, 2002), and phosphorylation induces Hrs to dissociate from the endosomal membrane, a process believed to be coupled to the formation of receptor containing internal vesicles (Urbe *et al.*, 2003). This dissociation may also result in the movement of newly freed receptors to the edge of the clathrin-coated microdomain, where inward vesiculation occurs (Sachse *et al.*, 2002).

Fab1, a yeast lipid kinase that produces $PI(3,5)P_2$, also contains a FYVE domain (Odorizzi *et al.*, 1998; Gary *et al.*, 1998; Sbrissa *et al.*, 2002). A point mutation in the lipid kinase domain caused defects in transport of biosynthetic cargo through

the MVB (Shaw *et al.*, 2003). In cells expressing mutant Fab1, the morphology of the yeast vacuole is altered and sorting of endocytic cargo onto internal vesicles is defective. Similarly, a dominant negative mutant of the mammalian homologue, PIKFYVE, causes enlargement of endosomes in mammalian cells (Ikonomov *et al.*, 2001). Recent evidence supporting the involvement of PIKFYVE in protein sorting came from the discovery that a subunit of ESCRT-III (Vps24) interacts with $PI(3,5)P_2$ (Whitley *et al.*, 2003).

Phox (PX) domains are present in a number of proteins that bind phosphoinositides (PI). The sorting nexins (SNX) are a family of cytoplasmic and membrane-associated proteins, believed to function in the intracellular trafficking of plasma membrane receptors, including EGFR. SNX proteins exert their function through PX domain-mediated interaction with PI, although interactions with other proteins are thought to contribute to the membrane specificity (Xu *et al.*, 2001; Cozier *et al.*, 2002; Zhong *et al.*, 2002). SNX1 has been localised to endosomes in a PI3K dependent manner and is reported to play a critical role in the sorting of EGFR to lysosomes, as overexpression of SNX1 increased receptor degradation (Kurten *et al.*, 1996; Haft *et al.*, 1998; Zhong *et al.*, 2002). Additionally, SNX1 interacts specifically with Hrs on endosomes, where they form a complex devoid of EGFR, and it is believed that Hrs may negatively regulate EGFR transport through its interaction with SNX1 (Chin *et al.*, 2001). More recently SNX16 has also been reported to be a negative regulator of EGFR-mediated signalling pathway by sorting EGFR for degradation (Choi *et al.*, 2004).

1.3.4 Annexins and sorting

Although annexins, with the exception of annexin 6, have not been reported to be involved in the internalisation of growth factor receptors, their common ability to bind phospholipid membranes in a Ca^{2+} dependent manner has made them popular candidates to participate in membrane trafficking. However, several annexins have been ruled out as their Ca^{2+} requirement for membrane binding far exceeds that of cytosolic Ca^{2+}. Annexins 1, 2 and 6 are able to associate with membranes at much lower and more physiological Ca^{2+} concentrations. Using light and electron

microscopy annexins 1 and 2 have been localised to early endosomes (Emans *et al.*, 1993; Harder and Gerke, 1993; Seemann *et al.*, 1996b; Seemann *et al.*, 1997; Diakonova *et al.*, 1997; Rescher *et al.*, 2000). Annexin 1 has also been localised to MVBs (Futter *et al.*, 1993), while annexin 2 colocalised with Rab11 in recycling endosomes (Zobiack *et al.*, 2003). Annexin 6 has also been localised to endocytic membranes (Jackle *et al.*, 1994; Seemann *et al.*, 1996b; Pol *et al.*, 1997; Ortega *et al.*, 1998; Massey-Harroche *et al.*, 1998). Interestingly, all three annexins were identified on phagosomes from macrophages (Desjardins *et al.*, 1994; Diakonova *et al.*, 1997) and annexin 2 has also been observed on pinosomes (Merrifield *et al.*, 2001).

At the beginning of this project, no functional studies supporting a role for annexin 1 in membrane trafficking had been reported, although a plethora of data exists regarding the anti-inflammatory role of annexin 1 in glucocorticoid function. Meanwhile, the use of a dominant negative mutant pointed to a role for annexin 2 in the organisation of early endosomes (Harder and Gerke, 1993). Annexin 2 was also shown to be involved in endosome fusion using an *in vitro* homotypic endosome fusion assay (Emans *et al.*, 1993). More recently, RNAi-induced depletion of annexin 2 has been used to further examine its role in membrane trafficking. In cells treated with annexin 2 RNAi, there was a dramatic relocalisation of recycling endosomes, with little effect on TfR recycling (Zobiack *et al.*, 2003). These findings are consistent with earlier work indicating that annexin 2 plays a role in positioning of endosomes (Harder and Gerke, 1993). Zobiack *et al.* (2003) also reported that lysosomal delivery was unaffected in annexin 2 depleted cells. However, conflicting data reported that knockdown of annexin 2 inhibited MVB biogenesis and delivery of EGFR to the lysosome (Mayran *et al.*, 2003).

Functional studies investigating the role of annexin 6 in later stages of endocytosis have revealed its involvement in trafficking of LDL from the pre-lysosomal compartment to degradation in the lysosome (Pons *et al.*, 2001). Expression of mutant annexin 6 caused LDL to accumulate in enlarged pre-lysosomal structures, which was accompanied by a significant inhibition of LDL degradation.

1.4 Receptor recycling

There are two recycling pathways, the rapid one from endosomes and the slower one through recycling endosomes. The majority of constitutively recycled receptors, e.g. TfR, recycle from endosomes but a certain amount are sorted into recycling endosomes from the perimeter membrane of MVBs. Sorting to the recycling pathway and lysosomal delivery are likely coupled, as lysosomal fusion occurs as soon as all the recycling receptors have been removed from the limiting membrane (Futter *et al.*, 1996).

In unstimulated cells, unoccupied EGFR are constitutively endocytosed and recycled back to the plasma membrane, ready to bind EGF (Herbst *et al.*, 1994). Ligand binding enhances endocytosis and also reduces the rate of receptor recycling, as active EGFR now become targeted for lysosomal degradation (Wiley *et al.*, 1991). Some ligand-bound EGFR are recycled, although this depends on the cell type and also on the level of receptor expression. In human A431 cells, which express high levels of EGFR, more recycling occurs than in a cell line that expresses low levels of receptors. This is due to the saturable nature of the sorting mechanisms. Until recently it was believed that the recycling pathway was the default pathway for EGFR, a hypothesis derived from many studies showing enhanced recycling in the absence of lysosomal targeting signals (Levkowitz *et al.*, 1998; Kil *et al.*, 1999; Stoorvogel *et al.*, 2004). However, a protein has been identified, the role of which suggests that recycling is an active process. Calcium-modifying cyclophilin ligand (CAML) is a ubiquitous protein, resident in the endoplasmic reticulum (Bram and Crabtree, 1994; Holloway and Bram, 1998). CAML was shown to be necessary for the efficient recycling of EGFR (Tran *et al.*, 2003). Cells lacking CAML fail to recycle EGFR but show normal levels of degradation, indicating that EGFR becomes trapped within the cell rather than recycled (Tran *et al.*, 2003). These findings suggest that CAML serves an opposite function to ESCRT-I, by preferentially binding non-ubiquitinated EGFR and aiding their transport back to the cell surface.

Recycling endosomes are Rab11 positive, Rab5 negative and are often characterized by the presence of TfR (Green *et al.*, 1997). A dominant negative Rab11 mutant has been shown to inhibit TfR recycling (Ullrich *et al.*, 1996; Ren *et al.*, 1998). Annexin 2 has been localised to Rab11 positive recycling endosomes (Pol *et al.*, 1997; Trischler *et al.*, 1999; Zeuschner *et al.*, 2001; Zobiack *et al.*, 2003) and is believed to play a role in controlling the localisation of recycling endosomes. Annexin 2 was observed associated with recycling endosomes and its depletion results in an increased number of endosomal buds that label heavily for clathrin (Zeuschner *et al.*, 2001; Zobiack *et al.*, 2003). However, clathrin does not seem to be essential for recycling and is believed to play a role in formation or organisation of recycling endosomes, rather than in concentrating receptors to be recycled. Similarly, little evidence exists for a role of adaptor proteins in recycling although in polarised cells AP-1/μ1B adaptor complex is involved in the efficient recycling of TfR and LDL-R to the basolateral membrane (Gan *et al.*, 2002).

1.5 Final stages of endocytosis

After receptors are sorted onto internal vesicles of MVBs and recycling receptors have been sorted back to the plasma membrane, the final stage is fusion of mature MVBs with lysosomal membranes. The contents of the MVB are exposed to internal hydrolases and become degraded (Futter *et al.*, 1996). Lysosomes are membrane-bound, hydrolase rich, acidic organelles. They can be distinguished from endosomes by their lack of mannose-6-phosphate (M6P) receptors and recycling surface receptors. Lysosomes are the final destination for many macromolecules taken up by endocytosis from the extracellular milieu and from the cell surface. Ligand induced activation of many cell surface receptors triggers downregulation of the receptors by internalisation and delivery to the lysosome. EGFRs with bound EGF are degraded in the lysosome (Wiley *et al.*, 1991). In contrast, receptors lacking the cytoplasmic tail fail to reach the lysosome and are recycled rapidly back to the cell surface (Herbst *et al.*, 1994).

For many years it was believed that lysosomes were simply "garbage-disposal units" (Luzio *et al.*, 2000). More recently it has been shown that lysosomes can

fuse with the plasma membrane and secrete their contents (for a review see Stinchcombe and Griffiths, 1999). Lysosomes can also be accessed via the biosynthetic pathway e.g. newly synthesized acidic hydrolases modified with mannose-6-phosphate groups bind to their receptors (MPRs) in the trans-Golgi network (TGN), after which they are transported to endosomes via an intracellular route. The hydrolase-MPR complex dissociates in the acidic pH of the endosomes and hydrolases are thus transported to the lysosome, while the receptors return to the TGN for further activity. Transport between late endosomes/MVBs and lysosomes has been studied in a cell free system (Mullock *et al.*, 1994; Mullock *et al.*, 1998). Three hypotheses have been proposed for the mixing of contents between MVB/late endosomes and lysosomes. The first proposes that there is vesicular transport between organelles. The second "kiss and run" hypothesis proposes a continuous repeated transient fusion and fission (Storrie and Desjardins, 1996). The third and most recent proposal is an extension of the kiss and run hypothesis as MVBs and lysosomes fuse. Data exists to support the latter hypothesis, which suggests that lysosomes and MVBs fuse directly but that lysosomes can be regenerated from this hybrid organelle (Mullock *et al.*, 1994; van Deurs *et al.*, 1995; Futter *et al.*, 1996; Bright *et al.*, 1997; Mullock *et al.*, 1998). Further evidence supporting the fusion of MVBs and lysosomes comes from both *in vitro* studies and *in vivo* studies using electron microscopy of cultured cells (Casciola-Rosen and Hubbard, 1991; Futter *et al.*, 1996; Tjelle *et al.*, 1996). Therefore, there is extensive evidence to back up the third proposal for MVB/lysosome fusion.

The fusion of late endosomes and lysosomes *in vitro* was found to be ATP, cytosol and temperature dependent (Mullock *et al.*, 1998). These studies also identified a requirement for NSF (*N*-ethylmaleimide sensitive factor) and SNAPs (soluble NSF attachment proteins). This fusion was inhibited by Rab-GDI, which implied the need for a Rab-GTPase. Both Rab7 and Rab9 have been localized to late endosomes (Chavrier *et al.*, 1990; Lombardi *et al.*, 1993). As Rab9 also localizes to the TGN, it is believed that this Rab GTPase is involved in transport between the TGN and lysosomes. More recently, Rab7 has been identified as necessary for the proper aggregation and fusion of late endocytic structures in the perinuclear region

and also for the proper biogenesis and maintenance of lysosomes (Bucci *et al.*, 2000).

1.6 Endocytosis and signalling

Activated EGFR undergo a conformational change, resulting in activation of the intracellular tyrosine kinase domain. In addition to autophosphorylation, this domain can phosphorylate a wide range of downstream molecules, a process that acts as the initiation step for several signalling pathways. EGF stimulation of cells activates a number of pathways, resulting in one of a number of processes, including cell proliferation, motility, differentiation and survival. One of the most studied pathways is the ERK1/2 (extracellular regulated kinase) MAPK pathway; a series of protein kinases to activate ERK1/2, which is able to translocate to the nucleus and stimulate mitogenesis.

1.6.1 How does endocytosis affect signalling?

Downregulation of EGFR is important for termination of signals leading to cellular growth and proliferation. However, as the rate of receptor internalisation far exceeds the rate of receptor degradation, it is clear that receptor internalisation is necessary for more than simply targeting receptors to the lysosome. It was originally thought that internalisation, and thus removal from the plasma membrane, of activated EGFR inhibited the ability of the receptor to signal. This theory was quashed by the finding that endocytosed EGFR are hyperphosphorylated compared to those at the plasma membrane (Lai *et al.*, 1989; Wada *et al.*, 1992; Di Guglielmo *et al.*, 1994; Burke *et al.*, 2001).

Although the majority of mitogenic signals are initiated at the plasma membrane (Di Fiore and Gill, 1999), there is growing evidence to suggest that some signalling cascades require endocytosis for activation. Inhibition of EGFR internalisation, using mutant dynamin, significantly inhibited signalling through the MAPK pathway, showing that endocytosis of EGFR is required for full activation of this

pathway (Vieira *et al.*, 1996). However, this work also showed that phospholipase C γ (PCLγ) signalling was increased by inhibiting EGFR internalisation, indicating that endocytosis can also regulate some signalling pathways by separating the receptor from its downstream signalling partners at the plasma membrane (Vieira *et al.*, 1996). Other signalling pathways do not require receptor internalisation for their activation as shown by phosphorylation of IRS1 (insulin receptor substrate 1) in the absence of insulin receptor (IR) internalisation. However, although blocking IR internalisation had no effect on Akt kinase phosphorylation or activation, it partially inhibited phosphorylation of other downstream substrates, Shc and ERK1/2 (Ceresa *et al.*, 1998)

Several proteins involved in the endocytosis of EGFR also play roles in signalling, especially through the MAPK pathway. Grb2 is recruited to the plasma membrane in response to receptor activation, either directly through an interaction with the receptor or indirectly through Shc. Grb2 is needed for the transient anchoring of EGFR at the rim of CCPs (Stang *et al.*, 2004). Additionally, Grb2 is constitutively associated with SOS (son of sevenless), a Ras guanine-nucleotide exchange factor (GEF), at the plasma membrane (Egan *et al.*, 1993) and the proximity of this complex with Ras is thought to mediate Ras activation. Ras-GTP can now bind to its effector Raf-1, thus recruiting it to the plasma membrane. Raf-1 is a MAPK kinase kinase, which phosphorylates and activates the MAPK kinase, MEK-1. MEK-1 phosphorylates and activates MAPK/ERK1/2. Activated ERK1/2 can translocate to the nucleus and stimulate mitogenesis, or it can remain in the cytosol and phosphorylate other cytosolic proteins.

The formation of signalling complexes has not only been observed at the plasma membrane, but also on endosomal structures. Grb2 and SOS are associated with activated EGFR at the plasma membrane and also been localised to endosomal membranes (Di Guglielmo *et al.*, 1994; Sorkin *et al.*, 2000; Burke *et al.*, 2001; Jiang and Sorkin, 2002). Therefore, Ras activation can occur both at the plasma membrane and on endosomes (Jiang and Sorkin, 2002). Other members of the ERK1/2 MAPK pathway have also been localised to endosomes, including Raf-1, which translocates to endosomes after receptor activation (Di Guglielmo *et al.*,

1994; Pol *et al.*, 1998; Rizzo *et al.*, 2000), MAPK and MEK, thus creating a signalling endosome (Howe *et al.*, 2001; Luttrell *et al.*, 2001). MAPK and MEK are recruited to endosomes by kinase-substrate interactions, but also by scaffolding proteins. MP1 (MEK1 partner) specifically binds MEK1 and results in ERK1 activation (Schaeffer *et al.*, 1998). Recently, an additional scaffold protein, p14, has been shown to interact with MP1 on late endosomes (Wunderlich *et al.*, 2001) and act as an endosomal adaptor protein for MP1. The endosomal localisation of p14/MP1 scaffold complex is required for efficient ERK signalling (Teis *et al.*, 2002).

Activated EGFR are able to tyrosine phosphorylate a wide range of downstream molecules at the plasma membrane, many of which are involved in the internalisation of the receptor. However, some downstream targets are not accessible to EGFR at the plasma membrane and are only phosphorylated once the receptor has been internalised. Hrs is involved in EGFR sorting within the endosomal clathrin coat. Its phosphorylation, by kinases downstream of the active EGFR, occurs at the endosomes, indicating that receptor endocytosis is necessary for Hrs phosphorylation to occur (Urbe *et al.*, 2000; Bache *et al.*, 2002). Eps8 is another substrate of the EGFR tyrosine kinase and is thought to mediate the transfer of signals between Ras and Rac (Scita *et al.*, 1999). Eps8 is only associated with internalised EGFR within endosomes, an association that is enhanced by EGF stimulation (Burke *et al.*, 2001). Similarly annexin 1, another substrate of the EGFR tyrosine kinase, is only phosphorylated by EGFR, or associated kinases, within MVBs (Futter *et al.*, 1993). Although the exact nature of the role of annexin 1 in EGFR endocytosis remains unclear, the fact that it is only phosphorylated by internalised EGFR provides another example of how endocytosis is necessary for signalling.

1.6.2 How does signalling affect endocytosis?

EGFR endocytosis has been shown to be necessary for efficient signal transduction. Therefore, the processes of endocytosis and signalling are intimately linked and appear to influence each other. The involvement of many proteins in both

signalling and trafficking raises the question of whether signalling receptors or downstream signalling pathways can modulate the endocytic machinery.

Although CCPs form constitutively on the surface of cells, the density of CCPs is increased upon EGF stimulation (Connolly *et al.*, 1984). Activation of EGFR results in tyrosine phosphorylation of the clathrin heavy chain by a downstream kinase, c-src, resulting in clathrin translocation to the plasma membrane and formation of CCPs (Beattie *et al.*, 2000). Additionally, EGFR can activate PI(4,5)K1β, leading to the localised generation of PIP_2 and recruitment of PIP_2-binding proteins involved in clathrin coat formation (Barbieri *et al.*, 2001). These data show that signalling from the EGFR is required for the enhanced formation of many CCPs, which in turn are necessary for efficient internalisation of EGFR, and thus EGFR controls its own endocytosis. Eps15 interacts with clathrin-associated adaptor proteins and is required for budding of CCPs (Confalonieri *et al.*, 2000). Eps15 is recruited to the plasma membrane upon EGF stimulation and is phosphorylated by the EGFR. Eps15 phosphorylation is necessary for its activity in EGFR endocytosis, but not for constitutive endocytosis (Confalonieri *et al.*, 2000).

Rab5 participates in both regulation of endocytosis and in signalling. Rab5a is activated by EGF stimulation and its activation is essential for EGFR endocytosis (Barbieri *et al.*, 2000). Activation of Rab5a is mediated through RIN1 (Ras inhibitor), a Rab5 GEF (Tall *et al.*, 2001) or by physical separation from RN-tre (Related to the N-terminus of TRE), its GTPase activating protein (GAP) (Martinu *et al.*, 2002). Grb2 is involved in the activation of Ras but has recently been shown to signal to Rab5a through its interaction with RN-tre. Therefore, the signalling activity of EGFR activates Rab5a and stimulates internalisation. Activated Rab5 recruits EEA1 to endosomes, where it acts as a tether and is necessary for endosomal fusion (Christoforidis *et al.*, 1999; Barbieri *et al.*, 2000). A second potential Rab5 effector is PI3K (human homologue of Vps34). Rab5 recruits hVps34 to endosomes, where Vps34 is important in the production of PI3P, which is necessary for the membrane binding of FYVE-domain containing proteins, such as EEA1 and Hrs (Murray *et al.*, 2002). Additionally, hVps34 has been shown to

mediate internal vesicle formation within MVBs, which is important in the downregulation of EGFR signalling (Futter *et al.*, 2001).

1.7 Properties of annexins – clue to function?

The annexin family has been well studied over the years, in terms of structure and general properties. Some of these properties have given rise to proposed roles for annexins in membrane trafficking, in particular annexins 1 and 2, although little conclusive evidence has yet been collected.

1.7.1 Regulation of annexin binding to endosomal membranes

The localisation of several annexins to endosomal structures, coupled with their generic membrane binding properties, has led to proposed roles for annexins in membrane trafficking. Both annexins 1 and 2 have been localised to endosomal membranes and their possible roles in receptor sorting have already been discussed. Another common property of the annexin family is Ca^{2+} binding, although the requirement for Ca^{2+} for membrane binding differs between family members. Annexins contain two types of calcium binding motifs, type II and type III. Type II sites appear to have a higher affinity for Ca^{2+} and are therefore regarded as the likely candidates for regulation of annexin function within cells (Thiel *et al.*, 1992; Jost *et al.*, 1994). Inactivation of one type II Ca^{2+} binding site dramatically changed the intracellular distribution of both annexin 1 and 2, from punctate membrane or cytoskeletal associated, respectively, to diffuse, cytoplasmic staining with no sign of membrane association (Jost *et al.*, 1994; Rescher *et al.*, 2000).

Typically annexins bind membranes in a Ca^{2+} dependent manner and, in the presence of Ca^{2+}, annexin 1 has been localised to endosomal membranes in living cells (Rescher *et al.*, 2000). A rise in intracellular Ca^{2+} is known to alter the localisation of several annexins, presumably by allowing annexins to bind membranes in a Ca^{2+} dependent manner (Babiychuk *et al.*, 1999; Babiychuk and Draeger, 2000). Interestingly, EGF stimulation induces a rise in intracellular Ca^{2+}

(Moolenaar *et al.*, 1988; Pandiella *et al.*, 1988; Qiu and Green, 1991; Obermeier *et al.*, 1993; Tinhofer *et al.*, 1996). However, the effect of EGF stimulation on annexin localisation has not yet been studied. Although Ca^{2+} is required for the association of annexin 1 with early endosomes, Ca^{2+} independent membrane binding has also been shown *in vitro* at a more acidic pH (Rosengarth *et al.*, 1998), and *in vivo* by a mutant form of annexin 1 lacking Ca^{2+}-binding sites that was still able to bind endosomes in BHK cells (Jost *et al.*, 1997). Additionally, phosphorylation was shown to convert annexin 1 from a Ca^{2+} independent membrane binding protein to a Ca^{2+} dependent species (Haigler and Schlaepfer, 1990). Ca^{2+} independent binding of annexin 1 was also suggested by Futter *et al.* (1993), where MVBs fractionated through a gradient containing EDTA still contained annexin 1 (Futter *et al.*, 1993). *In vitro* phosphorylation reactions of isolated MVBs showed that phosphorylated annexin 1 was released from the membrane in the presence of EDTA, but not in the presence of Ca^{2+}, supporting the notion that phosphorylated annexin 1 requires Ca^{2+} for membrane association (Futter *et al.*, 1993). However, it was later shown that in living cells non-phosphorylated annexin 1 requires intact Ca^{2+} binding sites in order to bind to early endosomal membranes (Rescher *et al.*, 2000). The discrepancy in these findings could be explained by a requirement for Ca^{2+} for association with endosomes but, once associated, annexin 1 is not readily released by treatment with EDTA. Furthermore, phosphorylated annexin 1 is more susceptible to N-terminal proteolysis (Chuah and Pallen, 1989; Ando *et al.*, 1989). The N-terminal domain contains the early endosomal localisation signal and its loss results in a relocalisation of annexin 1 from early endosomes to late endosomes (Seemann *et al.*, 1996b; Rescher *et al.*, 2000).

Unlike wild type annexin 1, a large fraction of endosomally associated annexin 2 remains bound to the organelle membrane in the presence of Ca^{2+} chelating agents (Emans *et al.*, 1993; Harder *et al.*, 1997). Annexin 2 can be released from membranes, along with a group of actin-binding proteins, by sequestration of cholesterol (Harder *et al.*, 1997). It was proposed that the atypical (Ca^{2+} independent) binding of annexin 2 to membranes most likely requires a specific membrane composition and configuration. Annexin 2 associates with membrane rafts in both a Ca^{2+} dependent and independent manner. In smooth muscle cells

annexin 2 binds to lipid rafts following a rise in intracellular Ca^{2+} (i.e. during muscle contraction) (Harder and Gerke, 1994; Babiychuk and Draeger, 2000). Interestingly, this rise in Ca^{2+} induces the relocalisation of annexin 6 from the cytoplasm to the plasmalemma in these cells (Babiychuk *et al.*, 1999).

Annexin 2 interacts preferentially with cholesterol rich membranes and cholesterol appears to be necessary for annexin 2 Ca^{2+} independent membrane binding. The plasma membrane and early endosomes contain the largest amounts of cholesterol and annexin 2 is found associated with both of these types of membrane (Harder *et al.*, 1997). Additionally, the intracellular distribution of cholesterol was found to modulate the location of annexin 2, as observed in cells from patients with the cholesterol storage disorder, Niemann-Pick C, where annexin 2 was found in enlarged MVBs (Mayran *et al.*, 2003). Annexin 2 has therefore been proposed to form cholesterol-containing platforms on early endosomal membranes, which are involved in receptor trafficking.

1.7.2 Annexin binding to actin and other cytoskeletal proteins

Microtubules have long been shown to be required for endocytosis, both in the positioning of endocytic organelles (Matteoni and Kreis, 1987; McGraw *et al.*, 1993; Nielsen *et al.*, 1999) and for transport from early to late endosomes (Aniento *et al.*, 1993). More recently, roles for actin filaments have been identified in the initial uptake of ligands and later for their delivery to the lysosome (van Deurs *et al.*, 1995; Durrbach *et al.*, 1996). Inhibition of actin filament assembly impairs lysosomal delivery and disrupts the organisation of endosomes (van Deurs *et al.*, 1995; Barois *et al.*, 1998). A member of the Diaphanous group of proteins, hDia2C, has been identified as the downstream effector of RhoD and together these proteins function to position endosomes along actin filaments, which requires the recruitment and activation of c-src (Gasman *et al.*, 2003). Further evidence that actin is required for endocytosis comes from the localisation of MM1α, a member of the myosin family with actin-based motor properties, to both endosomes and lysosomes. Expression of a non-functional mutant MM1α inhibits transport of fluid phase cargo to the lysosome. Through its interaction with actin, MM1α is

thought to be required for the close apposition of endosomes and lysosomes necessary for their fusion (Raposo *et al.*, 1999). In addition to its role in positioning endosomes, actin is involved in the movement of intracellular vesicles. Pinosomes were identified as having dynamic actin comet tails (Willingham *et al.*, 1981; Merrifield *et al.*, 1999). Sustained actin assembly on the surface of the newly formed pinosome is thought to propel it through the cytoplasm. Similarly, actin comet tails have been identified on MVBs and lysosomes, and shown to contain N-WASP, which is intimately associated with the endosomal membrane (Taunton *et al.*, 2000). Movement of these structures is believed to be mediated through actin-assembly nucleated by Arp2/3, the downstream effector of N-WASP (Taunton *et al.*, 2000). Taken together, these studies highlight the importance of actin both in the proper positioning of endosomes and also in their movement through cells.

Although actin-binding, unlike membrane binding, is not a common property of the annexin family, several annexins have been shown to interact directly with polymerised actin *in vitro* and this is consistent with proposed annexin functions in mediating, stabilising and/or regulating membrane-actin interactions. Both annexins 1 and 2 have been shown to bind F-actin in a Ca^{2+}-regulated manner (Gerke and Weber, 1984; Glenney, 1986a; Glenney, 1986b).

Annexin 2 is capable of binding to, and bundling, actin in a Ca^{2+}-dependent manner, both as a monomer or as part of a heterotetramer with S100A10 (Gerke and Weber, 1985; Glenney, Jr. *et al.*, 1987). Actin binding is mediated through a specific 9 amino acid sequence at the end of the C-terminal region of annexin 2 (Filipenko and Waisman, 2001). Annexin 2 is believed to play a role in the organisation of membrane-associated actin at sites of cholesterol-rich microdomains, as cholesterol sequestering agents specifically release annexin 2 along with several other cytoskeleton proteins (Harder *et al.*, 1997). Annexin 2-S100A10 forms a complex with actin and AHNAK at the plasma membrane via S100A10 (Benaud *et al.*, 2004). AHNAK has been reported to organise the cell cytoarchitecture and it has been revealed that annexin 2 is necessary for this to occur, as depletion of annexin 2 results in release of AHNAK into the cytoplasm (Benaud *et al.*, 2004).

Like annexin 2, annexin 1 has also been associated with the cytoskeleton through its F-actin binding property (Glenney, Jr. *et al.*, 1987; Schlaepfer and Haigler, 1987). Additionally, annexin 1 binds the G-actin-binding protein, profilin, which regulates actin polymerisation, and this provides another link between annexin 1 and cytoskeleton organisation (Alvarez-Martinez *et al.*, 1996). These later studies failed to show any binding of annexin 1 and actin, and proposed that another protein might form a bridge between the two. Another interesting finding was that annexin 1 binding to profilin is Ca^{2+} independent, although the binding affinity was greater when Ca^{2+} was present. Work from the same group later showed that annexin 1 reduces the inhibitory effect of profilin on actin polymerisation (Alvarez-Martinez *et al.*, 1997). Conversely, profilin inhibits annexin 1 binding to membranes and this can be disrupted by the addition of PIP_2.

Therefore, the ability of annexins 1 and 2 to bind actin indicates that they may play roles in the positioning, or movement, of endocytic structures, as well as providing a link between endosomal membrane and the actin cytoskeleton.

1.7.3 Interactions with protein ligands

The localisation of annexin 2 to endosomes is mediated through its specific N-terminus and this property can be conferred onto other annexins by switching their N-terminal regions (Harder *et al.*, 1997; Jost *et al.*, 1997; Konig and Gerke, 2000). The N-terminal domain also contains binding sites for a member of the S100 subfamily of EF hand proteins, several of which form complexes with annexins. The formation of a heterotetrameric complex between annexin 2 and S100A10 (p11) is the best characterised so far. The interaction appears to be dependent on N-terminal acetylation of annexin 2 (Konig *et al.*, 1998). Co-fractionation of annexin 2 with early endosomal membranes does not require Ca^{2+} or S100A10 (Konig and Gerke, 2000), although binding of S100A10 is required for stabilisation of annexin 2 binding in the absence of Ca^{2+} (Konig and Gerke, 2000). It is believed that annexin 2, as part of a complex with S100A10, provides a link between the cytoplasmic face of the plasma membrane and the cortical actin cytoskeleton, and

that this function is regulated by membrane cholesterol content and by Ca^{2+} concentration (Gerke and Moss, 2002).

Annexin 1 also contains N-terminal binding sites for a S100 protein, S100A11 (S100C). The formation of a heterotetrameric complex is based on similar principles to annexin 2/S100A10, except that annexin 1/S100A11 binding requires Ca^{2+} (Mailliard *et al.*, 1996; Seemann *et al.*, 1996a; Rety *et al.*, 2000). Annexin 1 can target S100A11 to early endosomes (Seemann *et al.*, 1997). However, the *in vivo* interaction of annexin 1 and S100A10 remains to be identified.

Both annexins, in complex with their S100 binding partners, are thought to be able to link membranes, although the exact function of this property has not been revealed. The annexin 2/S100A10 complex exists in resting cells and is not dependent upon Ca^{2+}, whereas it is predicted that the annexin 1/S100A11 complex is dependent on transient intracellular calcium rises and plays an important role in Ca^{2+} regulated membrane transport (Gerke and Moss, 2002).

1.7.4 Modulation of annexin function by phosphorylation

The annexins are well known targets for post-translational modifications, including phosphorylation. Annexin 2 was originally identified as a substrate of v-src protein kinase (Erikson *et al.*, 1981). Annexin 2 can also be phosphorylated by the IR tyrosine kinase, in a manner that resembles annexin 1 phosphorylation by EGFR tyrosine kinase. Annexin 2 is only phosphorylated by IR as it undergoes internalisation (Biener *et al.*, 1996), while EGF-stimulated annexin 1-phosphorylation also occurs at a post-internalisation stage (Futter *et al.*, 1993). Tyrosine phosphorylation (on Tyr-23) of annexin 2 was increased in the presence of Ca^{2+} (Glenney, Jr., 1985), but tyrosine phosphorylation of annexin 2 decreased its membrane binding (Powell and Glenney, Jr., 1987; Hubaishy *et al.*, 1995). Similarly, annexin 1 phosphorylation alters its membrane binding properties by increasing the requirement for Ca^{2+}. Phosphorylation also increases the susceptibility of annexin 1 to N-terminal proteolysis (Chuah and Pallen, 1989;

Ando *et al.*, 1989) and a N-terminally truncated annexin 1-GFP chimera has been shown to relocate from early to late endosomes (Rescher *et al.*, 2000).

Protein kinase C (PKC) is a serine/threonine kinase and is known to phosphorylate a number of annexins, although annexin 5 is able to inhibit PKC (Schlaepfer *et al.*, 1992). PKC phosphorylation of annexin 2, as a result of nicotine stimulation, is required for Ca^{2+} regulated exocytosis in adrenal chromaffin cells (Sarafian *et al.*, 1991; Delouche *et al.*, 1997). However, PKC-induced phosphorylation of annexin 1 inhibits its ability to aggregate chromaffin granules (Wang and Creutz, 1992) or phospholipid vesicles *in vitro* (Johnstone *et al.*, 1993).

1.7.5 Summary of annexin property-related functions

The ability of annexins 1 and 2 to bind both membranes and cytoskeletal proteins points to a role for these proteins in the organisation of membranes. Although structurally similar, annexins 1 and 2 have different binding partners and Ca^{2+} dependencies, reflecting their different intracellular functions. Annexin 1 is thought to be involved in a specific aspect of EGFR trafficking, at the level of the MVB, and the identification of the annexin 1-S100A11 complexes within these structures is awaited. Annexin 2 appears to play a role in the organisation of membrane-associated actin at sites of cholesterol-rich membrane domains, but may also be involved in the proper positioning of endocytic organelles, through its interaction with the actin cytoskeleton.

1.8 Recent technological advances utilised to investigate annexin function

Although the amount of published data on growth factor receptor endocytosis is increasing exponentially, there appears to be little conclusive data on the exact nature of the roles of annexins in receptor sorting.

1.8.1 Annexin knockout models

To study the function of annexins further, several have been targeted for the creation of knockout mouse models (Srivastava *et al.*, 1999; Herr *et al.*, 2001; Hannon *et al.*, 2002; Hawkins *et al.*, 2002; Brachvogel *et al.*, 2003; Ling *et al.*, 2004). Generally the deletion of a single annexin has little effect on the viability of the mice and provides little in the way of clear-cut phenotypes. The exception was the annexin 7 -/- mouse described by Srivastava *et al.* (1999), which was reported to be lethal (Srivastava *et al.*, 1999). This group also produced a heterozygous mouse, which exhibited an insulin secretion defect and tumour phenotypes. In contrast, a second group reported an annexin 7 null strain that was viable, healthy and without visible/obvious defects (Herr *et al.*, 2001). However, more recently, this group has reported that the loss of annexin 7 affects membrane fusion within red blood cells and platelets (Herr *et al.*, 2003).

The annexin 1 knockout mouse was reported to be viable and healthy. However, so far the analysis of the annexin 1 knockout mouse has been restricted to studies of the inflammatory response (Roviezzo *et al.*, 2002; Hannon *et al.*, 2002). These studies reported an increased response to inflammatory stimuli and a decreased response to the anti-inflammatory glucocorticoids. Interestingly, several other annexins are upregulated in cells taken from these mice (annexins 2, 5 and 6), in addition to other genes involved directly in inflammation (COX-2 and $cPLA_2$) (Croxtall *et al.*, 2003). The upregulation of other annexins caused concern that the actual phenotype is being masked by the compensatory action of other annexin family member.

An annexin 2 null mouse has recently been created and used to investigate the role of annexin 2 in cell surface plasmin generation. These mice are viable but show markedly decreased neovascularization of fibroblast growth factor-stimulated cornea and oxygen primed neonatal retina (Ling *et al.*, 2004). An annexin 2 -/- DT40 (B lymphocyte) cell line already exists and was created together with an annexin 5 -/- cell line to investigate the effects of loss of these annexins in response to apoptotic stimuli (Hawkins *et al.*, 2002). However, while the loss of annexin 2

had no effect on apoptosis, the annexin 5 -/- cells were more resistant to induced apoptosis.

1.8.2 RNAi-induced annexin depletion

To overcome the potential problems of compensatory upregulation of alternative proteins in knockout mice, a relatively new technology has been utilised. RNA interference (RNAi) technology was originally used in insect cell lines to "knock-down" the expression of specific proteins. RNAi works by transfecting cells with short double stranded RNA sequences specifically designed against the desired protein. This activates the Dicer complex within cells to destroy the synthetic RNA sequence and also any naturally occurring RNA with the same sequence, thus destroying the usual cell transcripts. More recently the use of RNAi has been extended to mammalian cells (Elbashir *et al.*, 2001) and since this demonstration the use of RNAi has become commonplace in many publications. However, its use in studies of annexin function has not been widely published. The use of conventional RNAi to deplete annexin 2 has been reported by several groups (Mayran *et al.*, 2003; Zobiack *et al.*, 2003). Although annexin 1 RNAi has not yet been reported to deplete cellular annexin 1, use of annexin 1 antisense cDNA to reduce endogenous annexin 1 expression has been used to investigate annexin 1 inhibition of $cPLA_2$ (Solito *et al.*, 1998).

1.9 Aims of this work

Although the discovery of many members of the annexin family occurred years ago, further studies are still needed to identify and confirm specific roles for each family member. Annexins 1 and 2 have been implicated in various aspects of membrane trafficking, as well as playing roles in other processes that require their specific interactions with membranes and cytoskeletal proteins.

Annexin 1 is a well-known substrate of the EGFR tyrosine kinase (Haigler *et al.*, 1987) and has been shown to become phosphorylated only in MVBs and not at the

plasma membrane (Futter *et al.*, 1993). Tyrosine phosphorylation of annexin 1 increases the susceptibility of the protein to N-terminal proteolysis (Haigler *et al.*, 1987; Chuah and Pallen, 1989; Ando *et al.*, 1989) and loss of the N-terminal domain alters the membrane binding capabilities of annexin 1, possibly through disruption of the putative heterotetrameric complex with S100A11. Taken together, these data led to a proposed role for annexin 1 in formation of internal vesicles within MVBs and/or receptor sorting. However, the exact nature of this role remains unknown. Recently, annexin 2 has been implicated in MVB biogenesis (Mayran *et al.*, 2003). As annexins 1 and 2 share considerable homology, it is possible that they are involved in similar processes and may even be able to functionally compensate for each other. As a substrate of the EGFR tyrosine kinase, annexin 1 is more likely to be involved in a specific aspect of EGFR trafficking, while annexin 2, which is a poor substrate for EGFR tyrosine kinase, is more likely to play a functionally distinct role.

Therefore, the major aims of these studies were to investigate the effects of loss of annexins 1 and 2 on the formation of MVBs, including inward vesiculation, and the intracellular sorting of growth factor receptors, concentrating on EGFR. In addition, the effects of loss of these annexins on fluid phase endocytosis and endocytosis of the non-kinase receptor TfR were explored. During these studies RNAi-induced protein depletion, an annexin 1 -/- cell line (derived from the annexin 1 knockout mouse), and an annexin 2 knockout DT40 cell line were all used to investigate the intracellular morphology and kinetics of receptor trafficking. The effects of EGF stimulation on MVB formation and localisation of annexin 1 were explored using a combination of fluorescence, transmission electron microscopy and cryo-immuno electron microscopy. Finally, the effect of loss of annexin 1 on cell shape and EGF-stimulated cell motility was investigated by comparing the annexin 1 -/- cell line with a cell line derived from a wild type mouse.

Chapter 2 - Materials and Methods

2.1 Materials

2.1.1 Cell Culture

All reagents used in tissue culture were obtained from GibCo and all cell culture flasks and plates from Nunclon, except 3cm diameter Mattek™ dishes from BDH.

2.1.2 Molecular Biology

T4 DNA ligase, calf intestinal alkaline phosphatase (CIP), *pfu* DNA polymerase, dNTPs, DNA markers and gel loading buffer were all obtained from Promega UK Ltd. Restriction enzymes were from New England Biolabs. XL-1 blue supercompetent *Escherichia coli* were from Stratagene Ltd. TAE and TE buffer (50x stock) were from National Diagnostics. All primers, Lipofectamine™ and Oligofectamine™ were from Invitrogen. pGFP-N1 was from Clontech. Human EGFR was a gift from Alexander Sorkin (University of Colorado, Denver, USA). All RNAi oligonucleotides were ordered from Qiagen.

2.1.3 Electron Microscopy

Gold (10nm and 5nm) was obtained from British Biocell International. The anti-human EGFR antibody (108) was a gift from Joseph Schlessinger (Yale Medical School, USA). Protein A gold (10nm and 15nm) was obtained from the Utrecht Medical School (The Netherlands) every 3 months and used at 1:65-80 depending on the batch. Thermanox coverslips were from Nalgene.

2.1.4 Miscellaneous

All other chemicals were from Sigma, unless otherwise stated. Biotinylated human EGF was from Molecular Probes. ^{125}I-labelled human EGF was from Amersham. 125I-labelled human Tf was from Perkin Elmer. The Nucleofector™ machine, reagents and equipment were obtained from Amaxa Biosystems.

2.1.4 Antibodies

Mouse antibodies are monoclonal and all other species polyclonal, unless otherwise stated. The name of the antibody, the species it was raised in, and the domain it was raised against, are given in brackets.

Primary Antibody	**Use**			**Obtained from**
	ImmunoEM	**IF**	**W.blot**	
Anx 1 (74/3, mouse monoclonal)	1:50	1:100		Gift from C. Isacke
Anx 1 (sheep)			1:4000	Gift from J. Croxtall
Anx 2 (HH7, mouse)	1:50	1:500	1:4000	Gift from V. Gerke
EGFR (goat, cytoplasmic)			1:1000	Santa Cruz
EGFR (sheep, cytoplasmic)	1:250			Europa
GFP (rabbit, full length)	1:90		1:25	Clontech
Mek1/2 (rabbit)			1:1000	Cell Signaling
p44/42 (rabbit)			1:1000	Cell Signaling
P-Mek1/2 (rabbit, S217/221)			1:250	Cell Signaling
P-p44/42 (mouse, T202/Y204)			1:1000	Cell Signaling
Phosphotyrosine (mouse, PY99)			1:2000	Santa Cruz
TfR (H68.4, mouse, cytoplasmic)	1:25			Zymed
TfR (B3/25, mouse, extracellular)	1:20			
α-Tubulin (mouse)			1:2000	Zymed
Secondary Antibody				
Sheep HRP (donkey)			1:5000	Sigma
Goat HRP (donkey)			1:2000	DAKO
Mouse HRP (goat)			1:2000	DAKO
Rabbit HRP (goat)			1:2000	DAKO
Mouse Cy2 (donkey)		1:100		Molecular Probes
Mouse IgG (rabbit)	1:180			DAKO
Goat IgG (rabbit)	1:180			DAKO
Rabbit IgG (swine)	1:180			DAKO
Other				
EGF-AlexaFluor555		1:1000		Molecular Probes
Tf -AlexaFluor555		1:500		Molecular Probes
Phalloidin- AlexaFluor547		1:20		Molecular Probes

2.2 Cell Culture

Standard cell culture conditions (37°C, 5% CO_2) were used, unless otherwise stated. To serum starve cells, DMEM without foetal bovine serum (FBS) was used.

2.2.1. Human cell lines

HEp2, HeLa and A431 cells were all cultured in DMEM, containing 10% FBS, penicillin/streptomycin (5mg/ml) and L-glutamine (20mM). Cells were incubated

in 25cm^2 tissue culture treated flasks to form confluent monolayers. To passage cells, medium was removed and cells were washed with 1x PBS before incubating with 2ml 1x Trypsin/EDTA for 3-5 minutes. Full medium was added to cells to inhibit trypsin action before centrifuging at 1200 rpm (Eppendorf Centrifuge 5810R, A-4-62 rotor) for 4 minutes. Supernatant was removed and cells were resuspended in medium and transferred into fresh flasks at the appropriate dilution.

2.2.2 JACRO cell lines

Mouse lung fibroblasts from wild type and annexin 1 knockout mice (JACRO cells) were provided by Jamie Croxtall (St Bartholemew's Medical School, London, UK). Cells were cultured in DMEM F-12 containing 10% FBS, 5mg/ml penicillin/streptomycin and 10mM L-glutamine and passaged as described above.

2.2.3 DT40 cell lines

DT40 cells (chicken B lymphocytes) were cultured in suspension in DMEM containing 10% FCS, 1% chicken serum, penicillin/streptomycin and L-glutamine. DT40 cells were cultured at 40°C in 25ml medium in 25cm^2 flasks to a maximum density of 1 x 10^6 per ml before passaging at a dilution of 1:15-1:20.

2.3 Molecular Biology

2.3.1 Annexin 1-GFP Construction

The human annexin 1 gene was amplified using PCR from an I.M.A.G.E. Consortium [LLNL] cDNA clone ID3459615, using the following primers designed to contain *Xho*1 and *Bam*H1 restriction sites (underlined sequences). Bases in italics are extra bases or changed bases to keep annexin 1 in frame with GFP, to introduce appropriate restriction sites and to change the stop codon to allow read-through from annexin 1 into GFP.

Forward: *Xho*1 – 5'-CAAGAAG<u>CTCGAG</u>ATAAAGACACG-3'

Reverse: *Bam*H1 – 5'-CAAGG<u>G*GATCCGCG*</u>GTTTCCTCC-3'

These restriction enzymes were then used to clone annexin 1 into pGFP-N1, which contains the appropriate restriction sites within its multiple cloning site. Full annexin 1 sequence, including primers, is shown in Appendix 1 (Fig. S.1):

2.3.1.1 Restriction Digest of pGFP-N1 Plasmid DNA

pGFP-N1 DNA (0.5µg) was digested using 0.5U *Xho*1 and *Bam*H1 (in NEB buffer 2 (10x), 0.1mg/ml acetylated BSA, in a total volume of 25µl) for 2 hours at 37°C. Digestion was confirmed by analysis of 5µl of the restriction digest by electrophoresis on a 1% agarose gel containing ethidium bromide in cold 1x TAE buffer. A 1Kb DNA ladder was used as a marker and gels were run at 50V. Gels were visualised using Syngene UV Transilluminator and Gene Snap Gene Genius software. Bands were excised from the agarose gel and purified using QIAEX® II Gel extraction Kit (Qiagen). Digested pGFP-N1 was incubated with 1µl CIP for 30 minutes at 37°C. Excess CIP was removed after incubation using QIAquick PCR purification kit according to the manufacturer's instructions.

2.3.1.2 Ligations and Cell Transformations

For a 3:1 ratio of insert to vector the following calculation was used:

$$\frac{\text{Amount of vector (ng) x size of insert (kb)}}{\text{Size of vector (kb)}} \times \frac{\text{insert}}{\text{vector}} = \text{insert (ng)}$$

Ligations were performed in a total volume of 10µl containing plasmid DNA, insert DNA, T4 DNA ligase (1µl) and buffer (1µl of 10x stock). Reactions were incubated for 3 hours at room temperature or overnight at 4°C.

Supercompetent *E.coli* (100µl per transformation) were thawed on ice in pre-chilled 1.5ml microcentrifuge tubes. DNA (approximately 1µl of a typical ligation reaction) was gently mixed with cells and left on ice for 30 minutes. Cells were subjected to heat shock at 42°C for 45 seconds and returned to ice for 2 minutes. Pre-warmed LB broth (1ml) was added to cells and the contents of the tubes transferred to an incubation tube and incubated at 37°C shaking for 1 hour. Transformed cells were plated out onto selective LB agar plates and incubated

overnight at 37°C. Colonies were picked and plasmid DNA prepared (see 2.3.1.3). Purified plasmids were cut using restriction enzymes to check for the presence of the insert and suitable clones were sequenced for further verification (see 2.3.3).

2.3.1.3 Purification of Plasmid DNA

Plasmid DNA was extracted and purified from picked colonies using the Miniprep system from Qiagen according to manufacturers instructions. The same method was used to extract and purify plasmid DNA from *E.coli* grown in LB medium (cells were pelleted by centrifugation at 6000g for 15 minutes at 4°C). DNA was eluted in 1ml TE buffer. DNA was quantified by measuring absorption at λ=260nm (1 OD unit = 50μg double stranded DNA).

2.3.2 Annexin 1 Phosphorylation Site Mutation

Primers were designed to create a point mutation (bold underlined) at the site of EGFR phosphorylation of annexin 1, to change tyrosine (TAT) to phenylalanine (TTT) (Y21F) and abolish the phosphorylation site. For full annexin 1 sequence, including amino acids, see Appendix 1 (Fig. S.2).

Forward: 5'-GAA GAG CAG GAA T**T**T GTT CAA ACT GTG AAG TC-3'
Reverse: 5'-CTT CTC GTC CTT A**A**A CAA GTT TGA CAC TTC AG-3'

2.3.2.1 Mutagenesis PCR

QuikChange™ Site directed Mutagenesis kit (Stratagene) was used to create the point mutation in annexin 1 (within the pGFP-N1 vector). The experimental reaction and a control mutagenesis reaction were prepared according to manufacturers instructions. Mutagenesis reactions were carried out in an Eppendorf Master Cycler Gradient PCR Machine as follows: 95°C 30 seconds; {95°C 30 seconds, 55°C 1 minute, 68°C 11 minutes} x12; 4°C 2 minutes. Dpn1 (10U) was then added to each mutagenesis reaction and incubated at 37°C for at least 1 hour to degrade parental supercoiled dsDNA.

2.3.2.2 Cell Transformations

Transformations were performed using *E.coli* XL1-Blue supercompetent cells and 2µl of Dpn1 digested DNA according to manufacturers instructions. In addition a transformation efficiency control was performed using 1µl pUC18 (0.1ng). Colonies were picked from sample mutagenesis plates and incubated in LB broth, containing kanamycin, overnight at 37°C. The following day plasmid DNA was purified using Qiagen spin miniprep kit (as described in 2.3.1.3). Each DNA sample was sequenced (see 2.3.3) to check for presence of the desired mutation.

2.3.3 Sequencing

To sequence annexin 1-GFP, primers were designed for the multiple cloning site of pGFP-N1 (Primer 1) and for the middle of annexin 1 (Primer 2). Primer 1 was used to sequence Y21F annexin 1-GFP to check for the presence of the desired mutation. For the sequence of primers and results of sequencing see Appendix 1 (Fig. S.3 & S.4). Sequencing reactions were carried out in 10µl volume according to the Big Dye® Terminator v3.1 Cycle Sequencing Kit (Applied Biosystems). DNA was purified by adding 2.5µl 125mM EDTA, 25µl 100% ethanol and transferring to 1.5ml microcentrifuge tubes for 15 minutes room temperature. Tubes were centrifuged at 13000rpm in an Eppendorf Centrifuge 5415D using a F-45-24-11 rotor at 4°C for 15 minutes, before carefully discarding supernatants and washing DNA pellets with 70% ethanol. After a repeat spin pellets were resuspended in 12µl HiDi formamide and loaded onto the ABI sequencing machine.

2.4 Transfections of cell lines

2.4.1 Lipofectamine™ Ttransfection of HEp2 cells

Annexin 1-GFP plasmid DNA was transiently transfected into HEp2 cells using Lipofectamine™, according to the manufacturer's instructions, and expression of the construct confirmed using the BioRad confocal to visualise annexin 1-GFP.

2.4.2 Calcium Phosphate Transfection to create a stable cell line

HEp2 cells were seeded into wells of a 6-well plate to reach ~30% confluency after 24 hours. The following day cells were transfected with annexin 1-GFP plasmid DNA as follows: DNA (20μg) was added to 0.5ml 2x HEPES buffer (0.5M HEPES pH7.1, 3M NaCl, 1M $NaPO_4$, freshly made and filter sterilised) and vortexed continuously whilst adding 0.5ml $CaCl_2$ dropwise to precipitate DNA. The precipitate was allowed to form at room temperature for 30 minutes before vortexing and adding 1ml to cells. Cells were incubated at 37°C for 10 minutes before a further 2.5ml medium was added to each well and plates incubated overnight under standard conditions. The following day medium was removed and 1-2ml 12.5% glycerol (filter sterilised, in medium containing 10mM Hepes pH7.4) added for 2 minutes at room temperature. Glycerol was removed, cells washed twice in PBS and full medium added. Cells were incubated at 37°C for 48 hours. At this point normal medium was removed and full medium containing 0.5mg/ml G418 was added to select for transfected cells. Cells were left for approximately 10-14 days and medium changed every 3-5 days to removed dead cells. Single transfected cells grew into colonies, which were picked using a small amount of trypsin to detach cells within an area defined using sterile cloning rings. Cells were transferred into wells of a new 24 well plate. Expression of annexin 1-GFP was determined using fluorescence microscopy and a cell line derived from a single clone was chosen for its uniform low expression of the plasmid.

2.4.3 Nucleofection of JACRO cells

JACRO wild type and annexin 1 -/- cells (5x 10^5) were transfected with 2.5μg hEGFR, wild type or Y21F annexin 1-GFP DNA using Normal Human Dermal Fibroblast™ kit and programme U-23 according to manufacturers instructions.

2.5 RNAi

2.5.1 Annexin 2 RNAi

For annexin 2 siRNA, the first oligonucleotide was ordered using the published sequence (Mayran *et al.*, 2003). The second oligonucleotide was designed against

human annexin 2 using the Qiagen protocol. For experiments, the two oligonucleotides were used together. Full human annexin 2 sequence is shown in Appendix 1 (Fig. S.6):

RNAi1 – start 131 - 5'-AAGTGCATATGGGTCTGTCAA-3'
RNAi2 – start 820 - 5'-AACCTGGTTCAGTGCATTCAG-3'

A431, HeLa, HEp2 or JACRO wild type cells (4x 10^4) were seeded in 12 well plates and incubated overnight. The following day medium was replaced with 500µl antibiotic free medium and RNAi was prepared as follows (per well). Each RNAi oligonucleotide (20µM) was added to 50µl OptiMEM in tube 1. In tube 2, 3µl Oligofectamine™ was added to 12µl OptiMEM. Tubes were incubated at room temperature for 7-10 minutes before the contents of tubes 1 and 2 were mixed and incubated for 25 minutes at room temperature. OptiMEM (32µl) was added to the mixture and 100µl of the transfection mixture was added to cells. Cells were incubated with RNAi for 3 days, or split 1:3 on day 3 and allowed to settle for 1 hour before re-transfecting with RNAi for a further 3 days. Cells were collected for western blot analysis by scraping 2 wells into 100µl 2x reducing sample buffer. Cell lysates were blotted for tubulin as a loading control and annexin 2 (see 2.6).

2.5.2 Annexin 1 RNAi

The first 4 oligonucleotides were designed against human annexin 1 using the Dharmacon protocol. The final oligonucleotide was designed against human and mouse annexin 1 using the new Qiagen protocol. All oligonucleotides were used to transfect cell lines, as described in 2.4.1. Full annexin 1 sequence including oligonucleotide sequences is shown in Appendix 1 (Fig. S.5).

LBA1A – start 201 – 5'-AATCCATCCTGGATGTCGCT-3'
LBA1B – start 291 – 5'-AACAATGCACAGCGTCAACAG-3' - Control
LBA1C – start 247 – 5'-AAGGTGTGGATGAAGCAACCA-3'
LBA1D – start 1048 – 5'-AAGCCATCCTGGATGAAACCA-3'
LBA1X – start 240 – 5'-ATGGTTAAAGGTGTGGATGAA-3'

LBA1A and LBA1X were also used to transfect HeLa and A431 cells using nucleofection (2.3.3). Cells ($1x10^6$) were nucleofected with 5µl of each oligonucleotide using Kit V and programme T-28, as per manufacturers instructions, and left to settle for 24 hours in antibiotic free medium. After 24 hours, cells were trypsinised, resuspended in 100µl solution V and re-nucleofected. Cells were plated (1:10) onto wells of 24-well plate or onto coverslips and left for 48 hours before collection for western blotting (section 2.6) or experimentation.

2.5.3 Annexin 1 and 2 RNAi

HeLa cells were treated with both annexin 2 oligonucleotides and annexin 1 oligonucleotides LBA1A and LBA1X, using nucleofection, as described in 2.5.2.

2.6 Western blotting

2.6.1 Preparation of Samples

To investigate the effects of EGF stimulation, cells were serum starved for 1 hour before stimulating with 100ng/ml EGF for the appropriate length of time. In the absence of EGF-stimulation, cells were washed with PBS before scraping into 2x RSB. DNA was sheared using a 0.6 gauge needle before boiling samples at 95°C for 5 minutes and briefly centrifuging to remove any debris.

2.6.2 SDS Polyacrylamide Gel Electrophoresis (PAGE)

Typically 10µl of each sample or 8µl of rainbow molecular weight markers (Amersham) was loaded in each well. Samples were resolved by SDS-PAGE using a 10% polyacrylamide gel run at 0.25A (per mini-gel) for 50 minutes.

2.6.3 Western blotting

After SDS-PAGE, proteins were transferred to Protran nitrocellulose transfer membrane (Schleicher and Schuell) using the BioRad Transfer unit at 100V for 50

minutes. Membranes were washed in PBS and then blocked in 5% (w/v) dried powdered skimmed milk, or 5% BSA for phosphotyrosine antibodies, for 30 minutes at room temperature. After blocking, membranes were incubated with primary antibody for at least 1 hour at room temperature or overnight at 4°C. Membranes were washed in PBS/Tween before incubation with secondary antibody-HRP conjugate for 45 minutes at room temperature. Membranes were washed thoroughly in PBS/Tween before 1 minute incubation with Supersignal West Pico Chemiluminescent substrate (Pierce). Antibody binding was visualised using Fujifilm intelligent dark box II and Las-1000 Pro software (version 2.3).

2.6.4 Semi-Quantitative Analysis of Western Blots

To compare the effect of RNAi treatment on protein levels, western blot images were analysed using AIDA 2D densitometry software. For each experiment tubulin was used as a loading control. The intensity of tubulin bands and the appropriate protein band were measured and the background signal subtracted. Results were each protein assayed were normalised against that for tubulin. The difference in intensity of the desired band was then compared between treated and control cells and recorded as a percentage of the control. The mean ± SEM were calculated from at least 5 independent experiments.

2.7 Reverse Transcriptase PCR of annexin 2

Total RNA was isolated from $1x10^7$ wild type or annexin 2 knockout DT40 cells using RNeasy Mini Kit protocol (Qiagen) and used to synthesise cDNA using ProStar First Strand RT-PCR kit (Stratagene). At the same time a control reaction (supplied with the kit) was performed. For both control and experimental cDNA synthesis random primers were used. Control cDNA was used in the control PCR amplification reaction to produce a 1.3Kb PCR product. Primers were designed to run from exon 1 to exon 4 across introns to produce a 239bp product (full chicken annexin 2 sequence is shown in Appendix 1, Fig. S.7).

Forward: 5'- TTAAGGCTTACTCAAACTTTGATGCTGACCG-3'
Reverse: 5'-TGGTGTCTTCAGCAAGCCCAA-3'

Reactions were performed according to manufacturers instructions. Experimental and control PCR reactions were run on 1% agarose gel containing ethidium bromide to visualise DNA. Experimental samples were run alongside PCR markers (New England Biolabs) and control samples with 1Kb markers.

2.8 Iodinated EGF and Tf experiments

2.8.1 EGF recycling & degradation in JACRO cells

JACRO cells were seeded on 3cm diameter dishes overnight and serum starved for 1 hour. To measure EGF degradation, cells were incubated with 6ng/ml ^{125}I-EGF for 10 minutes at 37°C in serum free medium containing 0.5% BSA (binding medium). After incubation cells were placed on ice and washed 5 times using pre-chilled binding medium to removed excess ^{125}I-EGF. Surface bound EGF was stripped during 2x 3 minute ice-cold acid washes (0.1M glycine, 0.9% NaCl pH3.0). The acid washes were collected into labelled screw-capped 1.5ml tubes. Cells were washed twice with cold binding medium before adding 250µl warm medium and returning to 37°C. For EGF recycling and degradation experiments cells were chased (with warm binding medium) for 10, 35, 50, 80 and 110 minutes. At each time point, medium was collected into a labelled tube and replaced with fresh warm medium. After the final time point cells were lysed using 250µl ice-cold 1% Tx100 for 10 minutes at 4°C. Cell lysates were collected into tubes. Counts per minute (cpm) were measured for each sample using a Packard Cobra II Gamma counter, counting for 2 minutes. After counting, medium samples were replaced on ice and TCA added, to a final concentration of 20%, for 1 hour. Tubes were centrifuged for 10 minutes at 14000rpm in an Eppendorf Centrifuge 5415D, using a F-45-24-11 rotor, at 4°C. Supernatants were collected into fresh tubes and cpm counted.

2.8.2 EGF recycling & degradation in annexin 2 RNAi treated HeLa cells

HeLa cells were seeded at $1.5x10^4$ cells per well of a 4 well plate overnight. The following day 2 wells were treated with annexin 2 RNAi and the other 2 with

control RNAi. After 3 days of RNAi treatment cells were serum starved for 1 hour. ^{125}I-EGF (1ng/ml) was added to each well in 250µl binding medium. The experiments were performed as described above for JACRO cells (section 2.8.1).

2.8.3 Tf Recycling

JACRO cells were plated, as described in 2.7.1, and preloaded with 0.3µg/ml of ^{125}I-Tf for 1 hour at 37°C before washing off excess ligand with cold medium. Surface bound Tf was removed, by incubating cells with ice-cold acid wash for 2x 3 minutes, collected and cpm measured. Cells were incubated with warm binding medium for 10, 25, 30, 60 and 120 minutes, medium was collected and cpm measured. Cell lysates were collected to count Tf remaining in cells.

2.8.4 Calculating percentage of ^{125}I ligand degraded or recycled

To calculate the total (in cpm) amount of Tf or EGF internalised, the cpm from the cell lysates sample was added to the combined cpm total of the media samples.

Total cpm internalised = all media samples + cell lysates

To determine the percentage internalised, the total cpm internalised was divided by the combined total of cell lysates plus media samples plus both acid washes.

$$\% \text{ internalised} = \frac{\text{Total cpm internalised}}{\text{Total cpm + acid washes}} \times 100$$

To calculate the percentage Tf recycled, the medium sample from that time point (or the cumulative media samples up to that time point) was divided by the total cpm internalised.

$$\% \text{ Tf recycled} = \frac{\text{cpm in medium sample}}{\text{total cpm internalised}} \times 100$$

At each time point recycled EGF is found in the TCA precipitate, while the TCA soluble supernatant contains the iodotyrosine released from degraded EGF. As the pellet is not counted with the same efficiency as liquid samples, the cpm in the supernatant was subtracted from the cpm in the pre-TCA medium sample. This

figure gave the cpm recycled at that time point. Therefore, to calculate the percentage EGF recycled at a given time point:

$$\% \text{ EGF recycled} = \frac{\text{cpm medium} - \text{cpm TCA supernatant}}{\text{total cpm internalised}} \times 100$$

The cpm from degraded EGF are present in the TCA supernatant so to calculate the percentage EGF degraded at a given time point, this figure was divided by the total cpm internalised.

$$\% \text{ EGF degraded} = \frac{\text{cpm TCA supernatant}}{\text{total cpm internalised}} \times 100$$

Finally, to calculate the total percentage of Tf or EGF recycled, or EGF degraded:

$$\text{Total \% recycled} = \frac{\text{cpm all medium} - \text{cpm all TCA supernatants}}{\text{Total cpm internalised}} \times 100$$

$$\text{Total \% degraded} = \frac{\text{all TCA supernatants}}{\text{Total cpm internalised}} \times 100$$

2.9 Live cell imaging

2.9.1 Phase and Fluorescent Imaging

JACRO cells were plated on 3cm Mattek™ dishes, allowed to settle and serum starved overnight. Cells were visualised using a Zeiss Axiovert 100M microscope (x20 objective). To visualise cells and fluorescent ligands, cells were washed thoroughly to remove DMEM and medium replaced with phenol red free L-15, as phenol red affects visibility of green fluorescence.

2.9.2 Cell Area Quantitation

Phase images of unstimulated or EGF-stimulated JACRO cells were taken using a Zeiss Axiovert 100M microscope and Improvision OpenLabs software. MetaMorph 4.6r9 was used to measure cell area and cell perimeter. Each cell was outlined and, once calibrated for the appropriate microscope and objective,

MetaMorph Integrated Photometric analysis used to calculate the area of each cell and its perimeter.

2.9.3 Cell Motility assay

JACRO wild type, annexin 1 -/- or transfected annexin 1 -/- cells were serum starved overnight. The following day cells were washed; for cells transfected with annexin 1-GFP constructs serum free medium was replaced with phenol red free L-15 medium. Unstimulated or EGF-stimulated cells were imaged every 5 minutes for 90 minutes using a Zeiss Axiovert 100M microscope (x20 objective) and Improvision OpenLabs software. The object tracking mode (MetaMorph v4.6r9) was used taking the nucleus as the centre point of the cell. Any movement of the nucleus was recorded and the total distance per cell (μm) recorded after 90 minutes. The average velocity (μm per second) was also calculated and recorded. For each transfection or treatment the movements of at least 20 cells were recorded.

2.10 Immunofluorescence

Cells were plated out in full medium onto 13mm glass coverslips overnight to reach approximately 70% confluency. The following day cells were serum starved for 1 hour before incubation with appropriate ligand. Cells were washed using PBS before fixing in 1ml 3% paraformaldehyde (in serum free medium) for 20 minutes. Coverslips were washed with PBS and free aldehyde groups quenched using 15mM glycine (in PBS) for 2x 10 minutes before blocking and permeabilising using PBS/1% BSA/0.1% saponin for 30 minutes. All antibodies were diluted in PBS/1% BSA/0.01% saponin. For antibody incubations, coverslips were turned (cells facing down) onto 40μl drops of diluted antibody and incubated for 1 hour (primary) or 45 minutes (secondary) at room temperature in a humidified chamber. Between antibodies and after secondary antibody incubation coverslips were washed 4x PBS/saponin and finally 2x PBS. Coverslips were mounted onto glass slides using anti-fade mounting medium (90% glycerol, 3% N-propyl-galate in PBS) and nail varnish before storing at 4°C.

Cells were visualised using a Radiance 2000 AGR-3 (Q) confocal microscope (BioRad) attached to an inverted microscope (model Axiovert S100TV; Carl Zeiss MicroImaging Inc.) and LaserSharp (version 5) software. Images were analysed using LaserPix (version 5) or Metamorph Image Analysis package 4.6r9 (Universal Imaging).

2.11 Transmission Electron Microscopy

2.11.1 Preparation of EM markers

2.11.1.1 Anti-human EGFR (108)-10nm gold

The pH of 10nm gold was adjusted to 9.3 using 0.2M K_2CO_3. 108 (anti-human EGFR antibody) was passed through PD10 column pre-equilibriated with 2mM borax. To determine the minimum amount of antibody necessary to stabilise the gold, increasing amounts of antibody were diluted in borax to a final volume of 12µl in 1.5ml microcentrifuge tubes and 250µl gold was added to each tube. Tubes were vortexed and incubated at room temperature for 5 minutes. NaCl (50µl of 20% solution) was added to aggregate any gold that had not been stabilised. All tubes were vortexed and centrifuged at 14000rpm, in an Eppendorf 5415D centrifuge, for 1 minute. 150µl supernatant was removed into wells of 96 well plate and the most pink fraction determined by eye. This corresponds to the lowest concentration of antibody that will stabilise the gold and was used to calculate the amount of antibody necessary to make a larger quantity of anti-EGFR-gold. The appropriate amount of gold was placed into a sterile tube and stirred vigorously whilst the minimum amount of antibody was added. After 5 minutes of stirring the antibody-gold was stabilised further using 10% BSA (in H_2O, pH9.0 filtered 0.45µm filter) to a final concentration of 1% BSA. The gold conjugate was centrifuged at 45000 rpm in a Sorval RC M150 GX centrifuge (using a S80At3-0051 rotor) for 10 minutes at 4°C to remove any free antibody and the fluid pellet resuspended in an appropriate volume (1/10) of 20mM Tris, 1% BSA pH 8.3, 0.02% azide. When using anti-hEGFR-gold, an appropriate volume was taken, diluted in serum free medium containing 0.5% BSA and centrifuged at 45000rpm,

4°C for 15 minutes to remove azide. The fluid pellet was resuspended in serum free medium containing BSA before incubation with cells at 37°C.

2.11.1.2 BSA-5nm gold

BSA-gold was prepared in the same way as described above for anti-EGFR-gold with the following changes. 1mg/ml BSA was dissolved in 2mM borax. The pH of 5nm gold was adjusted to 5.5, the pI of BSA. BSA-gold was pelleted by centrifuging at 65000 rpm, 4°C, 15 minutes and resuspended in serum free medium containing BSA before incubation with cells at 37°C.

2.11.1.3 Chick B-cell receptor-10nm gold

Anti-chicken IgMκ (Southern Biotechnology Associates Inc. clone M-4- 0.5mg/ml in borate buffered saline pH 8) was passed through PD10 column pre-equilibriated with 2mM borax. Fractions (0.5ml) were collected and the Pierce Protein Detection Kit was used to determine which fraction(s) contained the antibody. Antibody-gold conjugation was performed as described for anti-hEGFR in section 2.11.1.1.

2.11.1.4 EGF-HRP

Biotinylated EGF (0.328μg) was mixed with Streptavidin-HRP (5μg) in 100μl PBS, to achieve a 1:1 molar ratio, and incubated rotating at 4°C overnight. To test EGF-HRP, cells were cultured in a 24-well plate overnight to reach ~80% confluency. Cells were serum starved for 1 hour and incubated with increasing dilutions of EGF-HRP for 30 minutes at 37°C. For each concentration a competition reaction was set up, where cells were also incubated with 100x excess of non-labelled human EGF. Cells were washed thoroughly after incubation and solubilised in 200μl 0.5% Tx100 (in PBS containing protease inhibitor cocktail) for 10 minutes at 4°C. Solubilised cells were collected and centrifuged at 13000rpm in an Eppendorf Centrifuge 5415D (using a F-45-24-11 rotor) at 4°C for 5 minutes to pellet nuclei. The supernatant (35μl) was added to 65μl OPD reaction mix (1mg/ml OPD in 10ml citrate buffer pH 4.5 and 7.7μl H_2O_2, added immediately prior to reaction) and colour change allowed to develop. Reactions were stopped using

100µl 1M H_2SO_4. Absorbance at λ=450nm was read using a Safire Plate Reader. In the competition reaction, excess EGF should out-compete EGF-HRP and prevent binding. In the non-competition reaction EGF-HRP binding, as measured by increased amounts of EGF-HRP within cells and increased absorbance reading, should reach a plateau as >90% of receptors become saturated. The lowest concentration, where binding plateaued and could be prevented by addition of excess non-labelled EGF, was chosen as the concentration of EGF-HRP to use for experiments.

2.11.1.5 Tf-HRP

SPDP (N-succinimidyl 3-(2-pyridyldithio)propionate), 30mM, was added to a 2mg solution of iron-saturated human-Tf, in 1ml 0.1M phosphate buffer. In a separate tube SPDP was added to 5mg HRP (in 1ml 0.1M phosphate buffer and 0.15M NaCl). Both tubes were rotated at room temperature for 30 minutes. To remove the unbound SPDP, PD10 columns were pre-equilibriated using 0.1M phosphate buffer and 0.15M NaCl for Tf, or 0.1M sodium acetate pH 4.5 for HRP. Tf-SPDP or HRP-SPDP mixtures were passed through the appropriate column and 0.5ml fractions collected. HRP was visible as coloured fractions, which were collected and pooled. For Tf, fractions were analysed using the Pierce Protein Detection Kit, according to manufacturers instructions, and the absorbance read at λ=450nm to identify the Tf containing fraction. Meanwhile, DTT was added to the HRP mixture (final concentration 8 mg/ml) before rotating at room temperature for 20 minutes. To remove free HRP, the mixture was passed through a PD10 column pre-equilibriated with 0.1M phosphate buffer. HRP-containing fractions were collected. Tf-SPDP fractions and reduced HRP were mixed and incubated rotating overnight at 4°C.

Tf-HRP was tested as described above for EGF-HRP (see 2.11.1.4) and used at the chosen concentration, diluted in serum free medium.

2.11.2 Embedding of HeLa and JACRO cells

Cells were seeded onto sterile cell culture coated Thermanox coverslips. On the day of treatment cells were serum starved for 1 hour before incubation with HRP, anti-hEGFR-gold, Tf-HRP or EGF-HRP in serum free medium containing 0.5% BSA, to limit non-specific binding. After incubation, cells were washed thoroughly with PBS before fixation with 2% PFA/2% glutaraldehyde (in 0.1M cacodylate) for 30 minutes at room temperature. For cells incubated with HRP, or HRP conjugates, a DAB (diaminobenzidine) reaction (1% DAB in 10ml 0.1M Tris + 7.7µl H_2O_2) was performed, after fixation, for 30 minutes at room temperature in the dark to cross-link HRP molecules. Cells were then incubated with 1% osmium/1.5% potassium ferricyanide in 0.1M cacodylate for 1 hour at 4°C in the dark. To increase membrane resolution cells were incubated with 1% tannic acid (freshly made in 0.05M cacodylate) for 40 minutes at room temperature. Cells were washed thoroughly with cacodylate between each step. Cells were dehydrated using 70%, 90% and, finally 2x 10 minute washes in 100% ethanol with special care taken to prevent coverslips from drying out. After the second 100% ethanol wash, coverslips were placed into foil dishes containing 1:1 mixture of propylene oxide (PO) and EPON resin for 1 hour at room temperature. After an hour PO/EPON was removed and replaced with EPON for a further hour. EPON was changed once more before placing coverslips cell side down onto EPON stubs and baking overnight at 60°C. Coverslips were removed by heating, leaving the layer of cells on face of the stub.

2.11.3 Embedding of DT40s

DT40 cells were grown in suspension to a concentration of 2 x10^6 cells/ml. Cells were incubated with 1mg/ml HRP for 2 or 4 hours at 42°C. For incubation with BSA-5nm gold, 4ml cells were resuspended in 1.5ml medium and 1.5ml BSA-gold diluted 1:5 for 4 hours followed by a 20 hour chase in full medium at 42°C. For washes, cells were centrifuged for 3 minutes at 1000rpm in an Eppendorf Centrifuge 5415D (using a F-45-24-11 rotor). Cells were washed three times before fixation in 2% PFA/2% glutaraldehyde (in 0.1M cacodylate) for 30 minutes.

After fixation cells were washed at a higher speed (4000rpm). After washing cells were incubated with DAB (as described in section 2.10.2). DAB reaction mixture was washed off cells during three washes in 0.1M cacodylate and cells were incubated with 1% osmium/1.5% potassium ferricyanide for 1 hour at 4°C. Cells were washed three times before dehydration using 70%, 90% and finally two 10 minutes incubations in 100% ethanol. After the 90% ethanol step, cells were transferred from 1.5ml screw capped microcentrifuge tubes to 0.4ml thin centrifuge tubes. Cells were pelleted by centrifuging horizontally at 10000rpm in a Biofuge Primo centrifuge (Heraeus Instruments) using a HTA 13.8 rotor for 5 minutes. Ethanol was removed and 1:1 mixture of PO/EPON added for 1 hour at room temperature. PO/EPON was removed and excess PO allowed to evaporate for 10 minutes. EPON was added for another hour, removed and fresh EPON added for a further hour. Tubes were baked overnight at 60°C. The following day pellets were cut out of tubes, re-embedded in EPON coffins and baked overnight at 60°C.

2.11.4 Ultrathin sectioning and staining

Samples were sectioned using a Leica microtome and a Diatome Ultra diamond knife (size 4). Ultrathin sections (60-70nm) were stained using Reynold's lead citrate for 5 minutes at room temperature. Sections were then observed using a JEOL 1010 transmission electron microscope.

2.11.5 Morphometric Analysis of MVBs

To calculate the number of MVBs per unit cytoplasm (μm^2), at least 25 photos were taken of cells, chosen at random at a low magnification. The area of cytoplasm per photo was measured using LaserPix and the number, area and internal vesicle frequency of MVBs per photo was also recorded. MVBs were defined as vacuoles $\geq$ 200nm in diameter and containing $\geq$ 1 internal vesicle. For each experiment the total number of MVBs was divided by the total area cytoplasm to calculate the number of MVBs per μm^2. For each cell line or each treatment at least three independent experiments were performed.

2.12 Immuno Electron Microscopy

Cells were grown in 92mm diameter tissue culture treated dishes overnight and serum starved for 1 hour the following day. After EGF stimulation, cells were fixed in 4% PFA/0.1% glutaraldehyde for 2 hours at room temperature and then 0.5% PFA for at least an hour at room temperature or overnight at 4°C. Free aldehyde groups were quenched by 5 washes using 20mM glycine (in 0.1M phosphate buffer). Cells were scraped into 500µl 1% gelatin and centrifuged horizontally at 1500rpm in a Biofuge Primo centrifuge (Heraeus Instruments) using a HTA 13.8 rotor for 1 minute. Cell pellet was resuspended in 10% gelatin and immediately centrifuged horizontally at 5000rpm for 1 minute. Most of the gelatin was removed and the tube was placed on ice for 15 minutes. The pellet was then cut out of the tube, placed in a fresh tube containing 2.3M sucrose and rotated vertically for 15 minutes at 4°C. Cell pellets were then cut into 4-6 blocks, depending on size of pellet, and incubated in sucrose for a further 2 hours at 4°C. Pellet blocks were placed onto pins (scuffed and washed in acetone) and immediately stored in liquid nitrogen.

2.12.1 Immunolabelling of cryosections

Ultra thin cryosections (60-70nm) were cut using a Leica cryo ultra microtome and Diatome Cryo P diamond knife. Sections were stored in 1:1 mixture of methylcellulose (MC) and 2.3M sucrose on Formvar/carbon coated hexagonal mesh grids at 4°C. For immunolabelling, grids were turned over onto 100µl 2% gelatin (in PBS) for 20 minutes at room temperature, followed by 2x 5 minutes 15mM glycine. Sections were blocked using 1% BSA (from 10% stock centrifuged for 1 hour at 45000rpm and filtered)/0.1% BSA-c before primary antibody incubation for 1 hour. Sections were washed in 0.1% BSA/0.01% BSA-c before incubation with a bridging antibody (30 minutes at room temperature). After a second round of washing sections were incubated with protein A gold (45 minutes at room temperature). For double labelling sections were washed thoroughly after gold incubation and fixed in 1% glutaraldehyde for 10 minutes. Sections were washed in PBS and free aldehyde groups quenched using 5x 2 minutes on 20mM glycine.

Antibody incubations were carried out in the same way as for the first antibody. After the second fixation in glutaraldehyde sections were washed 8x in double distilled H_2O before being placed onto a drop of 1:4 uranyl acetate (UA)/MC on ice. Grids were moved through 3 drops of UA/MC before 5 minute incubation on the final drop in the dark. Grids were picked up using small wire loops, excess UA/MC drained onto filter paper and allowed to dry before storage.

2.13 Scanning electron microscopy

JACRO cells were seeded onto glass coverslips overnight. The following day cells were serum starved for 1 hour. Cells were fixed in 1% PFA/2% glutaraldehyde in 0.08M cacodylate for 1 hour at room temperature. After fixation cells were treated with 1% osmium in 0.08M cacodylate for 1 hour at 4°C. Cells were dehydrated in 70%, 90% and finally 2x 10 minutes in 100% ethanol. Finally cells were washed for 3x 2 minute incubations in hexamethyl disilazane (HMDS) and allowed to dry by evaporation. After fixation, coverslips were mounted onto stubs using conductive silver paint and sputter coated with gold. Specimens were then examined in a JOEL 6100 scanning electron microscope.

2.14 Flow cytometry

Jacro wild type or annexin 1 -/- cells ($1x10^5$) were collected, resuspended in PBS/2mM EDTA (to avoid clumping) and placed on ice. Cell size was analysed by FACS (Flow assisted cell sorting) analysis using FAC SCAN (Becton Dickinson) and 25,000 events were recorded passing a λ=488nm argon ion laser. Forward and side scatter were measured and plotted on XY axis. The mean value for each axis was recorded for each cell type.

To compare the two cell lines at the same time, wild type cells were incubated with Vybrant™ CFDA SE (carboxy-fluorescein diacetate, succinimidyl ester) for 10 minutes at 37°C. Cells were washed and then left to rest for 30 minutes at room temperature. Cells were washed again and then mixed with annexin 1 -/- cells before analysis using FACS (see above).

Chapter 3 – Annexin 1 and MVB formation

3.1 Introduction

Annexins 1, 2 and 6 have been proposed to play roles in MVB formation and/or sorting within MVBs. The work described in this chapter focuses on annexin 1. Annexin 1 was proposed as a candidate protein in receptor sorting and/or MVB formation on the basis of its properties. Firstly, it interacts with both phospholipid membranes and the actin cytoskeleton (Glenney, Jr. *et al.*, 1987), and can promote vesicle fusion *in vitro* (Blackwood and Ernst, 1990). Secondly, annexin 1 is a major substrate for EGFR within MVBs, but not at the plasma membrane, providing a link between annexin 1 and endocytosed receptors (Futter *et al.*, 1993). Thirdly, EGFR-mediated phosphorylation of annexin 1 N-terminus is proposed to modulate the membrane binding activity of annexin 1.

Phosphorylation of annexin 1 is believed to have two major effects. The first is the increased requirement for Ca^{2+} in order to bind endosomal membranes (Haigler and Schlaepfer, 1990; Futter *et al.*, 1993). An element of controversy over the Ca^{2+} dependency of annexin 1 for membrane binding exists, but experiments in living cells showed that non-phosphorylated annexin 1 required intact Ca^{2+} binding sites in order to bind to early endosomal membranes (Rescher *et al.*, 2000). The discrepancy between these and earlier fractionation studies can be reconciled by the explanation that annexin 1 requires Ca^{2+} for association with endosomes, but once associated annexin 1 is not readily released by treatment with EDTA. The second effect of annexin 1 phosphorylation is an increased susceptibility to N-terminal proteolysis (Chuah and Pallen, 1989; Ando *et al.*, 1989). The N-terminal domain contains both the early endosomal localisation signal and the S100A11 binding site (Seemann *et al.*, 1996b; Rosengarth *et al.*, 2001). Loss of the N-terminus results in a relocalisation of annexin 1 from early endosomes to late endosomes (Seemann *et al.*, 1996b; Rescher *et al.*, 2000).

It has been proposed that annexin 1 and S100A11 could organise the limiting membrane for inward vesiculation. However, it is important to note that the heterotetrameric complex between annexin 1 and S100A11 has only been

demonstrated *in vitro* and it is not known whether it exists *in vivo*. Loss of the N-terminus, and thus loss of the S100A11 binding site, has been proposed to disrupt the heterotetrameric complex and allow internal vesicle fission (Gerke and Moss, 2002). Additionally, it was proposed that the release of annexin 1, through phosphorylation induced Ca^{2+} dependency, may be required for the release of vesicles into the lumen of the MVB (Gerke and Moss, 2002).

The aim of this work was to identify the exact nature of the role of annexin 1 in the formation of MVBs. Initially, an annexin 1 -/- cell line derived from an annexin 1 knockout mouse was used for this work (Hannon *et al.*, 2002; Croxtall *et al.*, 2003), but more recently it was possible to deplete levels of annexin 1 using RNAi technology. In cells lacking annexin 1, or with decreased levels of annexin 1, there was a reduction in numbers of internal vesicles in MVBs, although internal vesicles could still form. In the first set of experiments, EGF-stimulated cells were used so that an anti-EGFR antibody coupled to gold could be used as a marker of MVBs. Subsequently, by comparing EGF-stimulated cells with unstimulated cells, it was demonstrated that EGF stimulation increases inward vesiculation within MVBs. Basal inward vesiculation was unaffected by loss of annexin 1, but EGF stimulation of inward vesiculation is dependent on tyrosine phosphorylation of annexin 1.

3.2 Results

3.2.1 Loss of annexin 1 does not affect MVB formation

JACRO cells are lung fibroblast cell lines derived from either a wild type mouse or an annexin 1 -/- mouse (Hannon *et al.*, 2002; Croxtall *et al.*, 2003). To confirm that annexin 1 -/- cells did not express annexin 1, JACRO cell lysates were collected and blotted for tubulin, to ensure equal protein loading, and annexin 1 (Fig.3.1a). Annexin 1 protein was undetectable in annexin 1 -/- cells, compared with JACRO wild type cells. The same cell lysates were also blotted for other annexins to observe whether the loss of annexin 1 affected the expression of other annexin family members (Fig. 3.1a). Annexin 1 -/- cells show increased levels of annexins 2 and 6 compared with wild type cells, which is consistent with published data (Croxtall *et al.*, 2003). The expression of EGFR varies between cell lines and, as

one of the aims of this work was to investigate EGFR trafficking in the absence of annexin 1, the level of EGFR expression by JACRO cells was compared with that of HeLa cells, a human cell line known to express moderate levels of receptor (Fig. 3.1b). Both JACRO cell lines express much lower levels of EGFR than HeLa cells.

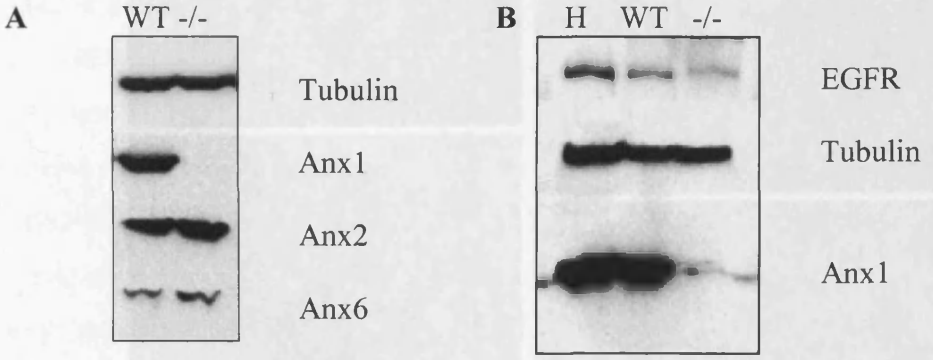

Figure 3.1. *Expression of annexins in JACRO cells.* JACRO wild type (WT) and annexin 1 -/- (-/-) cell lysates were blotted with antibodies against tubulin and annexin 1 to confirm -/- cells did not express annexin 1 (A). Lysates were also blotted for annexin 2 and annexin 6, both of which were upregulated in annexin 1 -/- cells. To compare levels of EGFR expression, HeLa (H) and JACRO cell lysates were blotted with anti-EGFR, anti-tubulin and anti-annexin 1 (B). JACRO cells expressed lower levels of EGFR compared to HeLa cells.

A major reason for investigating annexin 1 was to follow up a published study that identified annexin 1 as a substrate for EGFR within MVBs, and led to the proposal that annexin 1 participates in the formation of internal vesicles within MVBs (Futter *et al.*, 1993). To observe whether loss of annexin 1 had an effect on MVB formation, JACRO cells were serum starved, incubated with EGF conjugated to HRP (horseradish peroxidase) for 1 hour, and processed for transmission electron microscopy (TEM), as described in Materials & Methods section 2.11.2, including the DAB reaction to visualise HRP. EGF-HRP, visible as the dark DAB reaction product, was visible in many structures in both cell lines. The morphology of EGF-HRP containing MVBs was observed in wild type cells (Fig. 3.2) and revealed the presence of multiple EGF-HRP positive internal vesicles. EGF-HRP was also present in the lysosomes of wild type cells. In annexin 1 -/- cells, the morphology of MVBs was noticeably different, as they contained fewer internal vesicles than those seen in wild type cells. However, some of the small number of internal vesicles that formed still labelled with EGF-HRP, which was also found in the lysosomes of annexin 1 -/- cells.

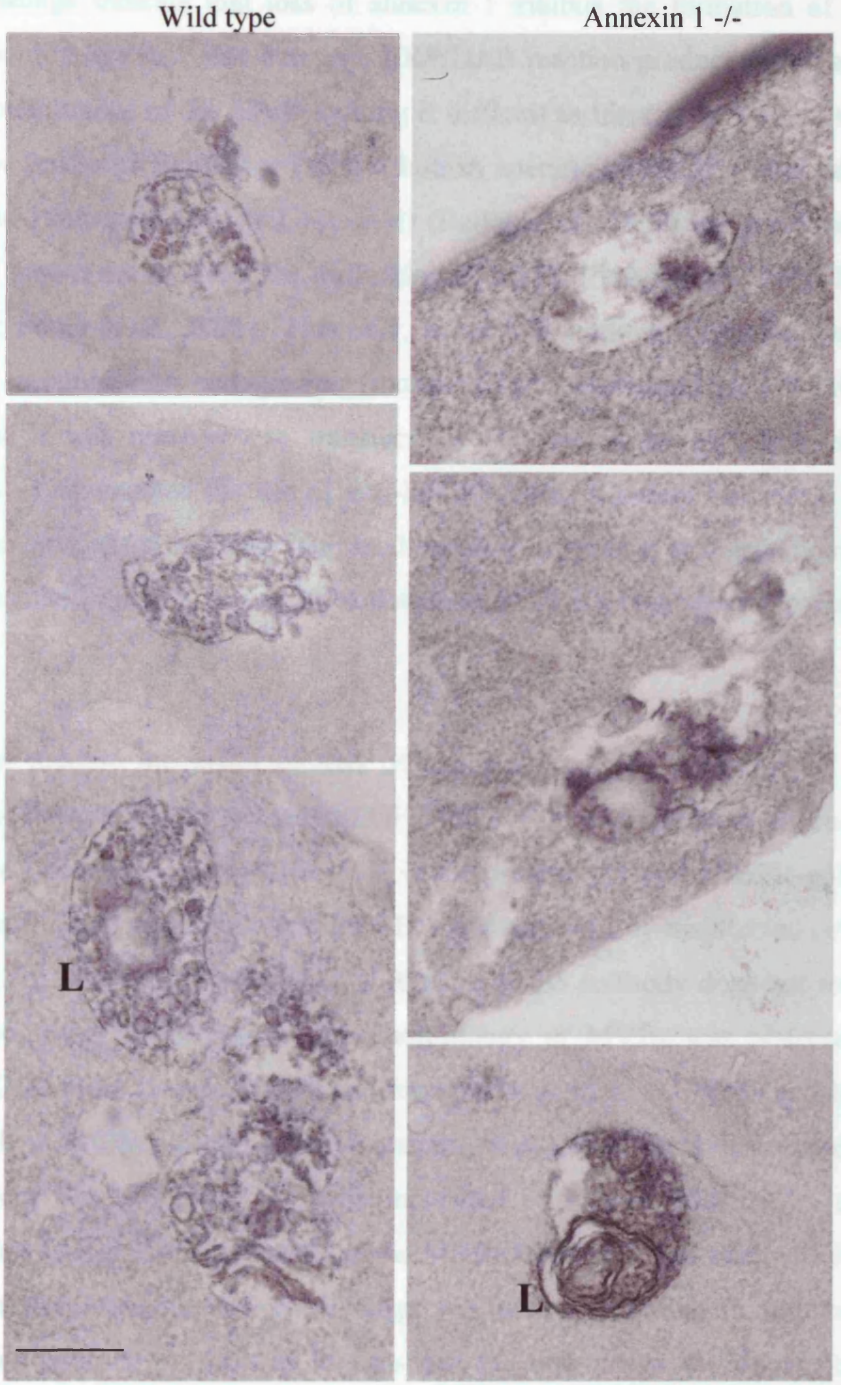

Figure 3.2. *Analysis of MVB morphology in JACRO cells.* JACRO cells were serum starved for 1 hour before stimulation with EGF-HRP for a further hour at 37°C. Cells were processed for TEM, including the DAB reaction. Ultrathin sections were cut and the morphology of MVBs analysed. Electron micrographs show typical EGF-HRP containing MVBs and lysosomes (L) from both cell lines. MVBs from annexin 1 -/- cells contained fewer internal vesicles, although EGF-HRP was present in lysosomes in both cell lines. Bar = 200nm.

These findings indicate that loss of annexin 1 inhibits the formation of internal vesicles within MVBs. However, the HRP/DAB reaction product can obscure the internal membranes of the MVB making it difficult to identify individual vesicles. To follow traffic of EGFR by TEM, a human specific anti-EGFR antibody (108) coupled to 10nm gold (anti-hEGFR-gold) (Bellot *et al.*, 1990) has previously been used and shown not to affect the trafficking of EGFR (Futter *et al.*, 1993; Futter *et al.*, 1996; Futter *et al.*, 2001). However, as the 108 antibody is human specific, it will not recognise the endogenous (mouse) EGFR expressed by JACRO cells. Therefore, it was necessary to transfect JACRO cell lines with human EGFR (hEGFR). This enabled the use of anti-hEGFR-gold, allowing individual internal vesicles to be counted, and also increased receptor expression to a level comparable with human cell lines, in which TEM detection of EGFR has been successful (Fig. 3.3A).

To further analyse the effect of loss of annexin 1 on the formation of MVBs, JACRO cells were transfected with hEGFR for 24 hours. Cells were serum starved for 1 hour before stimulation with EGF, in the presence of anti-hEGFR-gold, for a further hour. Cells were processed for TEM and successfully transfected cells were identified by the presence of anti-hEGFR-gold, as the antibody does not recognise endogenous (mouse) receptors. The morphology of MVBs was observed (Fig. 3.3B). MVBs were present in both cell lines but in annexin 1 -/- cells anti-hEGFR-gold positive MVBs contained fewer internal vesicles, as previously observed in MVBs from non-transfected -/- cells incubated with EGF-HRP. The electron micrographs in Fig. 3.3B represent typical MVBs from each cell line. The size of MVBs was not markedly different as larger MVBs were observed in both cell lines and images have been included to illustrate the size range of MVBs found in JACRO cells. There was less anti-hEGFR-gold in many of the annexin 1 -/- cells, and consequently less gold in MVBs, due to the fact that annexin 1 -/- cells were more difficult to transfect than wild type cells. However, in annexin 1 -/- cells that contain comparable amounts of hEGFR to wild type cells, anti-hEGFR-gold was visible in clusters at the perimeter membrane of MVBs containing few internal vesicles (Fig. 3.3B).

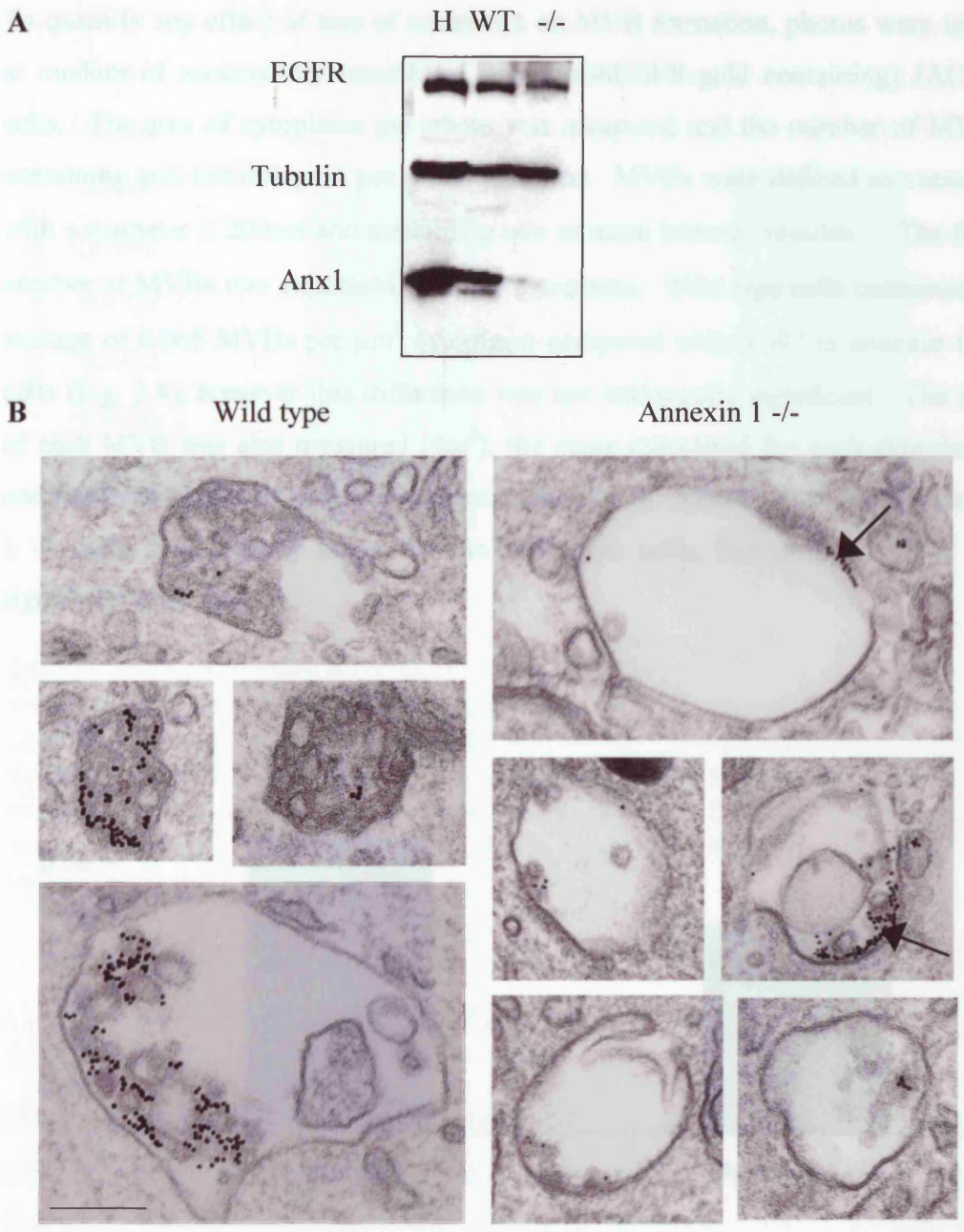

Fig. 3.3. *MVBs form in the absence of annexin 1 but contain fewer internal vesicles.* JACRO wild type (WT) and annexin 1 -/- (-/-) cells were transfected with hEGFR for 24 hours. HeLa (H) and JACRO cell lysates were blotted with antibodies against tubulin (to ensure equal loading), annexin 1 and EGFR, to detect receptor expression. Transfected JACRO cells expressed EGFR at a more comparable level to HeLa cells (A). Cells from these transfections were serum starved and stimulated with EGF (100ng/ml), in the presence of anti-hEGFR-gold, for 1 hour. Cells were processed for TEM and the morphology of anti-hEGFR-gold containing MVBs observed (B). MVBs in annexin 1 -/- cells contained fewer internal vesicles than MVBs from wild type cells. Arrows point to areas of clustered gold at the perimeter membrane. Bar = 200nm.

To quantify any effect of loss of annexin 1 on MVB formation, photos were taken at random of successfully transfected (i.e. anti-hEGFR-gold containing) JACRO cells. The area of cytoplasm per photo was measured and the number of MVBs containing anti-hEGFR-gold per photo recorded. MVBs were defined as vacuoles with a diameter ≥ 200nm and containing one or more internal vesicles. The final number of MVBs was expressed per μm^2 cytoplasm. Wild type cells contained an average of 0.065 MVBs per μm^2 cytoplasm compared with 0.047 in annexin 1 -/- cells (Fig. 3.4), however this difference was not statistically significant. The area of each MVB was also measured (nm^2), the mean calculated for each experiment and finally the mean of three experiments determined. Although MVBs in annexin 1 -/- cells were slightly larger than in wild type cells, this difference was not significant (Fig. 3.5).

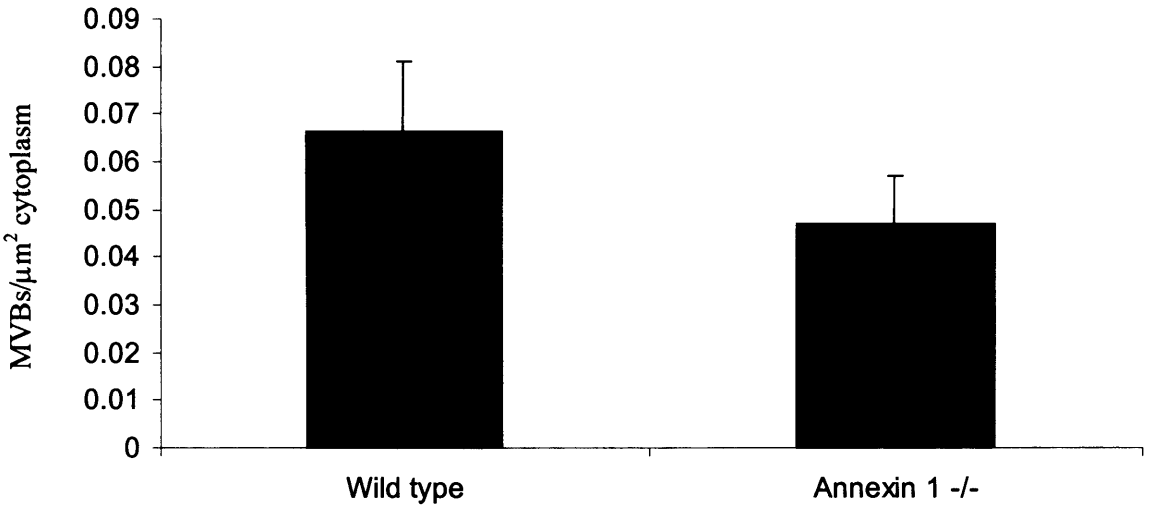

Figure 3.4. *Comparing numbers of MVBs in JACRO cells.* JACRO cells were transfected with hEGFR, serum starved and stimulated with EGF (100ng/ml), in the presence of anti-hEGFR-gold, for 1 hour. Cells were processed for TEM and at least 20 photos taken at random in anti-hEGFR-gold containing cells. The area of cytoplasm per photo was measured (nm^2). Number of MVBs per experiment were counted and expressed as number of MVB per μm^2 cytoplasm. Wild type cells contained slightly more MVBs than annexin 1 -/- cells but this difference was non-significant. Graph shows the mean ± SEM of three independent experiments.

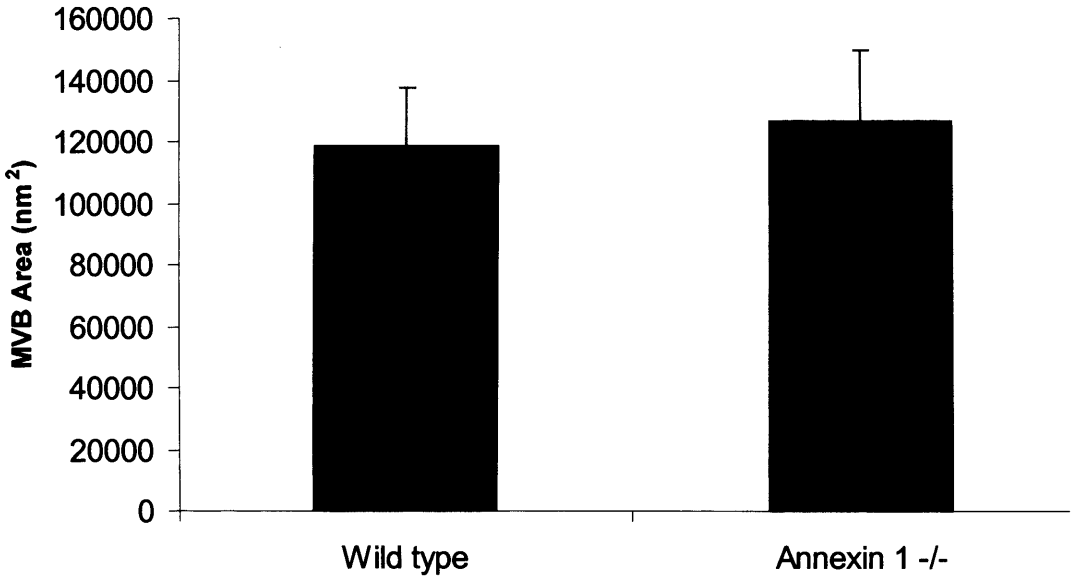

Figure 3.5. *Loss of annexin 1 does not alter the area of MVBs.* JACRO cells were transfected with hEGFR, serum starved and stimulated with EGF (100ng/ml), in the presence of anti-hEGFR-gold, for 1 hour. Cells were processed for TEM and at least 20 photos taken at random in anti-hEGFR-gold containing cells. The area of MVBs was measured (nm^2). The loss of annexin 1 did not alter the mean area of MVBs. Graph shows the mean ± SEM of three independent experiments.

3.2.2 Loss of annexin 1 inhibits internal vesicle formation within MVBs.

In the above experiments, the number of internal vesicles in each MVB was also counted and the mean number per MVB calculated for each experiment (Fig. 3.6A). The mean number of internal vesicles per MVB in annexin 1 -/- cells was significantly reduced compared to that of wild type (12.3 ± 0.9 compared to 21.6 ± 1.5), confirming the results of the MVB morphology described above (Fig. 3.2 & 3.3B). Although the mean number of internal vesicles per MVB was consistent between three independent experiments, within a single experiment there was a wide variation in the number of internal vesicles per MVB. Therefore, the effect of loss of annexin 1 on the distribution of number of internal vesicles per MVB was investigated, to observe whether loss of annexin 1 affected all MVBs or just those that contained higher numbers of internal vesicles.

MVBs from both cell lines were divided into categories based on different numbers of internal vesicles (Fig. 3.6B). As different numbers of MVBs were counted in each experiment, the number of MVBs in each group was expressed as a percentage of the total number of MVBs. The majority of MVBs from wild type cells contained 16 or more internal vesicles and the major effect of loss of annexin 1 was a shift in this trend towards the lower vesicle number categories. A significantly smaller percentage of MVBs from annexin 1 -/- cells contained more than 16 internal vesicles and instead the majority contained between 6 and 15 internal vesicles. These data show that loss of annexin 1 inhibits internal vesicle formation and results in fewer MVBs that contain high numbers of internal vesicles.

As JACRO wild type and annexin 1 -/- cells were derived from two different mice, it was possible that the differences observed in numbers of internal vesicles per MVB were due to factors other than the presence or absence of annexin 1. In order to provide further evidence that the reduction in numbers of internal vesicles per MVB was due to the loss of annexin 1, a method was devised to manipulate annexin 1 levels in cells so that the effects of annexin 1 depletion on internal vesicle formation could be examined in a single cell line.

The use of RNAi technology to deplete protein levels has increased rapidly since the beginning of these studies. Use of RNAi to knockdown annexin 1 has not been published; therefore it was necessary to optimise the design of RNAi oligonucleotides, and the methods and timing of transfections to obtain consistent annexin 1 depletion. Annexin 1 is an abundant protein and, in some cell types, the annexins constitute up to 1% of total cell protein. Unlike many other proteins, annexins are relatively stable proteins with long half lives, and work from the Moss group has shown that depletion of other members of the annexin family requires at least 3 days (Tomas *et al.*, 2004).

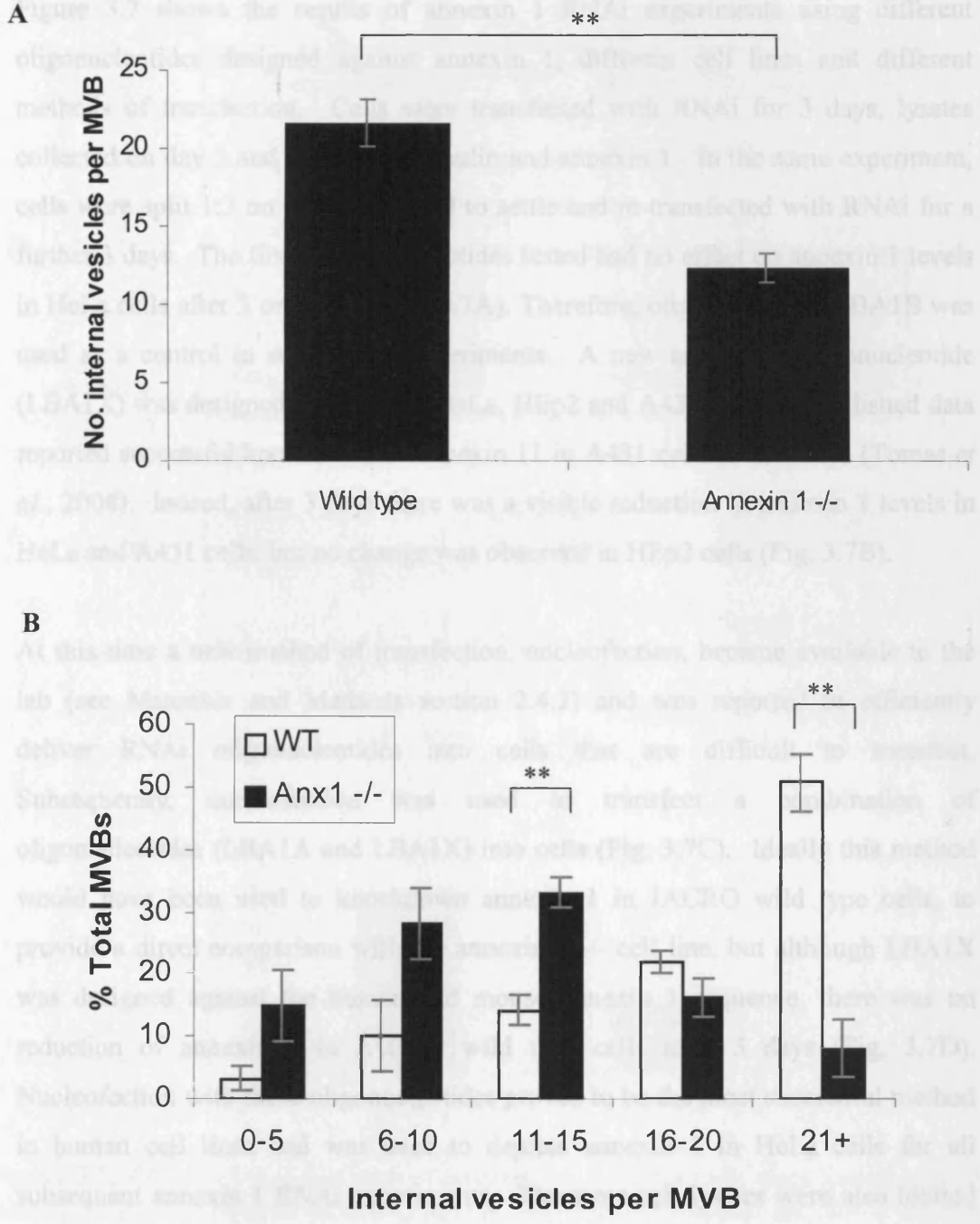

Figure 3.6. *Loss of annexin 1 reduces the number of internal vesicles per MVB.* JACRO cells were transfected with hEGFR, serum starved and stimulated with EGF (100ng/ml), in the presence of anti-hEGFR-gold, for 1 hour. Cells were processed for TEM and at least 20 photos taken at random in anti-hEGFR-gold containing cells. The mean number of internal vesicles per MVB was calculated (A). MVBs from these experiments were divided into groups according to number of internal vesicles, and expressed as a percentage of the total number of MVBs, to show the distribution of internal vesicles per MVB (B). MVBs from annexin 1 -/- cells contained fewer internal vesicles than those of wild type cells. Graph shows mean ± SEM of three independent experiments. ** $p<0.01$

Figure 3.7 shows the results of annexin 1 RNAi experiments using different oligonucleotides designed against annexin 1, different cell lines and different methods of transfection. Cells were transfected with RNAi for 3 days, lysates collected on day 3 and blotted for tubulin and annexin 1. In the same experiment, cells were split 1:3 on day 3, allowed to settle and re-transfected with RNAi for a further 3 days. The first 3 oligonucleotides tested had no effect on annexin 1 levels in HeLa cells after 3 or 6 days (Fig. 3.7A). Therefore, oligonucleotide LBA1B was used as a control in subsequent experiments. A new annexin 1 oligonucleotide (LBA1X) was designed and used in HeLa, HEp2 and A431 cells, as published data reported successful knockdown of annexin 11 in A431 cells after 3 days (Tomas *et al.*, 2004). Indeed, after 3 days there was a visible reduction in annexin 1 levels in HeLa and A431 cells, but no change was observed in HEp2 cells (Fig. 3.7B).

At this time a new method of transfection, nucleofection, became available to the lab (see Materials and Methods section 2.4.2) and was reported to efficiently deliver RNAi oligonucleotides into cells that are difficult to transfect. Subsequently, nucleofection was used to transfect a combination of oligonucleotides (LBA1A and LBA1X) into cells (Fig. 3.7C). Ideally this method would have been used to knockdown annexin 1 in JACRO wild type cells, to provide a direct comparison with the annexin 1 -/- cell line, but although LBA1X was designed against the human and mouse annexin 1 sequence, there was no reduction of annexin 1 in JACRO wild type cells after 3 days (Fig. 3.7D). Nucleofection with these oligonucleotides proved to be the most successful method in human cell lines and was used to deplete annexin 1 in HeLa cells for all subsequent annexin 1 RNAi experiments. The same cell lysates were also blotted with an anti-annexin 2 antibody, to determine whether annexin 1 depletion altered levels of annexin 2. In cells treated with annexin 1 RNAi, levels of annexin 2 were slightly increased (Fig. 3.7D). Semi-quantitative analysis of several independent experiments showed that annexin 1 RNAi treatment reduced annexin 1 levels by ~60% in HeLa cells (Fig. 3.6E).

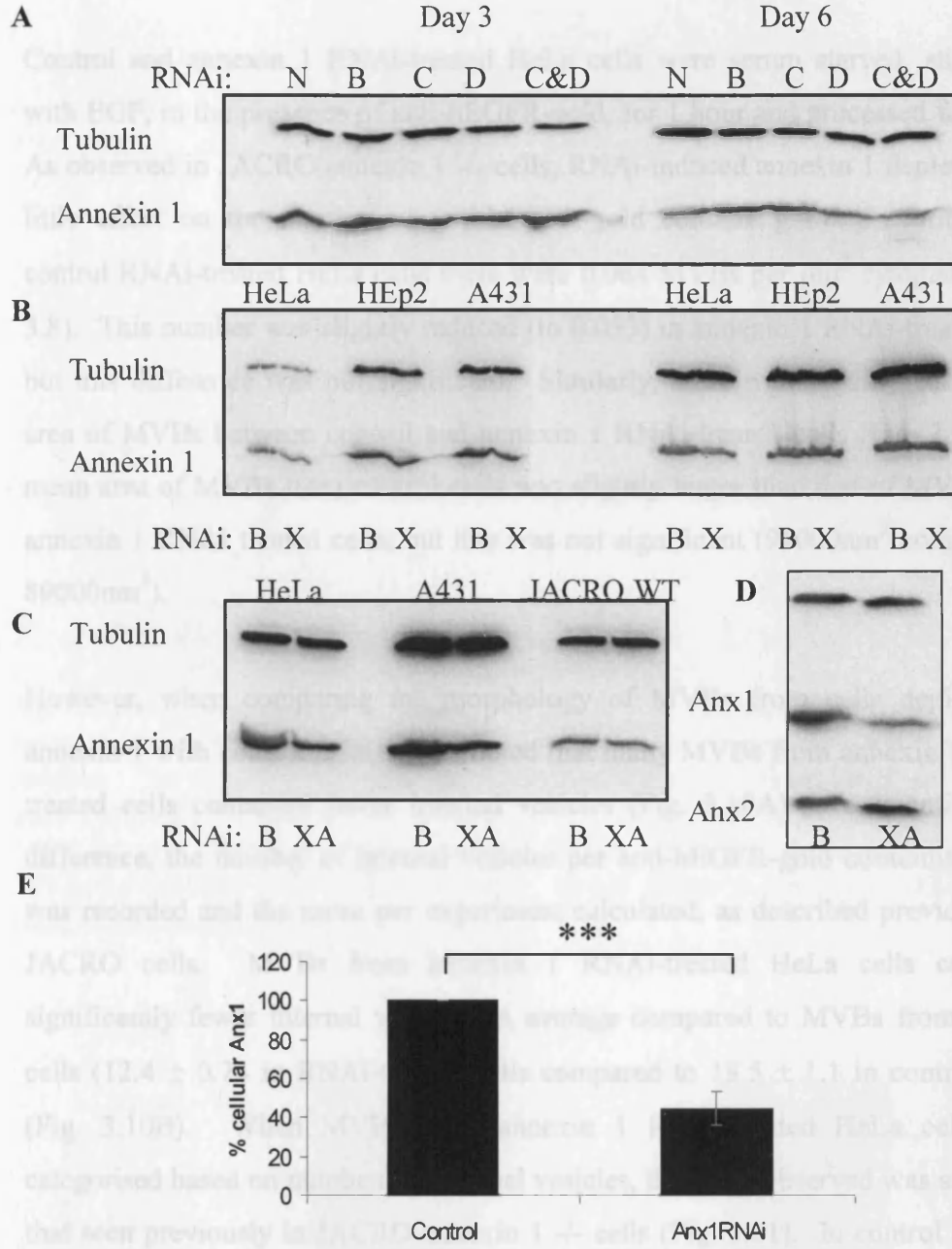

Figure 3.7. *RNAi-induced depletion of annexin 1.* A. HeLa cells were transfected with annexin 1 RNAi oligonucleotides (LBA1B, -C, -D) or no RNAi (N) for 3 days and lysates blotted for tubulin (loading control) and annexin 1, or transfected, split on day 3, retransfected & collected on day 6. No decrease in annexin 1 was observed. B. HeLa, HEp2 and A431 cells were treated with LBA1B (control) or LBA1X (annexin 1). After 3 days annexin 1 was slightly reduced in HeLa and A431 cells. C. HeLa, A431 and JACRO wild type cells were nucleofected with control or LBA1A & LBA1X for 24 hours, re-nucleofected and plated out for 48 hours before collecting for western blotting. There was significant reduction in annexin 1 levels in HeLa and A431 cells. D. Lysates were blotted for annexin 2 expression to determine whether it was upregulated in annexin 1 depleted HeLa cells. E. Semi-quantitative analysis of annexin 1 depletion was performed by measuring and comparing intensity of annexin 1 signals from at least 5 independent RNAi experiments in HeLa cells (see Materials & Methods section 2.4.2). *** $p<0.001$. All blots are representative of several experiments.

Control and annexin 1 RNAi-treated HeLa cells were serum starved, stimulated with EGF, in the presence of anti-hEGFR-gold, for 1 hour and processed for TEM. As observed in JACRO annexin 1 -/- cells, RNAi-induced annexin 1 depletion had little effect on the number of anti-hEGFR-gold containing MVBs formed. In control RNAi-treated HeLa cells there were 0.064 MVBs per μm^2 cytoplasm (Fig. 3.8). This number was slightly reduced (to 0.053) in annexin 1 RNAi-treated cells but this difference was not significant. Similarly, there was no difference in the area of MVBs between control and annexin 1 RNAi-treated cells (Fig. 3.9). The mean area of MVBs from control cells was slightly larger than that of MVBs from annexin 1 RNAi treated cells, but this was not significant ($91000nm^2$ compared to $89000nm^2$).

However, when comparing the morphology of MVBs from cells depleted for annexin 1 with control cells, it was noted that many MVBs from annexin 1 RNAi-treated cells contained fewer internal vesicles (Fig. 3.10A). To quantitate this difference, the number of internal vesicles per anti-hEGFR-gold containing MVB was recorded and the mean per experiment calculated, as described previously for JACRO cells. MVBs from annexin 1 RNAi-treated HeLa cells contained significantly fewer internal vesicles on average compared to MVBs from control cells (12.4 ± 0.74 in RNAi-treated cells compared to 19.5 ± 1.1 in control cells) (Fig. 3.10B). When MVBs from annexin 1 RNAi-treated HeLa cells were categorised based on numbers of internal vesicles, the trend observed was similar to that seen previously in JACRO annexin 1 -/- cells (Fig. 3.11). In control cells the majority of MVBs contained between 11 and 25 internal vesicles, whereas in annexin 1 RNAi-treated cells the majority shifted to between 6 and 15 internal vesicles. These data confirm that loss of annexin 1 affects inward vesiculation in EGF-stimulated cells.

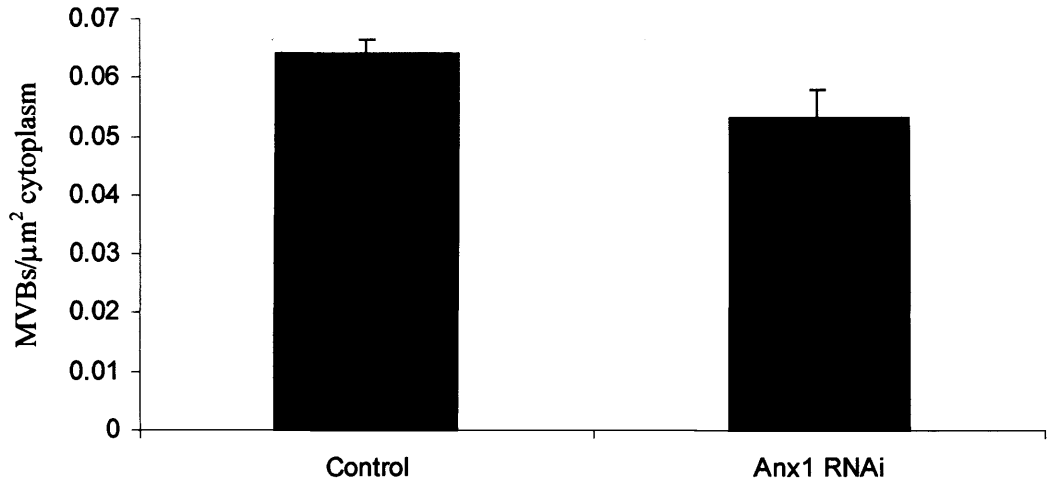

Figure 3.8. *Comparing numbers of MVBs in control and annexin 1 RNAi treated cells.* HeLa cells were transfected with control or annexin 1 RNAi for 3 days, serum starved and treated with EGF (100ng/ml), in the presence of anti-hEGFR-gold, for 1 hour. Cells were processed for TEM and at least 20 photos were taken of cells at random. The area of cytoplasm per photo was measured. Numbers of anti-hEGFR-gold containing MVBs per experiment were counted and expressed as number of MVB per μm^2 cytoplasm. There was a slight, non-significant, reduction in number of MVBs in annexin 1 RNAi treated cells. Graph shows the mean ± SEM of three independent experiments.

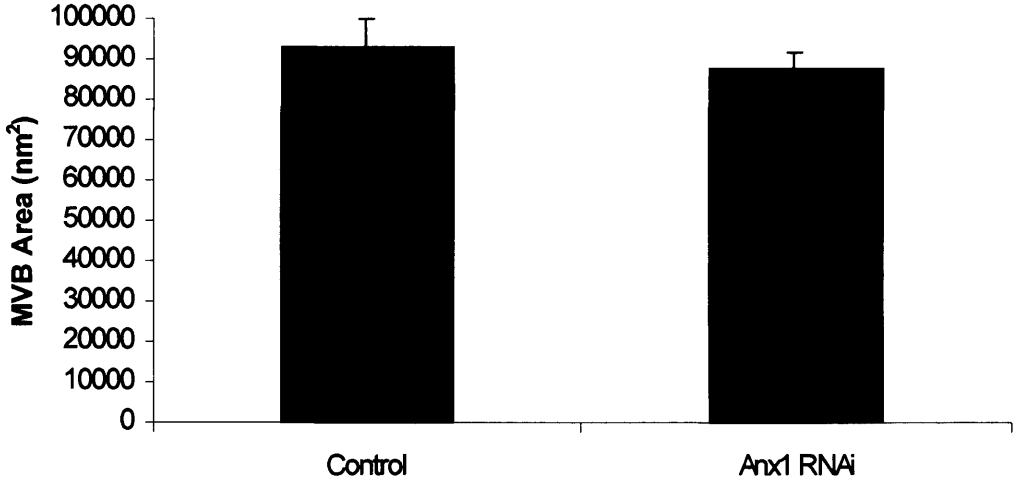

Figure 3.9. *Annexin 1 depletion does not alter area of MVBs.* HeLa cells were transfected with control or annexin 1 RNAi for 3 days, serum starved and treated with EGF (100ng/ml), in the presence of anti-hEGFR-gold, for 1 hour. Cells were processed for TEM and at least 20 photos were taken at random of cells. The area (nm^2) of each anti-hEGFR-gold containing MVB was measured. There was no difference in the average area of MVBs from control or annexin 1 RNAi treated cells. Graph shows the mean ± SEM of three independent experiments.

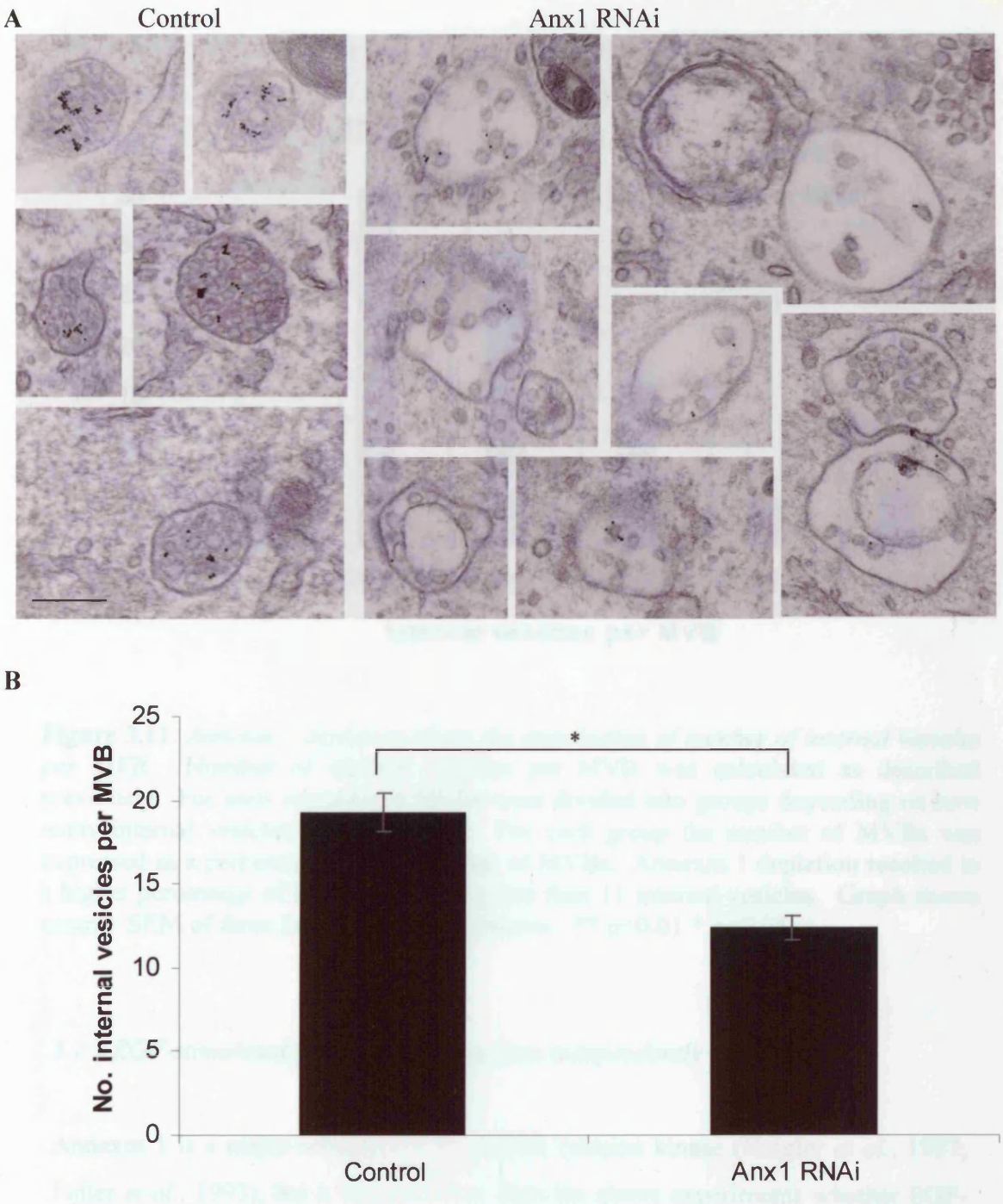

Figure 3.10. *Annexin 1 depletion reduces the number of internal vesicles per MVB.* HeLa cells were transfected with control or annexin 1 RNAi for 3 days, serum starved and treated with EGF (100ng/ml), in the presence of anti-hEGFR-gold, for 1 hour. Cells were processed for TEM to analyse the morphology of MVBs (A). At least 20 photos were taken at random and the number of internal vesicles per hEGFR-gold containing MVB was recorded (B). RNAi-induced annexin 1 depletion resulted in fewer internal vesicles per MVB. Graph shows mean ± SEM of three independent experiments. * $p<0.05$.
Bar = 200nm.

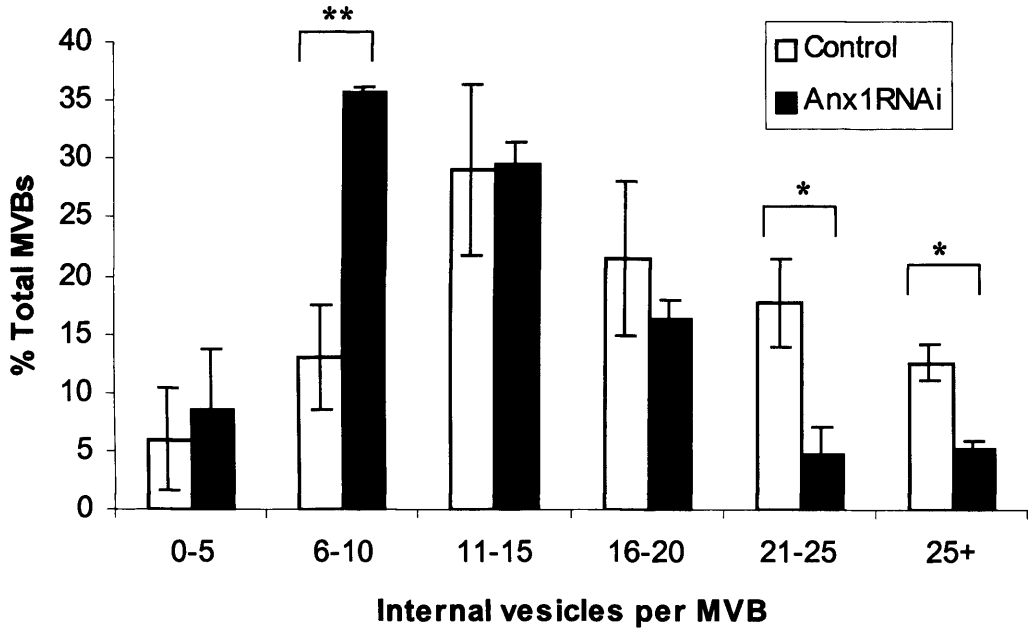

Figure 3.11. *Annexin 1 depletion alters the distribution of number of internal vesicles per MVB.* Number of internal vesicles per MVB was calculated as described previously. For each experiment MVBs were divided into groups depending on how many internal vesicles they contained. For each group the number of MVBs was expressed as a percentage of total number of MVBs. Annexin 1 depletion resulted in a higher percentage of MVBs containing less than 11 internal vesicles. Graph shows mean ± SEM of three independent experiments. ** $p<0.01$ * $p<0.05$.

3.2.3 EGF-stimulated MVB formation occurs independently of annexin 1

Annexin 1 is a major substrate of the EGFR tyrosine kinase (Haigler *et al.*, 1987; Futter *et al.*, 1993), but it was not clear from the above experiments whether EGF-stimulated phosphorylation of annexin 1 was required for the process of inward vesiculation as all cells were stimulated with EGF. EGFR is frequently used as a marker of MVB formation and so many studies investigating MVB formation and function have used EGF-stimulated cells. Unpublished observations, from the Futter group, have noted a much higher frequency of MVBs in EGF-stimulated cells, but these effects have never been documented. Therefore, experiments were designed that would both quantitate the effects of EGF stimulation on MVB formation and inward vesiculation, and determine whether these effects were dependent upon annexin 1.

To explore the effect of EGF stimulation on MVB formation, the above experiments were repeated using JACRO cells transfected with hEGFR, and comparing the effects of serum starvation with serum starvation followed by EGF stimulation. In these experiments it was necessary to count all MVBs, rather than only those that contain anti-hEGFR-gold, as in serum starved cells EGFR is not found in MVBs. EGF stimulation induced a significant increase in numbers of MVBs in both wild type and annexin 1 -/- cells (Fig. 3.12). In unstimulated cells the mean number of MVBs per μm^2 cytoplasm was the same (~0.028) in both cell lines. After EGF stimulation this number increased in both wild type and annexin 1 -/- cells, to 0.082 ± 0.009 and 0.067 ± 0.003, respectively. The small difference between numbers of MVBs in EGF-stimulated wild type and annexin 1 -/- cells was shown to be non-significant using Student's *t* test analysis, indicating that EGF stimulated MVB formation occurs independently of annexin 1.

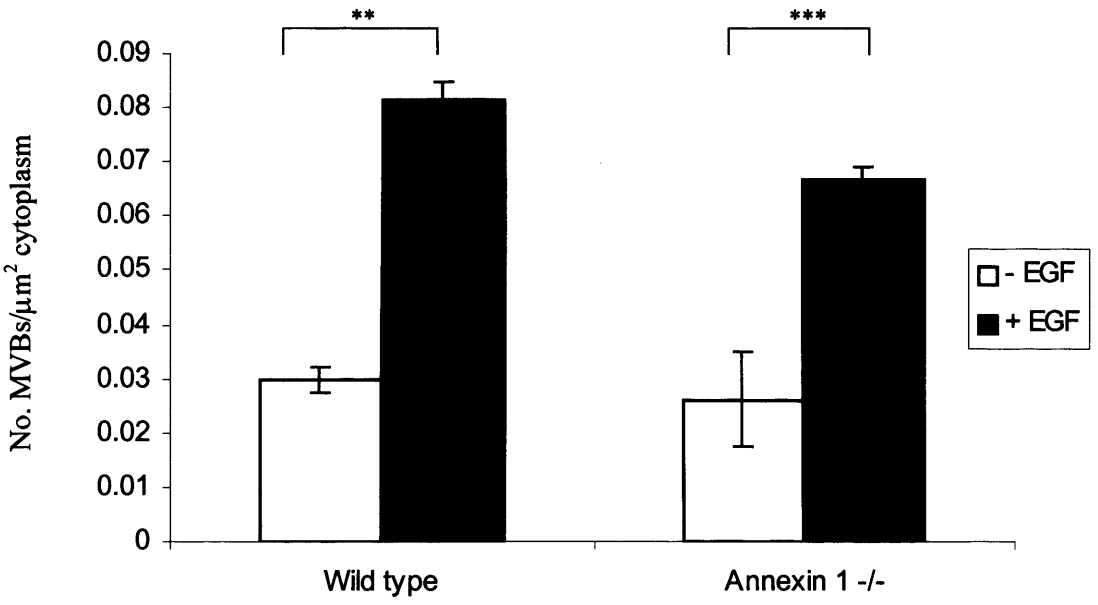

Figure 3.12. *EGF stimulates MVB formation in JACRO cells.* JACRO cells were transfected with hEGFR, serum starved and incubated in serum free medium for a further hour or stimulated with EGF (100ng/ml), in the presence of anti-hEGFR-gold, for 1 hour. Cells were processed for TEM and at least 20 random photos taken of cells. The area of cytoplasm per photo was measured, the total number of MVBs per experiment counted and expressed per μm^2 cytoplasm. EGF stimulation increased the number of MVBs in both cell lines. Graph shows the mean ± SEM of three independent experiments.
*** $p<0.005$ **$p<0.01$

The area of MVBs in unstimulated and EGF-stimulated cells was measured, and the mean per experiment calculated. EGF stimulation significantly increased the mean area of MVBs in both cell lines (Fig. 3.13). The effect of EGF stimulation observed in annexin 1 -/- cells was more extreme; the average area of MVBs increased from 79720 nm^2 ± 13900 to 119700 nm^2 ± 2097. However, the difference between cell lines was not significant, showing that the EGF-stimulated increase in MVB area does not require annexin 1.

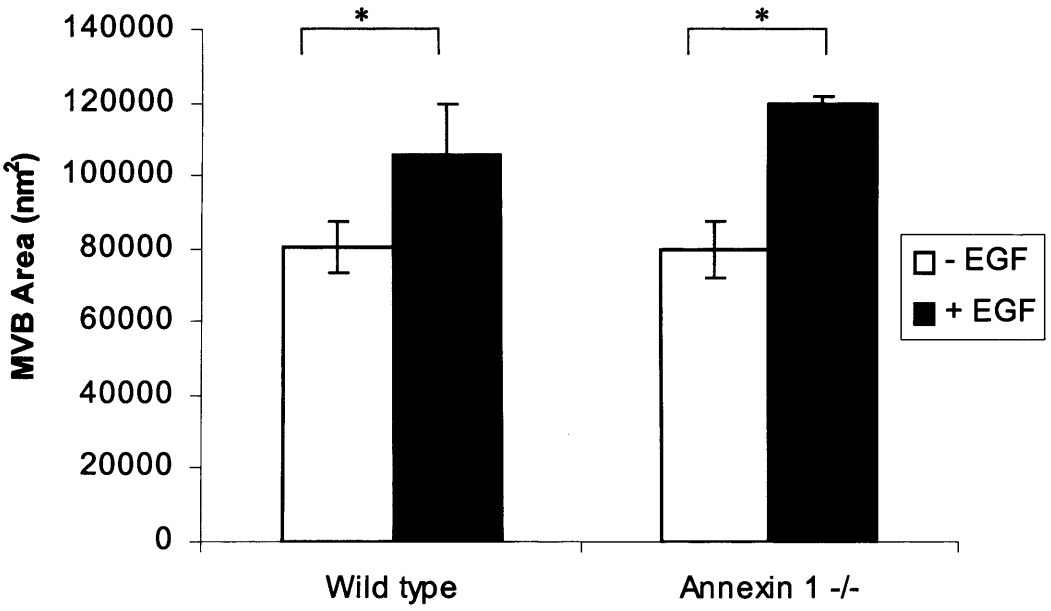

Figure 3.13. *EGF stimulation increases the mean area of MVBs.* JACRO cells were transfected with hEGFR, serum starved and incubated in serum free medium for a further hour or stimulated with EGF (100ng/ml), in the presence of anti-hEGFR-gold, for 1 hour. Cells were processed for TEM and at least 20 photos taken of cells at random. The area of all MVBs (nm^2) was measured. EGF stimulation increased the mean area of MVBs in both cell lines. Graph shows mean ± SEM of three independent experiments. * $p<0.05$

3.2.4 EGF stimulation increases internal vesicle formation in an annexin 1-dependent manner.

The data shown here provides evidence that loss of annexin 1 reduced numbers of internal vesicles in MVBs from EGF-stimulated cells (Fig. 3.6). To examine the full effect of EGF stimulation on inward vesiculation, the morphology of MVBs from unstimulated and EGF stimulated cells was observed using TEM (Fig.3.14A), and the mean number of internal vesicles per MVB calculated (Fig. 3.14B). EGF-stimulation of wild type cells significantly increased the mean number of internal vesicles per MVB over that of unstimulated cells (12.5 ± 0.8 increased to 17.5 ± 1.1). However, in EGF-stimulated annexin 1 -/- cells no increase was observed in the number of internal vesicles compared to unstimulated cells. Although the slight difference in number of internal vesicles between unstimulated wild type and annexin -/- cells (12.5 compared to 10.5) was non-significant, the difference between EGF-stimulated wild type and annexin -/- cells was statistically significant.

The data above show that EGF induced an increase in numbers of internal vesicles per MVB in wild type cells. That this did not occur in annexin 1 -/- cells demonstrates that EGF stimulation of inward vesiculation is mediated through annexin 1. To further investigate the effect of EGF stimulation on the process of inward vesiculation, the distribution of numbers of internal vesicle per MVB was observed and compared between unstimulated and EGF stimulated cells (Fig. 3.15). In unstimulated cells, the majority of MVBs from both cell lines contained between 6 and 16 internal vesicles, which is consistent with the average number of internal vesicles (~11 per MVB). However, EGF stimulation altered the distribution of number of internal vesicles per MVB in wild type cells so that a large proportion contained more than 16 internal vesicles (Fig. 3.15a). This EGF-mediated increase is also consistent with the increase observed in the average number of internal vesicles.

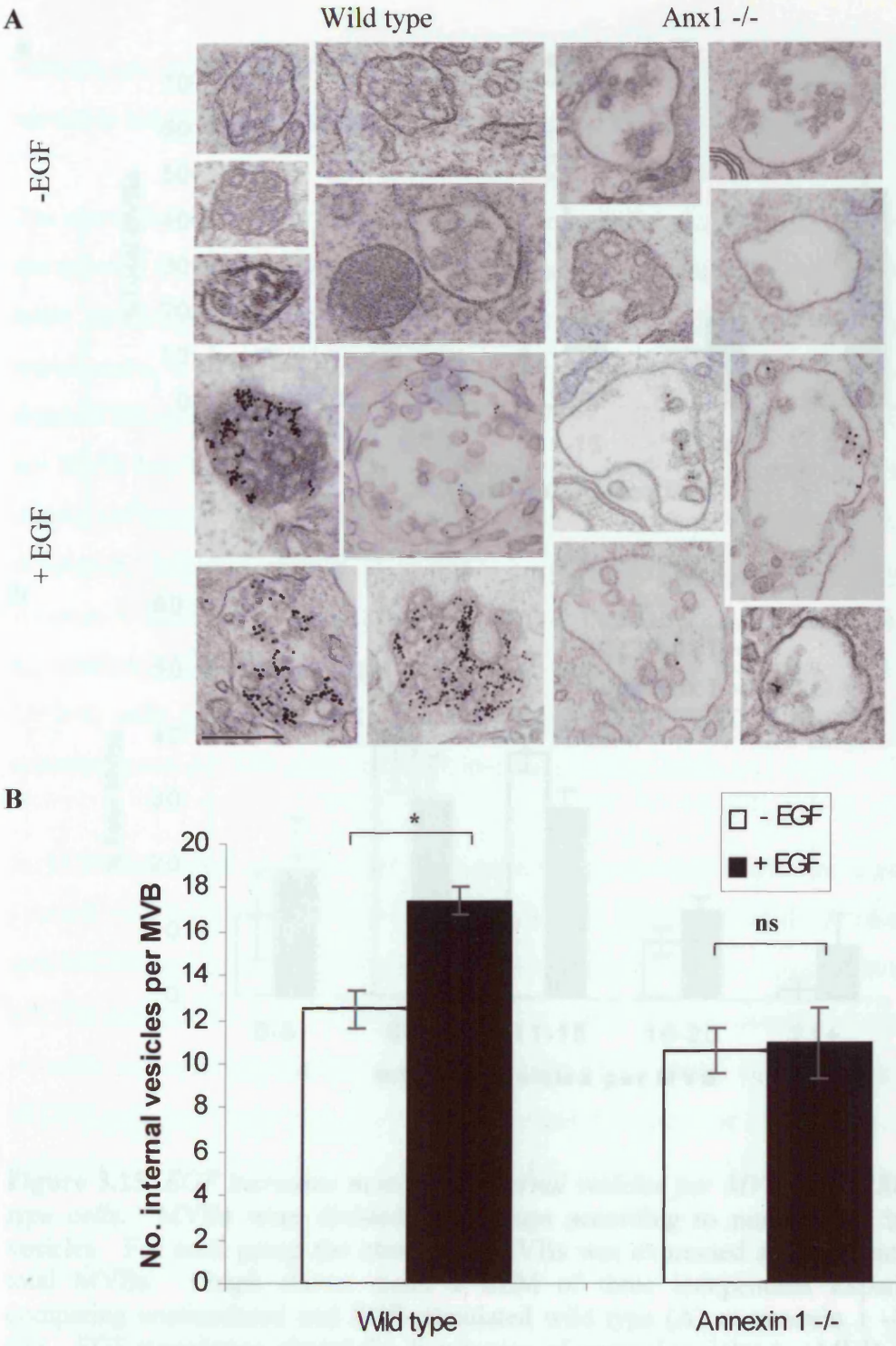

Figure 3.14. *Loss of annexin 1 inhibits EGF-stimulated increase in internal vesicle formation.* JACRO cells were transfected with hEGFR for 24 hours and serum starved for 1 hour. Cells were either kept in serum free medium or stimulated using EGF (100ng/ml), in the presence of hEGFR-gold, for 1 hour. Cells were processed for TEM and the morphology of MVBs in unstimulated or EGF-stimulated cells observed (A). Electron micrographs show typical MVBs from wild type and annexin 1 -/- cells. The number of internal vesicles per MVB was recorded for all MVBs in both unstimulated (white) and stimulated (black) cells. EGF stimulated an increase in number of internal vesicles in MVBs from wild type cells only. Graph shows mean ± SEM of three independent experiments. * $p<0.05$.

A

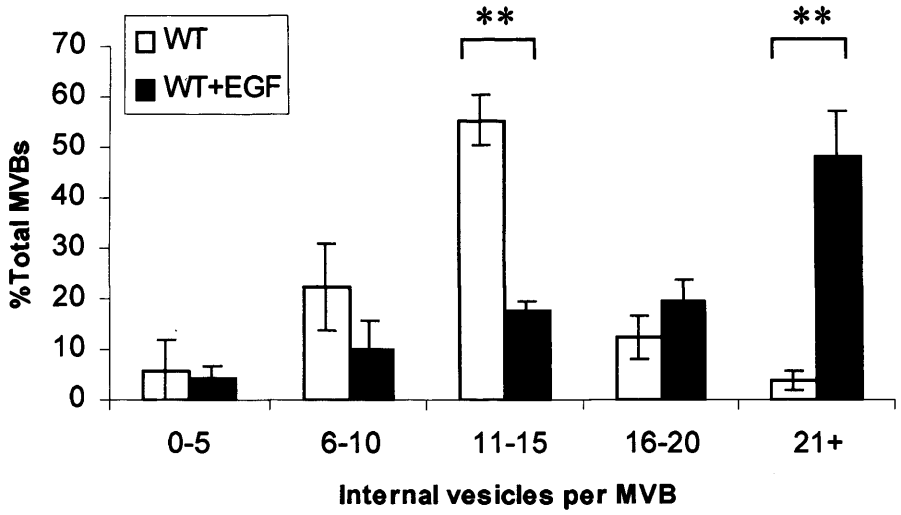

B

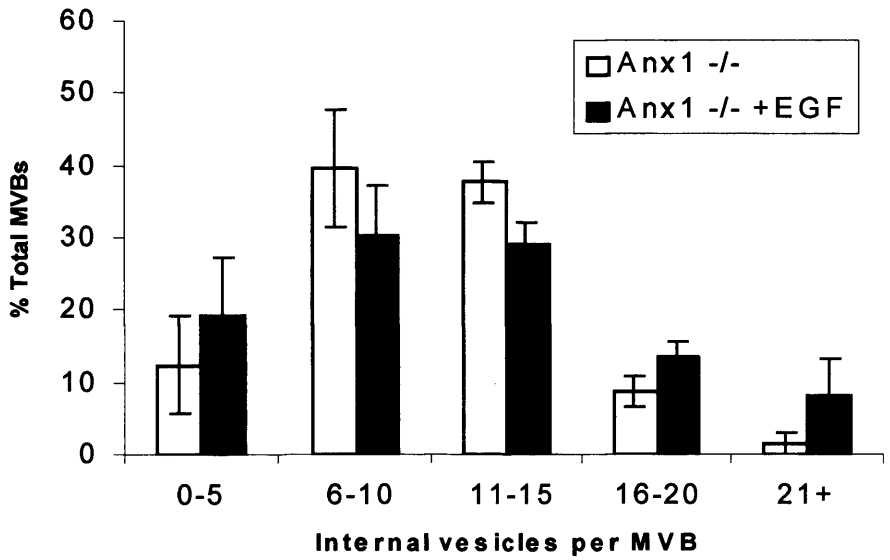

Figure 3.15. *EGF increases number of internal vesicles per MVB in JACRO wild type cells.* MVBs were divided into groups according to numbers of internal vesicles. For each group the number of MVBs was expressed as a percentage of total MVBs. Graph shows mean ± SEM of three independent experiments comparing unstimulated and EGF-stimulated wild type (A) or annexin 1 -/- cells (B). EGF stimulation altered the distribution of internal vesicles per MVB in wild type cells only. ** $p<0.01$, * $p<0.05$

In EGF-stimulated annexin 1 -/- cells no difference was observed in the distribution of numbers of internal vesicles per MVB compared with unstimulated cells (Fig. 3.15B). This finding is consistent with that derived from the previous figure, which showed that EGF stimulation had no effect on the average number of internal

vesicles per MVB. Therefore, these data further confirm that EGF stimulation increases internal vesicle formation in an annexin 1-dependent manner.

The above data show that EGF stimulation increases the number of MVBs, and also the number of internal vesicles per MVB, in JACRO wild type cells. Only the latter phenotype is affected by loss of annexin 1. Whilst performing these experiments, it was noted that not all MVBs, in EGF-stimulated cells, contained anti-hEGFR-gold. Having observed that the number of MVBs and internal vesicles per MVB was unaffected by loss of annexin 1 in unstimulated cells, annexin 1 is clearly not essential for formation of all MVBs or inward vesiculation within these structures. Taken together these findings posed the interesting question of whether annexin 1 mediates the formation of internal vesicles in all MVBs after EGF stimulation, or just the sub-population that contains EGFR. Therefore, MVBs from JACRO cells transfected with, and expressing, hEGFR were divided into those containing anti-hEGFR-gold and those that did not (Fig. 3.16).

In EGF-stimulated JACRO wild type cells, comparison of the mean number of internal vesicles in the two MVB sub-populations revealed that those containing anti-hEGFR-gold had significantly more internal vesicles than those without anti-hEGFR-gold (21.16 ± 0.67 compared to 14.1 ± 1.46). In EGF-stimulated annexin 1 -/- cells, two sub-populations were also observed i.e. those that contained anti-hEGFR-gold and those that did not. In contrast to wild type cells, there was no difference observed in the number of internal vesicles per MVB between those containing anti-hEGFR-gold and those without gold in annexin 1 -/- cells (10.89 ± 1.141 compared to 10.78 ± 1.71). These findings are consistent with earlier data showing that EGF-stimulates inward vesiculation through annexin 1, and provide evidence that this is only in a sub-population of MVBs that contain EGFR.

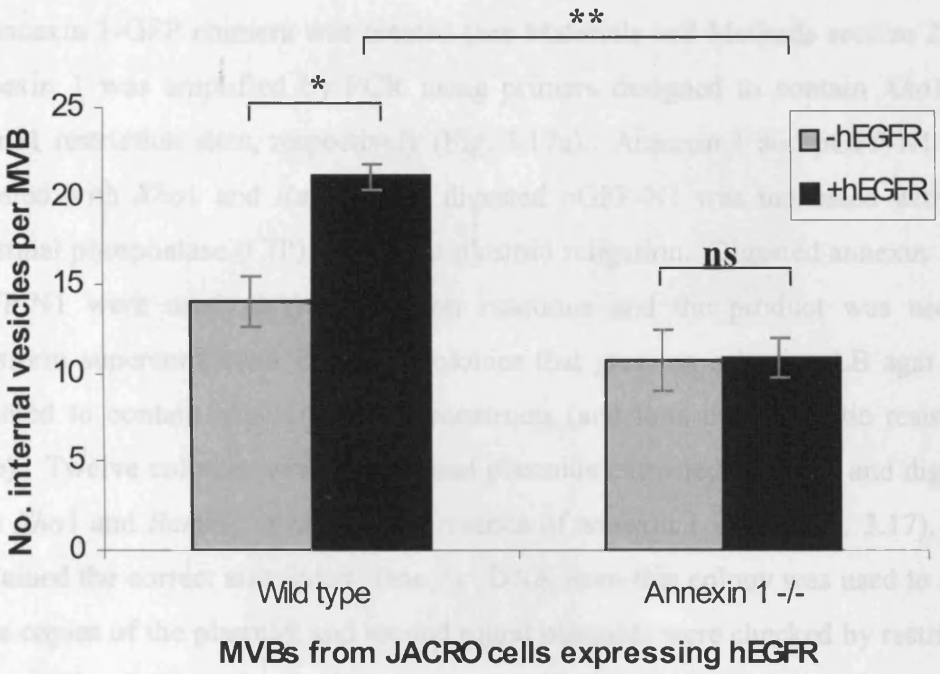

Figure 3.16. *MVBs with hEGFR-gold contain more internal vesicles in wild type cells.* From the previous experiment MVBs from EGF-stimulated hEGFR-expressing (i.e. anti-hEGFR-gold containing) JACRO cells were divided into MVBs containing one or more anti-hEGFR-gold particles (black), and MVBs that did not contain gold (grey). The average number of internal vesicles in these MVBs was calculated. Anti-hEGFR-gold containing MVBs from wild type cells contained more internal vesicles than MVBs without gold, but no difference was observed in annexin 1 -/- cells. Graph shows mean ± SEM of three independent experiments. * $p<0.05$ ** $p<0.01$ ns = non significant.

3.2.5 Reversal of phenotype observed in annexin 1 -/- cells

The data described above is consistent with previous published data implicating annexin 1 in the formation of internal vesicles within MVBs (Futter *et al.*, 1993). Although annexin 1 was found not to be necessary for formation of MVBs, it is necessary for EGF-stimulated inward vesiculation. To confirm that the phenotype observed in JACRO annexin 1 -/- cells was a direct consequence of the loss of annexin 1, it was necessary to re-express annexin 1 in annexin 1 -/- cells, to try to reverse the phenotype.

For use in these phenotype reversion experiments, and in future localisation studies, an annexin 1-GFP chimera was created (see Materials and Methods section 2.3.1). Annexin 1 was amplified by PCR using primers designed to contain *Xho*1 and *Bam*H1 restriction sites, respectively (Fig. 3.17a). Annexin 1 and pGFP-N1 were digested with *Xho*1 and *Bam*H1 and digested pGFP-N1 was incubated with calf intestinal phosphatase (CIP) to prevent plasmid religation. Digested annexin 1 and pGFP-N1 were used (3:1) in ligation reactions and the product was used to transform supercompetent *E. coli*. Colonies that grew on selective LB agar were assumed to contain annexin 1-GFP constructs (and thus the antibiotic resistance gene). Twelve colonies were picked and plasmids extracted, purified and digested with *Xho*1 and *Bam*H1 to check for presence of annexin 1 insert (Fig. 3.17). One contained the correct size insert (lane 7). DNA from this colony was used to make more copies of the plasmid, and second round plasmids were checked by restriction digests (Fig. 3.17). Single digestions (with *Xho*1, *Bam*H1 or *Xma*1) resulted in linearisation of the plasmid construct and a band of ~5.5kb, visible on 1% agarose gel. Double digestion with *Xho*1 and *Bam*H1 cut out the annexin 1 insert, which was visible as 1.2kb band. The annexin 1-GFP construct was sequenced to check for the presence of mutations and none were found when compared with wild type annexin 1 sequence (see Appendix 1, Fig. S.3).

Initially JACRO annexin 1 -/- cells were transiently transfected with annexin 1-GFP, to test the expression of this construct (Fig. 3.18). In cells expressing high levels of annexin 1-GFP, the construct was visible in the nucleus and throughout the cytoplasm, with little intracellular detail. In cells expressing lower levels of annexin 1-GFP, punctate labelling was observed in the cytoplasm. JACRO annexin 1 -/- cells were then transfected with annexin 1-GFP to make a stable cell line. However, creation of a stable cell line proved difficult due to cell death (personal observations and communication with Jamie Croxtall). Therefore, transient transfections had to be used. Despite obtaining an adequate level of transient transfection efficiency (~65%), this was insufficient to assume that the majority of cells would be transfected, especially as there was no way to determine which cells were expressing annexin 1-GFP in intact cells using TEM.

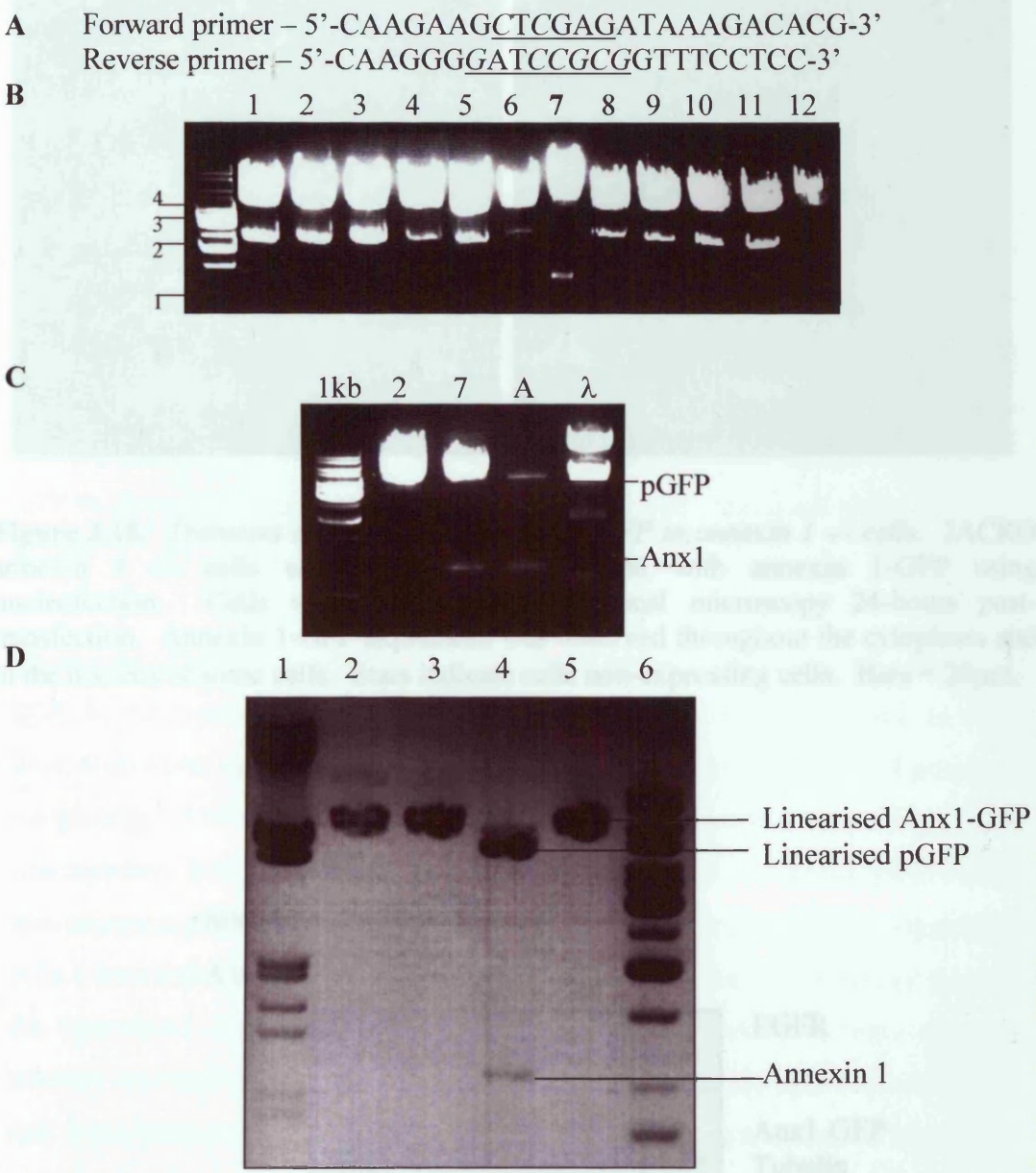

Figure 3.17. *Annexin 1-GFP construction.* Primers were designed to amplify annexin 1 and create *Xho*I and *Bam*HI restriction sites (A). Bases in italics indicate bases changed to allow restriction site but keep annexin 1 in frame. Underlined sequences show restriction sites. Annexin 1 and pGFP-N1 were digested with *Xho*I and *Bam*HI, treated with CIP and used in a ligation reaction. Ligations were used to transform supercompetent *E.coli* and plasmids were purified from these bacterial colonies. These samples were digested using *Xho*I and *Bam*HI to check for the presence of the correct size plasmid and insert (B). Lane 7 shows a band of 1.2kb that corresponds to annexin 1. DNA from samples 2 and 7 were digested again (C). Digested pGFP-N1 and annexin 1 were also loaded in lane A as a control. Sample 7 (annexin 1-GFP) was digested with *Xho*I (Lane 2), *Bam*HI (3), *Xho*I and *Bam*HI (4) or *Xma*1 (5). Lanes 1 & 6 were loaded with λ marker and 1kb marker respectively. Lanes 2, 3 & 5 show the presence of linearised plasmid (~5.5kb), whereas lane 4 shows a smaller linearised plasmid (~4.3kb) and annexin 1 insert (1.2kb)

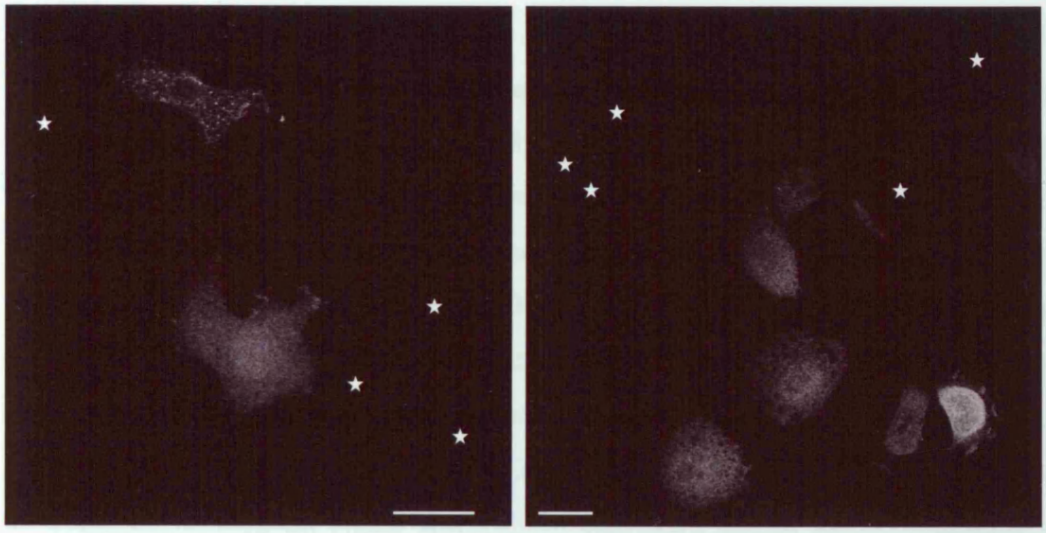

Figure 3.18. *Transient expression of annexin 1-GFP in annexin 1 -/- cells.* JACRO annexin 1 -/- cells were transiently transfected with annexin 1-GFP using nucleofection. Cells were imaged using confocal microscopy 24-hours post-transfection. Annexin 1-GFP expression was observed throughout the cytoplasm and in the nucleus of some cells. Stars indicate cells non-expressing cells. Bars = 20μm.

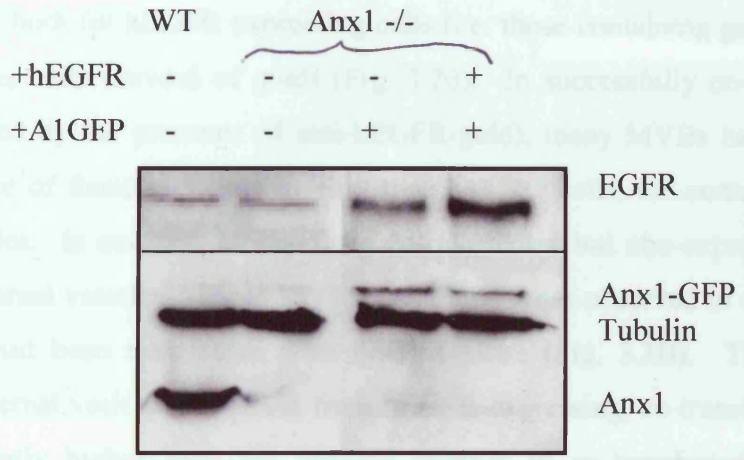

Figure 3.19. *Re-expression of annexin 1 in JACRO annexin 1 -/- cells.* JACRO annexin 1 -/- cells were transfected with annexin 1-GFP or annexin 1-GFP and hEGFR. Cell lysates were collected and blotted with anti-annexin 1 and anti-tubulin. Non-transfected JACRO wild type and annexin 1 -/- cells are included for comparison. Transfected cells blotted with an anti-annexin 1 antibody showed a band of approximately ~65kDa, which corresponds to the size of annexin 1-GFP.

Therefore, JACRO annexin 1 -/- cells were co-transfected with hEGFR and annexin 1-GFP, to be able to identify successfully transfected cells using anti-hEGFR-gold, assuming that cells expressing hEGFR would also express annexin 1-GFP. Figure 3.19 shows western blot analysis of non-transfected JACRO cells and JACRO annexin 1 -/- cells transfected with either annexin 1-GFP or co-transfected with annexin 1-GFP and hEGFR (co-transfected cells). Annexin 1 -/- cells transfected with annexin 1-GFP express relatively low levels of annexin 1-GFP, compared with endogenous annexin 1 levels in JACRO wild type cells. Annexin 1 -/- cells co-transfected with annexin 1-GFP and hEGFR expressed similar levels of annexin 1-GFP to those only transfected with annexin 1-GFP, but expressed higher levels of EGFR.

Co-transfected JACRO annexin 1 -/- cells were serum starved and stimulated with EGF, in the presence of anti-hEGFR-gold, for 1 hour. As loss of annexin 1 had little or no effect on the total number of MVBs, this was not measured. Instead, the morphology of MVBs was observed and the number of internal vesicles per MVB was recorded, both for hEGFR expressing cells (i.e. those containing gold) and for non-expressing cells (devoid of gold) (Fig. 3.20). In successfully co-transfected cells (identified by the presence of anti-hEGFR-gold), many MVBs had regained the appearance of those observed in wild type JACRO cells, i.e. contained more internal vesicles. In contrast, MVBs from co-transfected but non-expressing cells had fewer internal vesicles. These MVBs resembled those observed in annexin 1 -/- cells that had been transfected with hEGFR alone (Fig. 3.3B). The average number of internal vesicles per MVB from hEGFR-expressing, co-transfected cells was significantly higher than the average number in co-transfected but non-expressing cells (Fig. 3.21A).

Data from wild type and annexin 1 -/- cells, transfected with hEGFR only, were collected for comparison and show that there was no difference in the average number of internal vesicles per MVB between cells expressing hEGFR and non-expressing cells (Fig. 3.21A). This confirms that overexpression of hEGFR in JACRO cells had no effect on inward vesiculation and also shows that the increase in numbers of internal vesicles per MVB observed in successfully co-transfected

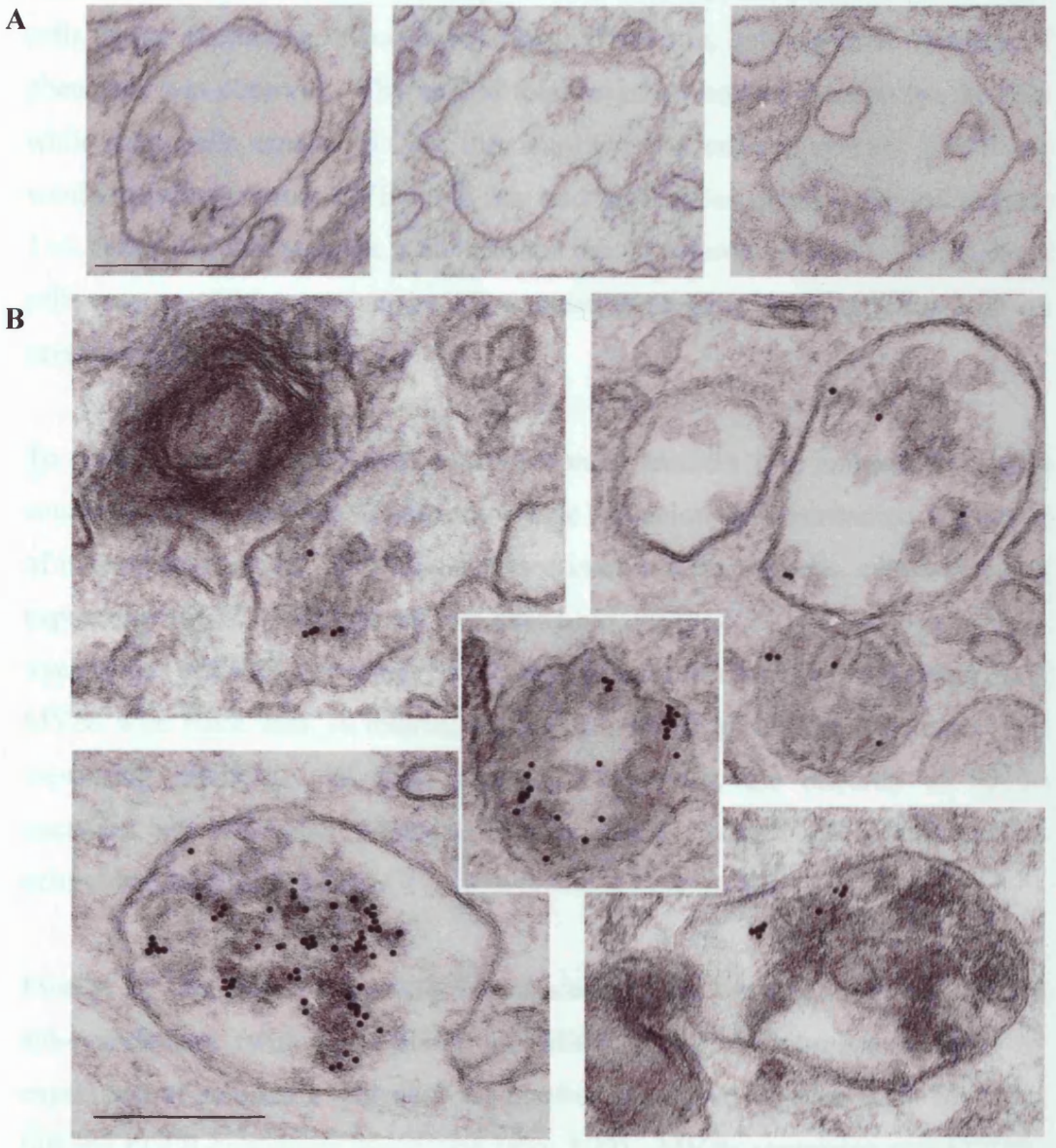

Figure 3.20. *MVB morphology after re-expression of annexin 1 in -/- cells.* JACRO annexin 1 -/- cells were co-transfected with annexin 1-GFP and hEGFR to re-express annexin 1 and reverse the effect of loss of annexin 1 on the number internal vesicles. After 24 hours cells were serum starved and stimulated with EGF (100ng/ml), in the presence of anti-hEGFR-gold, for 1 hour. Cells were processed for TEM and the morphology of MVBs analysed. (A) Typical MVBs in co-transfected annexin 1 -/- cells not expressing hEGFR. These MVBs contained few internal vesicles. (B) Typical MVBs from co-transfected annexin 1 -/- cells expressing hEGFR, showing increased numbers of internal vesicles. Bars = 200nm.

annexin 1 -/- cells is solely due to the expression of annexin 1-GFP. Although the mean number of internal vesicles per MVB was increased in successfully co-transfected cells, this number was significantly less than that observed in wild type cells (either expressing or non-expressing). Therefore, only a partial reversion of phenotype was observed. The lack of total reversion could be due to the fact that while some cells express hEGFR they may not also express annexin 1-GFP and would therefore possess MVBs with few internal vesicles, characteristic of annexin 1 -/- cells. Another possible reason for the partial reversal could be that, although cells were expressing annexin 1-GFP, expression may not be at sufficient levels to reverse the phenotype fully.

To further investigate whether re-expression of annexin 1 in annexin 1 -/- cells could reverse the decrease in internal vesicle formation, the distribution of number of internal vesicles per MVB was analysed in co-transfected cells, comparing cells expressing hEGFR and those not expressing hEGFR (Fig. 3.21B). Successfully co-transfected (hEGFR expressing) cells contained a significantly higher percentage of MVBs with more than 16 internal vesicles compared to untransfected cells (not-expressing hEGFR). In these non-expressing cells, the majority of MVBs contained between 6 and 15 internal vesicles, which is comparable to annexin 1 -/- cells only transfected with hEGFR from previous experiments.

Finally, MVBs from successfully co-transfected cells were divided into the two sub-populations (with or without anti-hEGFR-gold), to observe whether re-expression of annexin 1 increased the number of internal vesicles in all MVBs or just the EGFR-containing population (Fig. 3.22). MVBs containing anti-hEGFR-gold contained significantly more internal vesicles compared to MVBs that did not contain EGFR-gold (16.25 ± 0.58 compared to 9.78 ± 0.46). Expression of hEGFR alone in JACRO cells had no effect on inward vesiculation compared to non-expressing cells (Fig. 3.21). Similarly, there was no increase observed in the number of internal vesicles per anti-hEGFR-gold containing MVB in annexin 1 -/- cells, only transfected with hEGFR, compared to that seen in wild type cells (Fig. 3.16). Taken together these results provide further confirmation that, following co-transfection, a significant proportion of hEGFR-expressing annexin 1 -/- cells also express annexin 1.

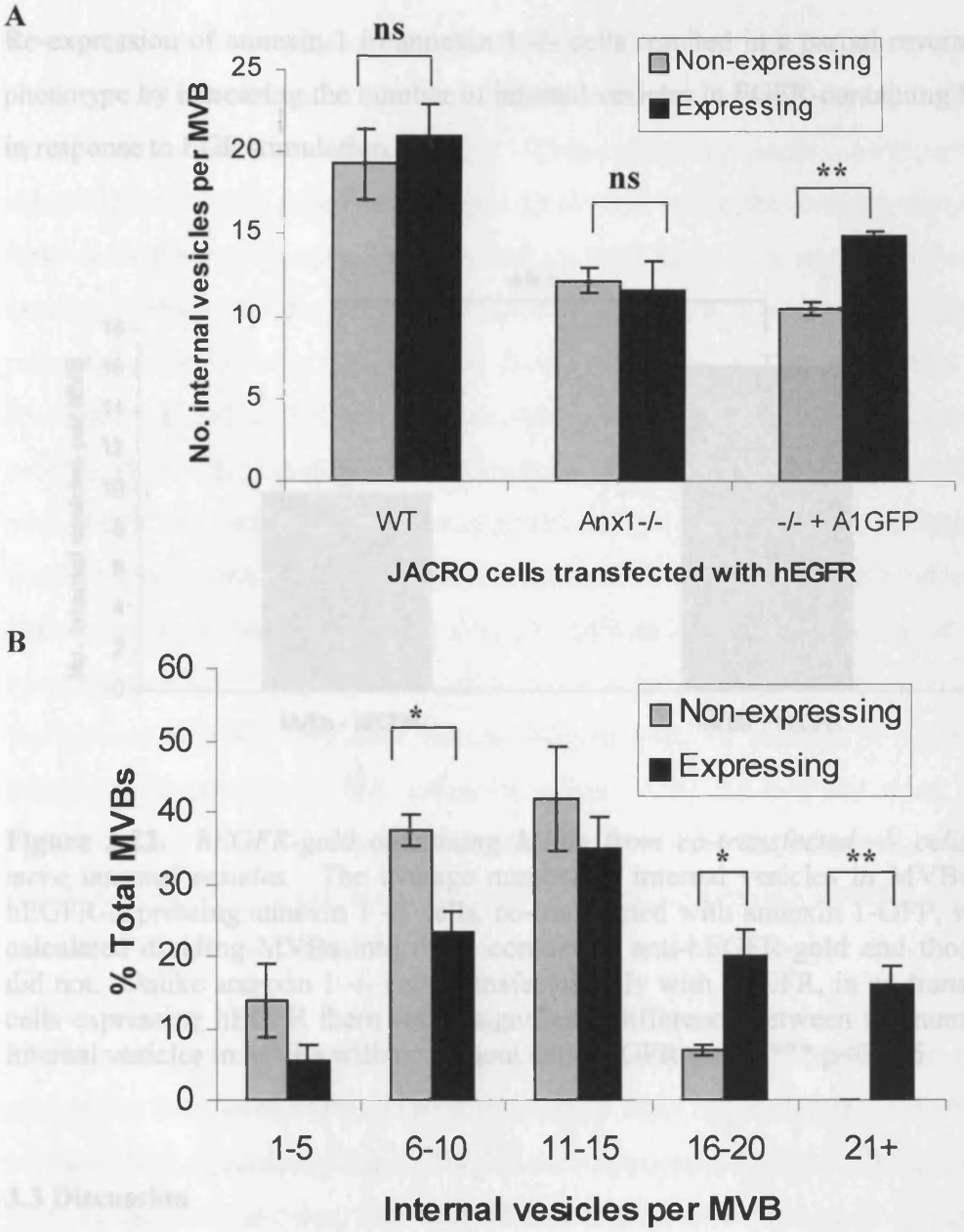

Figure 3.21. *Re-expression of annexin 1 in -/- cells increases the mean number of internal vesicles.* JACRO wild type and annexin 1 -/- cells transfected with hEGFR and annexin 1 -/- cells co-transfected with hEGFR and annexin 1-GFP (to reverse the phenotype seen in annexin 1 -/- cells) were serum starved and stimulated with EGF (100ng/ml) and anti-hEGFR-gold for 1 hour. For each cell type or transfection all MVBs were counted in cells expressing hEGFR (black) or not expressing (grey) (A). MVBs from successfully co-transfected annexin 1 -/- cells (expressing hEGFR) contained more internal vesicles than non-expressing cells. MVBs from annexin 1 -/- cells co-transfected with annexin 1 and hEGFR were divided into categories according to numbers of internal vesicles (B). Graph shows mean ± SEM of three independent experiments. * $p<0.05$ ** $p<0.01$.

Re-expression of annexin 1 in annexin 1 -/- cells resulted in a partial reversion of phenotype by increasing the number of internal vesicles in EGFR-containing MVBs in response to EGF stimulation.

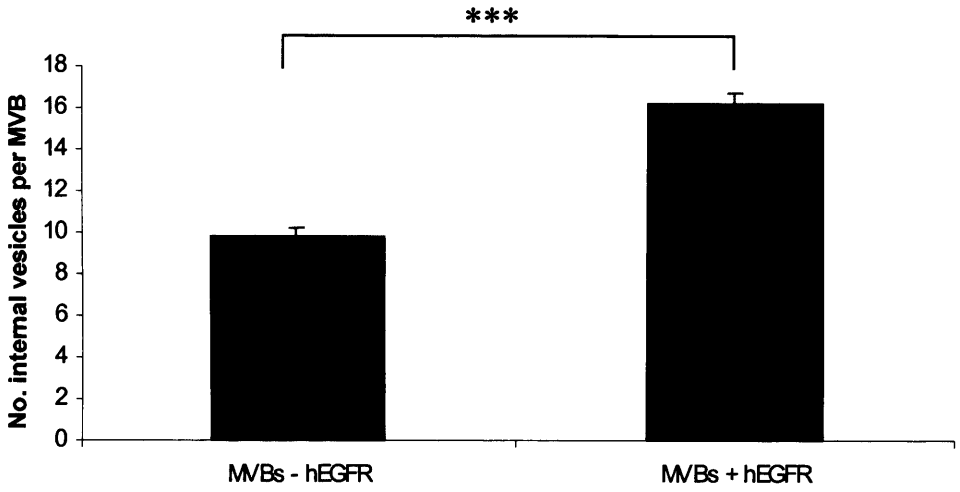

Figure 3.22. *hEGFR-gold containing MVBs from co-transfected -/- cells have more internal vesicles.* The average number of internal vesicles in MVBs from hEGFR-expressing annexin 1 -/- cells, co-transfected with annexin 1-GFP, was re-calculated dividing MVBs into those containing anti-hEGFR-gold and those that did not. Unlike annexin 1 -/- cells transfected only with hEGFR, in co-transfected cells expressing hEGFR there was a significant difference between the number of internal vesicles in MVBs with or without anti-hEGFR-gold. *** $p<0.005$

3.3 Discussion

3.3.1 EGF stimulation increases MVB formation in an annexin 1 independent manner

The formation of MVBs occurs as part of a maturation process (van Deurs *et al.*, 1993), whereby the limiting membrane of an endosome is induced to invaginate and forms internal vesicles. Many proteins have been implicated in the formation of internal vesicles, or sorting of lysosomally directed receptors onto these vesicles, and some proteins have been implicated in both e.g. Hrs (Urbe *et al.*, 2003; Bache *et al.*, 2003a). It is widely believed that the membrane binding properties of annexin 1 allow the protein to play a role in the formation of MVBs, although the exact nature has not been fully investigated (Gerke and Moss, 2002).

The results of the studies performed here show that MVBs are present in unstimulated cells, consistent with published work, which reports that MVBs form continuously (van Deurs *et al.*, 1993). These published studies were performed using HRP as a fluid phase marker and show that, while the average diameter of these structures does not alter significantly with time, the number of internal vesicles increases as the structure matures (van Deurs *et al.*, 1993). The data presented here, in both JACRO cell lines, show for the first time that EGF-stimulation significantly increases the total number of MVBs formed and the average MVB area, compared to unstimulated cells. These findings are consistent with unpublished work from the Futter group, using a human cell line (White *et al.*, under revision), and indicate that EGF-stimulated MVB formation is a widespread phenomenon. Although there was a slight decrease in the total number of MVBs formed in annexin 1 -/- cells, this difference was not significant and indicates that the process of MVB formation occurs independently of annexin 1. The small decrease in numbers of MVBs could be explained by the fact that when MVBs containing few internal vesicles from annexin 1 -/- cells are sectioned, there is a possibility that in any given section there may be no internal vesicles and these structures will not be counted as MVBs.

The increase in numbers of MVBs upon EGF stimulation in JACRO cell lines is such that at least some MVBs must be formed *de novo*. However, these findings do not rule out the possibility that EGFR can also enter pre-existing MVBs and further work is required to determine whether this is true. The increased numbers of internal vesicles per MVB, coupled with the increased numbers of MVBs, indicate that there is a substantial increase in the amount of cell membrane being delivered to the lysosome for degradation.

3.3.2 Annexin 1 is required for the EGF-stimulated increase in inward vesiculation

In addition to increasing MVB formation, EGF-stimulation also increases the number of internal vesicles per MVB. These findings regarding EGF stimulation were made in mouse lung fibroblasts, but are consistent with unpublished work using a human cell line (White *et al.*, under revision). As discussed above, neither the basal formation nor the EGF-stimulated formation of MVBs requires annexin 1.

While formation of internal vesicles in MVBs from unstimulated cells occurs independently of annexin 1, EGF-stimulated inward vesiculation is mediated through annexin 1. The use of RNAi to deplete annexin 1 in HeLa cells confirmed that the EGF-stimulated formation of internal vesicles is inhibited in cells lacking annexin 1. These data show that MVB formation and inward vesiculation within MVBs are separate processes that are regulated independently.

The formation of internal vesicles was believed to be necessary for lysosomal delivery of EGFR, but more recently it was shown that while inhibition of inward vesiculation had little effect on receptor degradation, it led to enhanced signalling from the activated receptor (Futter *et al.*, 2001). Therefore, it is possible that loss of annexin 1 could also enhance EGFR signalling through a failure to remove the tyrosine kinase domain from the cytoplasm.

3.3.3 Possible mechanisms for inward vesiculation

These data provide evidence that the mechanisms whereby EGF stimulation increases MVB formation and internal vesicle formation are distinct. However, it is probable that both mechanisms involve substrates of the EGFR tyrosine kinase or proteins that interact with phosphorylated EGFR. EGFR-mediated phosphorylation of c-Cbl activates c-Cbl ubiquitin ligase activity and induces receptor ubiquitination, which is believed to mediate receptor sorting onto internal vesicles of MVBs (Levkowitz *et al.*, 1998; de Melker *et al.*, 2001; Longva *et al.*, 2002). Hrs is believed to mediate sorting of ubiquitinated receptors, and is a substrate of a kinase downstream of activated EGFR (Bache *et al.*, 2002; Raiborg *et al.*, 2002; Katzmann *et al.*, 2003; Bache *et al.*, 2003b). Work on Hrs has provided evidence to link the processes of receptor sorting and inward vesiculation (Urbe *et al.*, 2003). However, EGF-stimulated phosphorylation of Hrs does not appear to modulate/enhance inward vesiculation as overexpression of a phosphorylation defective mutant has the same inhibitory effect on this process as wild type Hrs (Urbe *et al.*, 2003). Instead phosphorylation of Hrs releases it from the endosome, and is thought to allow other proteins to bind to the EGFR and mediate the actual process of inward vesiculation (Urbe *et al.*, 2003).

Annexin 1 is also a substrate for internalised EGFR, within MVBs, and has been proposed to mediate inward vesiculation (Futter *et al.*, 1993). Although loss of annexin 1 reduces the number of internal vesicles per MVB in EGF-stimulated cells, the studies here provide no conclusive evidence as to the specific role for annexin 1 within this process. Inward vesiculation can be divided into two stages: firstly, invagination of the endosomal membrane into the lumen of the endosome/MVB to form a vesicle, and secondly there is scission of the newly formed vesicle and its release into the lumen. The ESCRT complexes have been implicated in both processes. Vps4 is able to bind ESCRT-III (Bowers *et al.*, 2004) and is thought to induce the dissociation of ESCRT complexes and components of the endosomal clathrin coat, processes that appear to be linked to formation of internal vesicles (Babst *et al.*, 1998; Sachse *et al.*, 2003). To date there is no data to suggest that annexin 1 is involved, or interacts, with the ESCRT proteins. Furthermore, it is unclear whether annexin 1 promotes ESCRT/Vps4-mediated internal vesicle formation in response to EGF or whether there are two mechanisms of internal vesicle formation, one of which is annexin 1-dependent.

Overexpression of Hrs, downregulation of Tsg101 or disruption of ESCRT complex formation results in the inhibition of receptor sorting (Babst *et al.*, 2000; Bishop *et al.*, 2002; Lloyd *et al.*, 2002; Lu *et al.*, 2003; Urbe *et al.*, 2003; Morino *et al.*, 2004). In many cases MVBs are significantly enlarged and contain few internal vesicles. While loss of annexin 1 inhibits EGF-stimulated inward vesiculation, some vesicles still form and contain EGFR. These data suggest that receptor sorting still occurs but that annexin 1 might act downstream of Hrs/ESCRT proteins.

Annexin 1 may participate in membrane invagination or in scission of the newly formed vesicle. However, if annexin 1 is only involved in the latter process, membrane invagination should proceed normally and result in formation of budding profiles at the edge of MVBs (vesicles that fail to pinch off into the lumen). These structures were not observed in MVBs from cells lacking annexin 1, suggesting that annexin 1 is not involved in the scission step. It is, however, also possible that budding profiles are not stable and disassemble if fission fails to occur. Further evidence against a role for annexin 1 in vesicle scission comes from the observation

that in the absence of annexin 1 some internal vesicles still form. Therefore, it seems more likely that annexin 1 is involved in some aspect of membrane invagination, presumably controlled by EGFR-mediated phosphorylation.

3.3.4 Models of annexin 1-mediated internal vesicle formation

In a recent review, Gerke and Moss (2002) proposed a potential model for the mechanism by which EGFR-induced phosphorylation of annexin 1 mediates inward vesiculation (Fig. 3.23A). Annexin 1 is known to target its binding partner S100A11 to early endosomes (Seemann *et al.*, 1997) and is believed to form a heterotetrameric complex with S100A11 in a Ca^{2+} dependent manner, through which annexin 1 is able to bind to more than one membrane. The heterotetrameric complex is proposed to bring membranes together as other proteins e.g. ESCRT proteins, induce the actual process of membrane invagination. In this model, phosphorylation of annexin 1 by lysosomally targeted EGFR occurs just before the process of vesicle scission. Tyrosine phosphorylation of annexin 1 increases the susceptibility of annexin 1 to N-terminal proteolysis (Haigler *et al.*, 1987; Chuah and Pallen, 1989; Ando *et al.*, 1989). The N-terminal domain of annexin 1 contains the binding site for S100A11 and thus EGFR-mediated phosphorylation of annexin 1 could result in the loss of this site and disruption of the heterotetramer, which would in turn affect membrane binding. Evidence for loss of the N-terminus in MVB formation comes from the relocation of an N-terminally truncated annexin 1 from early to late endosomes (Seemann *et al.*, 1996a; Rescher *et al.*, 2000). Therefore, it is possible that the disruption of the heterotetrameric complex is coupled to vesicle fission.

A second model is proposed here based on the ability of annexin 1 to aggregate on membrane surfaces (Janshoff *et al.*, 2001) (Fig. 3.23B). Annexin 1 is known to bind to early endosomes and recruits S100A11 (Seemann *et al.*, 1996b; Seemann *et al.*, 1997; Rescher *et al.*, 2000). In this model, the annexin 1/S100A11 heterotetramer acts to stabilise the endosomal membrane. After receptor sorting, it is proposed that EGFR-mediated phosphorylation of annexin 1 disrupts annexin 1 binding to the endosomal membrane, through disruption of the heterotetramer as described in the above model. In a study using solid-supported membranes to observe the effect of annexin 1 in binding vesicles, it was shown that vesicle

adsorption to membrane-bound annexin 1 is mediated through two-dimensional annexin 1 clusters (Kastl *et al.*, 2004). N-terminally truncated annexin 1 showed a decrease in vesicle binding, thought to be due to the loss of binding sites (Kastl *et al.*, 2004). Release of annexin 1 from the endosomal membrane could destabilise the membrane allowing membrane invagination. However, this is unlikely because in the absence of annexin 1, this would lead to an increased number of internal vesicles within MVBs, the opposite effect to that observed in these studies. A modified version of the second model proposes that phosphorylation of annexin 1 alters its ability to cluster, through loss of its N-terminus, which may destabilise the membrane without loss of annexin 1, and/or allow members of the ESCRT complexes, involved in inward vesiculation, to bind. This is consistent with the localisation of N-terminally truncated annexin 1-GFP to late endosomes (Rescher *et al.*, 2000). However, as some internal vesicles form in the absence of annexin 1, it seems possible that ESCRT proteins may only mediate inward vesiculation within a subpopulation of MVBs.

Finally, a third hypothesis is proposes that Hrs-mediated EGFR sorting brings EGFR into close contact with annexin 1 (Fig. 3.23C). Phosphorylation of annexin 1 could result in a change in the conformation of annexin 1, through N-terminal proteolysis and disruption of the heterotetramer. In turn, this conformational change could recruit members of the ESCRT proteins, or other as yet unidentified proteins, to bind and form internal vesicles. In the absence of annexin 1, this recruitment would not occur, thus inhibiting inward vesiculation. However, as internal vesicles form normally in MVBs from unstimulated annexin 1 -/- cells, and some still form in EGF stimulated cells, it is unlikely that annexin 1 mediated inward vesiculation is solely dependent on the ESCRT proteins.

All three models are based on the known properties of annexin 1, but all include the formation of the putative heterotetrameric complex, which in the absence of annexin 1 would not form. From the data presented in this chapter, annexin 1 is promoting inward vesiculation in response to EGF stimulation. It is assumed that EGF-mediated phosphorylation of annexin 1 controls this process. Although annexin 1 is known to be phosphorylated by EGFR within MVBs, the role of phosphorylation in internal vesicle formation is unclear. More data is required to

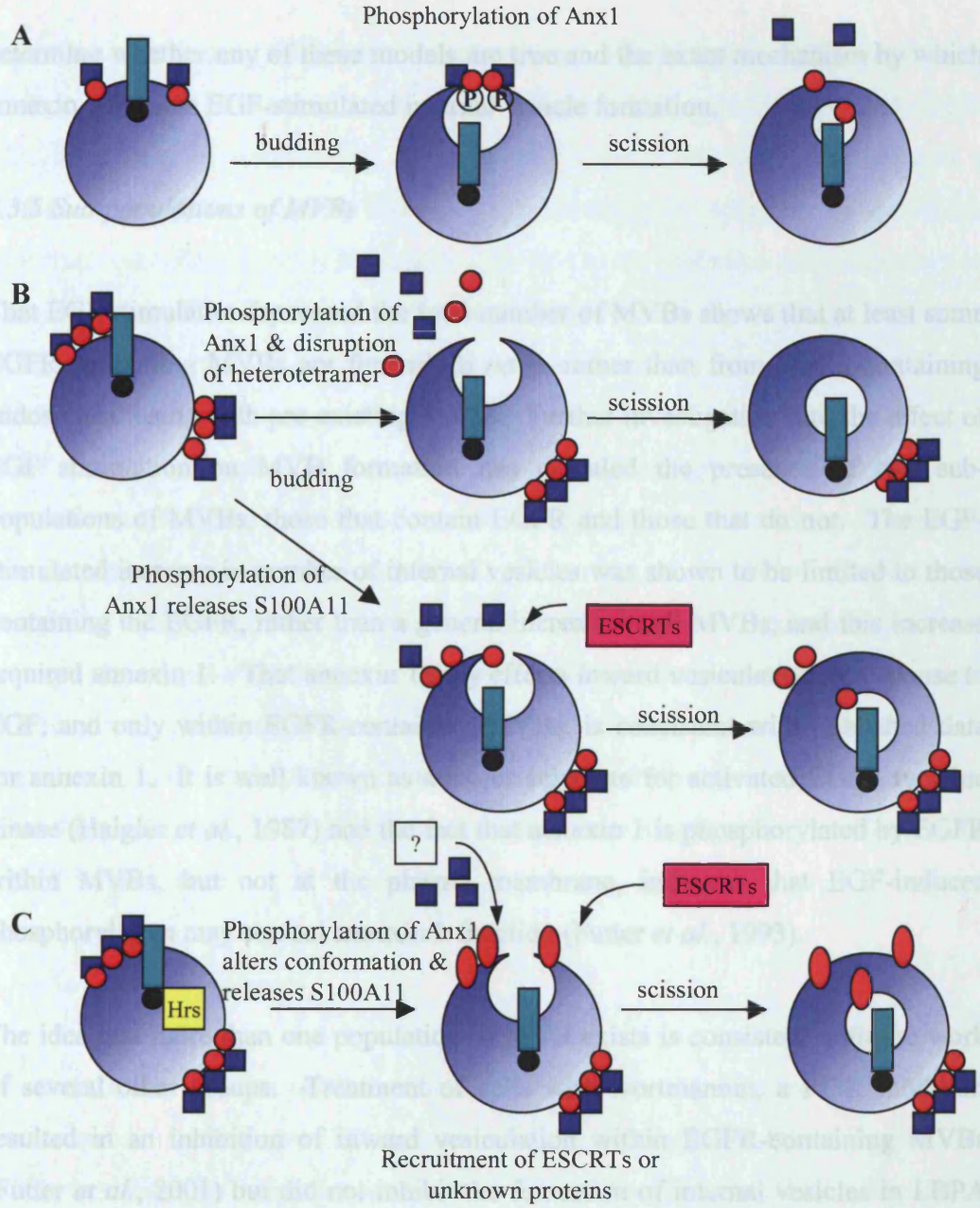

Figure 3.23. *Models of annexin 1-dependent inward vesiculation.* A - Gerke & Moss proposed that heterotetrameric complexes (containing annexin 1 (red) and S100A11 (blue)) on the surface of endosomes function to bring membranes together and stabilise this membrane-membrane interaction, as other proteins induce membrane invagination. The final stage of inward vesiculation is vesicle scission and this is proposed to be coupled to EGFR (green)-mediated phosphorylation of annexin 1, which disrupts the heterotetrameric complex. In Model B, annexin 1/S100A11 complexes form clusters on the cytoplasmic surface of the endosome, thus stabilising the membrane. Phosphorylation of annexin 1, by EGFR, disrupts this complex and either 1. releases annexin 1 from the membrane, causing membrane destabilization and allowing membrane invagination, or 2. alters the conformation of annexin 1, releasing S100A11, which may also destabilise the membrane and/or allow the binding of ESCRT proteins. Model C is based on Hrs-mediated EGFR sorting, allowing phosphorylation of annexin 1. Phosphorylation of annexin 1 induces a conformational change, which releases S100A11 and recruits ESCRT proteins, or unknown proteins, to induce formation of internal vesicles.

determine whether any of these models are true and the exact mechanism by which annexin 1 induces EGF-stimulated internal vesicle formation.

3.3.5 Sub-populations of MVBs

That EGF stimulation increased the total number of MVBs shows that at least some EGFR containing MVBs are formed *de novo*, rather than from EGFR-containing endosomes fusing with pre-existing MVBs. Further investigation into the effect of EGF stimulation on MVB formation has revealed the presence of two sub-populations of MVBs, those that contain EGFR and those that do not. The EGF-stimulated increase in number of internal vesicles was shown to be limited to those containing the EGFR, rather than a general increase in all MVBs, and this increase required annexin 1. That annexin 1 only effects inward vesiculation in response to EGF, and only within EGFR-containing MVBs, is consistent with published data for annexin 1. It is well known as a major substrate for activated EGFR tyrosine kinase (Haigler *et al.*, 1987) and the fact that annexin 1 is phosphorylated by EGFR within MVBs, but not at the plasma membrane, indicates that EGF-induced phosphorylation may control annexin 1 function (Futter *et al.*, 1993).

The idea that more than one population of MVB exists is consistent with the work of several other groups. Treatment of cells with wortmannin, a PI3K inhibitor, resulted in an inhibition of inward vesiculation within EGFR-containing MVBs (Futter *et al.*, 2001) but did not inhibit the formation of internal vesicles in LBPA containing MVBs (Bright *et al.*, 2001). Therefore, it seems likely that EGFR are trafficked through a Vps34, annexin 1 dependent MVB pathway, but that a separate group of MVBs that contain LBPA exist and these do not require Vps34. Furthermore, unpublished work confirmed that EGFR-containing MVBs are distinct from LBPA-containing MVBs, but that the two populations are morphologically identical (White *et al.*, under review). Interestingly, both sub-populations also labelled for the tetraspanin CD63 and this indicates that CD63 may be a more reliable MVB marker than EGFR or LBPA.

Wortmannin inhibited the formation of internal vesicles and caused EGFR to cluster at the perimeter membrane (Futter *et al.*, 2001). The phenotype observed in

annexin 1 -/- cells was similar but less drastic and was limited to EGFR-containing MVBs, whereas wortmannin treatment affected both constitutive and EGF-stimulated inward vesiculation. Additionally wortmannin treatment induced a marked enlargement of MVBs that could not be explained solely by the inhibition of inward vesiculation and was thought to be due to the inhibition of membrane exit from MVBs. This latter phenotype was not observed in annexin 1 -/- cells, although MVBs were slightly larger than those from wild type cells. If the only effect of loss of annexin 1 on MVBs was the inhibition of inward vesiculation, then some enlargement would be expected. That no significant vacuolar enlargement was observed suggests that loss of annexin 1 might have some additional effect on the delivery of membrane to the MVB. Retention of EGFR on the perimeter membrane of MVBs from wortmannin treated cells resulted in enhanced levels of tyrosine phosphorylation, due to an inhibition of signal attenuation. In control cells EGFR were sequestered onto internal vesicles and this is believed to attenuate signalling (Futter *et al.*, 2001). Therefore, it seems likely that annexin 1 mediated inward vesiculation in EGF-stimulated cells is necessary for attenuating its signalling properties.

3.3.6 Summary of findings

To summarise, this work shows that EGF stimulation increases both MVB formation and inward vesiculation within MVBs. Annexin 1 is not required for MVB formation but plays a specific role in formation of internal vesicles within MVBs. While annexin 1 is not required for the basal formation of MVBs or the EGF-mediated increase in MVB formation, it is necessary for the EGF-stimulated formation of internal vesicles. That annexin 1 is not involved in inward vesiculation within all MVBs is consistent with the recent idea that there is more than one population of MVBs. Therefore annexin 1 is necessary for the EGF-stimulated formation of internal vesicles in a sub-population of MVBs, which contain EGFR.

Chapter 4 – Does annexin 2 play a role in MVB formation?

4.1 Introduction

The results of the previous chapter showed that annexin 1 mediates the EGF-stimulated increase in inward vesiculation in a sub-population of MVBs. Although EGF stimulation also caused an increase in MVB formation, no evidence was found for a role of annexin 1 in MVB formation, either in the presence or absence of EGF. A recent published report suggested that annexin 2 is required for the biogenesis of MVBs and that annexin 2 depletion caused a failure of MVBs to "bud off" from endosomes (Mayran *et al.*, 2003). This morphological change was also reported to inhibit transport from early to late endosomes. In contrast, the findings of Zobiack *et al.* (2003) reported annexin 2 depletion had no effect on lysosomal delivery, but that the localisation of TfR positive recycling endosomes was altered (Zobiack *et al.*, 2003).

This chapter presents the results of a detailed investigation into the effect of loss, or depletion, of annexin 2 on MVB formation and inward vesiculation. Annexin 2 was depleted in HeLa cells using RNAi and the morphology of anti-hEGFR-gold containing MVBs observed. No difference was detected in the number of MVBs formed or the size of these MVBs between control and annexin 2 RNAi treated cells. Unlike annexin 1, annexin 2 is not required for the formation of internal vesicles in MVBs from EGF-stimulated cells. As the phenotype observed following RNAi-induced depletion is critically dependent on the efficiency of depletion, the effect of loss of annexin 2 was also investigated in a DT40 annexin 2 -/- cell line, where annexin 2 was completely absent due to the disruption of the annexin 2 gene. Experiments in these knockout cells further confirmed that annexin 2 is not required for any aspect of MVB formation examined.

4.2 Results

4.2.1 MVB formation occurs independently of annexin 2

To investigate whether annexin 2, unlike annexin 1, plays a role in MVB formation the effect of loss of annexin 2 on this process was investigated. RNAi has previously been used to deplete levels of annexin 2 in HeLa cells (Mayran *et al.*, 2003; Zobiack *et al.*, 2003). Therefore, HeLa cells were treated with annexin 2 or control RNAi for 3 days (see Materials and Methods section 2.5.1). Lysates were collected and blotted for annexin 2 to check the efficiency of knockdown (Fig. 4.1A). Cells treated with annexin 2 RNAi were significantly depleted of annexin 2 and semi-quantitative analysis of western blots from several independent RNAi experiments showed that annexin 2 RNAi treatment decreased protein levels by 70-80% in HeLa cells (Fig. 4.1B). Lysates were also blotted for annexin 1 and a small increase in the amount of annexin 1 was observed.

Coverslips from these RNAi experiments were processed and stained with an anti-annexin 2 antibody and fluorescent phalloidin to label actin and help to visualise annexin 2 depleted cells (Fig. 4.1C). Interestingly, while control HeLa cells grew in smooth-edged, round patches, annexin 2 RNAi treated cells tended to grow as single cells or as groups of cells without tightly formed cell-cell contacts (Fig. 4.1c). Levels of annexin 2 were reduced by approximately 75% in all experiments used, as shown by western blotting and by immunofluorescence. It is important to note that in 75% of cells annexin 2 was undetectable, while the remaining 25% of cells showed annexin 2 staining similar to control cells.

To observe the effect of annexin 2 depletion on MVB formation, HeLa cells were treated with control or annexin 2 RNAi. After 3 days cells were serum starved, incubated with EGF in the presence of anti-hEGFR-gold, or with EGF-HRP, for 1 hour and processed for TEM (see Materials & Methods section 2.11.2). Initially, the morphology of anti-hEGFR-gold, or EGF-HRP, containing MVBs was observed in both cell lines using TEM.

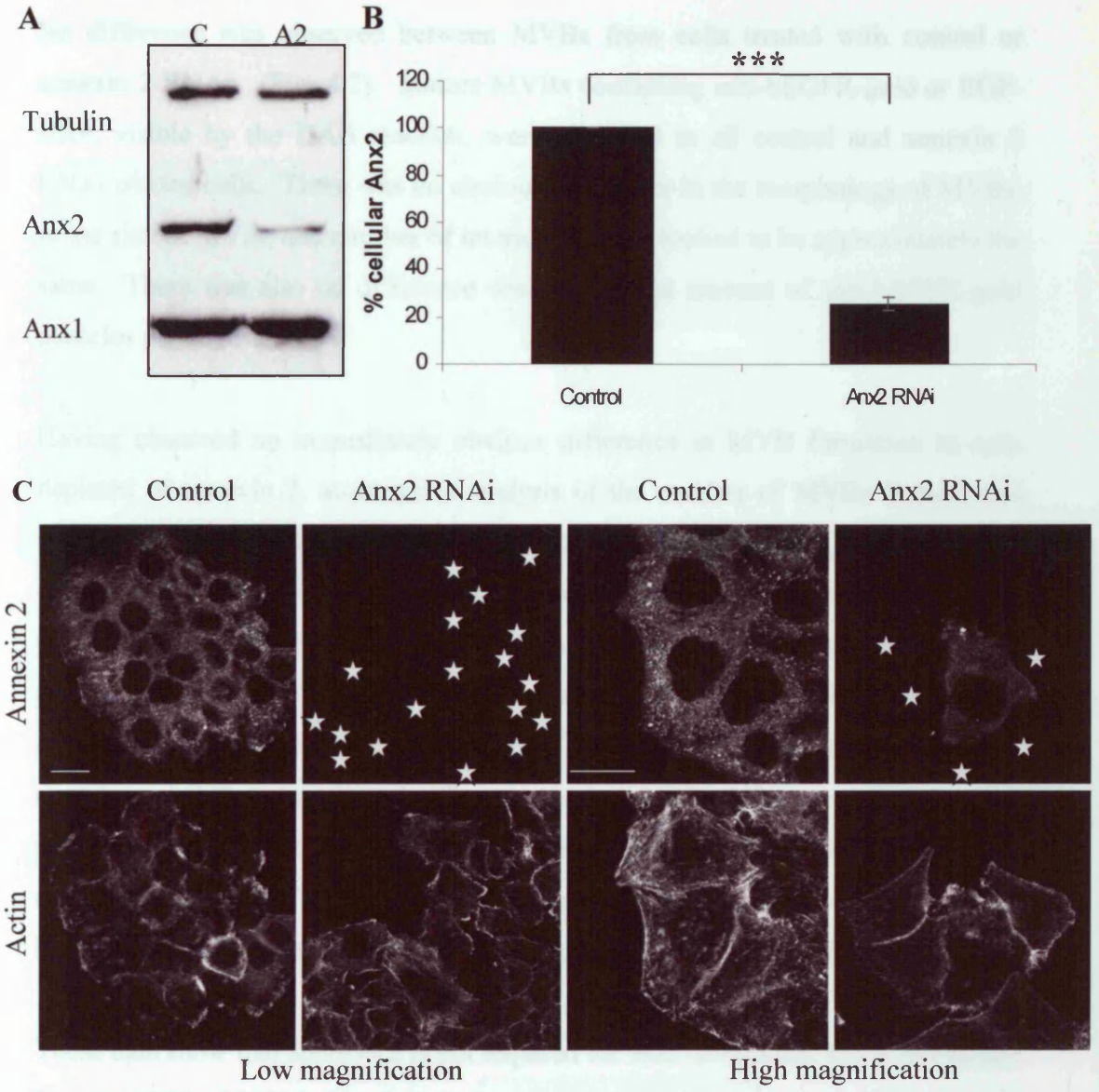

Figure 4.1. *Use of RNAi to deplete annexin 2 in HeLa cells.* HeLa cells were treated for 3 days with control (C) or annexin 2 RNAi oligonucleotides (A2). Cell lysates were collected and blotted with antibodies against tubulin, as a loading control, annexin 2 (anx2), to confirm the efficiency of knockdown, and annexin 1 (A). Semi-quantitative analysis if annexin 2 depletion was performed by measuring and comparing intensity of annexin 2 signal from control and annexin 2 RNAi treated cells (see Materials & Methods section 2.6.4) (B). Graph shows data ± SEM from at least 5 independent RNAi experiments. *** $p<0.001$. (C) Cells from the same experiment were fixed for immunofluorescence and labelled with anti-annexin 2 (top panel). Actin was stained using phalloidin-AlexaFluor 547. These are typical images of RNAi-treated cells at low power (left panels) or high power (right panels). White stars indicate cells apparently totally depleted of annexin 2. Bars = 20μm.

No difference was observed between MVBs from cells treated with control or annexin 2 RNAi (Fig. 4.2). Mature MVBs containing anti-hEGFR-gold or EGF-HRP, visible by the DAB reaction, were observed in all control and annexin 2 RNAi-treated cells. There was no obvious difference in the morphology of MVBs, as the size of MVBs and number of internal vesicles looked to be approximately the same. There was also no difference observed in the amount of anti-hEGFR-gold particles per MVB.

Having observed no immediately obvious difference in MVB formation in cells depleted of annexin 2, quantitative analysis of the number of MVBs formed was performed to reveal any subtle difference. As described in Chapter 3 for annexin 1, control or annexin 2 RNAi treated HeLa cells were incubated with EGF, in the presence of anti-hEGFR-gold, for 1 hour to label MVBs. At least 20 cells were photographed for each treatment in three independent experiments. The area of cytoplasm in each photo was measured (nm^2) and the number of anti-hEGFR-gold containing MVBs was counted. The mean number of MVBs per μm^2 cytoplasm was calculated, and compared between control and annexin 2 RNAi treated cells (Fig. 4.3). There was no significant difference in the number of MVBs formed in EGF-stimulated control or annexin 2 RNAi treated cells (0.075 compared to 0.078).

These data show that annexin 2 is not required for EGF-stimulated MVB formation. In spite of this, RNAi-induced depletion of annexin 2 does not target 100% of cells and, as a result, there are at least 20% of cells in each experiment that express wild type levels of annexin 2. The counting of a large number of cells should be adequate to overcome this problem. However, although in 80% of cells annexin 2 was reduced below the levels of detection, it may still be present at sufficient levels to perform its function. Therefore, it was necessary to analyse MVB formation in a cell line devoid of annexin 2 to confirm the above findings. DT40s are chick B lymphocytes and the annexin 2 -/- cell line does not express annexin 2 due to the disruption of the gene by the insertion of a neomycin cassette (Hawkins *et al.*, 2002). DT40 cell lysates were collected and blotted with an anti-annexin 2 antibody, against human placental annexin 2, but no signal was observed in either cell line, presumably because this antibody does not recognise the chicken protein.

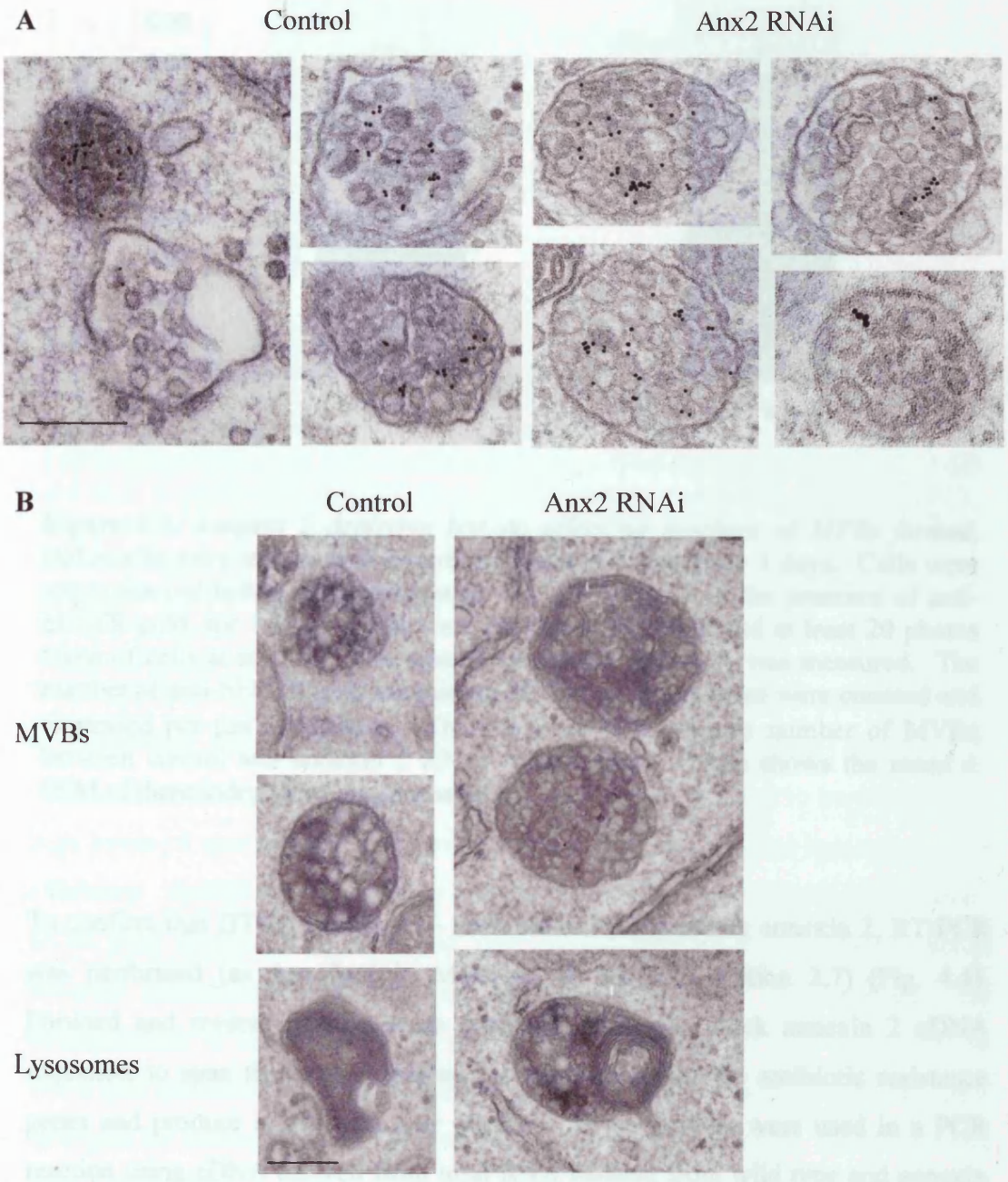

Figure 4.2. *Effect of annexin 2 depletion on MVB morphology.* HeLa cells were treated with control or annexin 2 RNAi. After 3 days cells were serum starved, stimulated with EGF (100ng/ml), in the presence of anti-hEGFR-gold (A), or EGF-HRP (B) for 1 hour, and processed for TEM. The morphology of MVBs was analyzed in many cells from several experiments. Electron micrographs show typical MVBs for control and RNAi-treated cells, and lower panels in B show typical EGF-HRP containing lysosomes. Bars = 200nm.

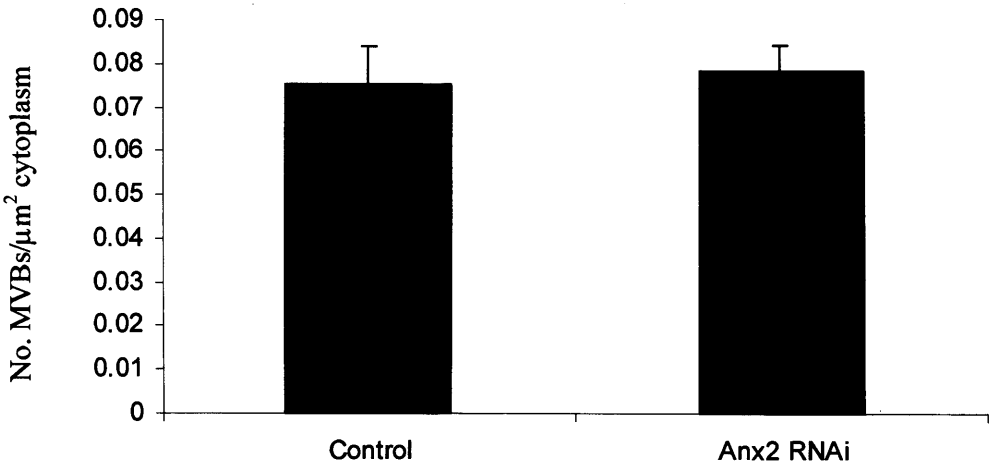

Figure 4.3. *Annexin 2 depletion has no effect on numbers of MVBs formed.* HeLa cells were treated with control or annexin 2 RNAi for 3 days. Cells were serum starved before stimulation with EGF (100ng/ml), in the presence of anti-hEGFR-gold, for 1 hour. Cells were processed for TEM and at least 20 photos taken of cells at random. The area of cytoplasm per photo was measured. The number of anti-hEGFR-gold containing MVBs per experiment were counted and expressed per μm^2 cytoplasm. There was no difference in number of MVBs between control and annexin 2 RNAi treated cells. Graph shows the mean ± SEM of three independent experiments.

To confirm that DT40 annexin 2 -/- cells were not expressing annexin 2, RT-PCR was performed (as described in Materials & Methods section 2.7) (Fig. 4.4). Forward and reverse primers were designed, using the chick annexin 2 cDNA sequence, to span the exon disrupted by the insertion of the antibiotic resistance genes and produce a 239 base pair product. These primers were used in a PCR reaction using cDNA derived from total RNA isolated from wild type and annexin 2 -/- DT40s. In the wild type cells there was a visible band at the correct size (~239bp) that was not observed in annexin 2 -/- cells. This confirmed that there was no detectable annexin 2 expression in the annexin 2 -/- cells.

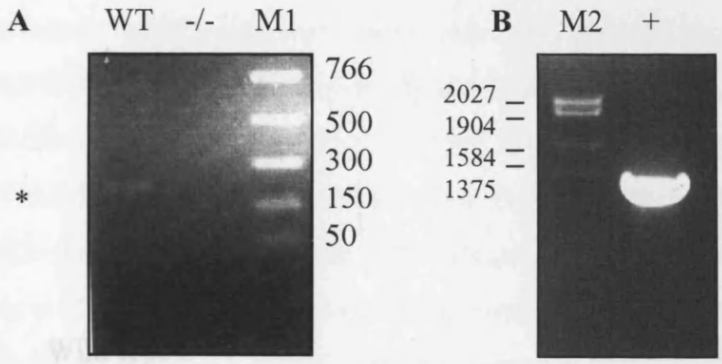

Figure 4.4. *RT-PCR analysis of annexin 2 expression in DT40 cells.* Total RNA was isolated from wild type and annexin 2 -/- DT40 cells and used to synthesize first strand cDNA. cDNA was used in a PCR reaction using primers designed against the chick annexin 2 sequence to produce a 239bp product. Wild type cells (WT) contained a band of the correct size (*), whilst annexin 2 -/- cells (-/-) did not (A). A control RT-PCR reaction (+) was also carried out to test the RT-PCR reaction and a 1.3Kb product is seen in lane 5 (B). Experimental samples were run alongside PCR markers (M1) and control reaction with λ DNA/*Eco*R1+*Hind*III markers (M2).

DT40 cells are chick cells and, consequently, do not express EGFR suitable for use of human EGF and anti-hEGFR-gold. To overcome this problem DT40 cells were transfected with hEGFR using nucleofection, but proved difficult to transfect due to high levels of spontaneous apoptosis (personal observations) and low transfection efficiency. Instead, an endogenous lymphocyte cell surface receptor was chosen. DT40 cells express high levels of cell surface IgM (B-cell receptor), which becomes internalised when activated by antigen binding. To investigate the internalisation of this receptor, an anti-chicken IgM antibody was conjugated to 10nm gold (Materials & Methods section 2.11.1.3). Cells were incubated with anti-IgM-gold for different lengths of time before processing for TEM. However, even after 2 hours, little gold was observed in cells and this may have been taken up by fluid phase endocytosis, rather than by receptor mediated endocytosis.

Therefore, to observe the effect of loss of annexin 2 on MVB formation, DT40 cells were incubated with markers taken up by fluid phase endocytosis. DT40s were incubated with HRP for 2 hours and processed for TEM (Material & Methods section 2.11.3). The morphology of MVBs was analysed but no difference was observed between wild type and annexin 2 -/- cells (Fig. 4.5).

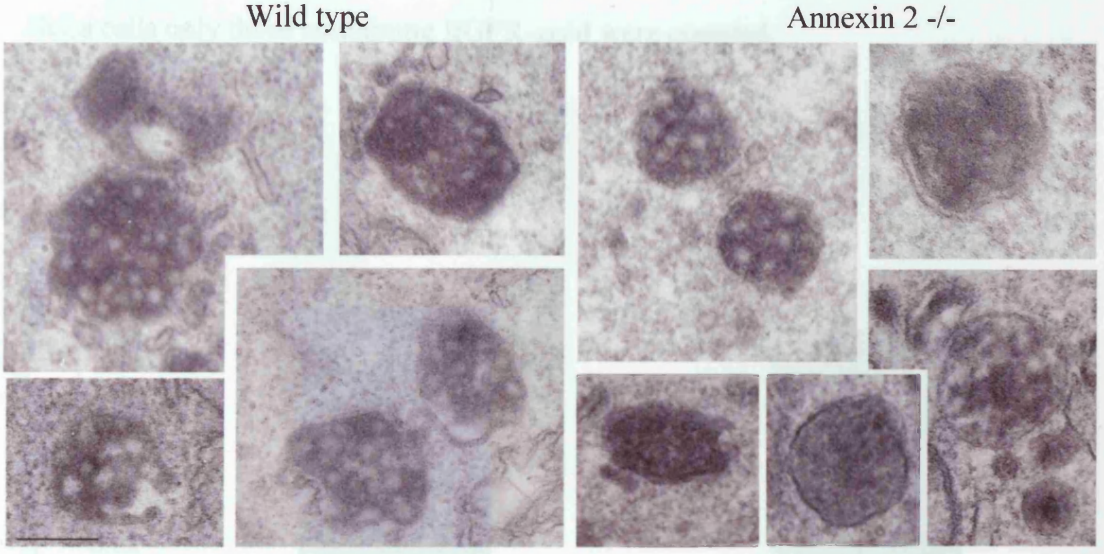

Figure 4.5. *Effect of loss of annexin 2 on MVB morphology.* DT40 cells were incubated with HRP for 2 hours, processed for TEM, including DAB reaction, and the morphology of MVBs analyzed. Electron micrographs show typical mature HRP-containing MVBs from each cell line. Loss of annexin 2 did not alter the morphology of HRP-containing MVBs, compared to those from wild type cells. Bar = 200nm.

Both cell lines contained MVBs with multiple internal vesicles, and the HRP/DAB reaction product was visible within these structures. MVBs from these DT40 cells, incubated with HRP, were counted to quantify the number of MVBs, as described above for RNAi-treated HeLa cells. No significant difference was observed in the number of MVBs formed in wild type or annexin 2 -/- cells (0.09 ± 0.003 compared to 0.085 ± 0.012) (Fig. 4.6). The number of MVBs per μm^2 cytoplasm was slightly higher than that seen in HeLa cells, but all MVBs were counted in DT40s, while in HeLa cells only those containing EGFR-gold were counted.

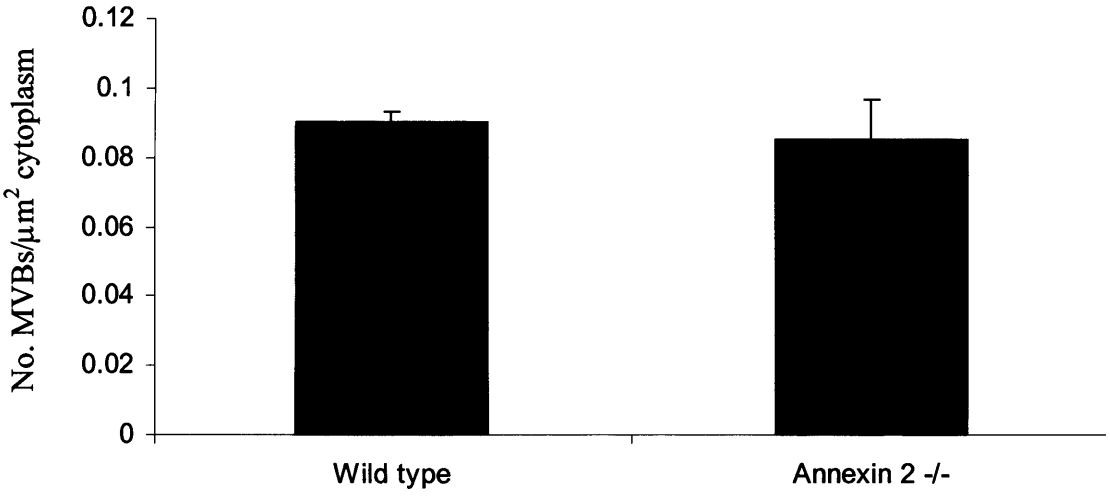

Figure 4.6. *Loss of annexin 2 has no effect on MVB formation.* DT40 cells were incubated with HRP for 2 hours, processed for TEM, including DAB reaction, and a number of random photos taken of each cell line. The area of cytoplasm per photo was measured. The number of MVBs per experiment were counted and expressed per μm^2 cytoplasm. There was no difference between cell lines. Graph shows the mean ± SEM of three independent experiments.

4.2.2 Loss of annexin 2 does not affect the size of MVBs formed

The depletion, or loss, of annexin 2 had no effect on the number of MVBs formed in either HeLa cells or DT40 cells. To analyse whether loss of annexin 2 altered the size of MVBs, the area of MVBs was measured in HeLa cells treated with control or annexin 2 RNAi, and also in both wild type and annexin 2 -/- DT40s. Fig. 4.7 shows that loss of annexin 2 does not affect the mean area of MVBs in

either HeLa or DT40 cells. The mean area of MVBs in annexin 2 RNAi-treated cells was slightly larger than that of control cells but this difference was not statistically significant. The mean area of MVBs in DT40 cells was smaller than that in HeLa cells (70000nm^2 in DT40s compared to 90000 nm^2 in HeLa cells), likely due to differences between species and/or cell types.

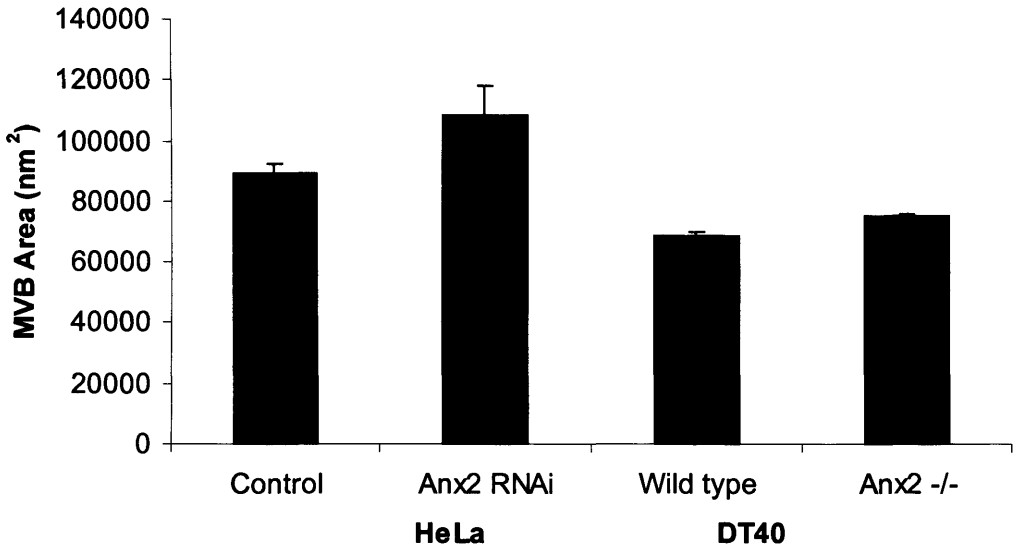

Figure 4.7. *Loss of annexin 2 has no effect on the area of MVBs.* The area (nm^2) of each MVB from the previously described HeLa annexin 2 RNAi and DT40 experiments was measured. For each cell line, the mean area of MVBs per experiment was calculated. The depletion, or total loss, of annexin 2 did not affect the area of MVBs. Graph shows the mean ± SEM of three independent experiments.

4.2.3 Inward vesiculation occurs independently of annexin 2

For each cell type (control or annexin 2 RNAi treated HeLa or wild type or knockout DT40), the number of internal vesicles per MVB was counted and the mean of 3 or more independent experiments calculated. There was a slight increase in the mean number of internal vesicles formed per MVB in annexin 2 RNAi treated cells, compared to control HeLa cells (26 ±1.5 compared to 22.8 ± 1.3) but this was not significant (Fig. 4.8). Similarly, there was no difference in the mean number of internal vesicles between wild type and annexin 2 -/- DT40s (Fig. 4.8). Both cell lines contained MVBs with an average of 17 internal vesicles. MVBs in

DT40 cells contained fewer internal vesicles than HeLa cells, but this was again probably due to the differences between species and/or cell type.

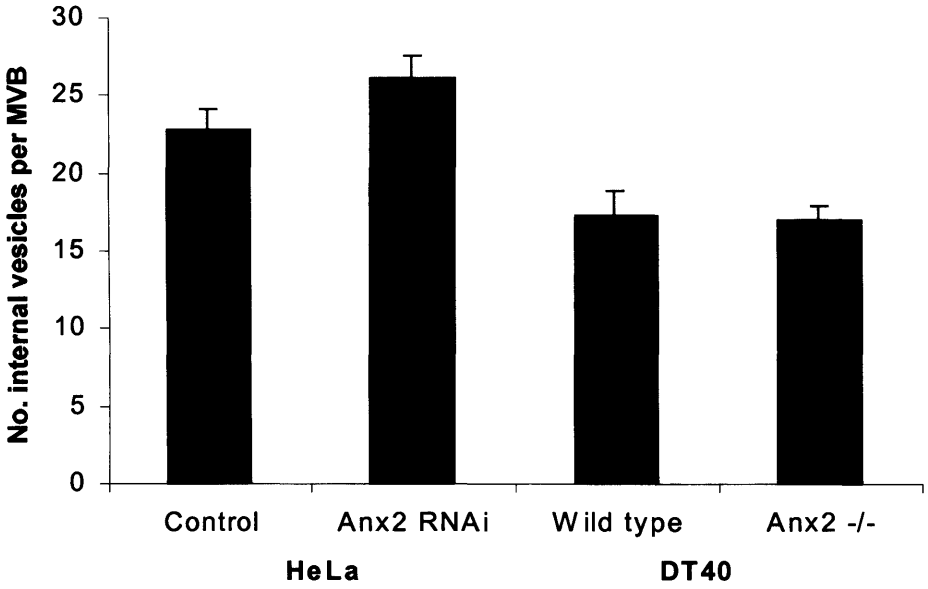

Figure 4.8. *Loss of annexin 2 does not alter inward vesiculation.* For each experiment the number of internal vesicles per MVB was counted and the mean per experiment calculated for HeLa cells and DT40s (A). Figure B shows the distribution of internal vesicles in a typical experiment. Loss of annexin 2 did not inhibit inward vesiculation. Graph shows the mean ± SEM of three independent experiments.

Although the mean number of internal vesicles per MVB did not differ between control and RNAi treated HeLa cells, or wild type and annexin 2 knockout DT40s, within a single experiment there was a range of MVBs containing different numbers of internal vesicles. To observe whether loss, or depletion, of annexin 2 altered the distribution of numbers of internal vesicles, MVBs were divided into different groups, based on number of internal vesicles, and expressed as a percentage of the total number of MVBs (Fig. 4.9). There was no significant difference between the percentages of MVBs in any group between control or RNAi-treated HeLa cells, or DT40 cell lines. The majority of MVBs in control or annexin 2 RNAi-treated HeLa cells contained 16 or more internal vesicles, and this was consistent with data from EGF-stimulated HeLa cells from the previous chapter investigating annexin 1. These data provide further confirmation that loss of annexin 2 has no effect on the process of inward vesiculation within MVBs.

A

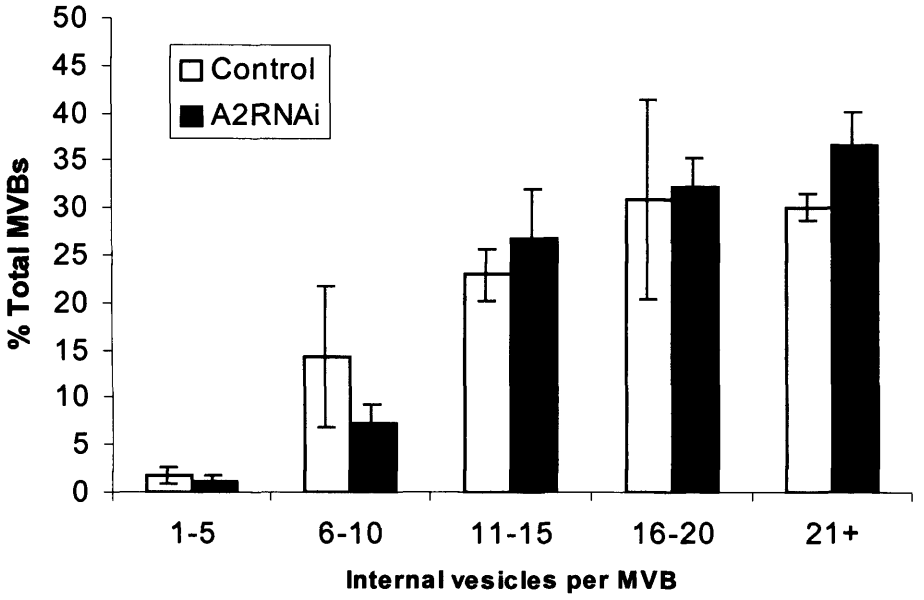

B

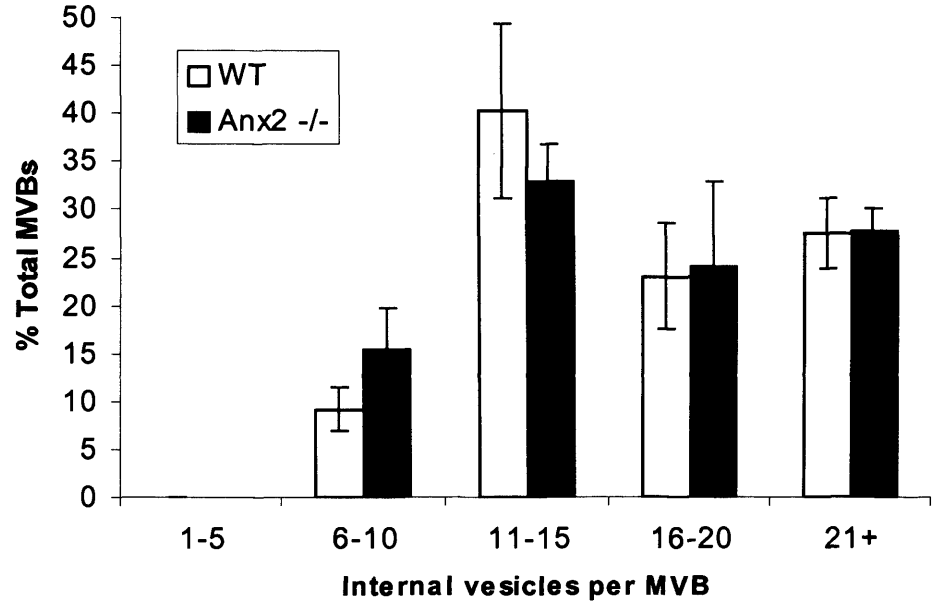

Figure 4.9. *Loss of annexin 2 does not affect the distribution of number of internal vesicles per MVB.* The numbers of internal vesicles per MVB were counted and MVBs divided into groups based on different numbers of internal vesicles in HeLa cells (A) and DT40s (B). Loss or depletion of annexin 2 had no effect on number of internal vesicles per MVB. Graphs show the mean ± SEM of three independent experiments

4.2.4 Depletion of annexin 1 and 2 has the same effect as loss of annexin 1 alone

RNAi-induced annexin 2 depletion, or total loss of annexin 2 through gene knockout, had no effect on MVB formation or inward vesiculation with MVBs in unstimulated or EGF-stimulated cells. As shown in the previous chapter, annexin 2 is upregulated in annexin 1 -/- cells, but cannot compensate for the loss of annexin 1 in EGF-stimulated internal vesicle formation. However, it is still possible that annexins 1 and 2 could compensate for each other in the process of MVB formation. Therefore, to investigate this possible functional redundancy, RNAi was used to deplete cells of both annexins 1 and 2. HeLa cells were treated with a combination of annexin 1 and annexin 2 RNAi oligonucleotides using nucleofection (described in Materials & Methods section 2.5.3). After 3 days, cell lysates were collected and blotted with anti-tubulin (loading control), anti-annexin 1 and anti-annexin 2 antibodies to determine the efficiency of knockdown (Fig. 4.10). Depletion of both annexins was similar to that observed in single RNAi experiments.

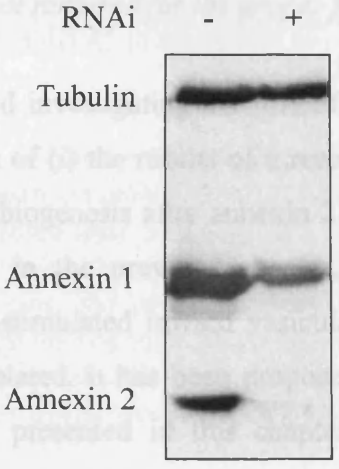

Figure 4.10. *RNAi-induced depletion of annexins 1 and 2 in HeLa cells.* HeLa cells were nucleofected with control (-) or a combination of annexin 1 and 2 RNAi oligonucleotides (+). After 24 hours, cells were re-transfected and left for 48 hours. On day 3, cell lysates were collected and blotted with anti-tubulin, anti-annexin 1 and anti-annexin 2. RNAi-treated cells were depleted for both annexins.

Having determined that depletion of both annexins at the same time did not affect cell viability, double RNAi-treated cells were serum starved, stimulated with EGF, in the presence of anti-hEGFR-gold, for 1 hour and processed for TEM. The morphology of anti-hEGFR-gold containing structures was observed in both control and double RNAi-treated cells. In both control cells and cells treated with annexin 1 and 2 RNAi, anti-hEGFR-gold containing MVBs were observed and there appeared to be no difference in the number or size of these structures. However, in the majority of cells treated with both annexin RNAi oligonucleotides, anti-hEGFR-gold containing MVBs contained few internal vesicles (Fig. 4.11). These MVBs were similar in morphology to those observed previously in annexin 1 RNAi-treated cells. These data indicate that neither annexin 1 nor annexin 2 is required for MVB formation. These findings provide further evidence that annexin 2 does not participate in EGF-stimulated inward vesiculation.

4.3 Discussion

4.3.1 Annexin 2 is not required for the proper formation of MVBs

The rationale behind investigating the role of annexin 2 in MVB formation came from a combination of (i) the results of a recently published study that reported an inhibition of MVB biogenesis after annexin 2 depletion (Mayran *et al.*, 2003), and (ii) data presented in the previous chapter, which reported that annexin 1 is necessary for EGF-stimulated inward vesiculation within MVBs. As annexins 1 and 2 are closely related, it has been proposed that they might play similar roles. However, the data presented in this chapter shows that neither RNAi-induced annexin 2 depletion nor loss of annexin 2, through gene knockout, had an effect on the formation of MVBs or on inward vesiculation within MVBs. It is important to note that within this study only anti-EGFR-gold containing MVBs were counted in annexin 2 RNAi-treated HeLa cells. As EGF-stimulation increased both MVB formation and inward vesiculation within MVBs (Chapter 3), these studies show that annexin 2 is not involved in EGF-stimulated MVB formation and also, unlike annexin 1, annexin 2 is not involved in EGF-stimulated inward vesiculation.

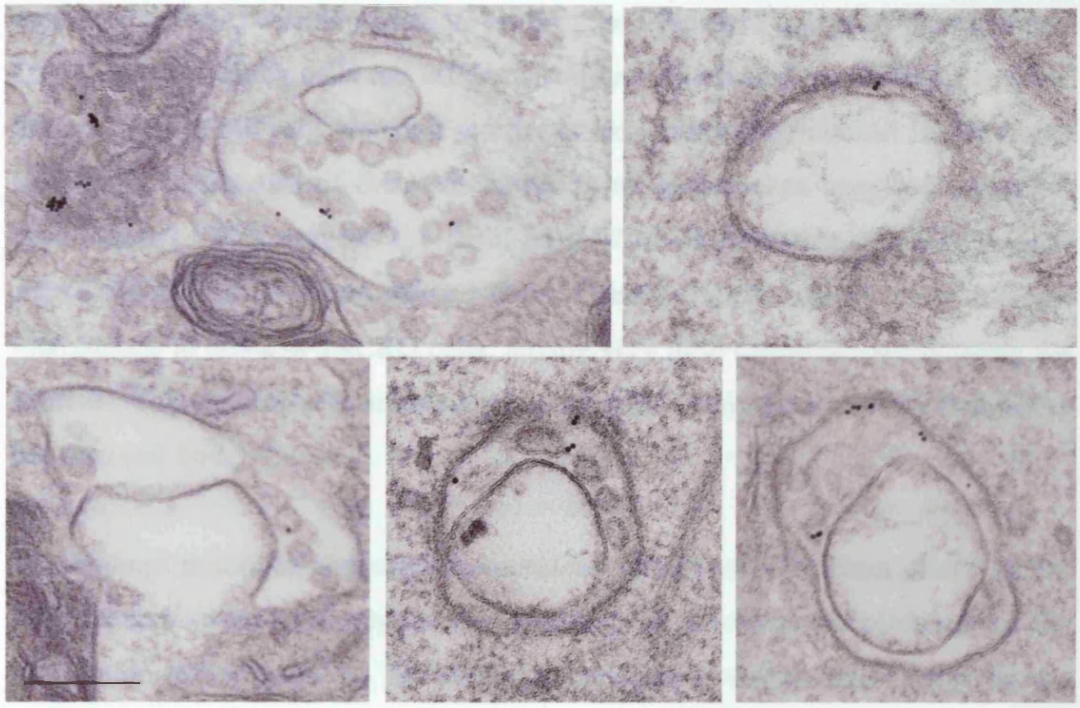

Figure 4.11. *Effect of double annexin depletion on MVB morphology.* HeLa cells were nucleofected with a combination of annexin 1 and 2 RNAi oligonucleotides. Cells were re-transfected after 24 hours and left for 48 hours. On day 3, cells were serum starved for 1 hour, stimulated with EGF (100ng/ml), in the presence of anti-hEGFR-gold, for 1 hour and processed for TEM. The morphology of MVBs was observed and electron micrographs show typical anti-hEGFR-gold containing MVBs from double RNAi-treated cells only, which show the same morphology as those observed in annexin 1 RNAi-treated cells, i.e. they contain few internal vesicles. Bar = 200nm.

DT40 cells were not EGF-stimulated and, therefore, the data from these cells is not directly comparable with that of annexin 2 RNAi-treated HeLa cells. However, studies using DT40 annexin 2 -/- cells show that annexin 2 is not required for MVB formation in unstimulated cells. Interestingly, the number of MVBs per μm^2 cytoplasm in DT40 cells was surprisingly high given the lack of EGF stimulation. There are several possible explanations for this. The first, and most likely, is that DT40 cells and HeLa cells are different cell types derived from different species. Secondly, the DT40 cells were not serum starved (unlike unstimulated JACRO cells in Chapter 3) because of their susceptibility to spontaneous apoptosis (personal observations). This suggests the basal level of MVB formation is higher in non-starved cells than in serum starved cells. Finally, DT40 cells have a different morphology to HeLa or JACRO cells, having very little cytoplasm surrounding the nucleus. This difference in morphology could affect comparisons of MVB numbers between cell lines.

The findings described above are inconsistent with those of Mayran *et al.* (2003). This group focussed initially on the influence of membrane cholesterol on the distribution of annexin 2, by studying cholesterol accumulation that occurs naturally in Niemann Pick C fibroblasts and through drug treatment in human skin fibroblasts. They reported that cholesterol accumulation in large swollen late endosomes and lysosomes caused a redistribution of annexin 2 to these structures, accompanied by an inhibition of transport from early to late endosomes, as observed by increased recycling of fluid phase markers. In the absence of cholesterol accumulation, annexin 2 was localised to the cytoplasm, the plasma membrane and early endosomes, in agreement with other published data (Harder and Gerke, 1993; Jost *et al.*, 1997).

Further investigation by Mayran *et al.* (2003) into the role of annexin 2 in endocytosis revealed that loss of annexin 2 inhibited early to late endosome transport of dextran and EGF. Dextran was recycled out of cells instead of being delivered to the lysosome, while EGF was retained in an enlarged EEA1 positive compartment. To determine whether the inhibition of transport from early to late endosomes was due to a failure of membrane fusion, an *in vitro* membrane fusion

assay was used. Depletion of annexin 2 from membranes and cytosol reduced membrane fusion by 50% but this reduction was insufficient to cause the dramatic inhibition of transport observed. Subsequently, the loss of annexin 2 on the *in vitro* formation of endosomal carrier vesicles/MVBs was investigated. This assay used early endosomes depleted of annexin 2 by drug treatment, and showed that these failed to form ECV/MVBs. Similarly, antibodies against annexin 2 inhibited ECV/MVB formation from normal endosomes. Finally, ultrastructural analysis of control cells showed HRP within MVBs of control cells, but in RNAi-treated cells HRP-containing structures were described as ring-shaped or tubular. However, annexin 2 was not involved in inward vesiculation as HRP was often present in multivesicular areas attached to these ring-shaped structures (Mayran *et al.*, 2003).

That annexin 2 is not involved in inward vesiculation is consistent with the data presented in this chapter. However, the ultrastructural analysis of MVB formation in HeLa cells depleted of annexin 2 performed here did not reveal any alteration in the morphology of MVBs compared to control cells. Normally inter-lab variations can be explained through the use of different cell lines or reagents. However, both sets of data used annexin 2 RNAi in HeLa cells. The studies in this chapter used a combination of two annexin 2 oligonucleotides, one of which is the published sequence from the work of Mayran *et al.* (2003). Having shown in the previous chapter that EGF-stimulation increases both MVB formation and inward vesiculation, it is possible that annexin 2 is involved in the formation of the non-EGFR containing sub-population of MVBs. Indeed the electron micrographs from Mayran *et al.* (2003) were from unstimulated cells, however, they also reported the inhibition of EGF transport to late endosomes. Therefore, it is unlikely that the work presented here and the work of Mayran *et al.* (2003) are looking at different populations of MVBs, as both sets of experiments used EGF stimulation. Additionally, the use of HRP, as a marker of fluid phase endocytosis, in unstimulated DT40 annexin 2 -/- cells failed to reveal any difference in MVB formation, when compared to wild type cells.

For ultrastructural analysis, Mayran *et al.* (2003) used nocodazole to depolymerise microtubules in HeLa cells before incubation with HRP. No reason was given for this treatment but it has commonly been used to accumulate MVBs by inhibiting

their transport from early endosomes to late endosomes/lysosomes. In control cells, normal MVBs formed, containing HRP, and failed to fuse with lysosomes due to the lack of microtubules. However, in cells lacking annexin 2 HRP-containing structures were shown to be mis-formed. Annexin 2 is required for the proper localisation of early endosomes (Harder and Gerke, 1993), and microtubules are required for the distribution of late endosomes and to facilitate delivery to the degradative pathway (van Deurs *et al.*, 1995; Durrbach *et al.*, 1996). It is therefore possible that loss of both annexin 2 and microtubules, at the same time, disrupts the localisation of endosomes, and that this mis-localisation is linked to the improper formation of MVBs observed by Mayran *et al.* (2003). In support of this theory, careful examination of the electron micrographs from the work of Mayran *et al.* (2003) shows a difference in the localisation of HRP-containing structures. In control cells, MVBs were present throughout the cytoplasm, whereas in RNAi-treated cells structures were shown close to the cell surface. This difference in localisation was not mentioned in the accompanying text. Taken together, it may be that efficient MVB formation and positioning may require both annexin 2 and intact microtubules.

However, the hypothesis described above does not explain the major finding of Mayran *et al.* (2003) that loss of annexin 2 inhibits delivery of EGF to the lysosome. The data presented in this chapter showed that EGF (as EGF-HRP) is delivered to lysosomes in annexin 2 depleted cells. This finding is consistent with those of the Gerke group, who reported that loss of annexin 2 had no effect on the delivery of fluid phase markers, or LDL, to the lysosome (Zobiack *et al.*, 2003).

The data presented in this chapter provides detailed quantitative measurement of the number and size of MVBs, and also the number of internal vesicles per MVB, from both EGF-stimulated HeLa cells depleted of annexin 2 and unstimulated annexin 2 -/- DT40 cells. In contrast, the finding of Mayran *et al.* (2003), that EGF transport to late endosomes is inhibited in cells depleted of annexin 2, was based on fluorescence images and no quantitation was performed. Quantitation of different HRP-containing structures was performed by Mayran *et al.* (2003), but only a small number of cells were observed to generate this data.

4.3.2 Differences in the nomenclature of endocytic compartments

A crucial difference between the work presented in this chapter and that of the Gruenberg lab (Mayran *et al.*, 2003) may stem from the definition of endocytic compartments. The definition of a MVB used here is a vacuole with a diameter ≥ 200nm and containing ≥ 1 internal vesicle. Although Mayran *et al.* (2003) gave no definition of a MVB, it appears that only MVBs with many internal vesicles were counted, and those that contained few internal vesicles were counted under a separate category. The data presented in both this chapter, and the previous chapter, showed that within a single experiment there is a wide range of MVBs containing different numbers of internal vesicles.

In a recent review, Gruenberg and Stenmark (2004) proposed a scheme whereby MVBs, also called endosomal carrier vesicles (ECVs), are defined as vacuoles that transport material from early to late endosomes, are multivesicular and LBPA negative (Gruenberg and Stenmark, 2004). According to this scheme, late endosomes contain both multivesicular and multilamellar regions and are LBPA positive. However, much data exists to suggest that MVBs/ECVs are more than just transport vesicles and also perform an important sorting function. This is shown by the gradual accumulation of lysosomally directed proteins, e.g. EGF and LDL, the gradual accumulation of internal vesicles and the gradual removal of recycling proteins, e.g. TfR (Hopkins *et al.*, 1990; van Deurs *et al.*, 1993; Futter *et al.*, 2001). Thus MVBs can be early and late; early MVBs have few internal vesicles and still contain recycling proteins, whereas late MVBs have many internal vesicles and lack recycling proteins. In conclusion, the differences in defining endocytic compartments need to be addressed, as the experiments in this chapter include a much wider variety of structure than those counted in the work of Mayran *et al.* (2003).

4.3.3 Annexin 2 is unable to functionally compensate for annexin 1

Annexins 2 and 6 are upregulated in JACRO annexin 1 -/- cells (Fig. 4.1) (Croxtall *et al.*, 2003), and it has been suggested that closely related annexins may

compensate for each other in various cellular function (Tomas *et al.*, 2003). In the previous chapter, RNAi was used to deplete levels of annexin 1 in HeLa cells for two reasons, to be able to use a human cell line but also to avoid the upregulation of annexin 2. However, even after 3 days of RNAi treatment annexin 2 was slightly upregulated in these cells. In this chapter, depletion of annexin 2 had no effect on MVB formation or inward vesiculation but these cells expressed slightly higher levels of annexin 1. Therefore, it is possible that the upregulation of these closely related members of the annexin family may partially compensate for each other. Furthermore, this compensation could mask the phenotype caused by loss of a single annexin. To explore this further, both annexins were targeted using RNAi-induced protein depletion. However, the effect observed on the formation of internal vesicles within MVBs was no greater, or different, to that observed with annexin 1 depletion alone. These data confirm that annexin 2 does not play a role in MVB formation or inward vesiculation.

4.3.4 Possible role for annexin 2

These studies provide extensive evidence that annexin 2 is not required for MVB formation in either unstimulated or EGF-stimulated cells, nor is it required for inward vesiculation. That annexin 2 is not involved with any aspect of MVBs investigated here is not surprising, as the majority of work on annexin 2 has identified it as associated with earlier endosomal structures, especially with recycling endosomes. Fractionation studies in rat hepatocytes failed to identify any annexin 2 associated with MVBs (Pol *et al.*, 1997). The apparent discrepancies between the data presented here and those of Mayran *et al.* (2003) could be due, in part, to the nomenclature used to describe endocytic compartments. Also, the lack of fusion activity *in vitro* does not always translate *in vivo*. It therefore seems more likely that annexin 2 is playing a role at a different stage of endocytosis, possibly within recycling endosomes (Zobiack *et al.*, 2003).

4.3.5 Summary of findings

These data provide conclusive evidence that annexin 2 is not required for the proper formation of MVBs in unstimulated DT40 cells, nor in the formation of EGF-stimulated MVBs in HeLa cells. Furthermore, unlike annexin 1, annexin 2 is not required for the formation of internal vesicles in MVBs of EGF-stimulated cells. This latter finding is consistent with those of Mayran *et al.* (2003), although this group also report that annexin 2 depletion inhibits early to late endosomal transport through a failure of MVBs to bud off from endosomes.

Chapter 5 – Annexins and receptor trafficking

5.1 Introduction

As shown in the previous chapters, neither annexin 1 nor annexin 2 were required for basal or EGF-stimulated formation of MVBs. Internal vesicles could form within MVBs in the absence of either, or both, annexins. However, annexin 1, but not annexin 2, was required for the EGF-stimulated increase in inward vesiculation. The inhibitory effect observed on EGF-stimulated inward vesiculation led to the proposal that annexin 1 may be involved in EGF/EGFR trafficking. Although internal vesicles form in the absence of EGF-stimulation, a proposed role of internal vesicle formation is to remove EGFR from the recycling pathway. Therefore, an inhibition of inward vesiculation, as seen in annexin 1 -/- cells, would be expected to alter EGFR trafficking, by promoting receptor recycling and thus reducing EGF/EGFR degradation. However, it is likely that inward vesiculation plays more than one role. Receptor sorting within MVBs can be divided into cargo selection for inclusion on internal vesicles and formation of internal vesicles. These processes are believed to be coupled through the FYVE-domain containing protein Hrs, which recruits the ESCRT complexes (Urbe *et al.*, 2003). However, Futter *et al.* (2001) showed that it was possible to uncouple receptor sorting from inward vesiculation, using wortmannin to inhibit PI3K dependent processes (Futter *et al.*, 2001). As seen with wortmannin treated cells, a small number of internal vesicles still form in MVBS from annexin 1 -/- cells and these often contained anti-hEGFR-gold, showing that EGFR could still be sorted onto internal vesicles. Quantification of EGFR sorting onto internal vesicles has proved difficult, as when internal vesicles are close to the perimeter membrane, it is not always clear whether the anti-hEGFR-gold is present on the limiting membrane or on the internal vesicle. Therefore, to obtain accurate quantitative measurements of the effect of loss of annexin 1 on receptor sorting in these studies, biochemical analysis of radio labelled EGF degradation and EGF/Tf recycling was performed.

Despite the failure to observe an effect of annexin 2 depletion on any aspect of MVB biogenesis, the question of whether annexin 2 is involved in receptor sorting has been raised. The data presented in the previous chapter contradicted published work from Mayran *et al.* (2003) that stated annexin 2 is required for MVB biogenesis. Work from the same group also reported that annexin 2 depletion inhibited the transport of EGF from early to late endosomes, but did not affect Tf internalisation or trafficking (Mayran *et al.*, 2003). However, these experiments were based on the use of fluorescent ligands and no quantitation was performed. The use of radio labelled EGF to measure degradation and recycling is very sensitive, even to small differences, and therefore was used in this chapter to compare EGF-trafficking in control and annexin 2 RNAi-treated cells.

The data presented in this chapter show that EGF degradation was unaffected by loss of either annexin, but that EGFR degradation was altered in cells lacking annexin 1, but not annexin 2. This delay in EGFR degradation, or inhibition of a small proportion of EGFR to become degraded, was accompanied by an enhancement of downstream phosphorylation i.e. signalling. Meanwhile, annexin 2 depletion was shown to have no effect on any aspect of EGF/EGFR trafficking. Instead, annexin 2 appears to be involved in the positioning of Tf positive recycling endosomes.

5.2 Results

5.2.1 EGF degradation is not affected by loss of annexin 1 or annexin 2 depletion

To measure the kinetics of EGF degradation in JACRO cells, both wild type and annexin 1 -/- cells were incubated with I-125 labelled EGF (^{125}I-EGF) for 10 minutes at 37°C to allow internalisation. Surface bound EGF was stripped and internalised EGF chased through cells using warm serum-free medium. At each time point, medium was collected and counts per minute (cpm) measured using a gamma counter. Cells were solubilised using Triton X-100 (Tx100) to release remaining EGF. Within the lysosome, EGF is degraded into single amino acids,

which releases the ^{125}I labelled tyrosine. After EGF degradation, iodotyrosines are able to freely diffuse across membranes, and so are rapidly released into the medium. At the same time recycled ^{125}I-EGF will also be present in the media. To distinguish between degraded and recycled label, all media samples were incubated with trichloroacetic acid (TCA) for 1 hour at 4°C and centrifuged to form a pellet. Iodotyrosines, from the degraded EGF, are soluble in TCA and remain in the supernatant, whereas ^{125}I-EGF that has been recycled is TCA precipitatable. The percentage of internalised EGF degraded was calculated for each time point (see Materials & Methods section 2.8.4).

Despite the marked change in morphology of EGFR-containing MVBs observed in annexin 1 -/- cells, there was no difference in the kinetics of EGF degradation between JACRO cell lines (Fig. 5.1A). After 1 hour, 20% EGF was degraded in both cell lines and the percentage of EGF degraded showed a linear increase up to 2 hours (46% degraded) and reached a plateau at 3 hours (56% EGF was degraded in both cell lines).

While the majority of EGF and its receptor are degraded, a small amount is constitutively recycled back to the cell surface. In the experiments described above, the percentage of EGF recycled at each time point was also calculated. Wild type cells recycled 7% more EGF than annexin 1 -/- cells after 3 hours incubation (Fig. 5.1B). This small increase was statistically significant ($p<0.05$). At each time point, wild type cells consistently recycled slightly more EGF than annexin 1 -/- cells and this increase was statistically significant at each time point after 25 minutes. As the percentage of EGF degraded was not increased in annexin -/- cells, the average percentage EGF remaining in the cell after 3 hours was calculated (Fig. 5.2). After 3 hours, 9.8% of internalised EGF remained in wild type cells compared to 13.8% annexin 1 -/- cells, and this difference was statistically significant.

A

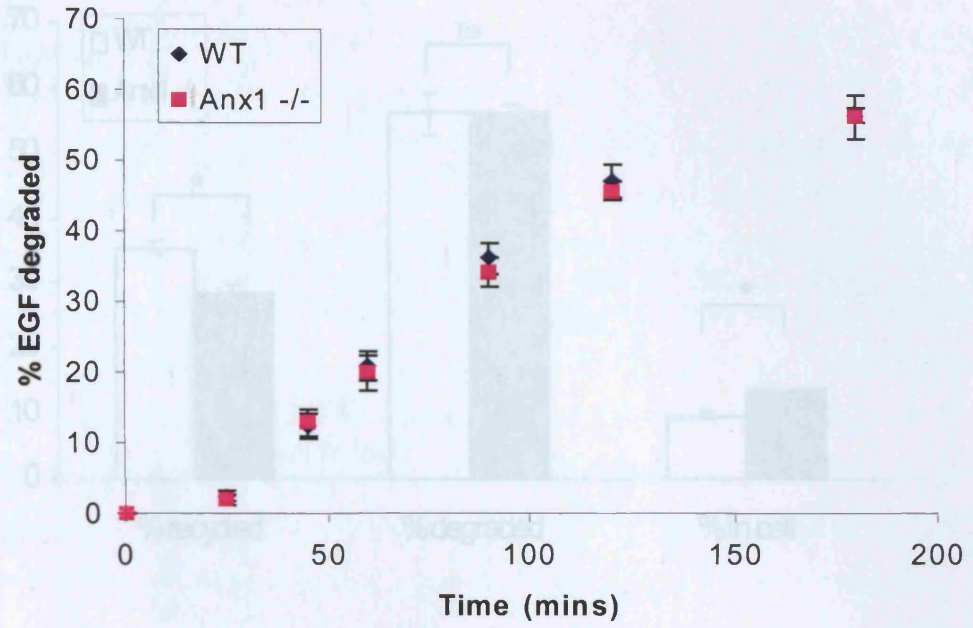

B

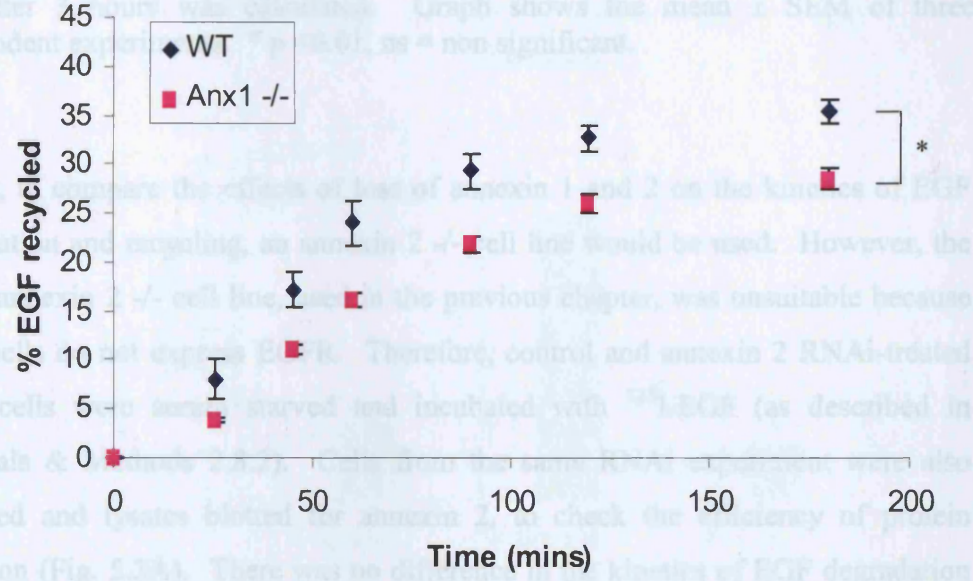

Figure 5.1. *Loss of annexin 1 does not affect the kinetics of EGF degradation.* JACRO cells were serum starved and incubated with ^{125}I-EGF for 10 minutes at 37°C. Surface bound EGF was stripped and cells were incubated with warm medium to chase EGF through the cell. Medium was collected at different time points and cpm measured. Each medium sample was TCA precipitated and the cpm in the TCA soluble supernatant measured. The percentage of EGF degraded (A) or recycled (B) was calculated (see Materials & Methods section 2.8.4). There was no difference between cell lines in the rate of EGF degradation, although loss of annexin 1 decreased the amount of EGF recycled. Graphs show mean ± SEM of three independent experiments. * $p<0.05$.

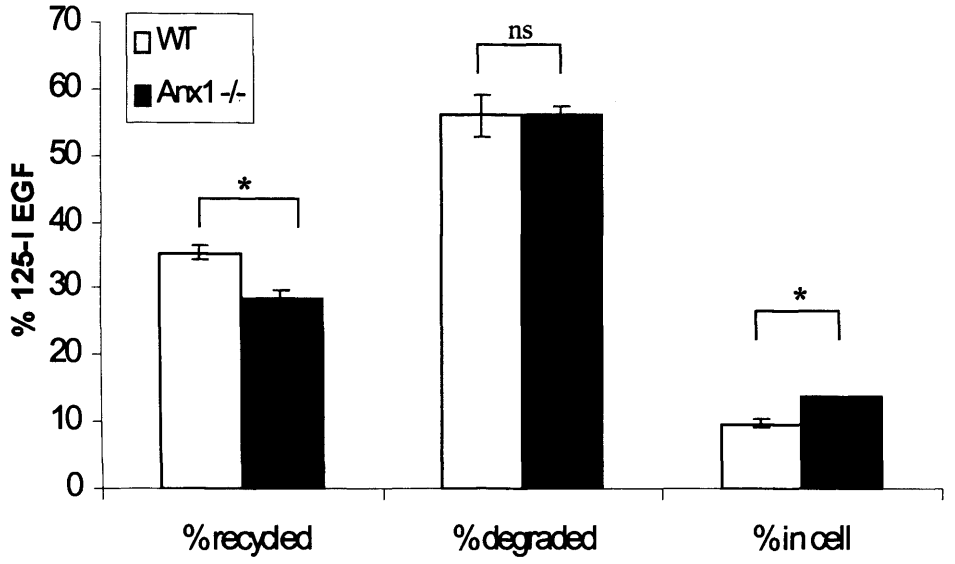

Figure 5.2. *Effect of loss of annexin 1 on EGF trafficking.* From the experiments shown in Fig. 5.1 the percentage of EGF recycled, degraded, and remaining in the cell, after 3 hours was calculated. Graph shows the mean ± SEM of three independent experiments. * $p < 0.01$, ns = non significant.

Ideally, to compare the effects of loss of annexin 1 and 2 on the kinetics of EGF degradation and recycling, an annexin 2 -/- cell line would be used. However, the DT40 annexin 2 -/- cell line, used in the previous chapter, was unsuitable because these cells do not express EGFR. Therefore, control and annexin 2 RNAi-treated HeLa cells were serum starved and incubated with ^{125}I-EGF (as described in Materials & Methods 2.8.2). Cells from the same RNAi experiment were also collected and lysates blotted for annexin 2, to check the efficiency of protein depletion (Fig. 5.3A). There was no difference in the kinetics of EGF degradation between control and annexin 2 RNAi-treated cells (Fig. 5.3A). After 4 hours, ~70% EGF had been degraded in both control and RNAi treated cells. Similarly, there was no significant difference observed at any time point in the percentage of EGF recycled between cell types (Fig. 5.3B). After 4 hours, ~16% EGF had been recycled out of control and annexin 2 RNAi-treated cells. Finally, there was no difference in the percentage of EGF remaining in cells after 4 hours. In both control and annexin 2 -/- cells, there was approximately 11% EGF remaining (Fig. 5.3C), which was consistent with the percentage calculated in JACRO cells.

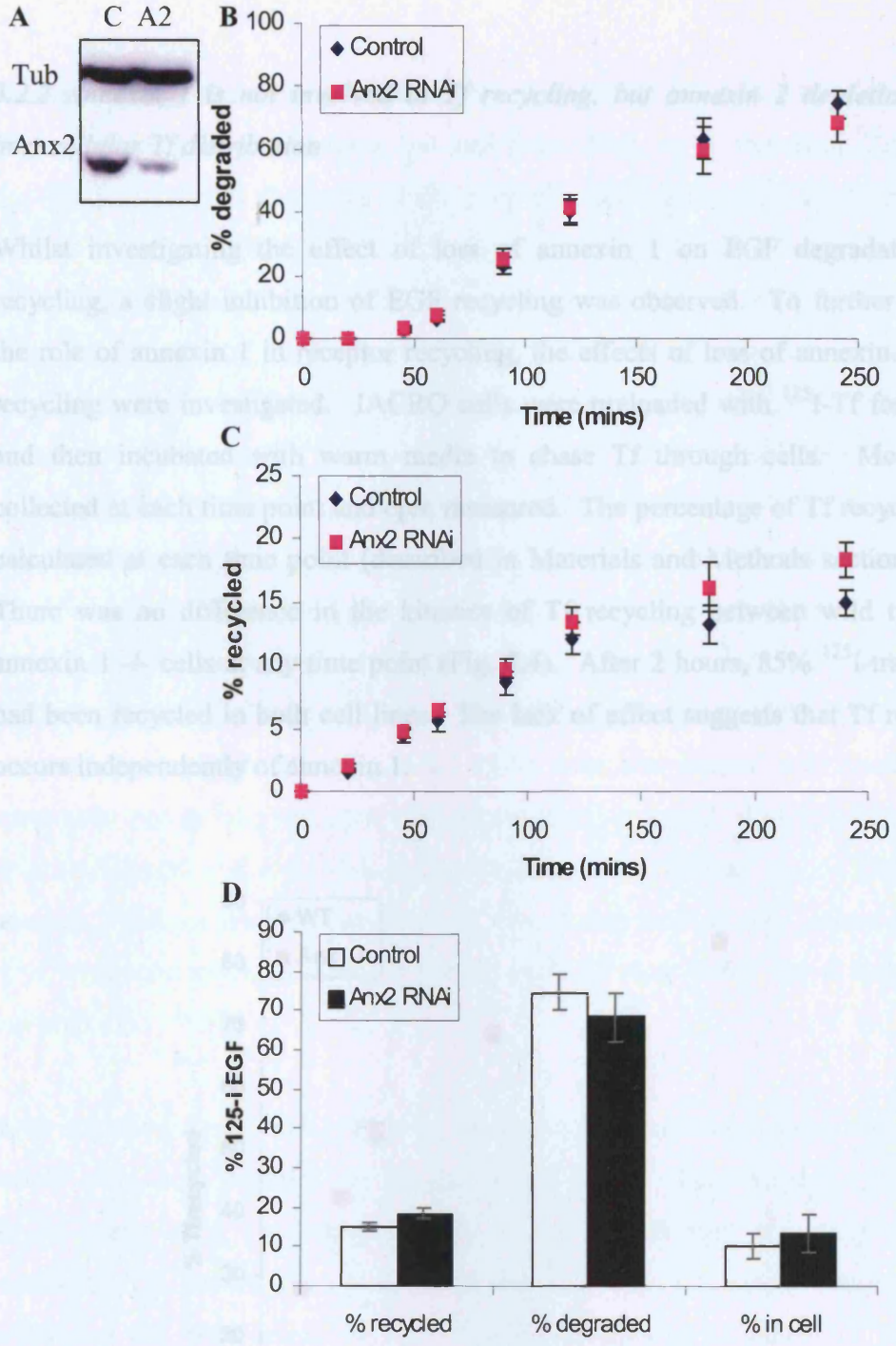

Figure 5.3. *Depletion of annexin 2 has no effect on EGF degradation or recycling.* HeLa cells were transfected with control (C) or annexin 2 RNAi (A2) for 3 days. Cell lysates were blotted with anti-tubulin (tub) and anti-annexin 2 (Anx2) to check efficiency of knockdown (A). Cells were serum starved before a 10 minute incubation with ^{125}I-EGF at 37°C. Surface bound EGF was removed and internalised EGF was chased through cells. Media was collected at each time point and EGF remaining in cells was released using 1% Tx100. All media samples were TCA precipitated to determine how much EGF was recycled or degraded at each time point. Graphs show percentage of EGF degraded (B), recycled (C) and a comparison of percentages (D). There was no difference between control and annexin 2 RNAi-treated cells in the kinetics of EGF degraded or recycled. Graphs show mean ± SEM of four independent experiments.

5.2.2 Annexin 1 is not involved in Tf recycling, but annexin 2 depletion alters intracellular Tf distribution

Whilst investigating the effect of loss of annexin 1 on EGF degradation and recycling, a slight inhibition of EGF recycling was observed. To further explore the role of annexin 1 in receptor recycling, the effects of loss of annexin 1 on Tf recycling were investigated. JACRO cells were preloaded with ^{125}I-Tf for 1 hour and then incubated with warm media to chase Tf through cells. Media was collected at each time point and cpm measured. The percentage of Tf recycled was calculated at each time point (described in Materials and Methods section 2.8.4). There was no difference in the kinetics of Tf recycling between wild type and annexin 1 -/- cells at any time point (Fig. 5.4). After 2 hours, 85% ^{125}I-transferrin had been recycled in both cell lines. The lack of effect suggests that Tf recycling occurs independently of annexin 1.

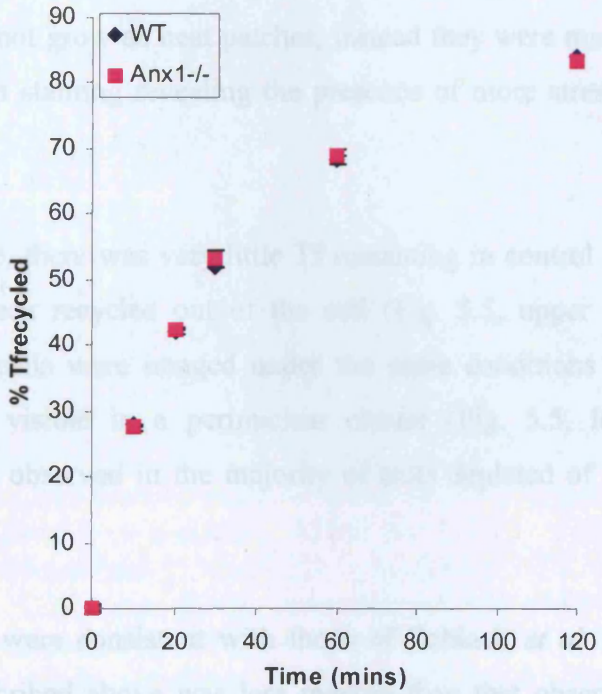

Figure 5.4. *Loss of annexin 1 has no effect on Tf recycling.* JACRO cells were preloaded with ^{125}I-Tf for 1 hour and then incubated with warm medium to chase Tf through cells. Medium was collected at different time points and cpm measured. The cpm in each media sample represents the recycled Tf and this was expressed as a percentage of the total Tf internalised. There was no difference in the kinetics of Tf recycling between cell lines. Graph shows the mean ± SEM of three independent experiments.

Recent studies have reported that annexin 2 depletion induced a relocalisation of Tf-positive recycling endosomes but had little effect on Tf recycling (Zobiack *et al.*, 2003). Around the same time, a conflicting report stated that annexin 2 depletion had no effect on Tf internalisation or the distribution of Tf positive endosomes (Mayran *et al.*, 2003). As the data presented in the previous chapter was inconsistent with the findings of Mayran *et al.* (2003), who also reported that annexin 2 depletion inhibited MVB biogenesis, these published experiments were repeated to determine the exact nature of the effect of annexin 2 depletion on the distribution of Tf-containing recycling endosomes. Therefore, HeLa cells treated with control or annexin 2 RNAi were serum starved, incubated with fluorescent Tf for 5 minutes followed by a 20 minutes chase with serum free media. Cells were fixed and processed for immunofluorescence (as described in Materials and Methods 2.10). Cells were labelled with an anti-annexin 2 antibody to identify successfully depleted cells (Fig. 5.5). Cells were also stained with phalloidin to label actin and to help visualise cells depleted of annexin 2. Control cells formed neat monolayers and actin staining was spread throughout the cell. Cells lacking annexin 2 did not grow as neat patches, instead they were mostly present as single cells with actin staining revealing the presence of more stress fibres than seen in control cells.

After the chase, there was very little Tf remaining in control cells, as the majority would have been recycled out of the cell (Fig. 5.5, upper panels). Annexin 2 RNAi-treated cells were imaged under the same conditions and many cells still contained Tf, visible in a perinuclear cluster (Fig. 5.5, lower panels). This difference was observed in the majority of cells depleted of annexin 2 but not in wild type cells.

These finding were consistent with those of Zobiack *et al.* (2003), although the phenotype described above was less marked than that observed in the published study. These Tf-containing structures were studied further using TEM. Cells were incubated with Tf-HRP for 5 minutes followed by a 20 minute chase, as a repeat of the experiment performed using fluorescence, and embedded for TEM. However, analysis of both control and annexin 2 RNAi-treated cells failed to reveal any Tf-HRP-containing structures, as identified by the product of the HRP/DAB reaction.

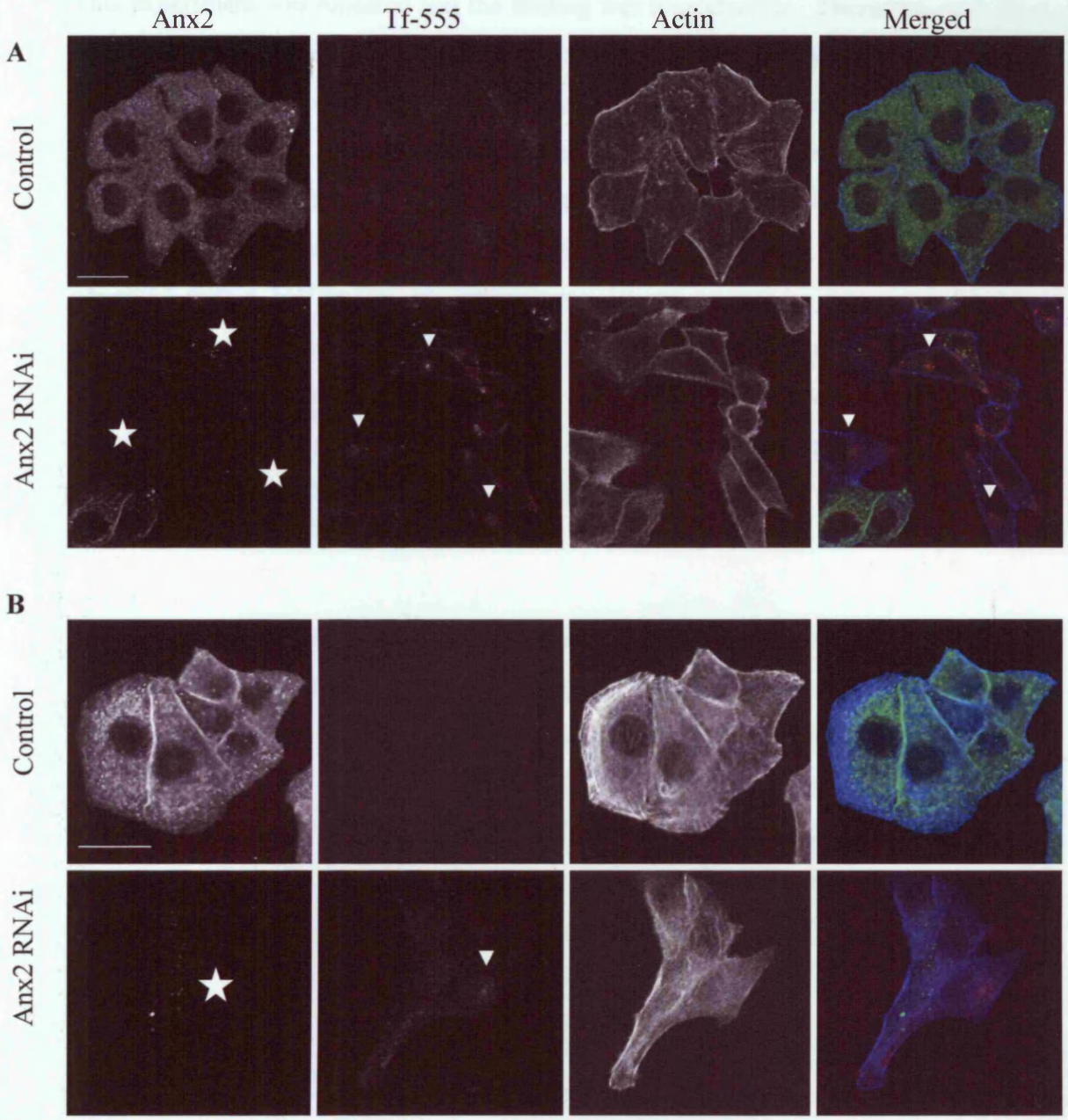

Figure 5.5. *Annexin 2 depletion causes a redistribution of Tf positive endosomes.* HeLa cells were treated with control or annexin 2 RNAi for 3 days. Cells were serum starved and incubated with Tf-AlexaFluor-555 (red) for 5 minutes at 37°C and then with media for 20 minutes at 37°C. Cells were fixed, permeabilised and stained using an anti-annexin 2 antibody (green) and phalloidin (blue), to label actin. Tf accumulated in cells depleted of annexin 2. Typical images are shown for each treatment (A - low magnification; B - higher magnification). Stars indicate some cells depleted of annexin 2. White arrows point to areas of concentrated Tf. Bars = 20μm.

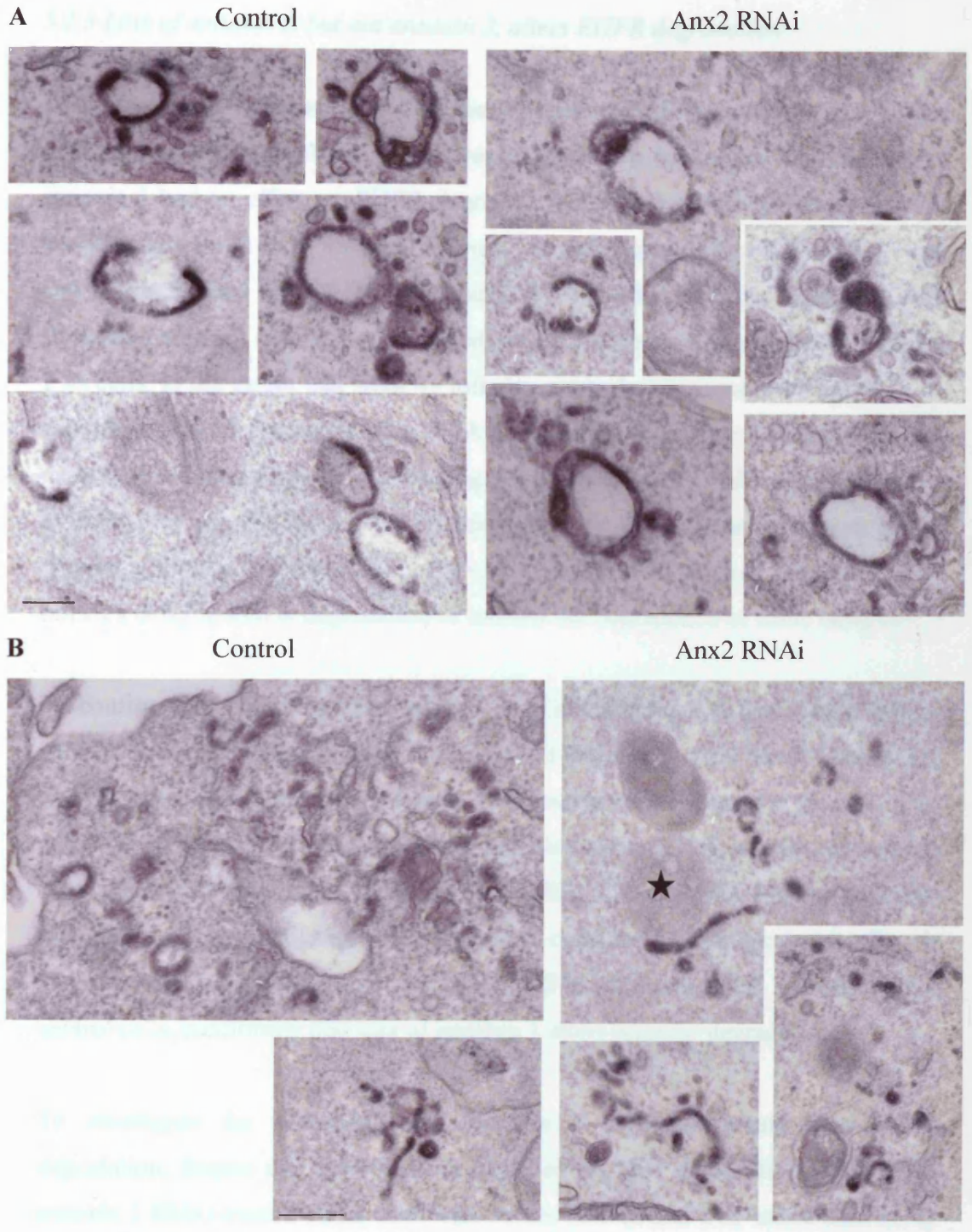

Figure 5.6. *Localisation of Tf-containing endocytic structures in annexin 2 RNAi-treated cells.* HeLa cells were treated with control or annexin 2 RNAi for 3 days. Cells were serum starved and incubated with Tf-HRP for 1 hour before processing for TEM. Typical Tf-HRP containing structures are shown (A) and tubular structures (B). Non-Tf-HRP containing MVB (*). Bar = 200nm

5.2.3 Loss of annexin 1, but not annexin 2, alters EGFR degradation

Loss of annexin 1 had no effect on the kinetics of EGF degradation, despite the inhibition of EGF-stimulated inward vesiculation. To investigate whether loss of annexin 1 had an effect on EGFR degradation, JACRO cells were serum starved and stimulated with EGF for up to 3 hours. At each time point cells were harvested and lysates blotted for EGFR and tubulin, as a loading control. Although EGF stimulated receptor degradation occurred in both cell lines, it was altered in annexin 1 -/- cells, to the extent that from 45 minutes onwards there was more EGFR in -/- cells than in wild type cells (Fig. 5.7A). Although wild type cells have slightly more EGFR than annexin 1 -/- cells (Fig. 3.1B), most of the EGFR signal was gone by 3 hours. At this time point in annexin 1 -/- cells, there was more EGFR remaining than in wild type cells. These data indicate that loss of annexin 1 either causes a delay in EGFR degradation or inhibits the degradation of some receptors.

To confirm that the alteration observed in EGFR degradation was due to loss of annexin 1, control and annexin 1 RNAi-treated HeLa cells were serum starved and stimulated with EGF for up to 3 hours. Cell lysates were collected at the same time points as in the JACRO cell experiment, and blotted for EGFR, tubulin and annexin 1, to check efficiency of knockdown (Fig. 5.7B). Western blot analysis indicated that annexin 1 was depleted in RNAi-treated cells, compared to control cells. In annexin 1 depleted cells, there was more EGFR remaining after 3 hours than in control cells, confirming that loss of annexin 1 alters receptor degradation.

To investigate the possibility that annexin 2 depletion would alter EGFR degradation, despite the lack of effect observed on EGF degradation, control and annexin 2 RNAi-treated HeLa cells were serum starved and EGF stimulated for up to 3 hours. Cell lysates were blotted for annexin 2 to check for efficiency of protein depletion (Fig. 5.7C). Lysates were also blotted with an anti-tubulin antibody, to ensure equal protein loading, and anti-EGFR, to analyse EGFR degradation. As expected, there was no difference in EGFR degradation between control and annexin 2 RNAi-treated HeLa cells. In both cell lines significant EGFR degradation had occurred by 90 minutes. By 180 minutes there was very little EGFR remaining in either cell line.

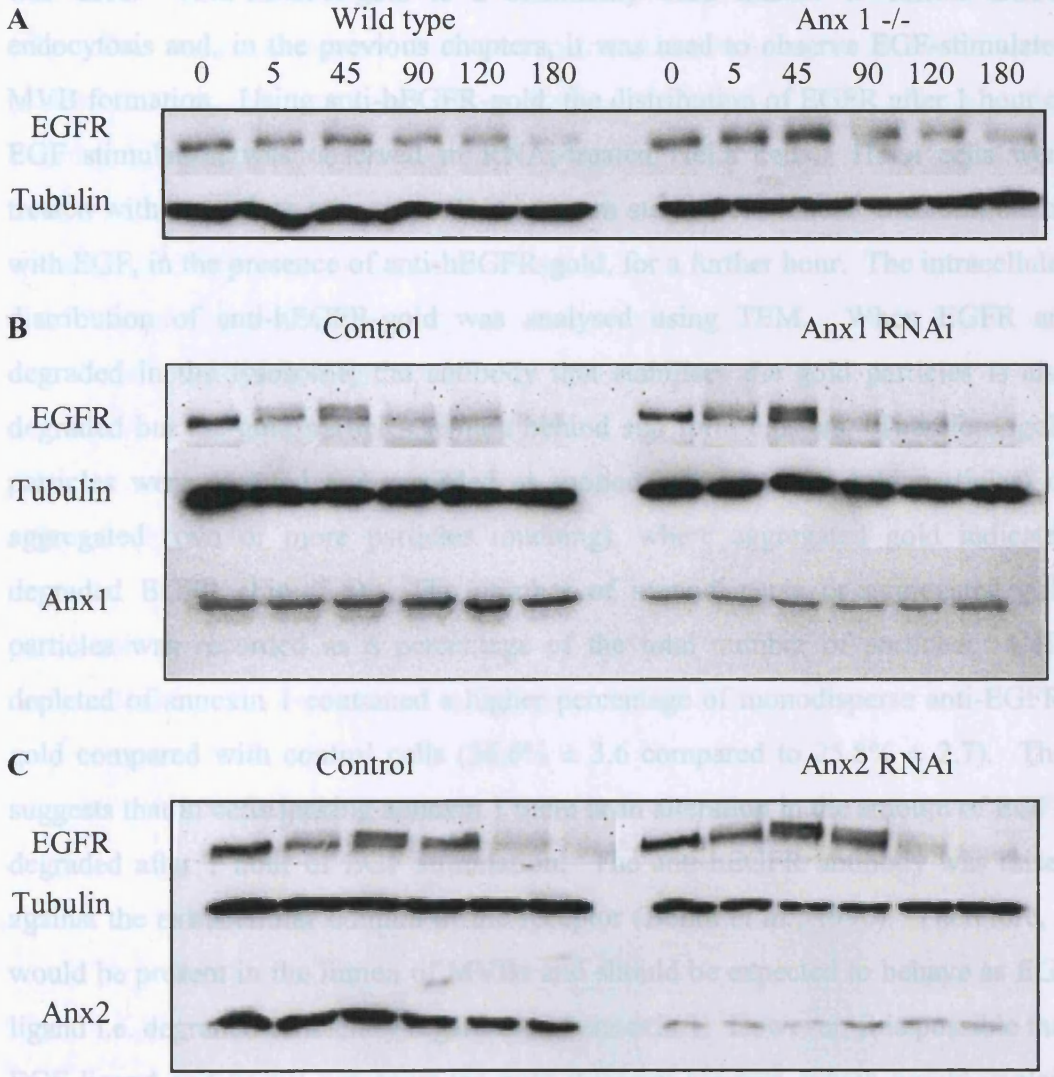

Figure 5.7. *Loss of annexin 1, but not annexin 2, alters EGFR degradation.* JACRO cells (A), annexin 1 RNAi-treated (B) or annexin 2 RNAi-treated HeLa cells (C) were serum starved, incubated with EGF and cell lysates collected at different time points of EGF stimulation. JACRO cell lysates were blotted with anti-EGFR and anti-tubulin. EGFR degradation was altered in annexin 1 -/- cells compared to wild type cells, as more remained undegraded in -/- cells after 3 hours. RNAi-treated cell lysates were blotted for EGFR, tubulin and annexin 1 (B) or annexin 2 (C), to check for efficient protein depletion. Annexin 1 depletion resulted in altered EGFR degradation, but depletion of annexin 2 had no effect.

The above data show that loss of annexin 1, but not annexin 2, alters the amount of EGFR degraded over 3 hours. As the effect observed on EGFR degradation was quite subtle, a further assay of the efficiency with which EGFR reach the lysosome was used. Anti-hEGFR-gold is a commonly used marker to follow EGFR endocytosis and, in the previous chapters, it was used to observe EGF-stimulated MVB formation. Using anti-hEGFR-gold, the distribution of EGFR after 1 hour of EGF stimulation was observed in RNAi-treated HeLa cells. HeLa cells were treated with control or annexin 1 RNAi, serum starved for 1 hour, then stimulated with EGF, in the presence of anti-hEGFR-gold, for a further hour. The intracellular distribution of anti-hEGFR-gold was analysed using TEM. When EGFR are degraded in the lysosome, the antibody that stabilises the gold particles is also degraded but the gold particles remain behind and form clusters. Therefore, gold particles were counted and recorded as monodisperse (single gold particles) or aggregated (two or more particles touching), where aggregated gold indicated degraded EGFR (Fig. 5.8). The number of monodisperse or aggregated gold particles was recorded as a percentage of the total number of particles. Cells depleted of annexin 1 contained a higher percentage of monodisperse anti-EGFR-gold compared with control cells (36.6% ± 3.6 compared to 25.8% ± 2.7). This suggests that in cells lacking annexin 1 there is an alteration in the amount of EGFR degraded after 1 hour of EGF stimulation. The anti-hEGFR antibody was raised against the extracellular domain of the receptor (Bellot *et al.*, 1990). Therefore, it would be present in the lumen of MVBs and should be expected to behave as EGF ligand i.e. degraded efficiently regardless of annexin 1. However, it is possible that EGF ligand and EGFR are degraded with different kinetics, which would explain the above result.

The previous chapters focused on the quantitation of MVBs following EGF stimulation. The biochemical experiments described above indicate that annexin 2 depletion had no effect on the kinetics of EGF/EGFR degradation. Nevertheless, annexin 2 has been proposed to play a role in maintaining the distribution of endosomes (Harder and Gerke, 1993) and so to investigate whether the loss of annexin 2 affected any part of the endocytic pathway, annexin 2 RNAi-treated HeLa cells were stimulated with EGF, in the presence of anti-hEGFR-gold, for different time periods and ultimately processed for TEM. The electron micrographs

in Figure 5.9 show typical anti-hEGFR-gold containing structures in both control and annexin 2 RNAi treated cells. No difference was observed in the distribution of anti-hEGFR-gold at any time point. After 10 minutes EGF stimulation, most anti-hEGFR-gold was near the cell surface, either in CCPs or in early endosomes (Fig. 5.9a). After 30 minutes EGF stimulation, there was more anti-hEGFR-gold present in both cell types and the majority was found in both immature (few vesicles) and mature (many vesicles) MVBs (Fig. 5.9b). Previous experiments have shown that after 1 hour of EGF stimulation mature, anti-hEGFR-gold containing MVBs were present in both control and annexin 2 RNAi treated cells (see Chapter 5). After 1 hour, a significant proportion of anti-hEGFR-gold was also found in lysosomes (Fig. 5.9c).

The percentage of monodisperse anti-hEGFR-gold compared to aggregated gold was calculated for annexin 2 RNAi treated cells, as described previously for annexin 1 RNAi treated cells (Fig. 5.8). There was no difference in the percentage of monodisperse anti-hEGFR-gold between annexin 2 RNAi-treated and control cells, indicating that annexin 2 is not involved in EGFR degradation.

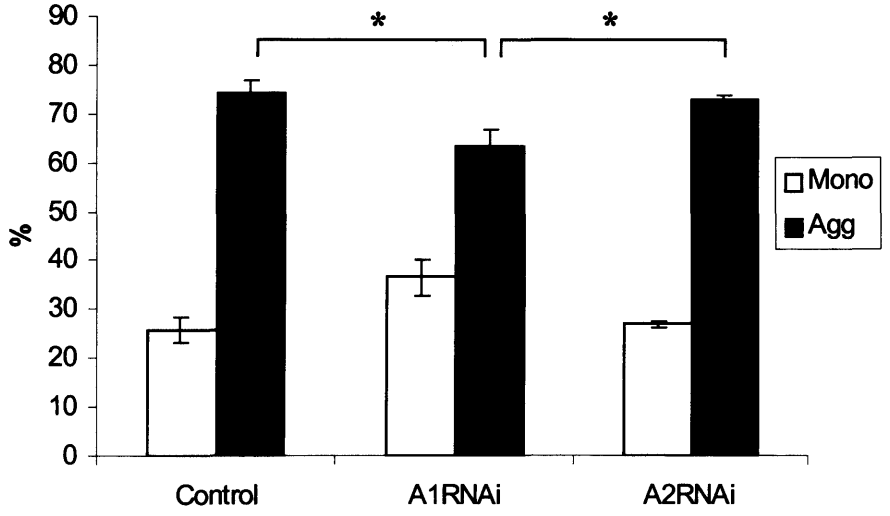

Figure 5.8. *RNAi induced depletion of annexin 1 delays EGFR degradation.* HeLa cells were treated with control, annexin 1 or annexin 2 RNAi for 3 days. Cells were serum starved before stimulation with EGF and anti-EGFR-gold for 1 hour. Cells were processed for TEM and the distribution of EGFR-gold was analysed. Gold particles were counted in a number of cells and recorded as monodisperse or aggregated (2 or more gold particles touching). Cells treated with annexin 1 RNAi showed a slight decrease in aggregated gold, compared to control or annexin 2 RNAi treated cells. Graphs show mean ± SEM of three independent experiments. In total, 10911 gold particles were counted. * $p<0.05$.

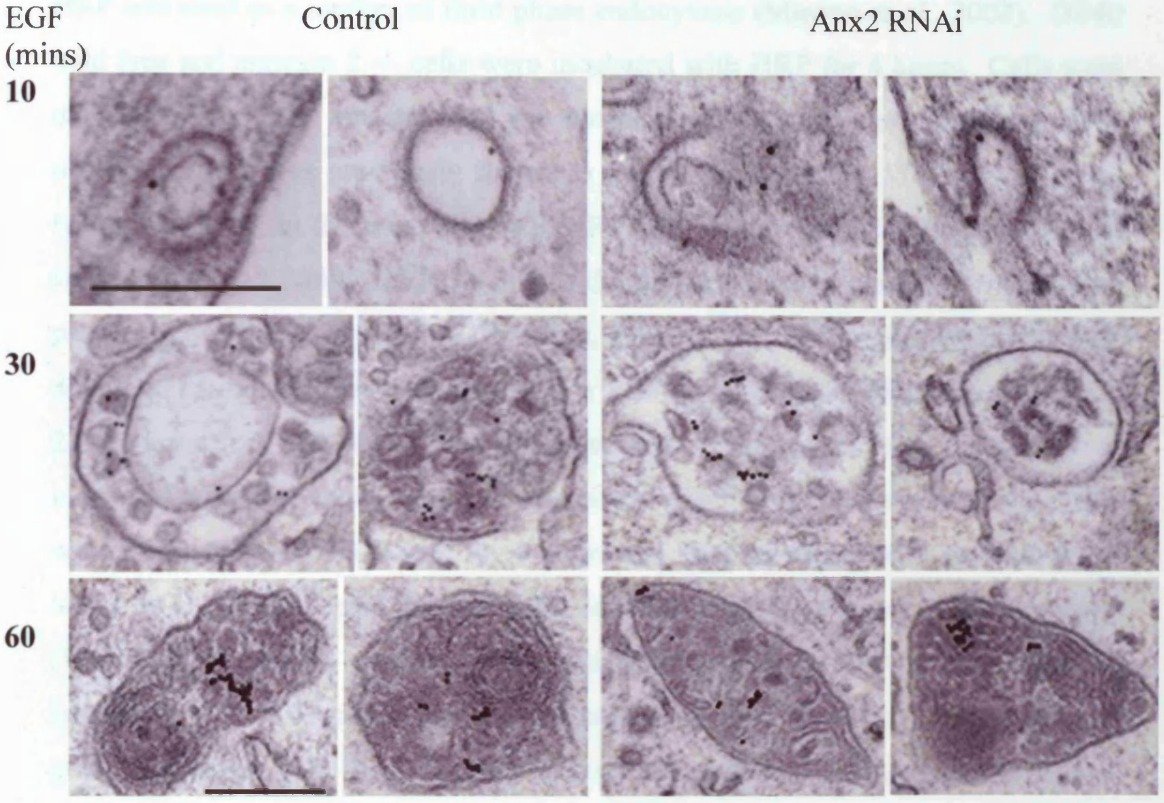

Figure 5.9. *Annexin 2 depletion does not affect lysosomal delivery of EGFR.* HeLa cells were treated with control or annexin 2 RNAi for 3 days. Cells were serum starved before stimulation with EGF (100ng/ml), in the presence of anti-hEGFR-gold, for 10, 30 or 60 minutes. Cells were processed for TEM and the distribution of anti-hEGFR-gold analysed. Electron micrographs show the location of anti-hEGFR-gold at each time point. There was no difference observed in the distribution of anti-hEGFR-gold between control and annexin 2 RNAi-treated cells. Bars = 200nm.

Having established that the effect of loss of annexin 1 induces an EGF-specific phenotype, but that annexin 2 depletion does not, it was necessary to investigate whether the loss of annexin 2 affected delivery of fluid phase markers to the lysosome. To compare the experiments performed here with published studies, HRP was used as a marker of fluid phase endocytosis (Mayran *et al.*, 2003). DT40 wild type and annexin 2 -/- cells were incubated with HRP for 4 hours. Cells were embedded for TEM analysis and the morphology of structures containing HRP observed. HRP was previously shown to be present in mature MVBs in both cell types (Fig. 4.5). In these experiments, HRP was also present in various lysosomal structures (Fig. 5.10A). HRP, visible as the dark HRP/DAB reaction product, was present in MVBs fused with the lysosome, and also in multilamellar lysosomes that do not contain multivesicular regions. For further confirmation that loss of annexin 2 does not affect delivery of fluid phase markers to the lysosome, DT40 cells were incubated with BSA-gold, which is also taken up by fluid phase endocytosis. Cells were incubated with BSA-gold for 4 hours and then incubated with medium or 20 hours, to chase BSA-gold through cells, in order to study delivery to the lysosome (Wettey *et al.*, 2002). As seen with anti-hEGFR-gold, as BSA-gold reaches the lysosome, BSA is degraded but the gold particle is not. Therefore, the presence of gold aggregates identifies the degradative compartment. Figure 5.10B shows typical lysosomes containing BSA-gold in both cell lines. Under these conditions, all BSA-gold was observed within multilamellar lysosomes in both cellslines. These data show that fluid phase endocytosis and delivery to the lysosome are unaffected in cells lacking annexin 2.

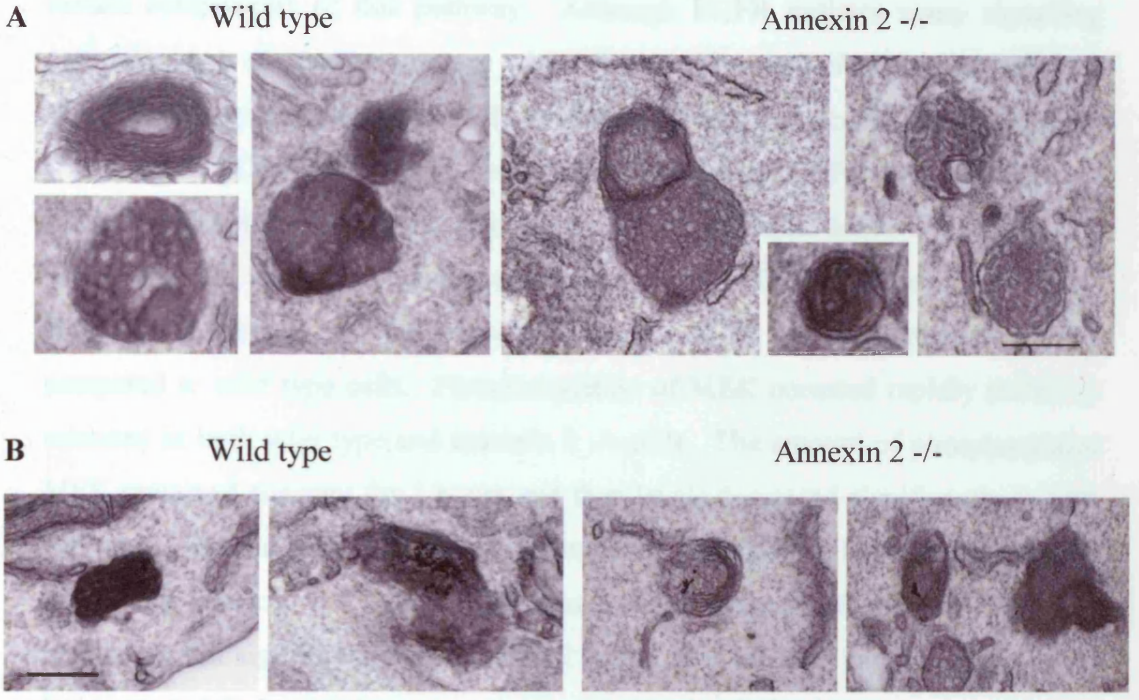

Figure 5.10. *Loss of annexin 2 does not affect delivery of fluid phase markers to the lysosome.* DT40 wild type and annexin 2 -/- cells were incubated with fluid phase HRP for 4 hours (A) or with BSA coupled to 10nm gold for 4 hours followed by a 20 hour incubation with normal DT40 cell medium (B). Cells were processed for TEM and the presence of these markers in lysosomes observed, as dark DAB reaction in A, or gold clusters in B. HRP and BSA-gold were observed in MVBs and lysosomes of both cell lines, and no difference in morphology was observed. Bars = 200nm.

5.2.4 Loss of annexin 1 prolongs MAPK signalling

Improper EGFR downregulation can result in the alteration of downstream signalling pathways. The ERK1/2 MAPK pathway is just one of many initiated by ligand-induced EGFR activation. This pathway has been well studied and it has been reported that EGFR endocytosis may be required for maximal activation of certain components of this pathway. Although EGFR initiates many signalling pathways, not all require receptor endocytosis. The well-characterised ERK1/2 MAPK pathway was chosen to study the effect of loss of annexin 1 on downstream signalling. JACRO cell lysates, collected for analysis of EGFR degradation, were blotted with antibodies against total MEK 1/2 and phospho-MEK 1/2 (Fig. 5.11). There was no difference in the total amount of MEK1/2 between cell types. However, in annexin 1 -/- cells levels of phospho-MEK 1/2 were greatly increased compared to wild type cells. Phosphorylation of MEK occurred rapidly (within 5 minutes) in both wild type and annexin 1 -/- cells. The amount of phosphorylated MEK remained constant for 2 hours and then levels decreased significantly in both cell types. In wild type cells there was almost no phospho-MEK 1/2 remaining at 3 hours. In annexin 1 -/- cells there was a small amount of phospho-MEK 1/2 remaining, but significantly less than at 2 hours. JACRO and annexin 1 or control RNAi-treated HeLa cell lysates were also blotted for ERK1/2 (p44/42 MAPK) and phospho ERK1/2 (phospho-p44/42). Again, there was no difference observed in the total cellular levels of the unphosphorylated protein between cell lines. Like MEK 1/2, phosphorylation of ERK1/2 occurred rapidly, within 5 minutes, in all cell types. Unlike phospho-MEK 1/2, phospho-ERK1/2 started to be dephosphorylated after 45 minutes in JACRO cells, and between 5 and 45 minutes in HeLa cells. In wild type JACRO cells and control HeLa cells, there was very little phospho-ERK1/2 remaining after 3 hours. However, in JACRO annexin 1 -/- cells and annexin 1 RNAi-treated HeLa cells there was significantly more phosphorylated protein remaining after 3 hours, especially in annexin 1 -/- cells. These data indicate that loss of annexin 1 prolongs signalling through the MAPK pathway.

The finding that loss of annexin 1 altered the amount or kinetics of EGFR degradation is novel, but that delayed receptor degradation resulted in prolonged

signalling has previously been reported (Babst *et al.*, 2000). Activated EGFR can signal, through tyrosine phosphorylation, to a wide range of downstream proteins, including the MAPK pathway. To investigate further the effect of loss of annexin 1 on EGFR tyrosine kinase activity, JACRO cell lysates from the above experiment were blotted with an anti-phosphotyrosine antibody (Fig. 5.12).

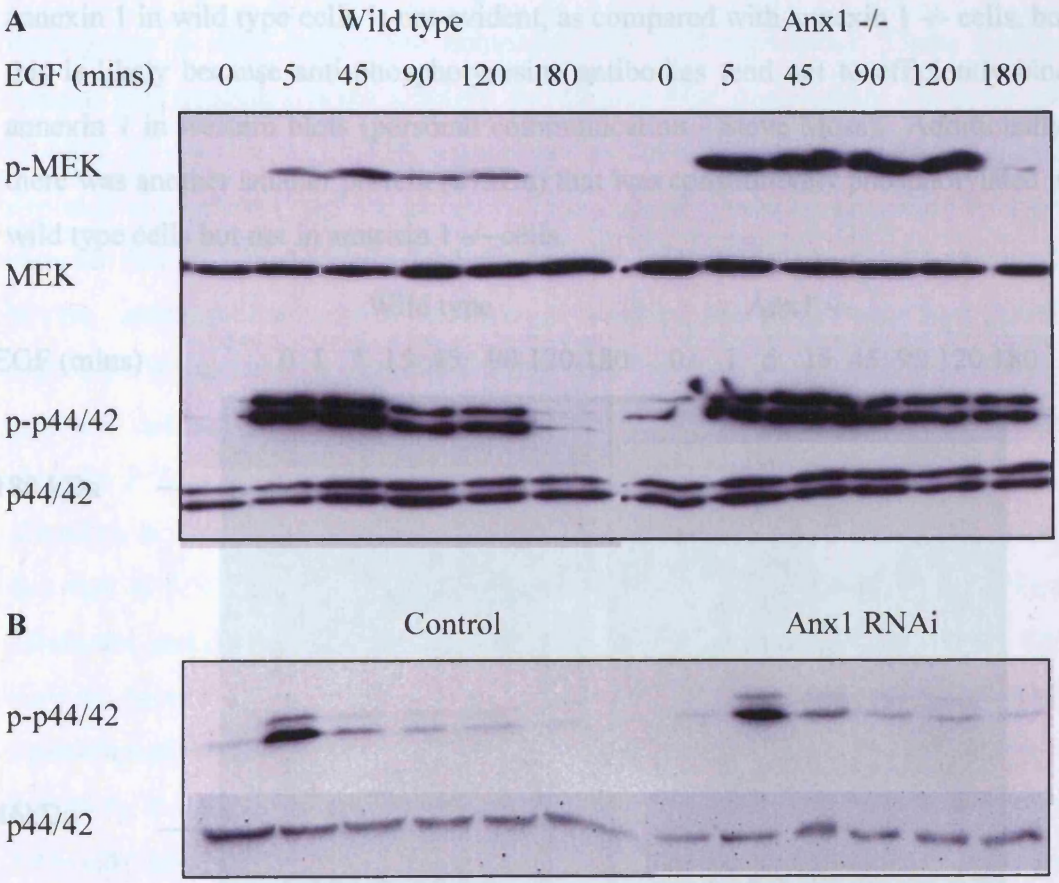

Figure 5.11. *Loss of annexin 1 prolongs MAPK signaling.* JACRO cells (A) or HeLa cells treated with control or annexin 1 RNAi (B) were serum starved, incubated with EGF and cell lysates collected at different time points of EGF stimulation. Lysates were blotted with anti-phospho (p) MEK, anti-MEK, anti-phospho p44/42 and anti-p44/42. Levels of phospho-MEK were increased in annexin 1 -/- cells and dephosphorylation of MEK and p44/42 was delayed.

EGFR is a major substrate of its own tyrosine kinase and phosphorylated EGFR was clearly visible as a large band near the top of the blot in both cells lines. There was more tyrosine phosphorylation following EGF stimulation in annexin 1 -/- cells, especially of larger proteins. In both cell lines, many proteins were rapidly

phosphorylated (within 1 minute) in response to EGF stimulation. There were also a number of proteins that are constitutively phosphorylated. In annexin 1 -/- cells there was one protein (46kDa) that was phosphorylated in response to EGF in wild type cells, but not detectable in annexin 1 -/- cells. The size of this protein corresponds to the size of annexin 1 (37kDa) plus S100A11 (10kDa), however there is no evidence that this dimer exists. Interestingly, the presence of phospho-annexin 1 in wild type cells is not evident, as compared with annexin 1 -/- cells, but this is likely because anti-phosphotyrosine antibodies tend not to efficiently bind annexin 1 in western blots (personal communication - Steve Moss). Additionally, there was another smaller protein (27kDa) that was constitutively phosphorylated in wild type cells but not in annexin 1 -/- cells.

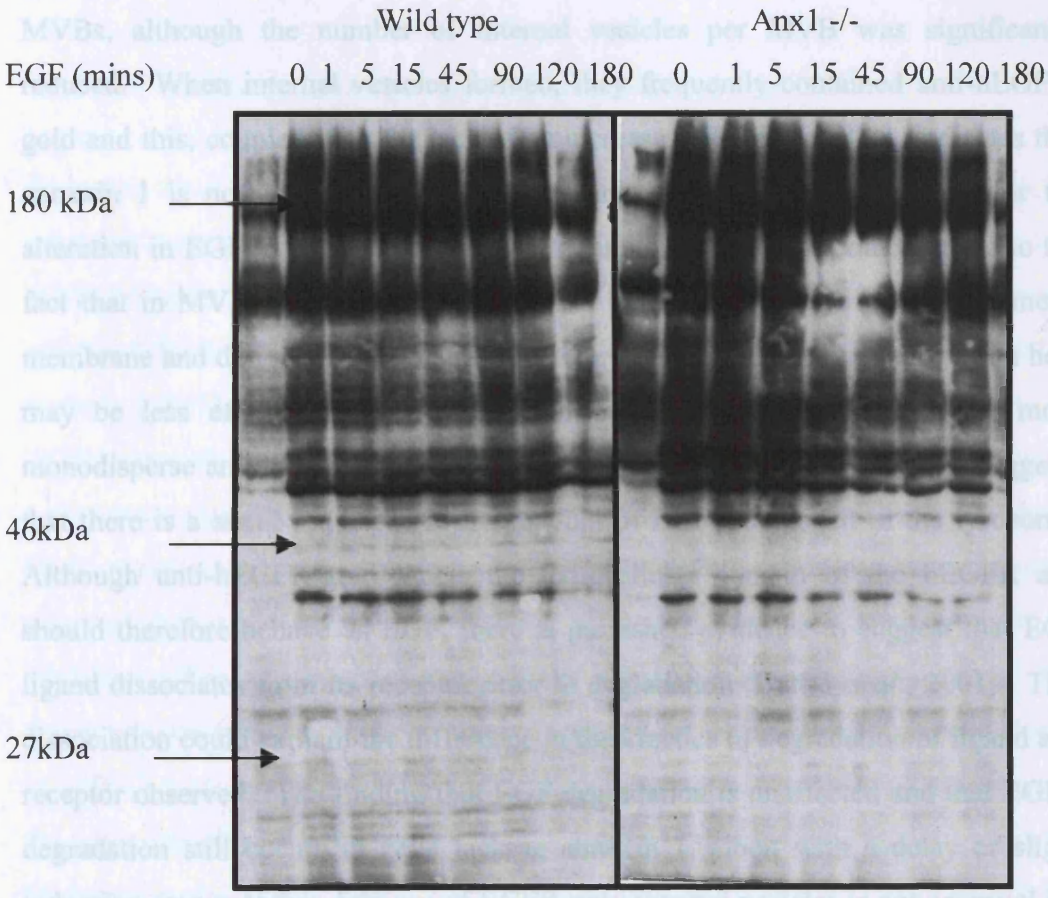

Figure 5.12. *Effect of loss of annexin 1 on EGF-stimulated tyrosine phosphorylation.* JACRO cells were serum starved before EGF stimulation. Cell lysates were collected at different time points of EGF stimulation and blotted with anti-phosphotyrosine. Phospho-EGFR is visible as a very large band (180kDa) near the top of the blot. There is a band at approximately 46kDa that is only phosphorylated in wild type cells.

5.3 Discussion

5.3.1 Loss of annexin 1 alters EGFR degradation and prolongs signalling

Despite the inhibition of EGF-stimulated inward vesiculation observed in MVBs from annexin 1 -/- cells (Chapter 3), there was no effect on the kinetics of EGF degradation in these cells when compared with wild type cells. These findings indicate that annexin 1 is not required for efficient EGF degradation. However, the kinetics, or amount, of EGFR degradation in these cells and also in HeLa cells depleted of annexin 1, but not annexin 2, was altered. Previous data, reported here, showed that in the absence of annexin 1 anti-hEGFR-gold was still present in MVBs, although the number of internal vesicles per MVB was significantly reduced. When internal vesicles formed, they frequently contained anti-hEGFR-gold and this, coupled with the lack of an increase in EGF recycling, indicates that annexin 1 is not involved in receptor sorting. A possible explanation for the alteration in EGFR degradation observed in annexin 1 -/- cells could be due to the fact that in MVBs lacking internal vesicles, EGFR are retained on the perimeter membrane and delivery to the degradative enzymes, within the lysosome, from here may be less efficient than delivery from the lumen. That there was more monodisperse anti-hEGFR-gold in annexin 1 -/- cells than wild type cells, suggests that there is a small reduction in the amount of EGFR degraded in the lysosome. Although anti-hEGFR-gold labels the extracellular domain of the hEGFR and should therefore behave as EGF, there is published evidence to suggest that EGF ligand dissociates from its receptor prior to degradation (Burke *et al.*, 2001). This dissociation could explain the difference in the kinetics of degradation of ligand and receptor observed. The finding that EGF degradation is unaffected and that EGFR degradation still occurs in cells lacking annexin 1, albeit with a delay or slight reduction, suggests that delivery of EGFR onto internal vesicles is not essential for lysosomal degradation.

These findings are similar to those of Futter *et al.* (2001) who reported that wortmannin treatment of cells resulted in formation of enlarged anti-hEGFR-gold containing vacuoles with few internal vesicles (Futter *et al.*, 2001). In these cells,

there was no difference in the kinetics or magnitude of EGF degradation. Further investigation revealed that retention of EGFR on the perimeter membrane, due to lack of inward vesiculation, resulted in an increased amount of tyrosine-phosphorylated proteins (Futter *et al.*, 2001). In this chapter, annexin 1 -/- cells exhibited enhanced and prolonged phosphorylation of MEK 1/2 compared to wild type cells, and phosphorylation of its downstream effector ERK1/2 was also prolonged in -/- cells. The overall level of tyrosine phosphorylated proteins in annexin 1 -/- cells was increased, supporting the hypothesis that sequestration of activated EGFR onto internal vesicles of MVBs is required to attenuate signalling. These data also provide evidence that annexin 1 may participate in the downregulation of EGFR signalling, through the formation of internal vesicles.

5.3.2 Loss of annexin 2 does not affect lysosomal delivery of EGF or EGFR

That annexin 2 depletion had no effect on delivery of EGF, or its receptor, to the lysosome was to be expected given that no effect had previously been observed on MVB formation in these studies (Chapter 4). However, these data contradict recent published findings, in which an inhibition of early to late endosomal transport in annexin 2 RNAi treated cells was reported (Mayran *et al.*, 2003). Mayran *et al.* (2003) found that fluorescent EGF was degraded after a 5 minute pulse followed by a 60 minute chase in control cells, but was still visible after the chase in enlarged EEA1 positive structures in annexin 2 RNAi-treated cells. However, these findings were not explored further using more detailed analysis and no quantitation of the inhibitory effect on lysosomal delivery was performed (Mayran *et al.*, 2003). The data presented in this chapter are more consistent with recent work from Zobiack *et al.* (2003), who reported that annexin 2 depletion had no effect on LDL delivery to the lysosome, although this group did not specifically investigate EGFR trafficking (Zobiack *et al.*, 2003). Additional studies of rat hepatocytes by Pol *et al.* (1997), using cellular fractionation techniques, demonstrated that while a significant amount of annexin 2 was present in fractions containing recycling endosomes, none was detected in the MVB fraction (Pol *et al.*, 1997). The findings presented in this chapter, taken together with data from previous chapters, show that annexins 1 and 2 do not functionally compensate each other, in terms of internal vesicle formation

and EGFR trafficking. Although annexin 2 is upregulated in annexin 1 -/- cells (Croxtall *et al.*, 2003), its loss had no effect on MVB formation or delivery of EGFR to the lysosome.

5.3.3 Annexin 1 and signalling

The finding in this chapter that loss of annexin 1 has a positive effect on EGFR signalling is consistent with a negative role of annexin 1 in this process. Loss of annexin 1 could alter signalling directly through its effect on EGF-stimulated inward vesiculation and, thus, dowregulation of EGFR signalling. However, it is possible that the prolonged MAPK signalling in annexin 1 -/- cells could occur independently of the effects observed on membrane traffic. Grb2 is a central molecule in EGFR internalisation and interacts with both c-Cbl and EGFR at the plasma membrane, and also within endosomes. Grb2 is recruited to the plasma membrane after ligand-induced receptor activation and is thought to be involved in anchoring receptors to the Eps15 complex, prior to CCV formation. Additionally, Grb2 is constitutively associated with SOS, which is part of the Ras signalling pathway. The N-terminal domain of annexin 1 contains a region, with sequence homology to SH2 recognition domains, that can bind Grb2 (Alldridge *et al.*, 1999; Croxtall *et al.*, 2000). Annexin 1 is believed to compete with Grb2 for binding to EGFR and inhibit the recruitment of further signalling factors (Croxtall *et al.*, 2000).

The role of annexin 1 in MAPK signalling also been investigated by groups working on LPS stimulation of macrophages (Alldridge and Bryant, 2003). In RAW macrophages overexpressing annexin 1, constitutive activation of ERK1/2 was observed, and resulted in decreased cell proliferation (Alldridge and Bryant, 2003). Although these findings are inconsistent with the work presented in this chapter and those of Croxtall *et al.* (2000), the effect of constitutive or enhanced signalling appears to be cell type specific, as ERK1/2 overexpression has been reported in transformed cells and allows translocation of phospho-proteins to the nucleus and subsequent phosphorylation of transcription factors (Marshall, 1995).

That annexin 1 plays a role in the regulation of EGFR signalling has previously been reported (Croxtall *et al.*, 2000), and the data presented here is consistent with a negative role for annexin 1 on EGF-stimulated signalling through the MAPK pathway. Efficient ERK1/2 signalling requires the formation of a scaffold complex on endosomes (Teis *et al.*, 2002). Given the membrane and actin binding properties of annexin 1, it is entirely possible that annexin 1 may play a scaffold or adaptor role to control the formation of signalling complexes, although no evidence exists to support this hypothesis.

5.3.4 Annexin 2 and Tf recycling

The majority of Tf is reported to recycle through the fast pathway from endosomes, and although some is retained on the perimeter membrane of MVBs and sorted to Rab 11 positive recycling endosomes (Ullrich *et al.*, 1996; Green *et al.*, 1997), these structures are not essential for Tf recycling (Sheff *et al.*, 2002). However, annexin 2 has been identified on both endosomes and recycling endosomes (Emans *et al.*, 1993; Harder and Gerke, 1993; Jost *et al.*, 1997; Zeuschner *et al.*, 2001; Zobiack *et al.*, 2003). Recently it was shown that depletion of annexin 2 caused a relocalisation of Tf positive recycling endosomes, although this had little effect on the kinetics of Tf recycling (Zobiack *et al.*, 2003). The data presented in this chapter is consistent with a role for annexin 2 in the proper positioning of recycling endosomes, although further work needs to be carried out to determine the ultrastructural nature and exact location of these organelles.

5.3.5 Summary of findings

The data presented in this chapter is consistent with previous chapters investigating the roles of annexins 1 and 2 in MVB formation and inward vesiculation. While annexin 2 is not involved in MVB biogenesis, annexin 1 is required for EGF-stimulated formation of internal vesicles within MVBs. The loss of annexin 1, therefore, not only inhibits this process, but is also accompanied by a delay in, or slight inhibition of, EGFR degradation. Subsequent downstream signalling events,

through tyrosine phosphorylation, are prolonged and this is consistent with published work that reports inward vesiculation is required to attenuate receptor signalling (Futter *et al.*, 2001). Meanwhile, loss of annexin 2 has no effect on these processes and instead is involved with the proper positioning of recycling endosomes, as reported by Zobiack *et al.* (2003).

Chapter 6 – Localisation of annexins in the endocytic pathway

6.1 Introduction

The data presented in the previous chapters demonstrates a role for annexin 1 within MVBs of EGF-stimulated cells. In contrast, no role for annexin 2 was identified in MVB formation or sorting within MVBs, regardless of whether or not cells were stimulated with EGF. Consistent with these findings, annexin 1 has been localised to MVBs (Futter *et al.*, 1993; Pol *et al.*, 1997) but annexin 2 was only reported to be found in MVBs in cells induced to accumulate cholesterol (Mayran *et al.*, 2003). The localisation of annexin 1 to MVBs used fractionation techniques, but more recently annexin 1-GFP was used to examine the subcellular distribution of annexin 1 in living cells. In these studies, using unstimulated HeLa cells, annexin 1-GFP was localised to Tf positive endosomes and only localised to fluorescent dextran-containing late endosomes as a N-terminally truncated construct (Rescher *et al.*, 2000). Annexin 2 has been localised to endosomes, both early and recycling, and this association is reportedly cholesterol dependent (Harder *et al.*, 1997; Zeuschner *et al.*, 2001; Mayran *et al.*, 2003; Zobiack *et al.*, 2003).

The effect of loss of annexin 1 on inward vesiculation suggests that annexin 1 is present on MVBs. Although the localisation of annexin 1 has been studied, whether it localises to internal vesicles or remains on the perimeter membrane remains unresolved. The finding that loss of annexin 2 had no effect on MVB formation or inward vesiculation within MVBs, taken together with the studies described above, suggests that annexin 2 is not part of the complex group of proteins that work within MVBs. However, this does not rule out the possibility that annexin 2 is present in MVBs, as a consequence of its localisation to early endosomes, which mature into MVBs.

A combination of fluorescence studies in living cells and cryo-immuno electron microscopy were used to investigate the intracellular locations of annexins 1 and 2. Given the EGF-stimulated effect mediated by annexin 1, it was important to also investigate whether EGF-stimulation altered the localisations of annexins 1 and 2. The main aim was to confirm the presence of annexin 1 in MVBs and to determine

whether it was found on the perimeter membrane of MVBs or on internal vesicles. The data presented in this chapter show that annexin 1 and annexin 1-GFP were both present on the perimeter membranes of MVBs, but also on EGFR-positive internal vesicles. The absence of a significant amount of annexin 2 in MVBs confirmed the specificity of labelling. In EGF stimulated cells, annexin 1 associated with EGFR-positive endosomes and remained associated with EGFR-positive structures until lysosomal degradation. As expected the localisation of annexin 2 did not alter upon EGF stimulation, and annexin 2 remained associated with a large number of TfR-positive membrane bound structures.

6.2 Results

6.2.1 Creating an annexin 1-GFP stable cell line to investigate the intracellular localisation of annexin 1

Annexin 1 has previously been localised to early endosomes containing fluorescent Tf (Seemann *et al.*, 1997; Rescher *et al.*, 2000). Annexin 1 is an abundant protein and conventional use of immunofluorescence to label endogenous annexin 1 proved inadequate to localise the protein to any particular intracellular structure, as annexin 1 is present throughout the cytoplasm and also in the nucleus (Fig. 6.1). Therefore, to overcome this problem an annexin 1-GFP chimera was expressed at low levels in HEp2 cells, and used to investigate the localisation of annexin 1 with Tf and EGF (see Materials & Methods section 2.2.1).

To test the expression of annexin 1-GFP, HEp2 cells were transiently transfected with the construct. Figure 6.2 shows HEp2 cells expressing annexin 1-GFP (left) or pGFP (right). Annexin 1-GFP was evident predominantly in the cytoplasm but a small amount was visible in the nucleus. It was also present as punctate regions throughout the cytoplasm. Cells transfected with pGFP showed diffuse GFP expression throughout the cytoplasm and high levels of expression in the nucleus. To create a stable cell line, HEp2 cells were transfected with annexin 1-GFP using the calcium phosphate transfection method (see Materials and Methods section 2.3.2). Medium was removed, 48 hours post-transfection, and replaced with selection medium containing G418. Over 2 weeks, cells that did not contain annexin 1-GFP, and therefore the antibiotic resistance gene, died and colonies

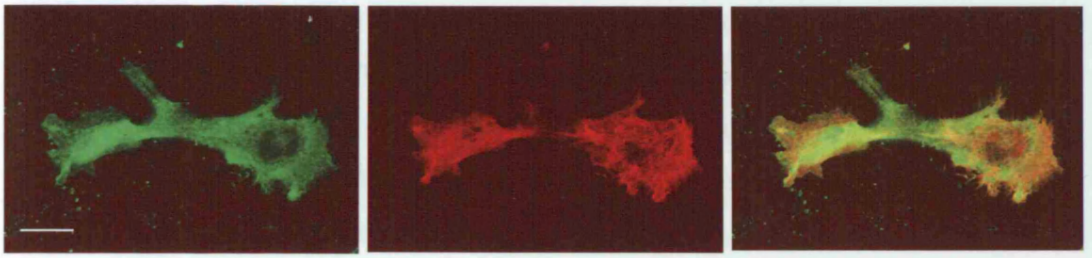

Figure 6.1. *Immunofluorescence staining of endogenous annexin 1.* HEp2 cells were fixed using 3% PFA and processed for immunofluorescence. Cells were labelled with anti-annexin 1 antibody (green) and phalloidin-AlexaFluor-547 (red) to label actin. Images show diffuse cytoplasmic annexin 1 staining with little intracellular detail and some nuclear staining. Bar = 20μm.

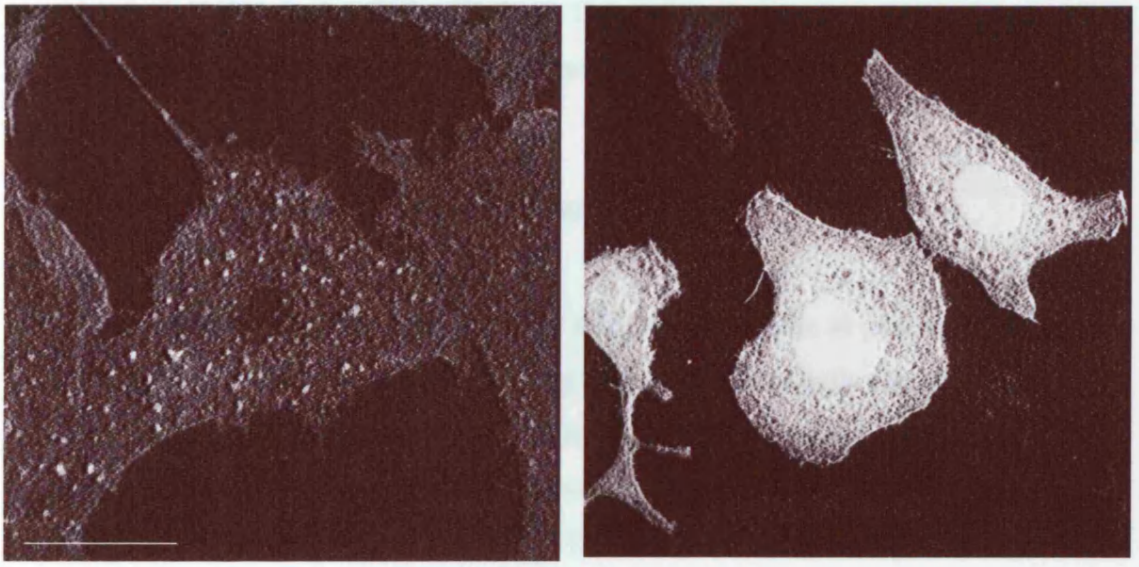

Figure 6.2. *HEp2 cells transiently expressing annexin 1-GFP.* HEp2 cells were transiently transfected with annexin 1-GFP (left), or pGFP-N1 (right), for 24 hours. Cells were imaged using confocal microscopy. Images shown are combined images, from 6 images taken in a Z-stack through the cell, and show that annexin 1-GFP expression is very different from GFP expression. Bar = 20μm.

formed from single cells that contained the plasmid. Colonies were picked and annexin 1-GFP expression observed using confocal microscopy. Cells derived from a single colony showed uniform expression of annexin 1-GFP (Fig. 6.3). One colony was chosen due to its low level expression, as it was difficult to identify intracellular structures in cells overexpressing annexin 1-GFP. Also, HEp2 cells express high levels of endogenous annexin 1 so overexpression of annexin 1-GFP could result in mislocalisation of the protein and/or an alteration in function.

Although the sequence of the annexin 1-GFP construct was correct (see Appendix 1, Fig. S.3) and its expression in cells in agreement with published data, a western blot was performed to further confirm the expression of annexin 1-GFP. HEp2 cells and cells from the stable cell line were harvested, and cell lysates blotted with anti-tubulin (loading control), anti-annexin 1 or anti-GFP antibodies (Fig. 6.4). In stably expressing cells blotted for annexin 1, there was an extra band of ~62 kDa visible that was not seen in control cells. This band corresponds to the size of annexin 1 (35kDa) plus GFP (27kDa). The levels of annexin 1-GFP expressed in these cells are much lower than that of endogenous annexin 1.

6.2.2 Annexin 1 colocalises with Tf in unstimulated cells

In live unstimulated cells annexin 1-GFP staining was visible as punctae throughout the cytoplasm, with some diffuse staining (Fig. 6.5). These cells express annexin 1-GFP at low levels and consequently little staining was visible in the nucleus. To identify the nature of the punctate annexin 1-GFP structures observed, cells were incubated with AlexaFluor555-labelled Tf for 10 or 60 minutes (Fig. 6.6). After 10 minutes, there was significant colocalisation between annexin 1-GFP and Tf in punctae around the cell periphery. There were also a number of structures that labelled for either Tf or annexin 1-GFP, but not both. After 60 minutes, the Tf-positive labelling had spread inwards from the cell periphery and some colocalisation with annexin 1-GFP occurred on large perinuclear structures, possibly MVBs before Tf has been sorted to the recycling pathway. However, there were also many single-labelled structures present around the nucleus.

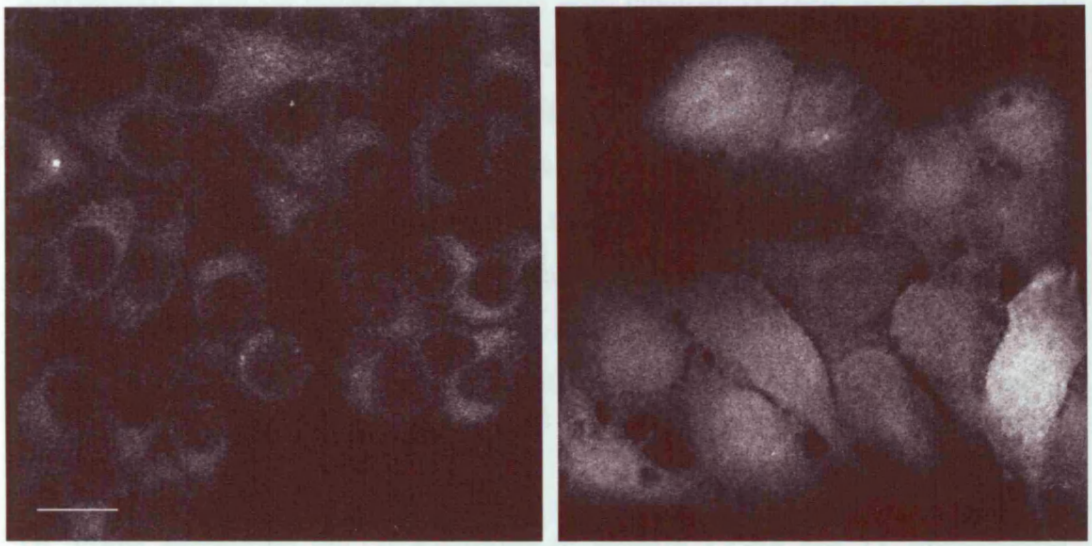

Figure 6.3. *Selection of stable cell line expressing annexin 1-GFP.* HEp2 cells were transfected with annexin 1-GFP, using calcium phosphate treatment, for 48 hours. Medium was replaced with selection medium containing 0.5mg/ml G418 for 10-14 days. Colonies were picked and annexin 1-GFP expression observed. Some colonies expressed low uniform annexin 1-GFP expression (left), whilst others were clearly derived from mixed colonies (right), showing different levels of expression.
Bar = 20μm.

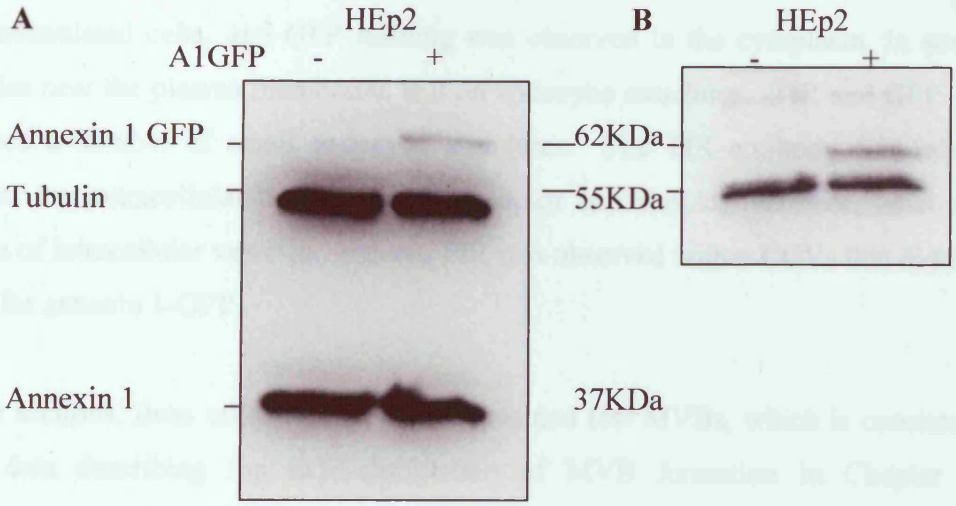

Figure 6.4. *Annexin 1-GFP expression in HEp2 cells.* HEp2 cells, stably expressing annexin 1-GFP (+), and control HEp2 cells (-) were collected for western blotting. Cell lysates were blotted for annexin 1 and tubulin (A) or GFP and tubulin (B). In transfected cells, there was an extra band visible of approximately 62kDa, which is around the correct size for annexin 1-GFP (35 + 27).

Interestingly, after 60 minutes incubation with labelled Tf, there was a significant number of Tf-positive vesicles just under the plasma membrane that did not colocalise with annexin 1-GFP, suggesting that annexin 1 is not involved in Tf internalisation. The small structures that only label for Tf could be endosomes returning Tf to the plasma membrane, via the fast recycling route. At later stages of Tf incubation, these single labelled structures were predominantly in a perinuclear distribution and it is likely that these are recycling endosomes. As this work was carried out in living cells, early or recycling endosomal markers, such as Rab5, EEA1 or Rab11, could not be used.

To further investigate the colocalisation of annexin 1-GFP and Tf, unstimulated HEp2 cells stably expressing annexin 1-GFP were fixed and processed for immuno-EM (see Materials & Methods section 2.11). Sections were labelled with anti-GFP and anti-TfR antibodies, followed by 10nm or 15nm Protein A Gold (PAG), respectively (Fig. 6.7). Sections from the same cells were also labelled with anti-GFP (10nm gold) and anti-EGFR (15nm gold) to further investigate the localisation of annexin 1 in the absence of EGF stimulation (Fig. 6.8).

In unstimulated cells, anti-GFP staining was observed in the cytoplasm, in small vesicles near the plasma membrane, and on endocytic structures. TfR and GFP co-labelled a number of small endocytic structures. The TfR antibody was raised against the extracellular domain of the receptor and should, therefore, label the lumen of intracellular vesicles. Indeed, TfR was observed within CCVs that did not label for annexin 1-GFP.

These sections, from unstimulated cells, contained few MVBs, which is consistent with data describing the EGF-stimulation of MVB formation in Chapter 3. However, a small number of MVBs were observed and many of these contained annexin 1-GFP labelling on internal vesicles (Fig. 6.7 & 6.8). Annexin 1-GFP was also present at the perimeter membrane of MVBs with TfR and on small vesicles near MVBs, which could be approaching endosomes ready to fuse with MVBs or recycling endosomes leaving the perimeter membrane. However, not all MVBs labelled for annexin 1-GFP. There was little EGFR labelling in MVBs in unstimulated cells.

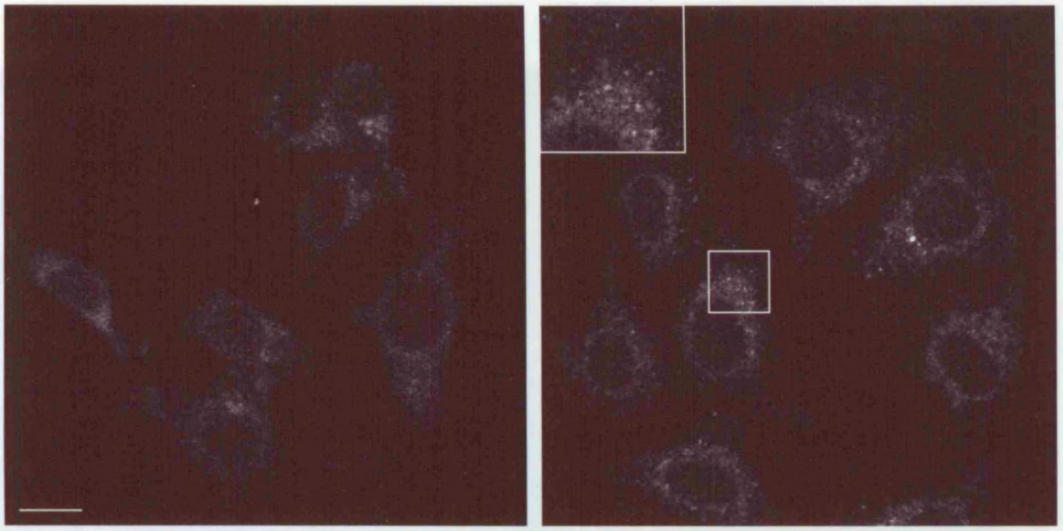

Figure 6.5. *Localisation of annexin 1-GFP in unstimulated cells.* HEp2 cells stably expressing annexin 1-GFP were serum starved for 1 hour and imaged using BioRad confocal microscope. Annexin 1-GFP was visible throughout the cytoplasm and as punctae especially near the nucleus (inset shows 2x magnification). Bar = 20μm.

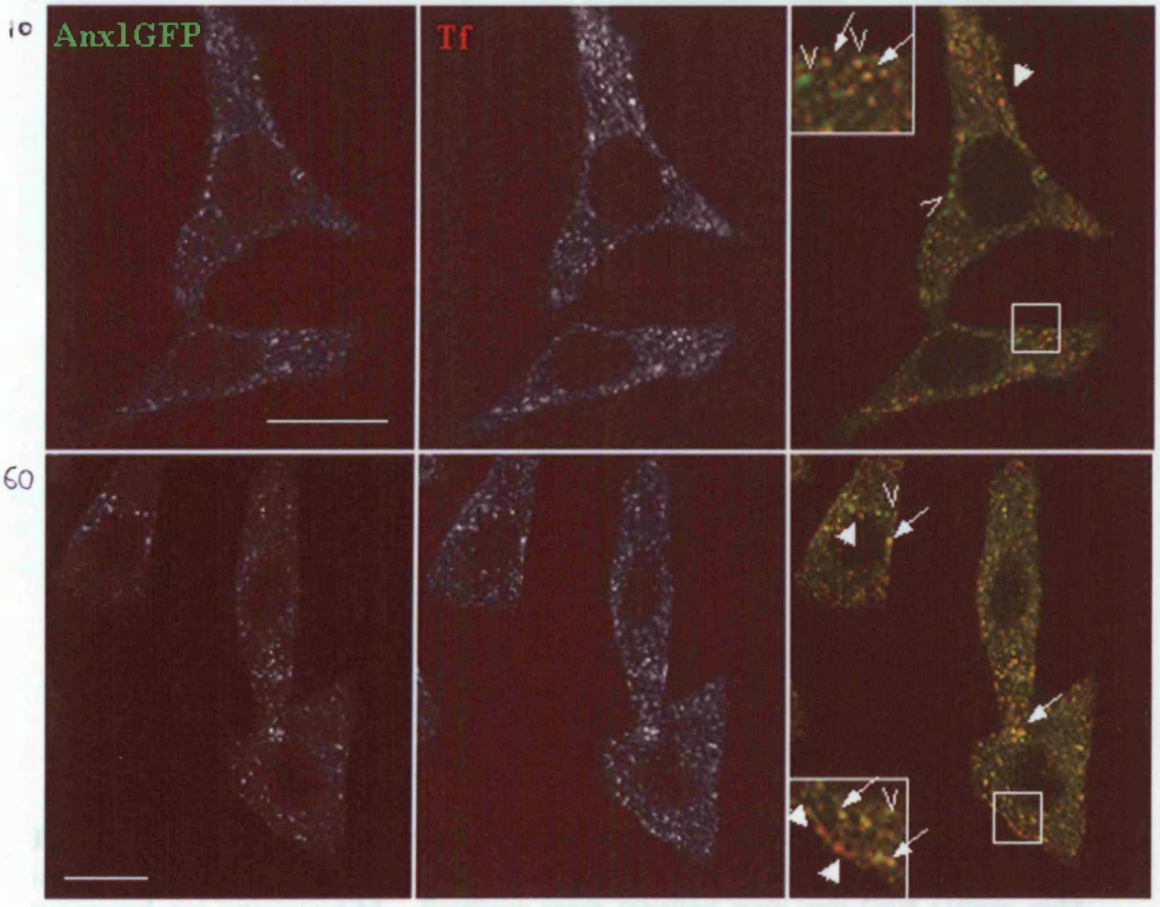

Figure 6.6. *Annexin 1-GFP colocalises with Tf in unstimulated cells.* Live unstimulated HEp2 cells, stably expressing annexin 1-GFP, were incubated with Tf-AlexaFluor 555 for 10 minutes or 60 minutes. Annexin 1-GFP colocalised with Tf in punctate structures, especially near the cell surface (arrows). Inset (2x magnification) shows that not all Tf and annexin 1-GFP are in the same punctae. Block arrowheads show Tf only positive structure near the membrane. Open arrowheads shown annexin 1-GFP only structures. Bars = 20μm.

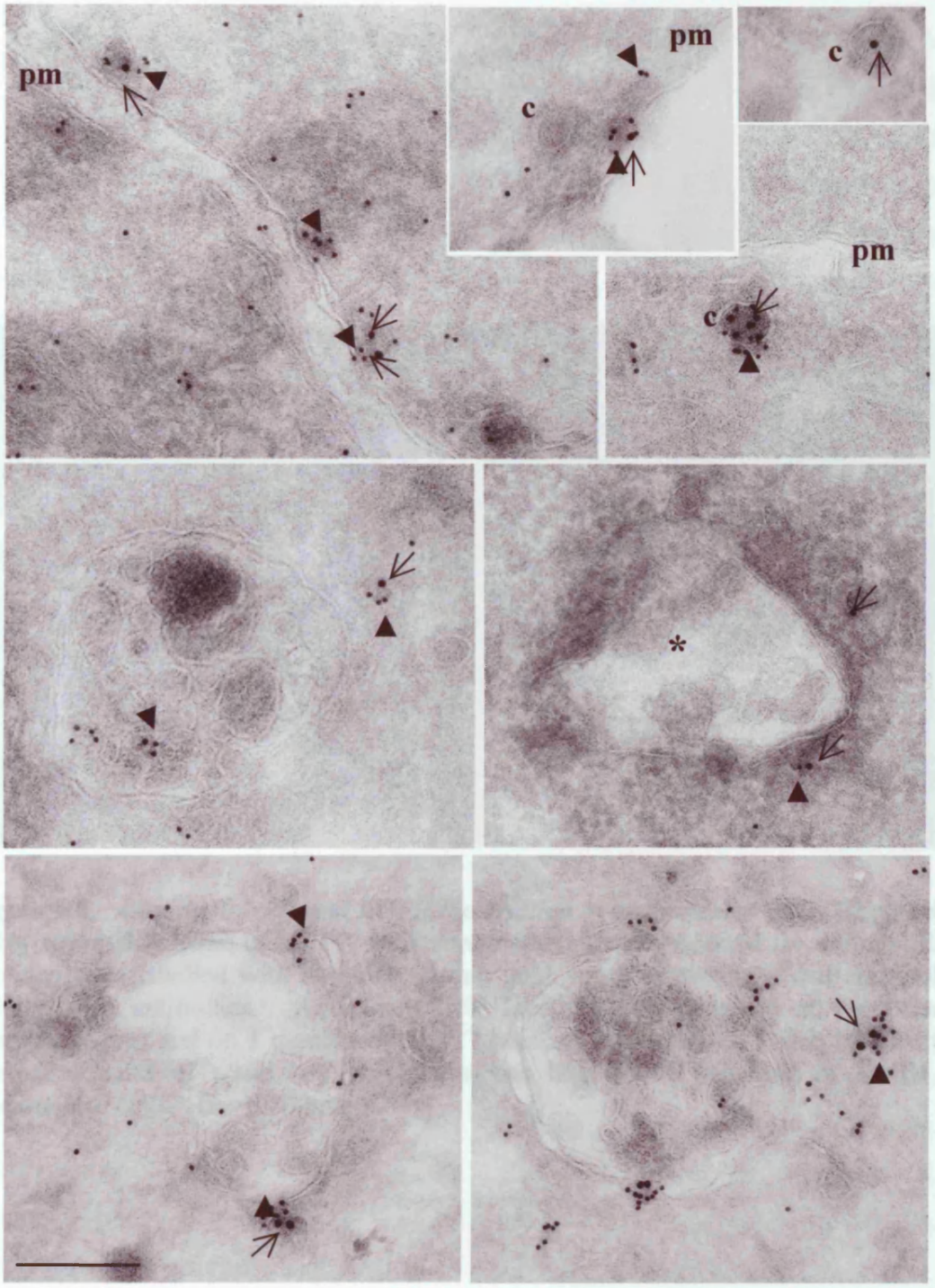

Figure 6.7. *Ultrastructural localisation of annexin 1-GFP and TfR in unstimulated cells.* HEp2 cells, stably expressing annexin 1-GFP, were serum starved and processed for immuno-EM. Sections were labelled with anti-GFP (10nm gold, block arrowheads) and anti-TfR (15nm gold, open arrows) antibodies. TfR labelling was found at the plasma membrane (pm), in CCVs (c) and within endosomes. Annexin 1-GFP labelled TfR positive structures and was found in the cytoplasm. Annexin 1-GFP also labelled most MVBs, but some MVBs contained no label (*). TfR labelling was not found within MVBs, but at the perimeter membrane with annexin 1-GFP, or in small vesicles nearby with annexin 1-GFP. Bar = 200nm.

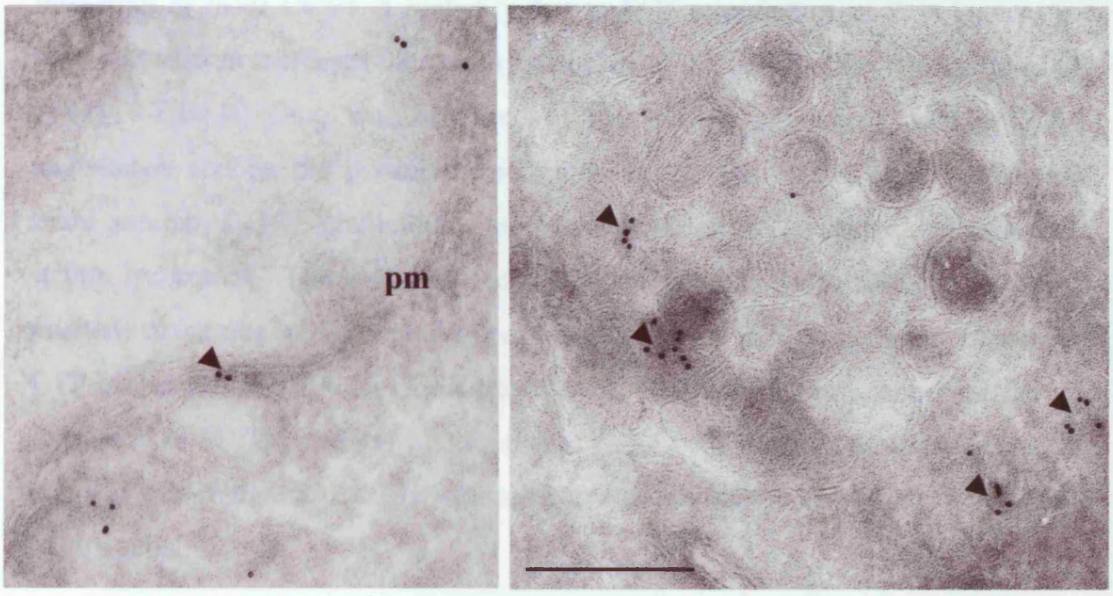

Figure 6.8. *Annexin 1-GFP and EGFR localisation in unstimulated cells.* HEp2 cells, stably expressing annexin 1-GFP, were serum starved and processed for immuno-EM. Sections were labelled with anti-GFP (10nm gold, block arrowheads) and anti-EGFR (15nm gold) antibodies. Annexin 1-GFP labelling was observed at the plasma membrane (pm) and on a number of small vesicles. Annexin 1-GFP also labelled the internal vesicles of some MVBs. There was little EGFR labelling of MVBs in unstimulated cells. Bar = 200nm.

To investigate whether EGF-stimulation had an effect on the colocalisation of annexin 1-GFP and Tf, sections from EGF-stimulated HEp2 cells, stably expressing annexin 1-GFP, were labelled with anti-GFP (10nm gold) and anti-TfR (15nm gold) antibodies and PAG (Fig. 6.9). After 30 minutes of EGF stimulation, the location of TfR staining was not markedly different to that seen in unstimulated cells, although more CCVs were observed with TfR labelling within. The formation of more CCVs is probably due to EGF stimulation, as it is known that EGF stimulation increases the density of CCPs at the cell surface (Connolly *et al.*, 1984). TfR labelling was observed at the plasma membrane, within CCVs, endosomes and on the perimeter membrane of MVBs. After EGF stimulation, more annexin 1-GFP labelled the internal vesicles of MVBs and was also present within lysosomes. These studies show that annexin 1-GFP is associated with TfR positive structures in unstimulated cells and that after EGF stimulation annexin 1-GFP is also associated with EGFR positive structures. EGF-stimulation induces the formation of MVBs, and the finding that annexin 1-GFP labelling was observed on many MVBs indicates that EGF-stimulation also alters the localisation of annexin 1 within cells.

6.2.3 Annexin 1 colocalises with EGFR after EGF stimulation

Following EGF stimulation, the localisation of TfR was unaffected but increased annexin 1-GFP labelling of internal vesicles of MVBs was observed. To investigate the exact nature of this EGF-stimulated effect, live HEp2 cells stably expressing annexin 1-GFP were stimulated with EGF and the localisation of annexin 1-GFP observed. After 10 minutes EGF stimulation, annexin 1-GFP and fluorescent EGF were present together in a number of peripheral structures (Fig. 6.10). EGF was also visible in annexin 1-GFP negative punctae. Annexin 1-GFP staining was visible throughout the cytoplasm, as described previously, and also in EGF negative vesicles distributed in a perinuclear location.

After 30 minutes of EGF stimulation, there was more colocalisation of annexin 1-GFP and EGF in larger structures throughout the cytoplasm (Fig. 6.11). There were also some single labelled vesicles, as observed after 10 minutes.

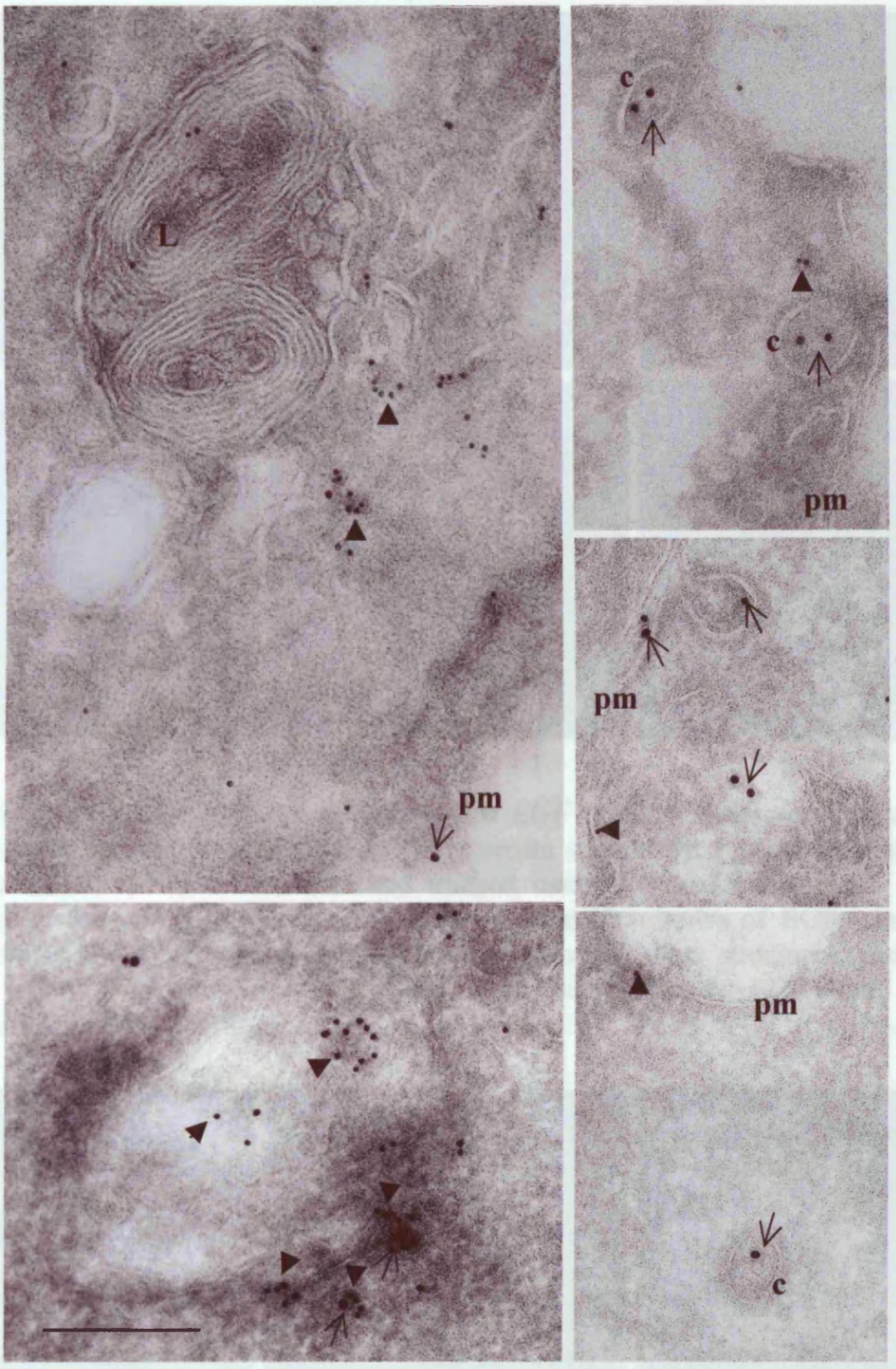

Figure 6.9. *Annexin 1-GFP and TfR localisation in EGF-stimulated cells.* HEp2 cells, stably expressing annexin 1-GFP, were serum starved, EGF stimulated for 30 minutes and processed for immuno-EM. Sections were labelled with anti-GFP (10nm gold, block arrowheads) and anti-TfR (15nm gold, open arrows) antibodies, to examine the localisation of annexin 1-GFP and TfR in EGF-stimulated cells. The localisation of TfR after EGF stimulation was not markedly different. TfR labelling was observed at the plasma membrane (pm), in CCVs (c) and in endosomes. TfR also labelled the perimeter membrane of some MVBs. Annexin 1-GFP labelling of internal vesicles of MVBs was significantly increased, compared to unstimulated cells. Annexin 1-GFP labelling was also observed in MVB/lysosomes (L). Bar = 200nm.

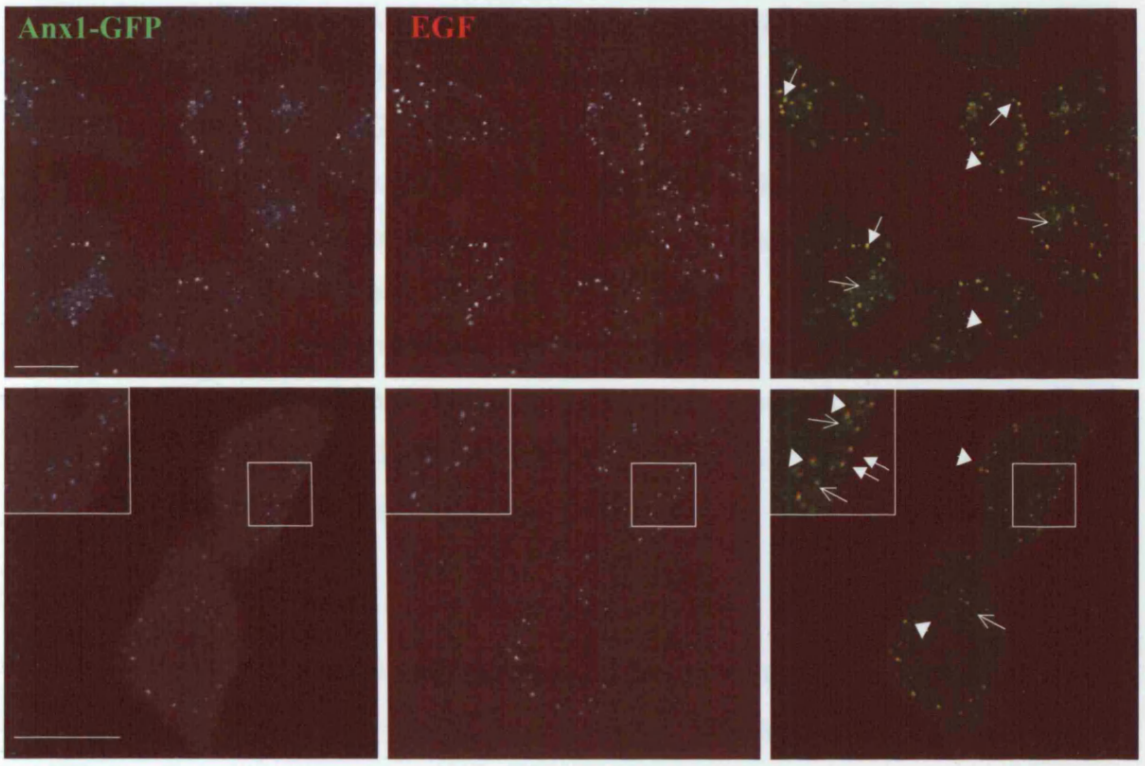

Figure 6.10. *Annexin 1-GFP colocalises with EGF in early endosomes.* Live HEp2 cells, stably expressing annexin 1-GFP, were serum starved for 1 hour, incubated with EGF-Alexafluor555 for 10 minutes and imaged using confocal microscopy. Images show typical annexin 1-GFP and EGF staining after 10 minutes of EGF stimulation. White arrows show areas of colocalisation, open arrows show structures positive for annexin 1-GFP alone, and block arrowheads structures positive for EGF alone. Inset = 2x magnification. Bars = 20μm.

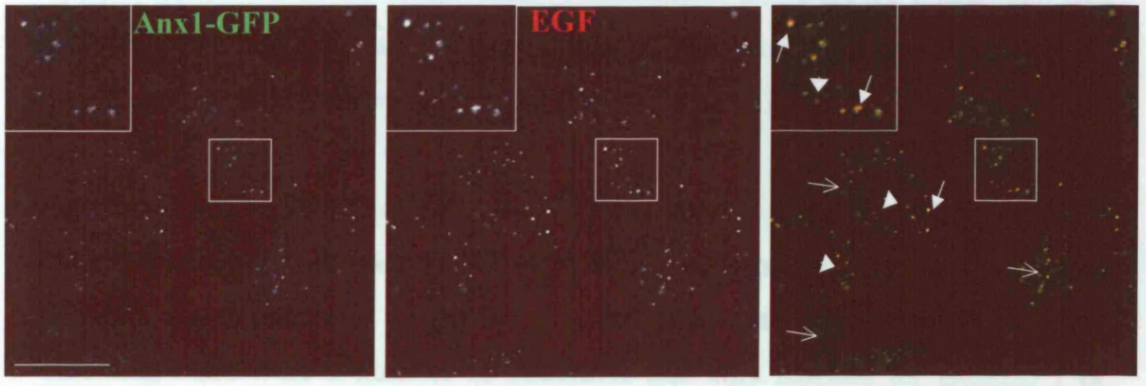

Figure 6.11. *Annexin 1 colocalises with EGF in later endocytic structures.* Living HEp2 cells, stably expressing annexin 1-GFP, were serum starved and incubated with EGF-Alexafluor555 for 30 minutes. There was significant colocalisation in punctae in a perinuclear distribution (white arrows). Open arrows show structures positive for annexin 1-GFP alone and block arrowheads structures positive for EGF alone Inset = 2x magnification. Bars = 20μm.

To observe the intracellular location of annexin 1-GFP with greater resolution, cryo-sections from EGF-stimulated HEp2 cells, stably expressing annexin 1-GFP, were labelled with anti-GFP (10nm gold) and anti-EGFR (15nm gold) antibodies (Fig. 6.12). After 30 minutes of EGF stimulation, EGFR labelling was observed on small endocytic structures and MVBs (Fig. 6.12). The anti-EGFR antibody was raised against the cytoplasmic domain of the receptor and, therefore, labelled the cytoplasmic side of the endosomal and MVB membranes, and the inside of internal vesicles. After 30 minutes, approximately equal amounts of EGFR labelled the perimeter membrane of MVBs and internal vesicles. Annexin 1-GFP also labelled EGFR-containing structures and was present on the same internal vesicles as EGFR.

Annexin 1-GFP showed extensive colocalisation with EGFR after EGF stimulation. To further confirm this finding, sections from EGF-stimulated HEp2 cells and HEp2 cells expressing annexin 1-GFP were labelled with anti-annexin 1 (10nm gold), to label endogenous annexin 1, and anti-EGFR (15nm gold) antibodies (Fig. 6.13). The anti-annexin 1 antibody would also be expected to recognise annexin 1-GFP but, as levels of endogenous annexin 1 are far higher (Fig. 6.4), the antibody should label predominantly the endogenous protein. In both wild type and annexin 1-GFP expressing HEp2 cells, anti-annexin 1 labelling was present throughout the cytoplasm, as well as on membranes. Furthermore, anti-annexin 1 labelling, like anti-GFP labelling, was also observed on EGFR-containing internal vesicles of MVBs and at the perimeter membrane of MVBs with EGFR.

As observed in unstimulated cells, there were a number of MVBs that did not label for either annexin 1, annexin 1-GFP or EGFR, and this provides further evidence of different sub-populations of MVBs. With both anti-GFP and anti-annexin 1 labelling, there were a number of structures that only labelled for annexin 1 or EGFR. This is consistent with fluorescence experiments that showed extensive, but not total, colocalisation of annexin 1-GFP and EGF. From these findings, it appears that annexin 1 is able to move with EGF and its receptor through the endocytic pathway. To investigate whether annexin 1 remains associated with EGFR until degradation in the lysosome, longer time points of EGF stimulation were examined.

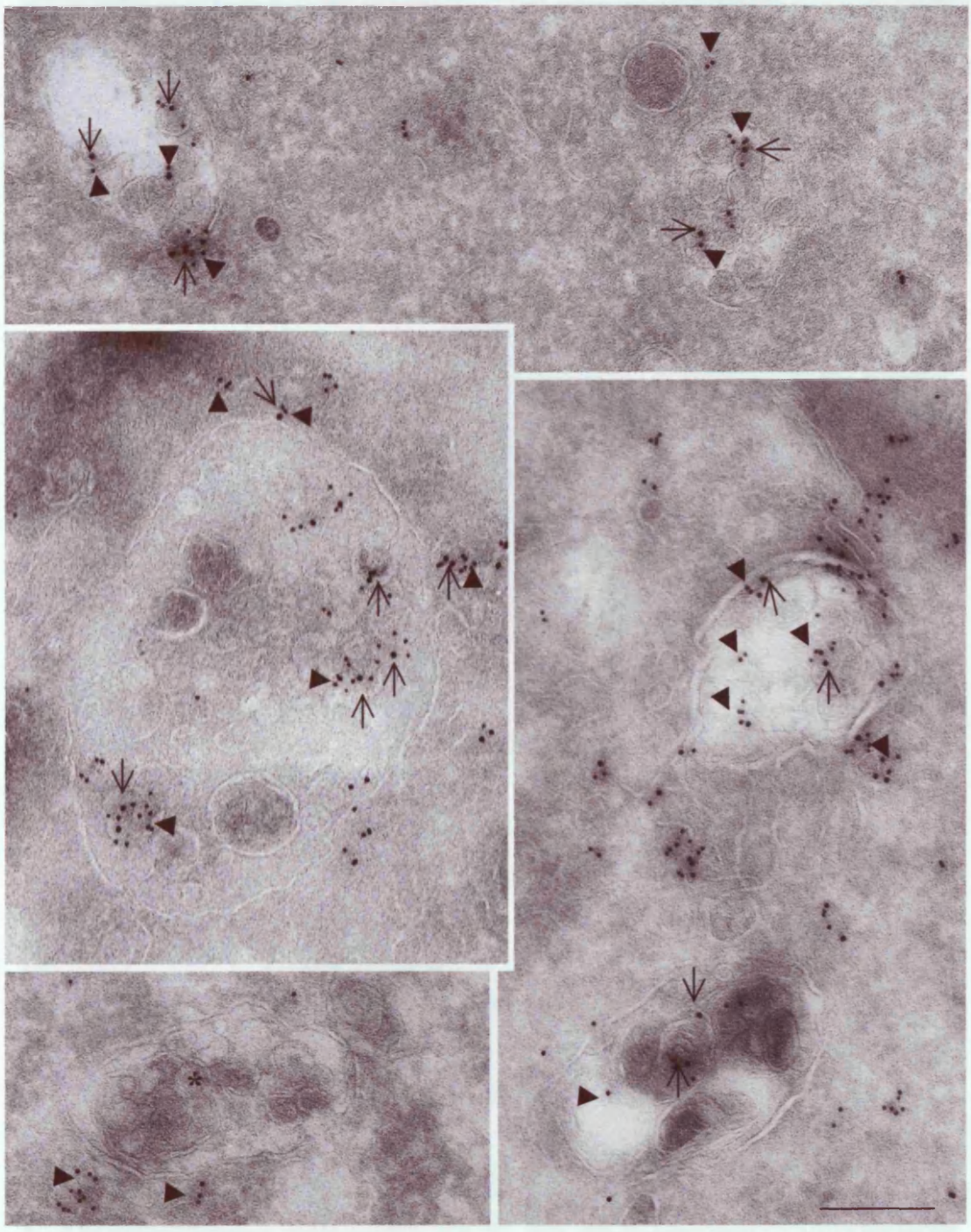

Figure 6.12. *Annexin 1 is present on EGFR positive internal vesicles.* HEp2 cells, stably expressing annexin 1-GFP, were serum starved, stimulated with EGF (100ng/ml) for 30 minutes and processed for immuno-EM. Sections were labelled with anti-GFP (10nm gold, block arrowheads) and anti-EGFR (15nm gold, open arrows) antibodies. EGFR labelling was observed on small vesicles, on the perimeter membrane of MVBs and also on internal vesicles. The majority of annexin 1-GFP labelling was on EGFR positive structures and annexin 1-GFP co-labels the same internal vesicles that contain EGFR. Unlabelled MVB is marked with a star. Bar = 200nm.

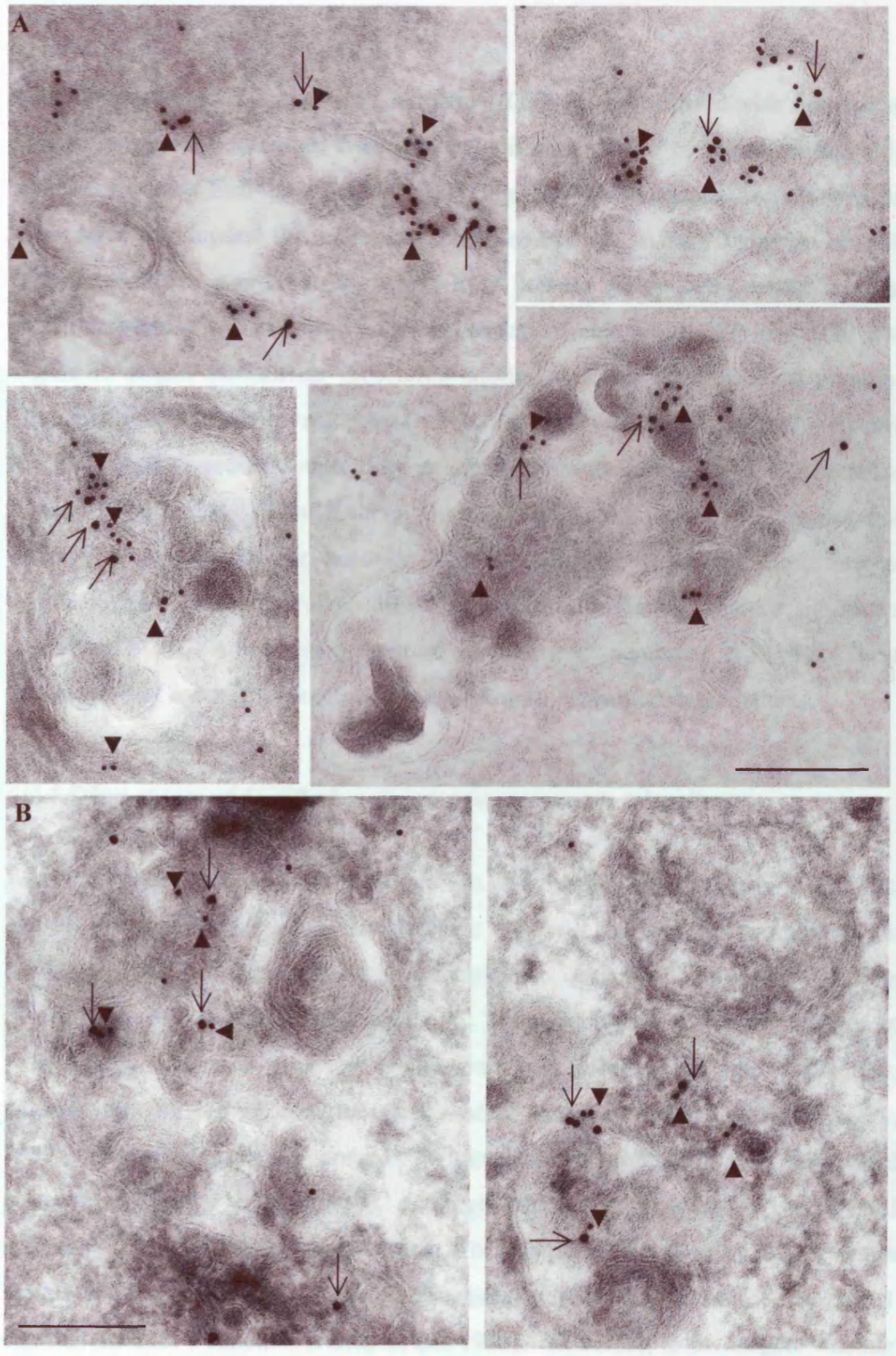

Figure 6.13. *Colocalisation of endogenous annexin 1 and EGFR.* HEp2 cells, stably expressing annexin 1-GFP (A) or wild type (B), were serum starved, stimulated with EGF (100ng/ml) for 30 minutes and processed for immuno-EM. Sections were labelled with anti-annexin (74/3) (10nm gold, block arrowheads) and anti-EGFR (15nm gold, open arrows) antibodies. EGFR labelling small endocytic vesicles and MVBs, as shown in Fig. 7.12. Endogenous annexin 1 labelling was observed in the cytoplasm, on endocytic vesicles, and with EGFR, both within MVBs and at the perimeter membrane. Bars = 200nm.

After 60 minutes EGF stimulation, annexin 1-GFP still colocalised with fluorescent EGF in living cells, although there was a significant number of structures that only labelled for either EGF or annexin 1-GFP (Fig. 6.14A). Colocalisation occurred in larger structures around the nucleus, likely to be MVBs. After 90 minutes of EGF stimulation, there was less fluorescent EGF present within cells, indicating that EGF degradation had occurred. Colocalisation of annexin 1-GFP and EGF was visible in larger, perinuclear structures similar to those seen after 60 minutes. Ultrastructural analysis revealed that annexin 1-GFP labels EGFR-positive mature MVBs and also lysosomal structures, as identified by the presence of multilamellar regions (Fig. 6.15). Although there was less EGFR staining after 60 minutes, due to receptor degradation, the majority of EGFR labelling was observed on internal vesicles of MVBs, compared to 30 minutes EGF stimulation where a significant proportion of EGFR was also present on the perimeter membrane of MVBs. These data show that annexin 1 remains with EGFR until lysosomal degradation.

6.2.4 Effect of loss of EGFR phosphorylation on annexin 1 localisation

After EGF stimulation a significant amount of annexin 1 was observed on MVBs, and on lysosomes after longer incubations. As little annexin 1 was observed on MVBs in unstimulated cells, it is possible that annexin 1 relocates from the cytoplasm to MVBs after EGF stimulation. It has been previously reported that an N-terminally truncated annexin 1-GFP construct localised to late endosomes, whereas the full length construct localised to early endosomes (Rescher *et al.*, 2000). Phosphorylation of annexin 1 increases its susceptibility to N-terminal proteolysis (Haigler *et al.*, 1987), although whether this occurs *in vivo* is still uncertain. The observation that annexin 1 is only phosphorylated by EGFR within MVBs led to the proposal that EGF-mediated phosphorylation of annexin 1 controls annexin 1 function (Futter *et al.*, 1993). Therefore, to investigate whether EGF-stimulated annexin 1 phosphorylation is required for the association of annexin 1 with later EGF-containing endocytic structures, an annexin 1-GFP mutant containing an amino acid substitution at the site of EGFR tyrosine phosphorylation (Y21F) was constructed (see Materials and Methods section 2.2.2). Y21F annexin 1-GFP was sequenced to confirm the presence of the mutation (see Appendix 1, Fig. S.4).

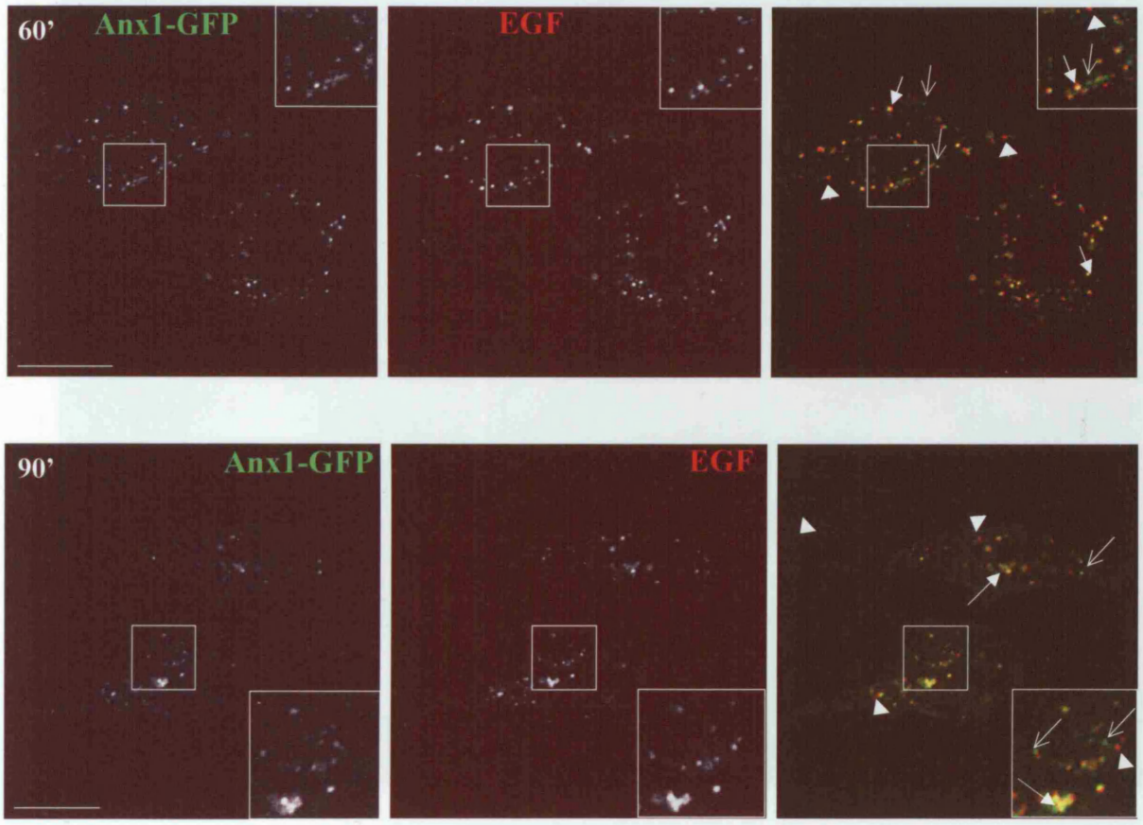

Figure 6.14. *Annexin 1-GFP moves with EGF to the lysosome.* Living HEp2 cells, stably expressing annexin 1-GFP, were serum starved and incubated with EGF-Alexafluor555 for 60 minutes or 90 minutes. There was significant colocalisation in juxtanuclear punctae (arrows), but also some structures that were only positive for annexin 1-GFP (open arrows) or EGF (block arrowheads). Insets = 2x magnification. Bars = 20μm.

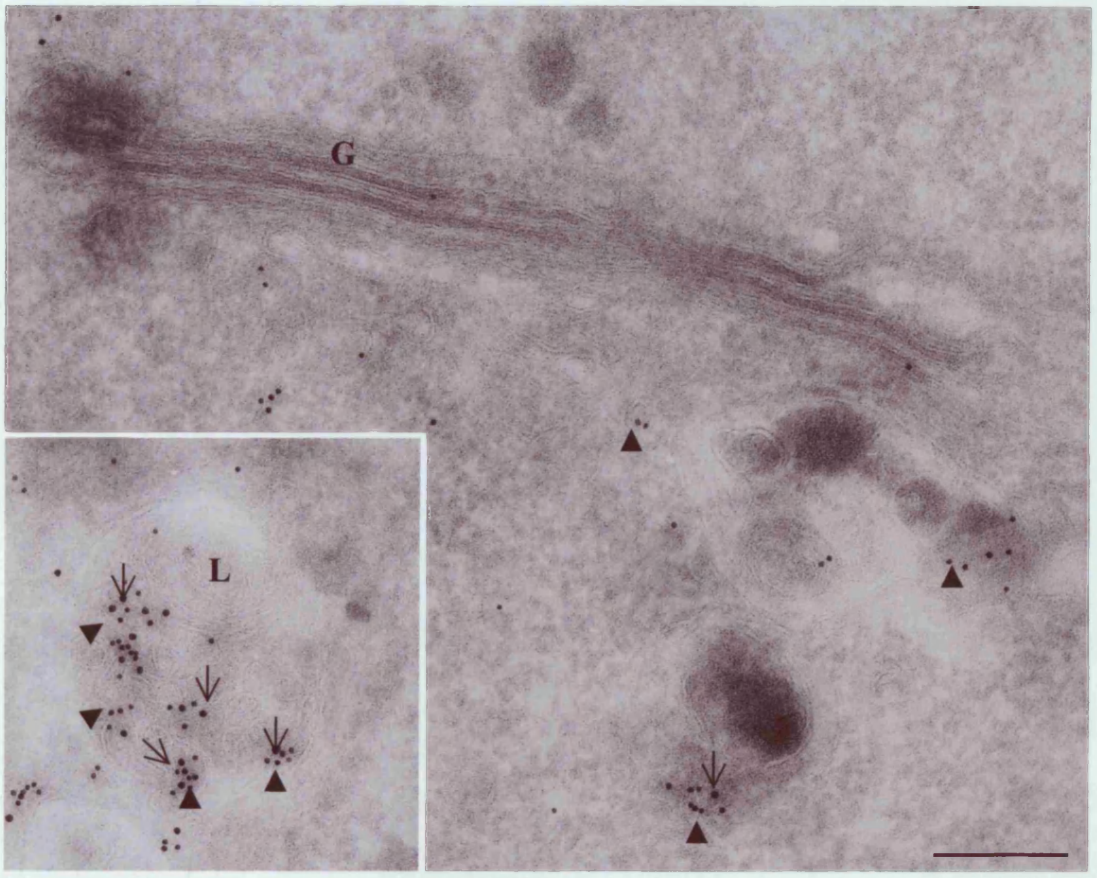

Figure 6.15. *Annexin 1-GFP remains associated with EGFR until the lysosome.* HEp2 cells, stably expressing annexin 1-GFP, were serum starved, stimulated with EGF (100ng/ml) for 60 minutes and processed for immuno-EM. Sections were labelled with anti-GFP (10nm gold, block arrowheads) and anti-EGFR (15nm gold, open arrows) antibodies. EGFR labelling of MVBs was primarily on internal vesicles, which also label for annexin 1-GFP. There was less EGFR labelling visible after 60 minutes, due to lysosomal degradation. Annexin 1-GFP and EGFR co-label both MVBs and lysosomes (L). G = Golgi apparatus. Bar = 200nm.

To test the expression of Y21F annexin 1-GFP, HEp2 cells were transiently transfected with the construct and its localisation observed after 24 hours. Y21F annexin 1-GFP (Y21F) was observed as diffused cytoplasmic staining with some areas of punctate staining in unstimulated cells (Fig. 6.16), and this localisation was similar to that of wild type annexin 1-GFP (Fig. 6.5). To examine whether loss of EGFR phosphorylation alters the localisation of annexin 1, cells were serum starved and observed after 10 minutes stimulation with fluorescent EGF (Fig. 6.17). The localisation of Y21F was not markedly altered after this short period of EGF stimulation. It was visible throughout the cytoplasm and also in a number of EGF-positive punctae, similar to those observed with wild type annexin 1-GFP, although there appeared to be less colocalisation in cells expressing Y21F. After 30 minutes of EGF stimulation, there was some colocalisation of Y21F and EGF, but a number of EGF positive vesicles were also visible (Fig. 6.18).

By 60 minutes, much EGF appeared to have been degraded. However, some colocalisation was still visible in a perinuclear distribution. The localisation of Y21F after EGF stimulation was not obviously different to that of wild type annexin 1-GFP, suggesting that EGFR phosphorylation of annexin 1 is not essential for its localisation.

6.2.5 Annexin 2 colocalises with TfR but not EGFR

The intracellular localisation of annexin 2 was examined to explore whether annexin 2 was present in MVBs despite its apparent lack of function in these structures. Previous immunofluorescence experiments (Chapter 5) revealed that annexin 2 was present throughout the cytoplasm, concentrating near the plasma membrane, and also on punctate structures throughout the cytoplasm.

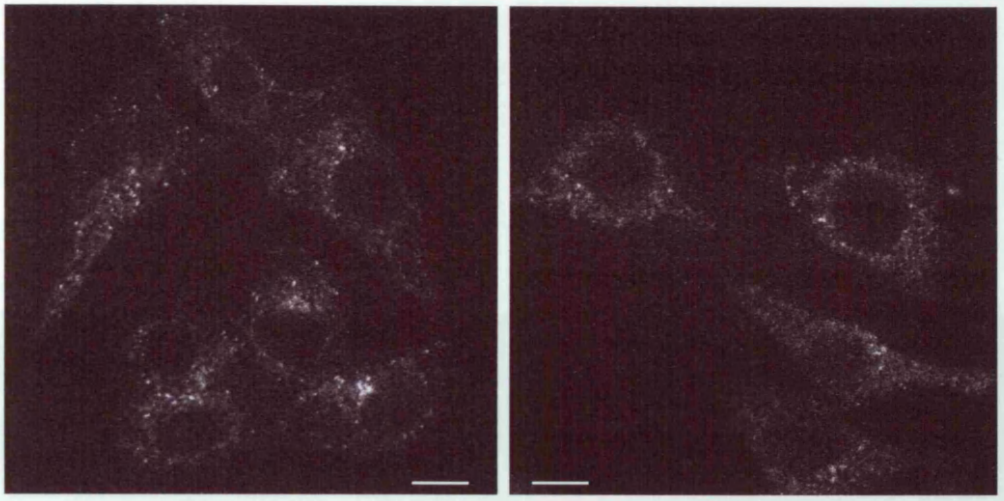

Figure 6.16. *Localisation of Y21F annexin 1-GFP in unstimulated cells.* HEp2 cells were transiently transfected with Y21F annexin 1-GFP for 24 hours. Living cells were serum starved for 1 hour and imaged using confocal microscopy. Y21F annexin 1-GFP was present throughout the cytoplasm and as punctae. Bars = 20μm

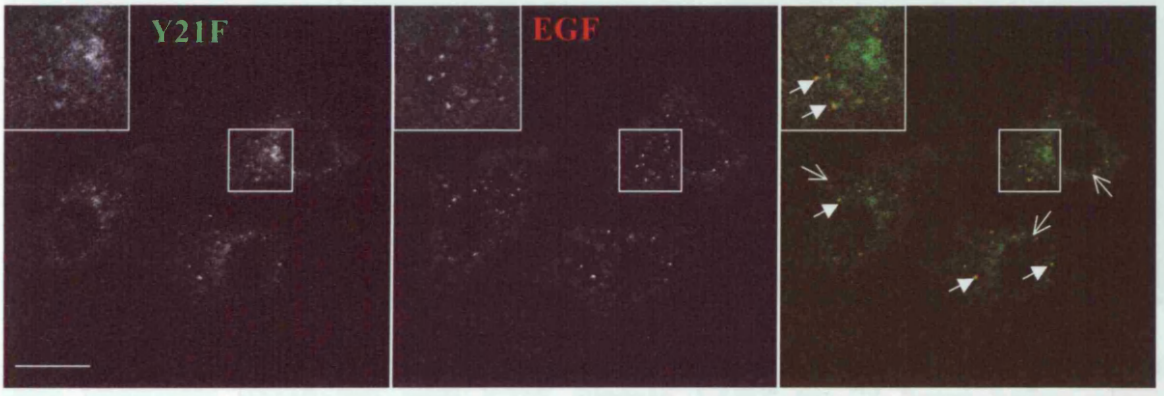

Figure 6.17. *Y21F annexin 1-GFP partially colocalises with EGF in early endosomes.* HEp2 cells were transiently transfected with Y21F annexin 1-GFP for 24 hours before serum starving for 1 hour. Cells were incubated with EGF-AlexaFluor555 for 10 minutes and imaged using confocal microscopy. Inset (2x magnification) shows areas of colocalisation between Y21F and EGF in peripheral punctae. Arrows point to punctae positive for Y21F and EGF, open arrows point to EGF-only positive structures.
Bar = 20μm.

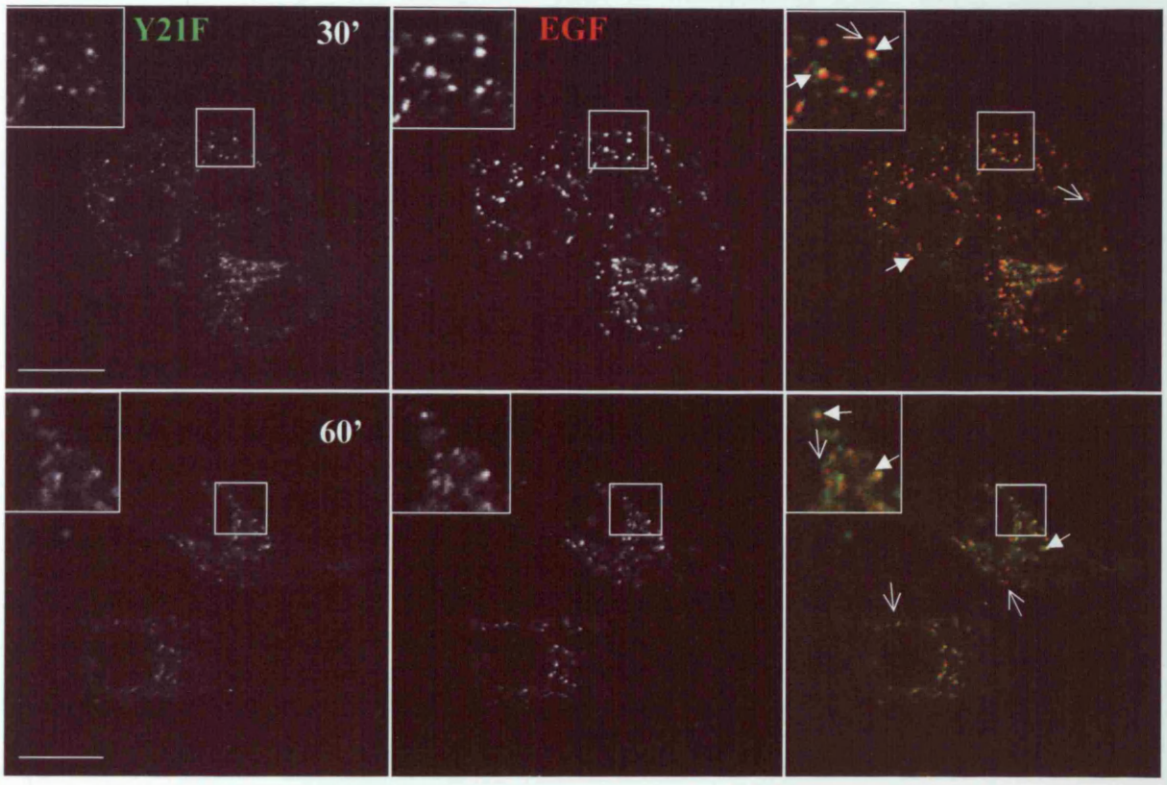

Figure 6.18. ***Y21F annexin 1-GFP localisation in EGF stimulated cells.*** HEp2 cells were transiently transfected with Y21F annexin 1-GFP for 24 hours before serum starving for 1 hour. Cells were incubated with EGF-AlexaFluor555 for 30 or 60 minutes and imaged using confocal microscopy. After 30 minutes there was some colocalisation, but many EGF-positive structures did not contain Y21F. After 60 minutes there was less EGF staining but still some colocalisation. Arrows point to punctae positive for Y21F and EGF, open arrows point to EGF-only positive structures. Insets = 2x magnification. Bars = 20μm.

To examine the localisation of annexin 2 in more detail, cryo-sections from unstimulated annexin 1-GFP expressing HEp2 cells were labelled with anti-annexin 2 (10nm gold) and anti-TfR (15nm gold) antibodies to identify whether annexin 2 localised to TfR positive structures (Fig. 6.19). Annexin 2 labelling was observed just underneath the plasma membrane, throughout the cytoplasm and on small membrane-bound vesicles, many of which co-labelled for TfR. Some structures that co-labelled were vesicular, whereas others were more tubular in shape, although the shape of the structure depends on the plane of sectioning. Although many structures labelled for both annexin 2 and TfR, some labelled only for annexin 2, especially in the cytoplasm.

As EGF stimulation appeared to increase annexin 1 labelling of MVBs, the effect of EGF stimulation on the localisation of annexin 2 was examined. Sections from EGF-stimulated cells were labelled with anti-annexin 2 and anti-TfR antibodies (Fig. 6.20). Previous work localising TfR showed that EGF stimulation had no effect on its localisation (Fig. 6.9). The data here show that EGF stimulation does not alter the localisation of annexin 2, as annexin 2 labelling was again observed on the membrane of TfR positive vesicles and tubular structures. Annexin 2 also co-labelled vesicles with TfR near unlabelled MVBs.

Having shown that EGF stimulation did not affect the localisation of annexin 2, it was necessary to investigate whether annexin 2 labelled any EGFR-positive structures. From published work, it was predicted that annexin 2 would label early endosomes containing EGFR, but whether annexin 2 is in EGFR-containing MVBs had not been investigated. Sections from EGF-stimulated cells were labelled with anti-annexin 2 (10nm gold) and anti-EGFR antibodies (15nm gold) (Fig. 6.21). As observed when investigating annexin 1 localisation, after 30 minutes of EGF stimulation much EGFR labelling was present on both the perimeter membrane and on the internal vesicles of MVBs. Unlike annexin 1, little annexin 2 labelling was observed on the internal vesicles of EGFR-positive MVBs. However, some annexin 2 labelling was observed on the perimeter membrane of a small number of MVBs.

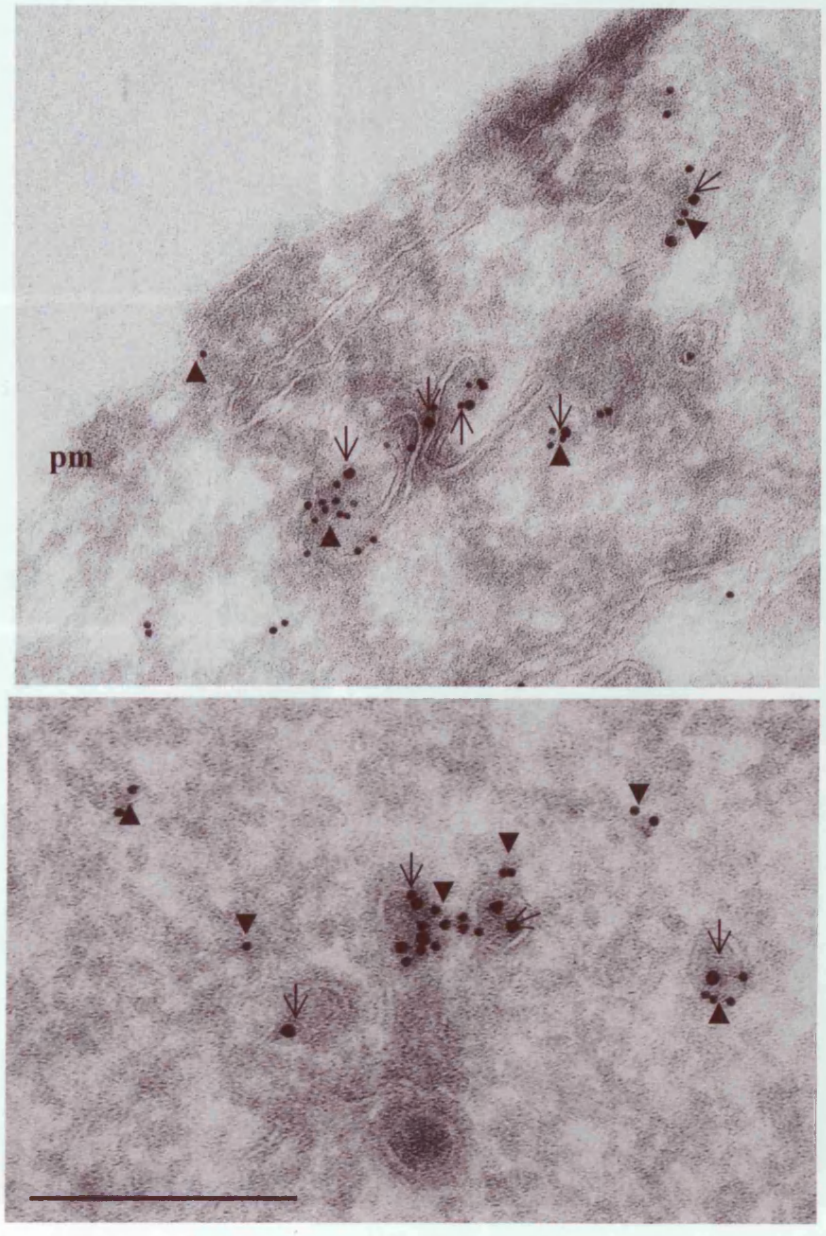

Figure 6.19. *Annexin 2 localises to TfR positive vesicles.* HEp2 cells, stably expressing annexin 1-GFP, were serum starved and processed for immuno-EM. Sections were labelled with anti-annexin 2 (HH7) (10nm gold, block arrowheads) and anti-TfR (15nm gold, open arrows) antibodies. Some annexin 2 labelling was observed just underneath the plasma membrane (pm). TfR labelled membrane bound vesicles and these co-labelled for annexin 2. Bar = 200nm.

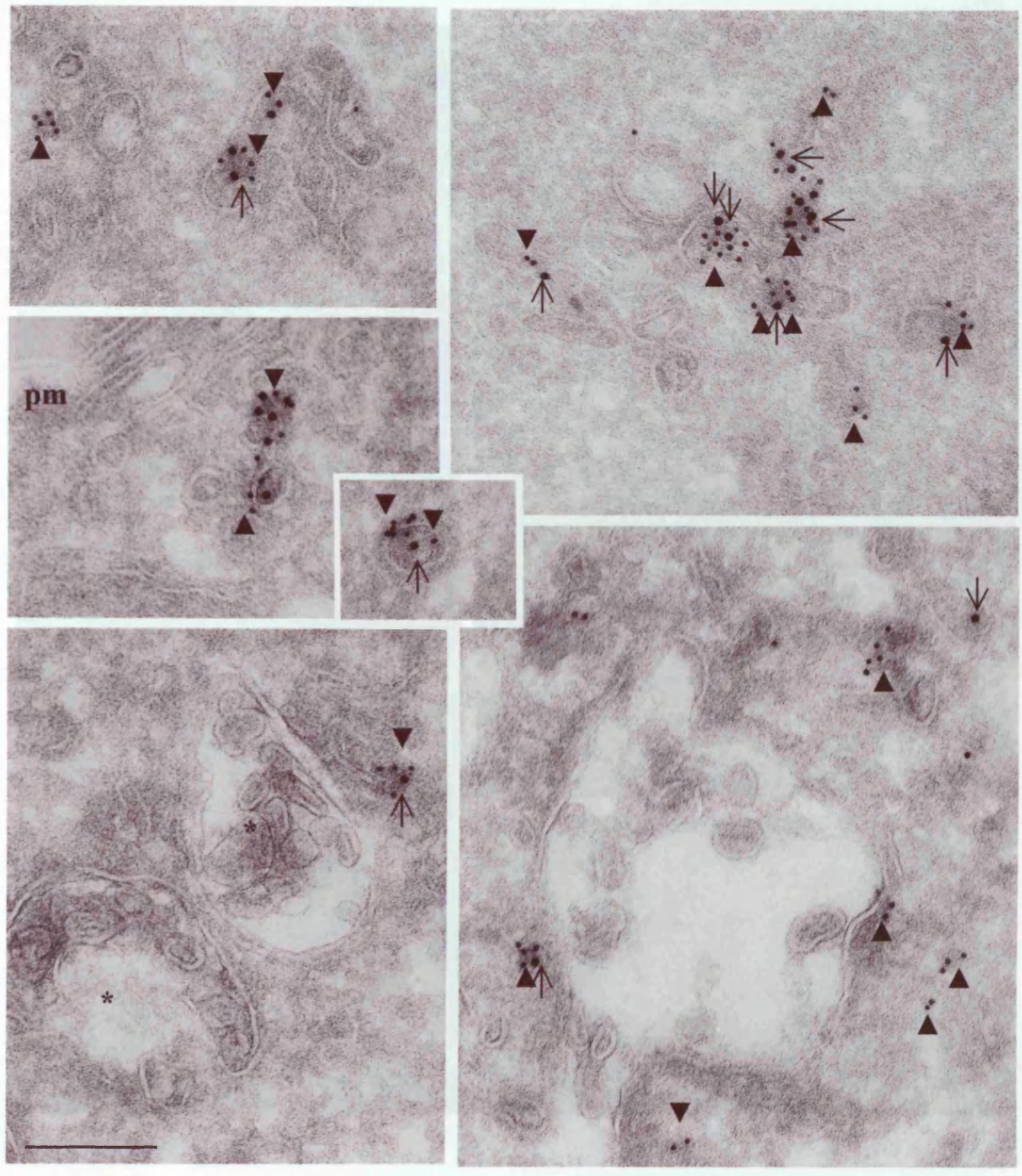

Figure 6.20. *Annexin 2 localisation in EGF-stimulated cells.* HEp2 cells, stably expressing annexin 1-GFP, were serum starved, EGF stimulated for 30 minutes and processed for immunoEM. Sections were labelled with anti-annexin 2 (HH7) (10nm gold, block arrowheads) and anti-TfR (15nm gold, open arrows) antibodies. Annexin 2 and TfR co-label many small endocytic structures, with TfR typically in the lumen of the vesicle or tubule, and annexin 2 on the membrane. Annexin 2 co-labels TfR positive vesicles that are close to MVBs, possibly recycling endosomes. Unlabelled MVBs are marked with a star. Bar = 200nm.

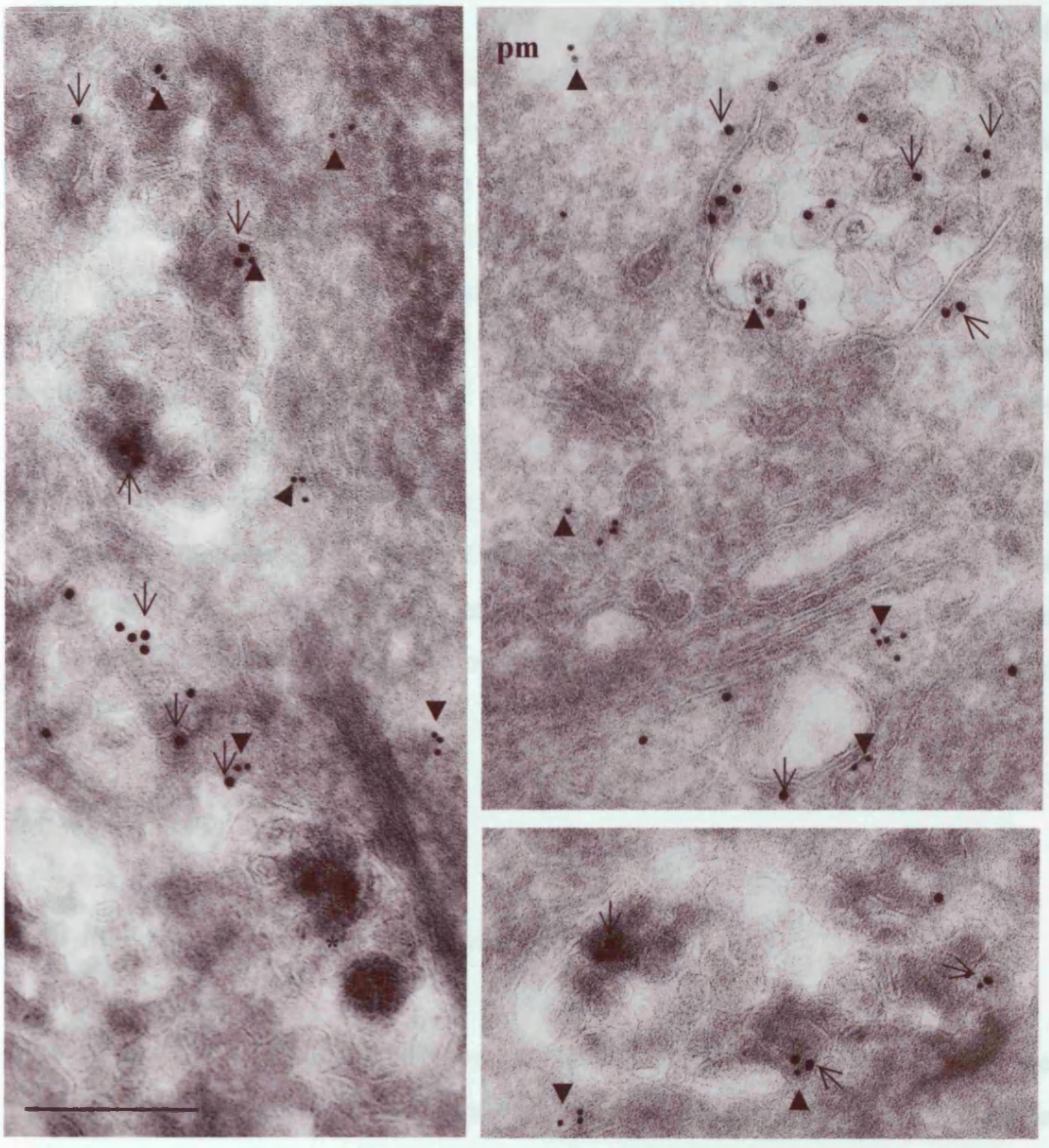

Figure 6.21. *Annexin 2 does not localise with EGFR in MVBs.* HEp2 cells, stably expressing annexin 1-GFP, were serum starved, EGF stimulated for 30 minutes and processed for immunoEM. Sections were labelled with anti-annexin 2 (10nm gold, block arrowheads) and anti-EGFR (15nm gold, open arrows) antibodies. EGFR labelling was observed in MVBs, both on the perimeter membrane (see MVB in upper right picture) and on internal vesicles. There was little annexin 2 labelling of these structures, although a small amount was observed on the perimeter membrane. Annexin 2 labelled small vesicles and near the plasma membrane (pm). Unlabelled MVB marked with a star. Bar = 200nm.

Thus far the functions described for annexin 1 do not apply to annexin 2. Annexin 1 has previously been localised to early endosomes and late endosomes after N-terminal proteolysis. Data shown here, for the first time, localised annexin 1 to the same internal vesicles as EGFR in MVBs of EGF stimulated cells, providing further evidence for its role in EGF-stimulated inward vesiculation in a subpopulation of MVBs. Annexin 2 did not label these structures to the same extent and instead colocalised extensively with TfR positive structures. Therefore, to further confirm that annexins 1 and 2 exhibit distinct cellular localisations, sections from EGF-stimulated cells were labelled with anti-GFP (15nm gold) and anti-annexin 2 (10nm gold) (Fig. 6.22). Both labelled the plasma membrane and throughout the cytoplasm. Annexin 1-GFP labelled the internal vesicles and perimeter membrane of MVBs, yet little annexin 2 labelling was observed on these structures. These data are consistent with those described above (Fig. 6.12 and 6.21), showing that annexin 1, not annexin 2, is involved in EGF-stimulated formation of internal vesicles.

6.3 Discussion

6.3.1 EGF stimulation alters the distribution of annexin 1

One of the aims of this study was to investigate the effect of EGF on the localisation of annexin 1. These data show, through a combination of fluorescence and cryo-immuno EM, that the localisation of annexin 1, as annexin 1-GFP, but not annexin 2, is altered after EGF stimulation. In unstimulated cells, annexin 1 is present both in the cytoplasm and on small vesicles near the plasma membrane, and on Tf/TfR positive early endosomes, consistent with published data (Seemann *et al.*, 1997; Rescher *et al.*, 2000). Following EGF stimulation, annexin 1-GFP co-labels small EGF positive endosomes and, after longer incubations, larger EGF positive structures distributed in a juxtanuclear position, which correspond to the usual location of MVBs. Immunolabelling of cryosections showed that these structures are EGFR-positive MVBs and that annexin 1 remains associated with EGF/EGFR positive structures until reaching the lysosome. This is the first report that annexin 1 is associated with EGFR containing endocytic structures until lysosomal degradation.

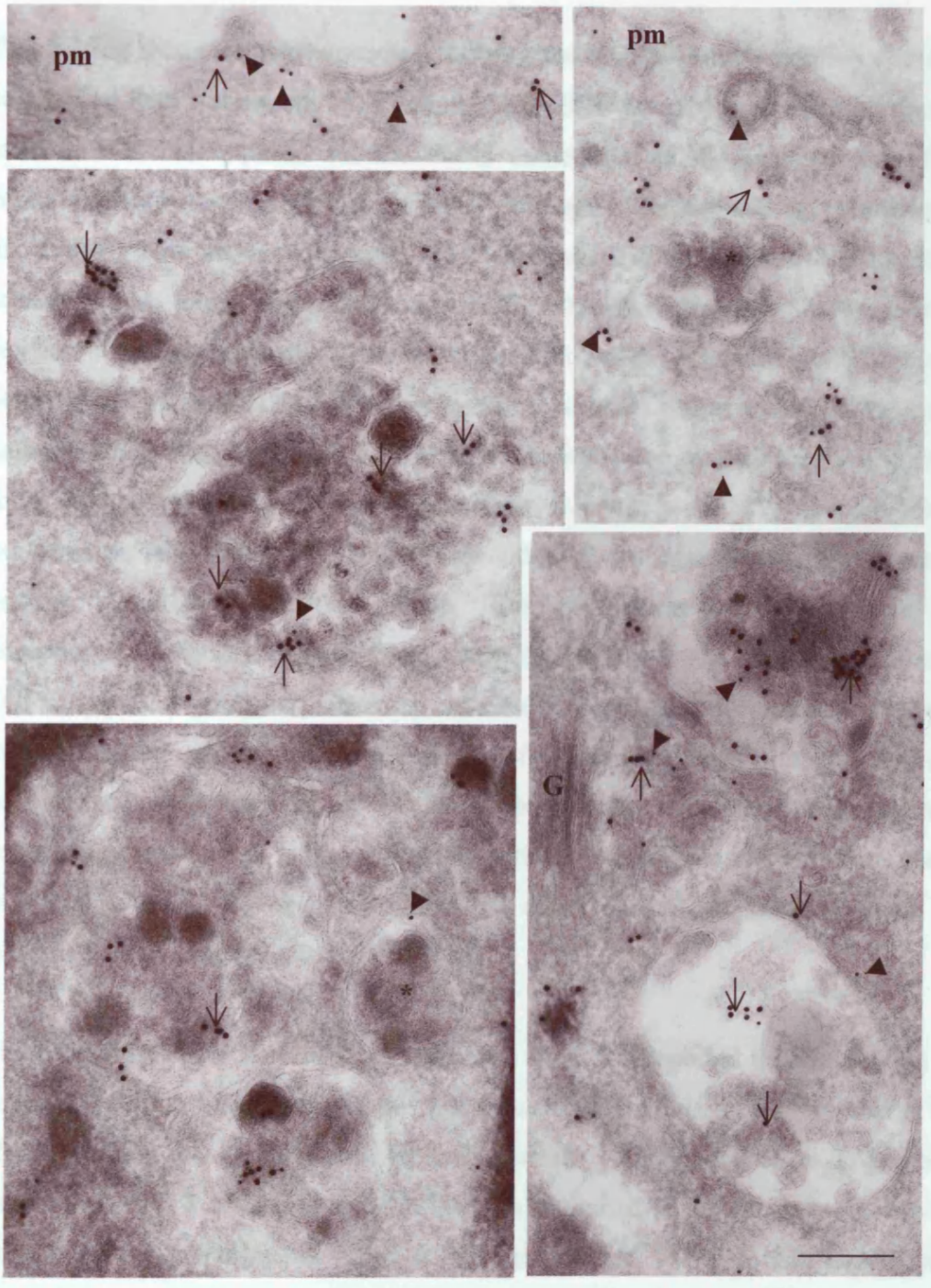

Figure 6.22. *Localisation of annexins 1 & 2 in EGF stimulated cells.* HEp2 cells, stably expressing annexin 1-GFP, were serum starved, EGF stimulated for 30 minutes and processed for immunoEM. Sections were labelled with anti-annexin 2 (HH7) (10nm gold, block arrowheads) and anti-GFP (15nm gold, open arrows) antibodies. Both annexins 1 and 2 labelled near, or just underneath, the plasma membrane (pm). The majority of annexin 1-GFP labelling was observed within MVBs. Unlabelled MVBs are marked (*). Annexin 2 preferentially labelled small vesicles throughout the cytoplasm, near MVBs and on the perimeter membrane of MVBs. G = Golgi apparatus. Bar = 200nm.

The finding that a mutant annexin 1 lacking the EGFR phosphorylation site still colocalised with fluorescent EGF indicates that EGF-stimulated phosphorylation of annexin 1 is not required for the initial association of the protein with EGF-containing endosomes, consistent with the findings of Seemann *et al.* (Seemann *et al.*, 1996). This mutant annexin 1-GFP construct still localised to EGF-positive structures after longer incubations with EGF. That the localisation of this mutant annexin 1 was not markedly different from that of wild type annexin 1-GFP could be explained by the fact that phosphorylation of annexin 1 does not occur until after annexin 1 has associated with EGF-positive endosomes. As endosomes mature to form MVBs, annexin 1 remains associated and it is within the MVB that annexin 1 performs its role in inward vesiculation, although the exact mechanism remains unclear. Therefore, even the mutant form of annexin 1-GFP, unable to be phosphorylated by EGFR, would be present on MVBs. It has been suggested that EGFR-mediated phosphorylation of annexin 1 is required for release of newly formed internal vesicles and so the effects of a phosphorylation mutant would not be observed until later stages of EGFR trafficking. As HEp2 cells express endogenous annexin 1, little functional evidence can be collected from these experiments as to the exact nature of the effect of loss of phosphorylation of annexin 1 on inward vesiculation.

These findings differ slightly from published work that reported the localisation of annexin 1-GFP in living cells for the first time (Rescher *et al.*, 2000). Rescher *et al.* (2000) showed that in unstimulated cells annexin 1-GFP localised to Tf-positive endosomes, which is consistent with the data presented in this chapter. However, these published experiments failed to localise annexin 1-GFP to late endosomes, marked by a pulse of fluorescent HRP (Rescher *et al.*, 2000). Only a N-terminally truncated annexin 1-GFP construct was found to label late endosomes (Rescher *et al.*, 2000). The data presented in this chapter can be reconciled with these published findings on the basis that annexin 1 plays a specific role within EGF stimulated cells. The experiments performed and described in this chapter show that annexin 1-GFP colocalises with EGF/EGFR in MVBs and lysosomes. In unstimulated cells there are fewer MVBs and these do not label as heavily for annexin 1-GFP. That some annexin 1-GFP was localised to MVBs in unstimulated cells, in this chapter, could be accounted for by the enhanced sensitivity of immuno EM compared with

immunofluorescence. Increased annexin 1 labelling of MVBs after EGF stimulation may be due, in part, to the increased number of MVBs. Therefore, the work of Rescher *et al.* (2000) in unstimulated cells provides further evidence that EGF-stimulation may alter the localisation of annexin 1, by promoting its association with endosomes and thus MVBs. The fact that only the core domain of annexin 1 localised to late endosomes (Rescher *et al.*, 2000) is consistent with the theory that phosphorylation induced N-terminal proteolysis of annexin 1 occurs, and that this process is coupled to inward vesiculation. However, the finding that annexin 1 lacking the EGFR phosphorylation site still localised to EGF-positive MVBs/late endosomes is inconsistent with the published work. One possible explanation could be that EGF stimulation induces the recruitment of annexin 1 to MVBs independently of annexin 1 phosphorylation, and that phosphorylation is only required for the release of internal vesicles within MVBs.

6.3.2 Annexin 1 is recruited onto internal vesicles of MVBs with EGFR

The finding that annexin 1 is associated with EGFR-positive MVBs confirms previously published fractionation studies (Futter *et al.*, 1993; Pol *et al.*, 1997). Furthermore, these experiments allowed the exact ultrastructural localisation to be examined, with regard receptor trafficking. The data presented here shows that not only is annexin 1 present within EGFR-positive MVBs, but that it labels the same internal vesicles as EGFR. While the EGFR antibody labelled the receptor cytoplasmic domain within the internal vesicles, it was not clear which side of the internal vesicle membrane annexin 1 labelled, partly due to the use of bridging antibodies. However, its localisation on internal vesicles is in keeping with a role for annexin 1 in allowing fission of newly formed vesicles into the lumen of the MVB. Some annexin 1 labelling was also found at the perimeter membrane and, although these experiments do not investigate it directly, this finding is consistent with the hypothesis that annexin 1 is phosphorylated by EGFR at the perimeter membrane, in order to induce N-terminal proteolysis of annexin 1, thus releasing the newly formed internal vesicle into the lumen of the MVB. These data also show that little annexin 2 was found within MVBs, although a small amount of labelling was observed, the majority of which was on the perimeter membrane.

This finding is in agreement with work suggesting a role for annexin 2 in TfR recycling, which also reports that loss of annexin 2 had no effect on delivery to the late endosome/lysosome (Zobiack *et al.*, 2003).

6.3.3 Further evidence for subpopulations of MVBs

In unstimulated cells there were fewer MVBs observed, consistent with the data shown in Chapter 3, and following EGF stimulation the number of MVBs was greatly increased. Annexin 1 and EGFR co-labelled the majority of MVBs observed. After 30 minutes of EGF stimulation, labelling was divided between the perimeter membrane and internal vesicles, whereas after longer incubations labelling was predominantly on internal vesicles. However, even after EGF stimulation, not all MVBs labelled for annexin 1 and EGFR. Those MVBs that did not label for EGFR did not label for annexin 1 either and are shown in Figures 6.7, 6.12 and 6.22. Taken together with previous findings (Chapter 3) showing that loss of annexin 1 did not affect the formation of all MVBs, these data provide further evidence for the existence of different sub-populations of MVBs.

Annexin 1-GFP labelled the majority of EGFR-positive MVBs, although some multivesicular structures labelled only for EGFR. This finding could be due to the fact that cells express far higher levels of endogenous annexin 1 than annexin 1-GFP, and that while endogenous annexin 1 may be present within MVBs, it was not recognised by the anti-GFP antibody. Within EGFR-positive MVBs, annexin 1-GFP only labelled certain internal vesicles, mostly those containing EGFR. Labelling of cryosections with an anti-annexin 1 antibody confirmed this finding and indicates that within MVBs there are at least two types of internal vesicle, those that label for annexin 1 and those that do not. Fractionation studies of late endosomal membranes separated MVB internal membranes into at least 2 populations, both of which contained the tetraspanin CD63. One of these populations contained the majority of cellular LBPA, while the other was enriched in phosphatidylcholine (Kobayashi *et al.*, 2002). However, from these experiments it was unclear whether there were two distinct populations of MVBs or two populations of internal vesicles within MVBs.

Unpublished data also identified the presence of at least two subpopulations of MVB (White *et al.*, under review), consistent with the data presented in this chapter. This work identified many EGFR-containing MVBs and a smaller number of morphologically similar MVBs that did not contain EGFR, but labelled for LBPA. The data from this chapter confirm the presence of two sub-populations of MVB, and also show that EGFR-containing MVBs label for annexin 1. Annexin 1 mediates the EGF-stimulated increase in inward vesiculation within MVBs, but only within those containing EGFR. Coupled with its localisation on EGFR-positive internal vesicles, it seems likely that annexin 1 is only present on one population of MVB and perhaps only one type of internal vesicle.

6.3.4 Annexin 2 and TfR

The majority of data discussed so far have concerned annexin 1 and its EGF-stimulated functions. That annexin 2 does not mediate any EGF-specific effect on MVB formation, or internal vesicle formation within MVBs, is not surprising, given that it is a poor substrate for the EGFR tyrosine kinase, unlike annexin 1. The data presented in this chapter confirm published studies that showed colocalisation of annexin 2 and early endosomes (Emans *et al.*, 1993). In the current study, the majority of annexin 2 labelling was observed on small membrane bound vesicles and a large amount was closely associated with TfR-positive structures. Although EGF stimulation did not markedly alter either annexin 2 or TfR localisation, in EGF stimulated cells annexin 2 and TfR co-labelled a number of vesicles near mature MVBs, possibly recycling endosomes.

These data support the evidence presented in the previous chapters that argue against a role for annexin 2 in MVB formation, but point towards a role in TfR trafficking, possibly in recycling. Annexin 2 is recruited to sites of actin polymerisation at both the plasma membrane and endosomes (Rescher *et al.*, 2004). Actin is known to be involved in TfR recycling and this provides another clue to the action of annexin 2 (Durrbach *et al.*, 1996).

6.3.5 Summary of findings

These data show, though a combination of fluorescence and immuno EM, that annexin 1 colocalises with EGF in early endosomes, but also in MVBs and lysosomes. That annexin 1 is present in early endosomes has been previously reported (Seemann *et al.*, 1997; Diakonova *et al.*, 1997; Rescher *et al.*, 2000), but the ultrastructural location of annexin 1 to MVBs is shown here for the first time. The finding that annexin 1 is present on the same internal vesicles as EGFR after EGF stimulation provides further evidence for its role in formation of EGF-stimulated internal vesicles. The absence of annexin 2 from MVBs and lysosomes, both in unstimulated and EGF-stimulated cells, supports previous findings that loss of annexin 2 does not affect MVB formation (Chapter 4) or lysosomal delivery (Chapter 5), and is consistent with published fractionation studies, in which no annexin 2 was associated with MVBs (Pol *et al.*, 1997). Instead, annexin 2 is closely associated with structures that also label for Tf/TfR. The localisation of annexin 2 does not alter after EGF stimulation, which is unsurprising as it is a poor substrate for the EGFR tyrosine kinase. Finally, detailed analysis of the intracellular locations of annexins 1 and 2 revealed that, although they are both present at the plasma membrane and throughout the cytoplasm, their localisations are very different and this could account for their distinct roles within EGFR trafficking.

Chapter 7 – A role for annexin 1 in the regulation of cell shape and motility

7.1 Introduction

JACRO annexin 1 -/- cells were studied in detail to investigate the effect of loss of annexin 1 on MVB formation and inward vesiculation (Chapter 3). Whilst using these cells, and the wild type cell line, a difference in cell size and shape was observed between cell lines. Croxtall *et al.* (2003) reported that annexin 1 -/- cells had more spindle-like appearance but did not investigate this further (Croxtall *et al.*, 2003). That annexin 1 may be involved in regulation of cell shape is consistent with its membrane- and actin-binding properties (Glenney, Jr. *et al.*, 1987). Regulation of the actin cytoskeleton is important for maintaining cell size and shape, and also in the regulation of cell motility. Additionally, annexin 1 is able to bind the actin-modifying protein, profilin (Alvarez-Martinez *et al.*, 1996; Alvarez-Martinez *et al.*, 1997).

The effects of growth factor stimulation on fibroblast motility have been widely investigated, in particular those of EGF (O'Neill *et al.*, 1985; Lin and Bertics, 1995; Xie *et al.*, 1998; Ware *et al.*, 1998; Wells *et al.*, 1999b) and fibroblast growth factor (FGF) (Taylor *et al.*, 1993; Ding *et al.*, 2000). EGF induces both mitogenic and motogenic responses in a variety of cell types, including fibroblasts (Chen *et al.*, 1994a&b). Fibroblast migration is stimulated by EGF receptor activation, in a process involving PLCγ mediated PIP_2 hydrolysis at the leading edge of cells and the localised release of the actin-modifying proteins, profilin and gelsolin (Goldschmidt-Clermont *et al.*, 1991; Banno *et al.*, 1992; Chen *et al.*, 1996a; Chou *et al.*, 2003). Annexins have also been implicated in cell migration although, in the case of annexin 1, the inhibition of the transendothelial migration of leukocytes by annexin 1 and N-terminal annexin 1 peptides is mediated by extracellular binding to members of the formyl peptide receptor family, rather than by direct interaction of annexin 1 intracellularly with the actin cytoskeleton (Walther *et al.*, 2000; Rescher *et al.*, 2002; Ernst *et al.*, 2004). The role of annexin 1 in EGF-stimulated cell motility has not yet been investigated. However, annexin 1 is phosphorylated by the EGFR tyrosine kinase and phosphorylation modifies the Ca^{2+} dependency of

membrane association and increases the susceptibility of annexin 1 to N-terminal proteolysis (Haigler *et al.*, 1987; Chuah and Pallen, 1989; Ando *et al.*, 1989; Futter *et al.*, 1993). The effect of tyrosine phosphorylation on actin binding and bundling activity has not been investigated directly, but EGF stimulation has been reported to induce colocalisation of annexin 1 with F-actin on membrane ruffles (Campos-Gonzalez *et al.*, 1990).

The initial aim of this study was to investigate the effect of loss of annexin 1 on the size and shape of mouse lung fibroblasts, using the JACRO cell lines. Cells lacking annexin 1 were slightly larger than wild type cells, but significantly flatter, as shown by an increased average area and confirmed using scanning electron microscopy. This increase in cell area was reversed by expressing annexin 1 in annexin 1 -/- cells. As annexin 1 plays a specific role in EGF-stimulated inward vesiculation, the effect of EGF was investigated and found that, although EGF-stimulation induced a change in cell shape, consistent with published data (Wells *et al.*, 1999a), no significant effect was observed in annexin 1 -/- cells compared with wild type cells. However, the use of EGF in these studies led to the observation that annexin 1 -/- cells appeared to move more in response to EGF stimulation.

The studies presented here show that EGF-stimulation enhanced cell motility in both cell lines, although the mean distance moved by annexin 1 -/- cells was markedly increased compared to that of wild type cells. This increase was reversed by re-expression of annexin 1, but not by expression of a mutant annexin 1 lacking the EGFR phosphorylation site. These data show that annexin 1 inhibits EGF-stimulated fibroblast motility, a process that requires EGFR-mediated annexin 1 phosphorylation.

7.2 Results

7.2.1 Loss of annexin 1 alters the morphology of JACRO cells

Both JACRO cell lines formed adherent confluent monolayers. Proliferation of annexin 1 -/- cells was slightly reduced compared to wild type cells (Croxtall *et al.*, 2003). To confirm the absence of annexin 1 in the -/- cells, JACRO cell lysates were collected and blotted for annexin 1 (Fig. 7.1A). The morphology of JACRO cells was observed using light microscopy, where JACRO annexin 1 -/- cells looked larger than wild type cells under sub-confluent conditions (Fig. 7.1B). The difference in cell morphology has already been reported, but focused on the more spindle-like appearance in the annexin 1 -/- cells compared to wild type cells (Croxtall *et al.*, 2003).

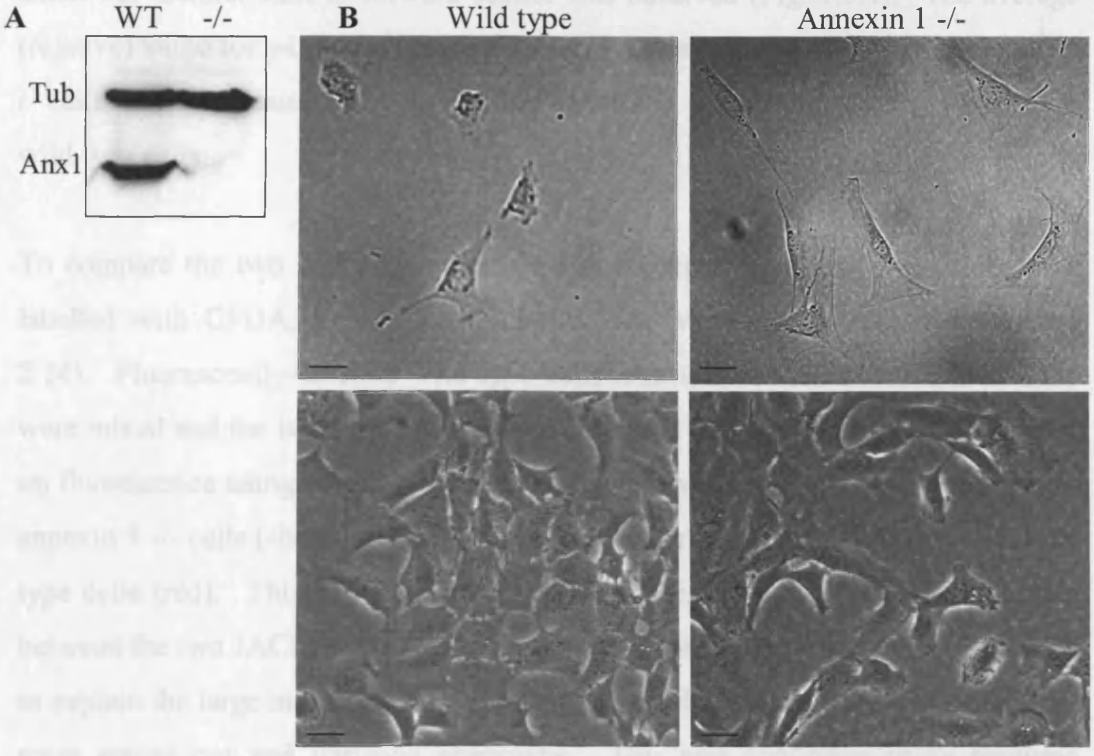

Figure 7.1. *Loss of annexin 1 alters morphology of JACRO cells.* (A) JACRO wild type (WT) and annexin 1 -/- cell lysates were blotted for annexin 1 and tubulin. (B) Wild type and annexin 1 -/- cells were imaged at subconfluency (top) or confluency (lower). Cells lacking annexin 1 have a more spindle-like, elongated shape. Bars = 10μm.

To further analyse the difference in cell morphology, phase images were taken of each cell line and the area of cells measured (see Materials and Methods section 2.9.2) (Fig. 7.2). JACRO annexin 1 -/- cells had a larger area than wild type cells (2.8-fold increase). These cells also had a greater cell perimeter than wild type cells under the same conditions, but the difference was not as great (1.4-fold).

The fact that there was a large difference in the area of JACRO cells was not surprising, having observed both cell lines in culture. However, when cells were trypsinised, for passaging or cell counting, the difference in size of rounded-up cells was not noticeably different. To compare the actual sizes of wild type and annexin 1 -/- JACRO cells, flow assisted cell sorting (FACS) analysis was used. To compare cell size, forward scatter was plotted on the X axis against side scatter on the Y axis. Comparing the data from wild type cells with annexin 1 -/- cells, a small but distinct shift in forward scatter was observed (Fig. 7.3A). The average (relative) value for wild type cell size was 417.6 compared to 456.14 in annexin 1 -/- cells. This indicates that cells lacking annexin 1 -/- cells are slightly larger than wild type cells.

To compare the two cell types within the same experiment, wild type cells were labelled with CFDA, a fluorescent marker (see Materials and Methods section 2.14). Fluorescently-labelled wild type cells and non-labelled annexin 1 -/- cells were mixed and the two populations were separated into two distinct groups, based on fluorescence using FACS (Fig. 7.3B). As observed in the previous experiment, annexin 1 -/- cells (shown in black) were located further along the X axis than wild type cells (red). This provides further evidence that there is a difference in size between the two JACRO cell lines. However, this small difference is not sufficient to explain the large increase in cell area, indicating that the annexin 1 -/- cells had a more spread out and flattened phenotype. This was confirmed using scanning electron microscopy (Fig. 7.4). JACRO cells were serum starved for one hour before being fixed and embedded for scanning electron microscopy (see Materials & Methods section 2.13).

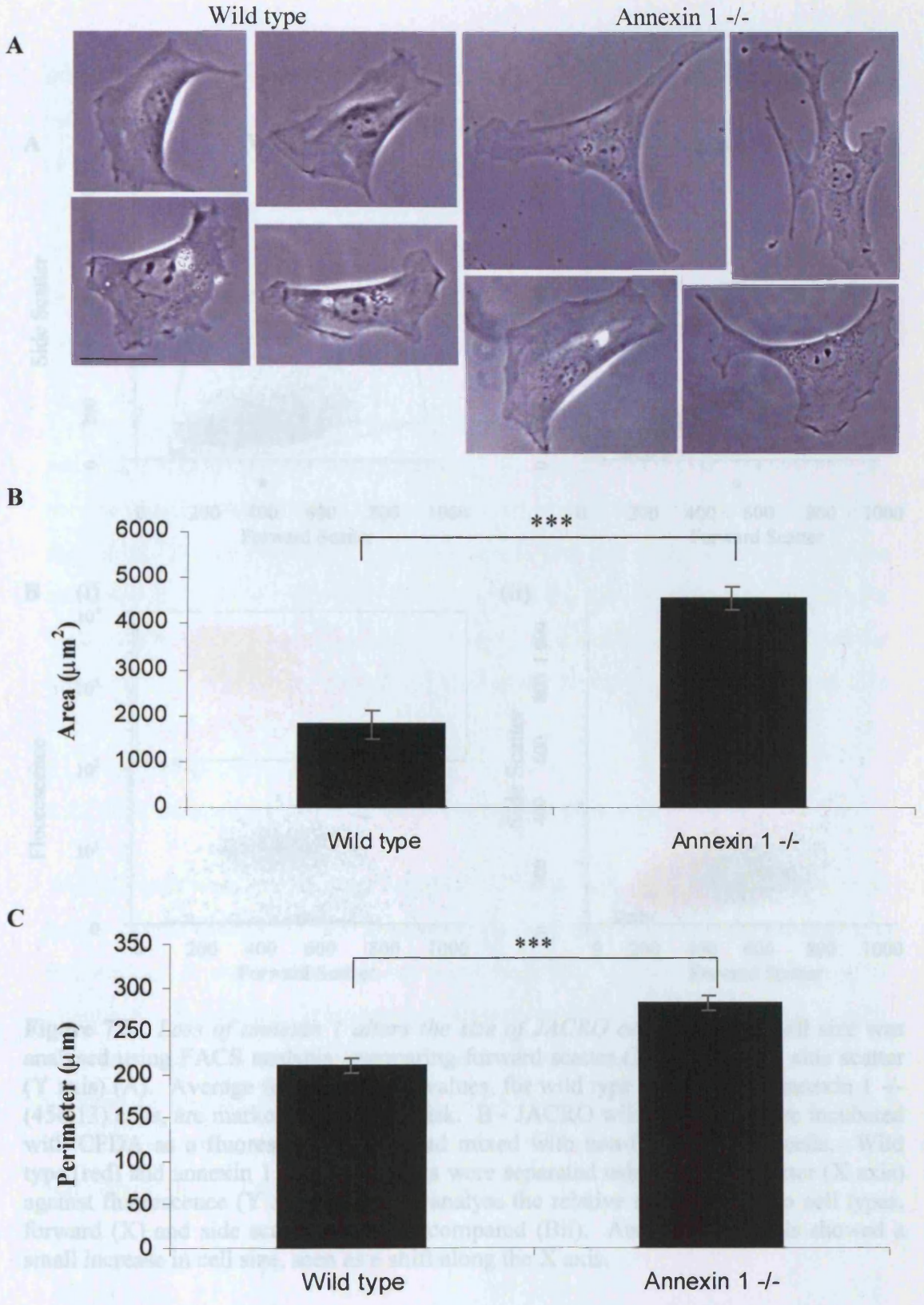

Figure 7.2. *Annexin 1 -/- cells have a greater area than wild type cells.* JACRO cells were plated on 3cm Mattek™ dishes for 24 hours and serum starved overnight. Several fields of cells were taken for each experiment and typical images shown for each cell type (A). Cell area (μm^2) and cell perimeter (μm) were measured for each cell and the mean calculated (B, C). JACRO annexin 1 -/- cells had a much greater area and perimeter than wild type cells. Graphs show the mean ± SEM of 4 independent experiments. Bar = 50μm. *** $p<0.005$.

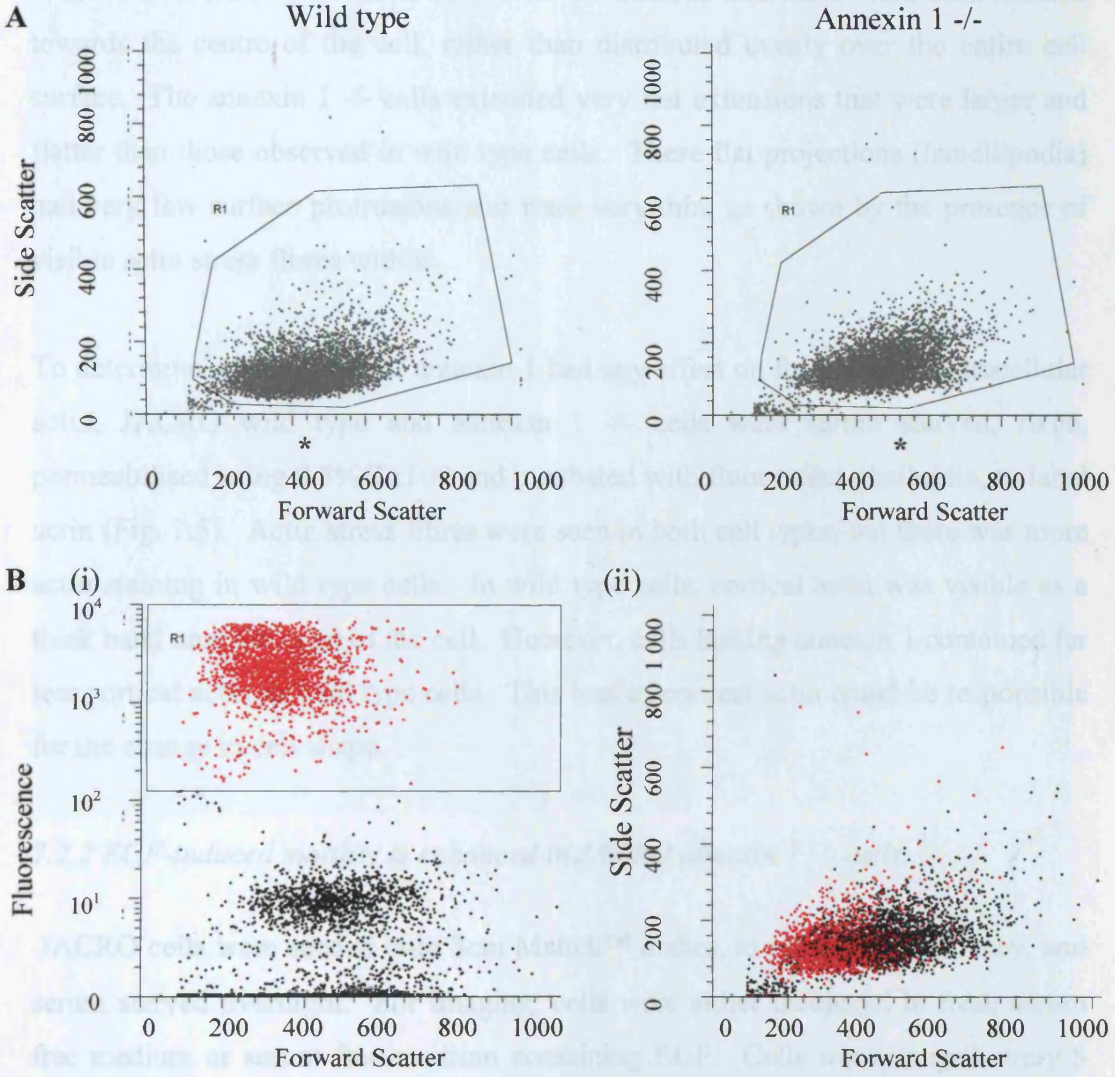

Figure 7.3. *Loss of annexin 1 alters the size of JACRO cells.* JACRO cell size was analysed using FACS analysis, comparing forward scatter (X axis) against side scatter (Y axis) (A). Average forward scatter values, for wild type (417.62) and annexin 1 -/- (456.13) cells, are marked with an asterisk. B - JACRO wild type cells were incubated with CFDA as a fluorescent marker and mixed with non-fluorescent -/- cells. Wild type (red) and annexin 1 -/- (black) cells were separated using forward scatter (X axis) against fluorescence (Y axis) (Bi). To analyse the relative sizes of the two cell types, forward (X) and side scatter (Y) were compared (Bii). Annexin 1 -/- cells showed a small increase in cell size, seen as a shift along the X axis.

Wild type cells had many surface protrusions spread over the entire surface of the cell, while annexin 1 -/- cells had fewer protrusions and these were concentrated towards the centre of the cell, rather than distributed evenly over the entire cell surface. The annexin 1 -/- cells extended very flat extensions that were larger and flatter than those observed in wild type cells. These flat projections (lamellipodia) had very few surface protrusions and were very thin, as shown by the presence of visible actin stress fibres within.

To determine whether loss of annexin 1 had any effect on formation of intracellular actin, JACRO wild type and annexin 1 -/- cells were serum starved, fixed, permeabilised using 0.5% Tx100 and incubated with fluorescent phalloidin, to label actin (Fig. 7.5). Actin stress fibres were seen in both cell types, but there was more actin staining in wild type cells. In wild type cells, cortical actin was visible as a thick band near the edge of the cell. However, cells lacking annexin 1 contained far less cortical actin as wild type cells. This loss of cortical actin could be responsible for the change in cell shape.

7.2.2 EGF-induced motility is enhanced in JACRO annexin 1 -/- cells

JACRO cells were seeded onto 3cm Mattek™ dishes, to reach subconfluency, and serum starved overnight. For imaging, cells were either incubated in fresh serum free medium or serum free medium containing EGF. Cells were imaged every 5 minutes for 90 minutes. The area and perimeter of each cell were measured at each time point of EGF stimulation, and the mean per experiment calculated. EGF stimulation did not induce a significant change in area or perimeter of JACRO cells. At each time point, the differences between wild type and annexin 1 -/- cell areas and perimeters were statistically significant (Fig. 7.6).

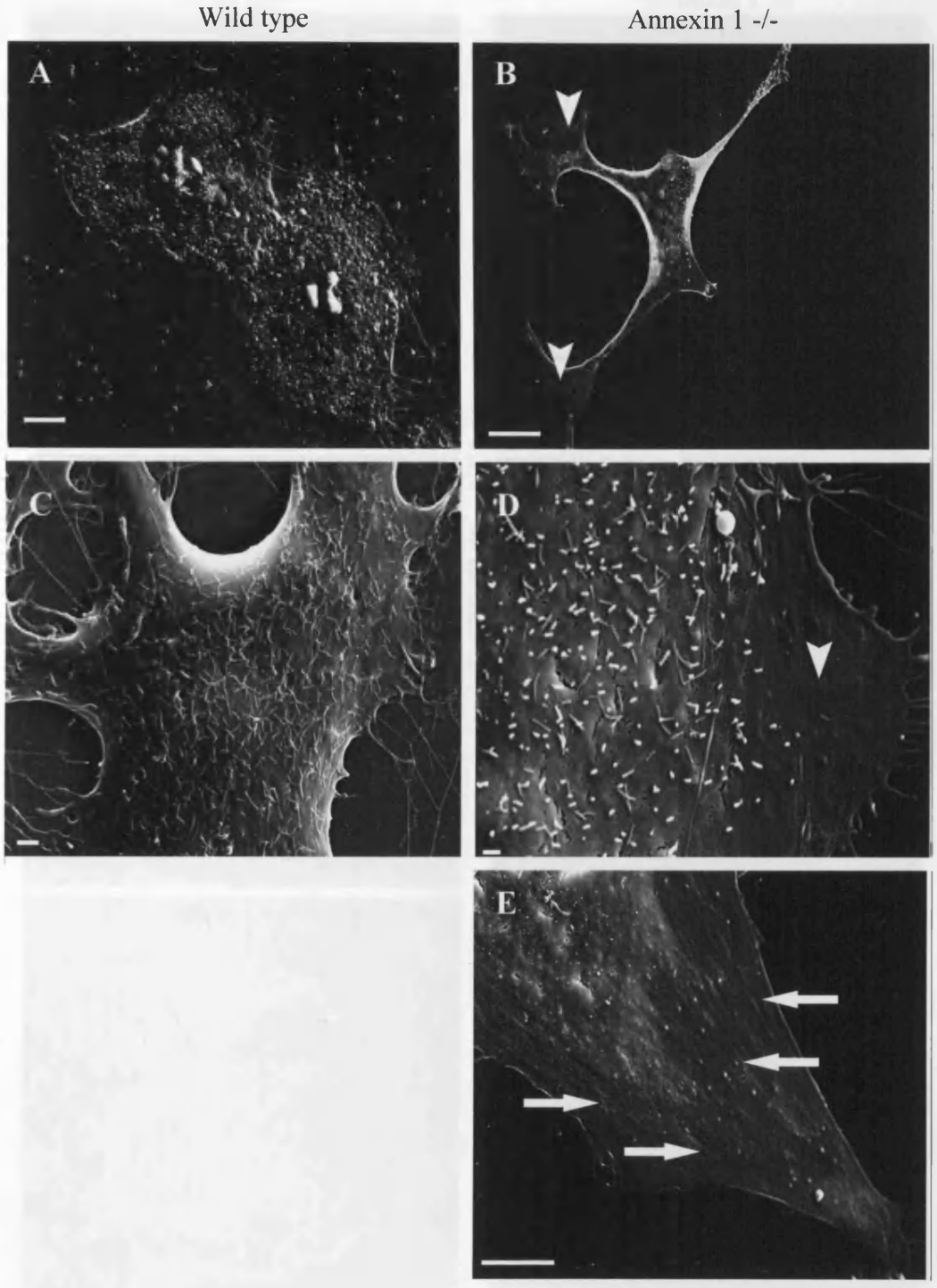

Figure 7.4. *Cells lacking annexin 1 are flatter and more spread out.* JACRO wild type (A & C) and annexin 1 -/- (B, D, E) cells were seeded onto glass coverslips overnight and serum starved for 1 hour. Cells were fixed for scanning electron microscopy. Low magnification (A & B) confirmed the difference in cell area previously observed. Higher magnification (C & D) revealed differences in cell surface protrusions. White arrowheads point to areas lacking surface protrusions, white arrows point to actin stress fibres visible within a very flattened lamellipodium. Annexin 1 -/- cells were flatter and more spread out, compared to wild type cells. Bars = 10μm (A, B, E) or 1μm (C, D).

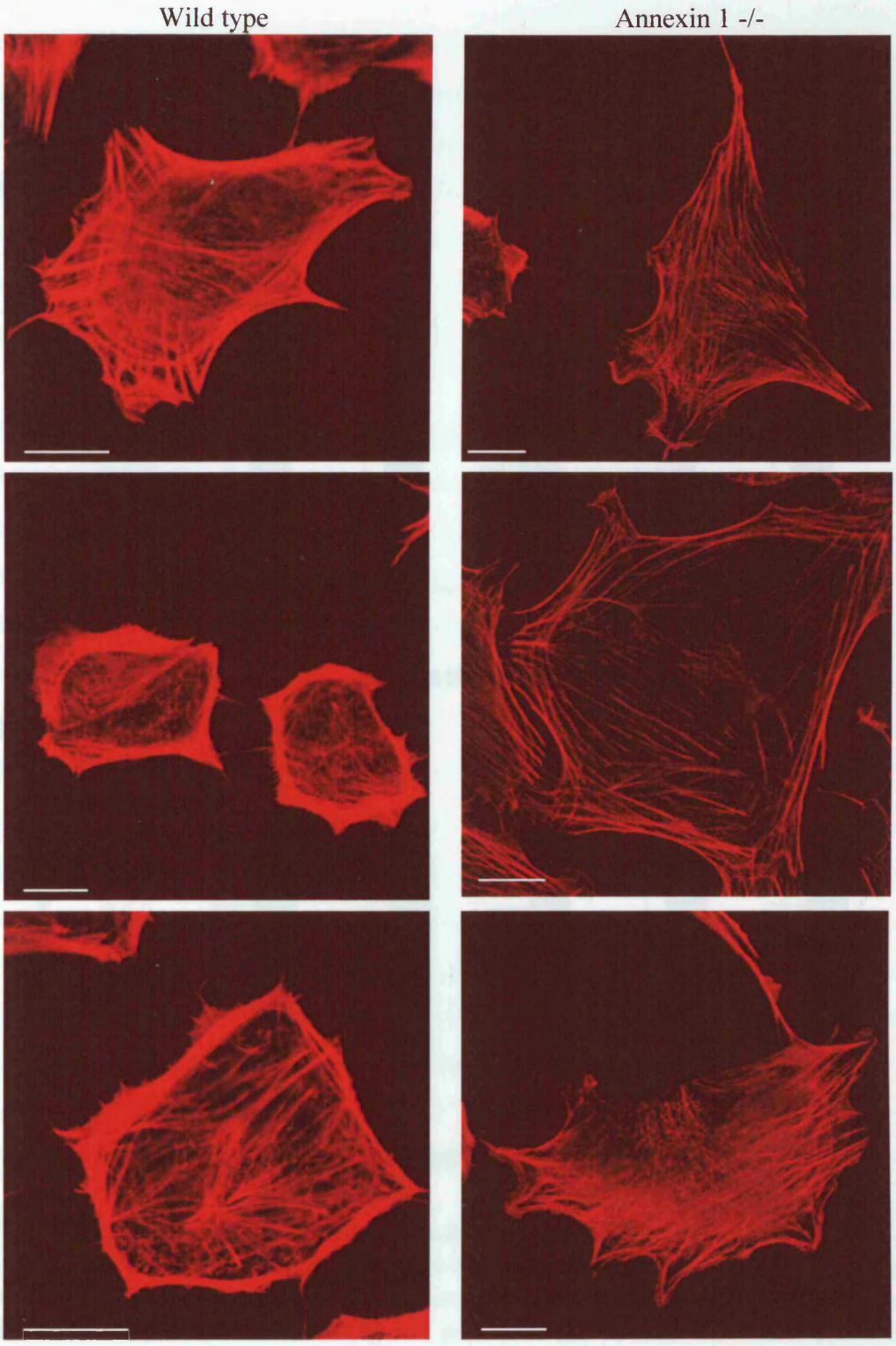

Figure 7.5. *Loss of annexin 1 reduces cortical actin.* JACRO cells were plated onto glass coverslips overnight and serum starved for 1 hour. Cells were fixed, permeabilised using 0.5% Tx100 and intracellular actin stained using phalloidin-547. These are typical images of regular actin staining in wild type cells and annexin 1 -/- cells, which show a loss of cortical actin. Bars = 20μm.

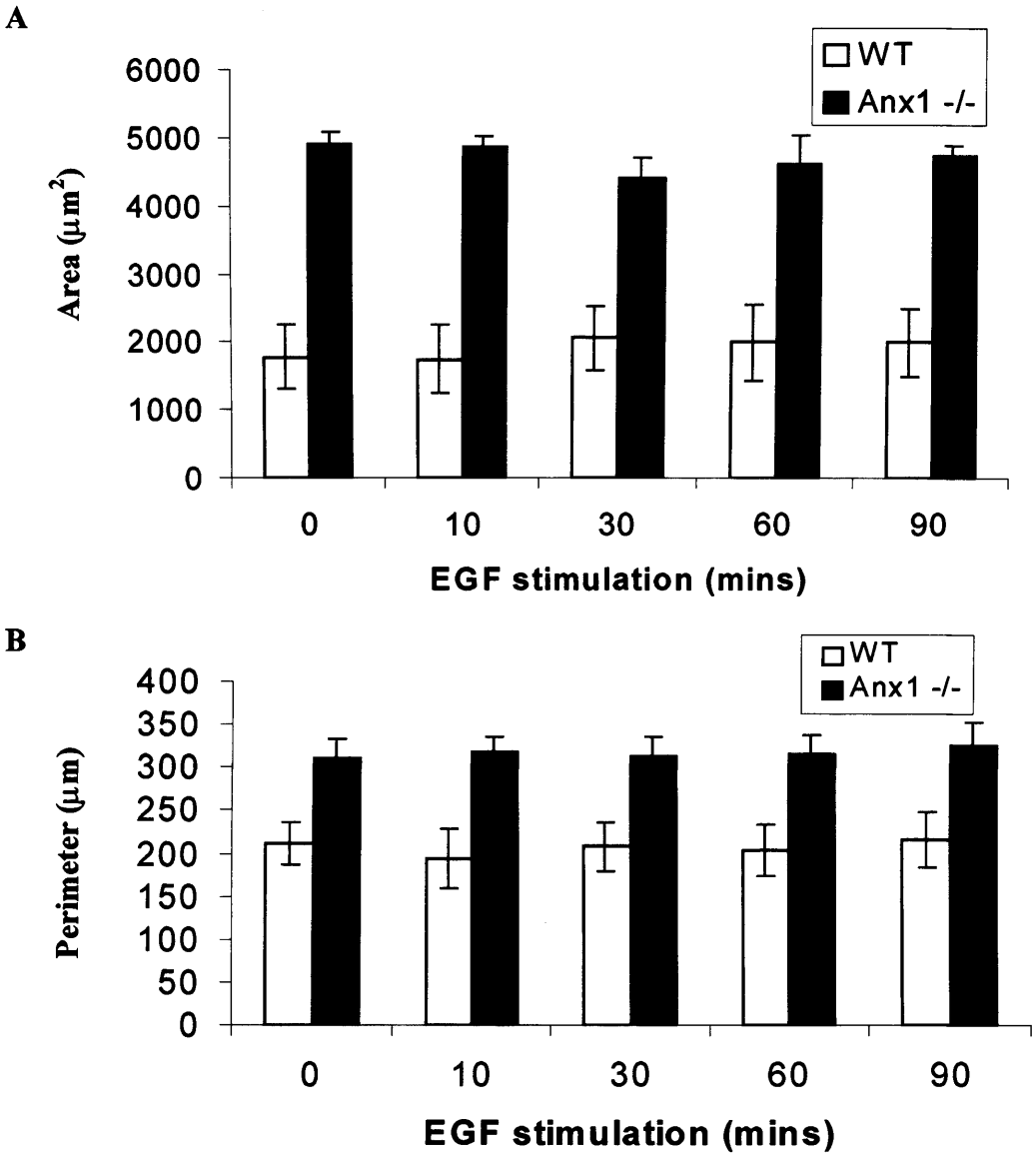

Figure 7.6. *EGF stimulation does not alter the area of JACRO cells.* JACRO cells were plated onto 3cm Mattek™ dishes and serum starved overnight. Images of unstimulated cells were taken. Cells were stimulated with EGF and images taken at different time points. The area (A) and perimeter (B) of each cell was measured and show that EGF stimulation did not induce a change in either cell line. Graphs show the mean ± SEM of 4 independent experiments.

Whilst imaging live JACRO cells for cell area and perimeter measurements, it was observed that annexin 1 -/- cells appeared to move more in response to EGF. To investigate this further, JACRO cells were imaged, in the absence or presence of EGF, every 5 minutes for 90 minutes. The movement of each cell was tracked over time using MetaMorph (v5). The nucleus was used as the central point of the cell and any movement of this point was recorded and plotted along an XY axis divided into 10μm sections.

Figure 7.7A shows a typical cell tracking experiment for the JACRO cell lines, in the absence or presence of EGF stimulation. Each colour represents a different cell and the difference between unstimulated and EGF-stimulated cell movement is clear in both cell lines. The data shown here also shows that EGF-stimulated annexin 1 -/- cell motility was significantly increased compared to EGF-stimulated wild type cells.

To quantify the effect of EGF stimulation on cell motility, the total distance (μm) moved, and the mean velocity of movement (μm/sec), for each were recorded. Both unstimulated JACRO cell lines moved a short distance, but there was no difference between cell types (Fig 7.7B). EGF stimulated JACRO cells moved significantly further and faster than unstimulated cells (approximately 2-fold increase after EGF stimulation) (Fig. 7.7B & C). However, the mean total distance moved by EGF-stimulated annexin 1 -/- cells was significantly increased compared to that of EGF-stimulated wild type cells (1.5-fold increase). The same significant increase was observed when comparing the mean velocity of EGF-stimulated annexin 1 -/- and wild type cells. These data confirm that cells lacking annexin 1 show enhanced motility in response to EGF.

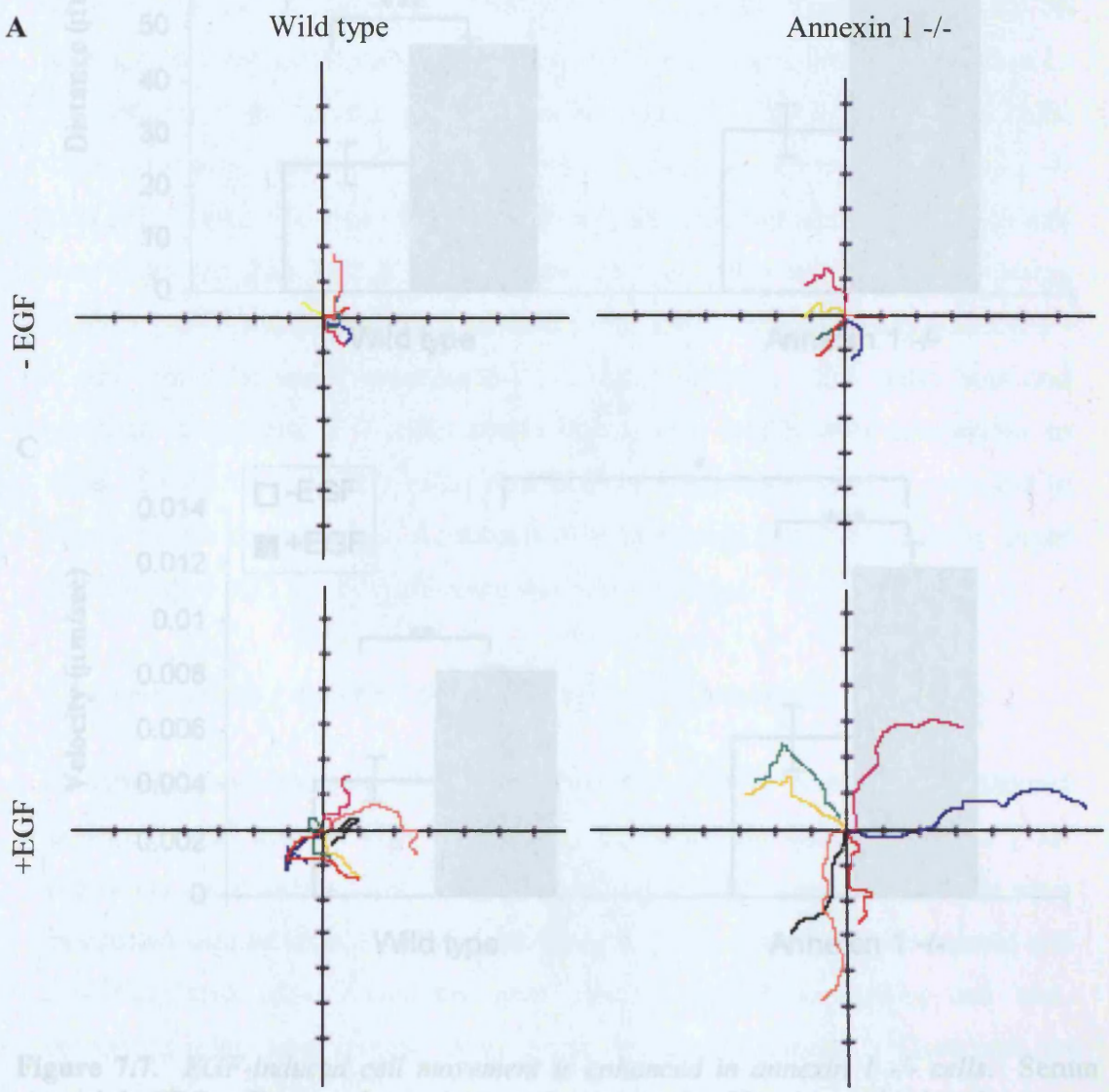

Figure 7.7. *EGF-induced cell movement in enhanced in annexin 1 -/- cells.* Legend overleaf (p206).

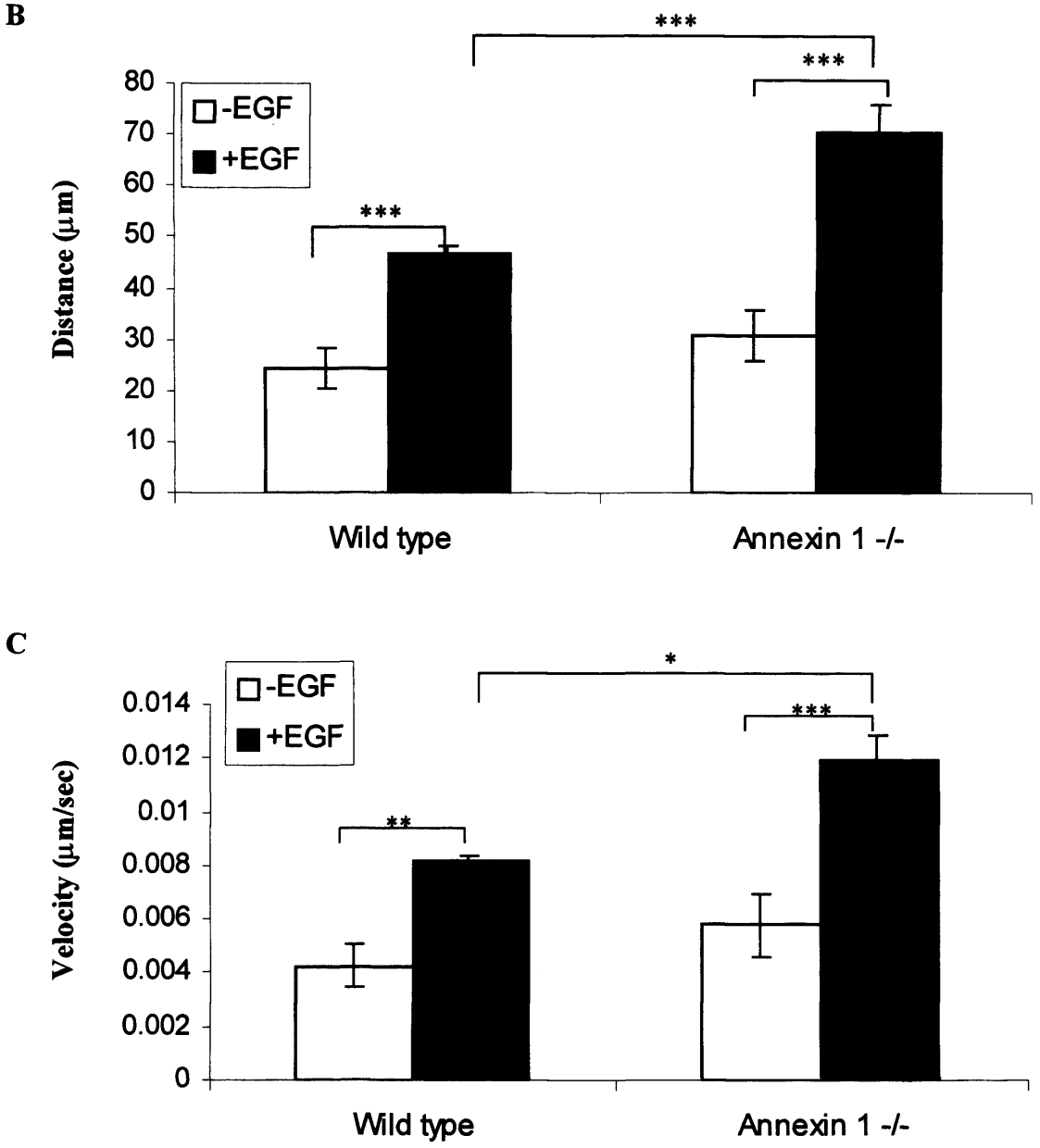

Figure 7.7. *EGF-induced cell movement is enhanced in annexin 1 -/- cells.* Serum starved JACRO cells were imaged every 5 minutes for 90 minutes in the absence or presence of EGF (100ng/ml). Cell movement was tracked using the nucleus as the central point of the cell. Figure A shows typical cell tracks for unstimulated and EGF-stimulated wild type and annexin 1 -/- cells. Each bar is 10µm. The total distance (µm) per cell was recorded and the mean per experiment calculated (B). The mean velocity (µm/sec) of cell movement was also determined (C). Cells lacking annexin 1 moved further and faster, than wild type cells, in response to EGF stimulation. Graphs show the mean ± SEM of 4 independent experiments. * $p<0.05$; ** $p<0.01$; *** $p<0.005$

7.2.3 Re-expressing annexin 1 decreases annexin 1 -/- cell area

To confirm that the change in cell area was due to the loss of annexin 1, JACRO annexin 1 -/- cells were transfected with an annexin 1-GFP chimera using nucleofection (see Materials and Methods section 2.4.3). Post-transfection (~36 hours), cells were serum starved overnight. Cells were washed and incubated in L-15 medium without phenol red to visualise annexin 1-GFP in transfected cells. Cells expressing annexin 1-GFP were smaller than non-expressing annexin 1 -/- cells (Fig. 7.8A). To quantify this difference, the area and perimeter of each cell were measured (Fig. 7.8B & C). The mean area and perimeter of cells expressing annexin 1-GFP were significantly reduced compared to non-expressing annexin 1 -/- cells from the same experiments (1.5-fold reduction). The mean area and perimeter of annexin 1 -/- cells expressing annexin 1-GFP were comparable to those of wild type JACRO cells (data from previous experiment is included in Figure 7.8 for comparison). Annexin 1-GFP expressing cells were slightly larger than wild type cells but this difference was not significant.

7.2.4 Re-expressing annexin 1 inhibits enhanced EGF-stimulated cell motility

Re-expression of annexin 1-GFP in annexin 1 -/- cells reversed the observed increase in cell area to wild type levels. To determine whether annexin 1 re-expression could reduce levels of EGF-stimulated motility, annexin 1 -/- cells were transfected with annexin 1-GFP, as described in 7.2.3. Fields of unstimulated and EGF-stimulated cells, containing both annexin 1-GFP expressing and non-expressing cells, were imaged every 5 minutes for 90 minutes. There was no difference in cell movement between unstimulated wild type, annexin 1 -/- or -/- cells expressing annexin 1-GFP. However, after EGF stimulation the mean distance travelled by annexin 1-/- cells expressing annexin 1-GFP was significantly reduced compared to non-expressing -/- cells (1.5-fold decrease) (Fig. 7.9). The distance and velocity of -/- cells expressing annexin 1-GFP was similar to the data collected for wild type cells, included in Figure 7.9 for comparison.

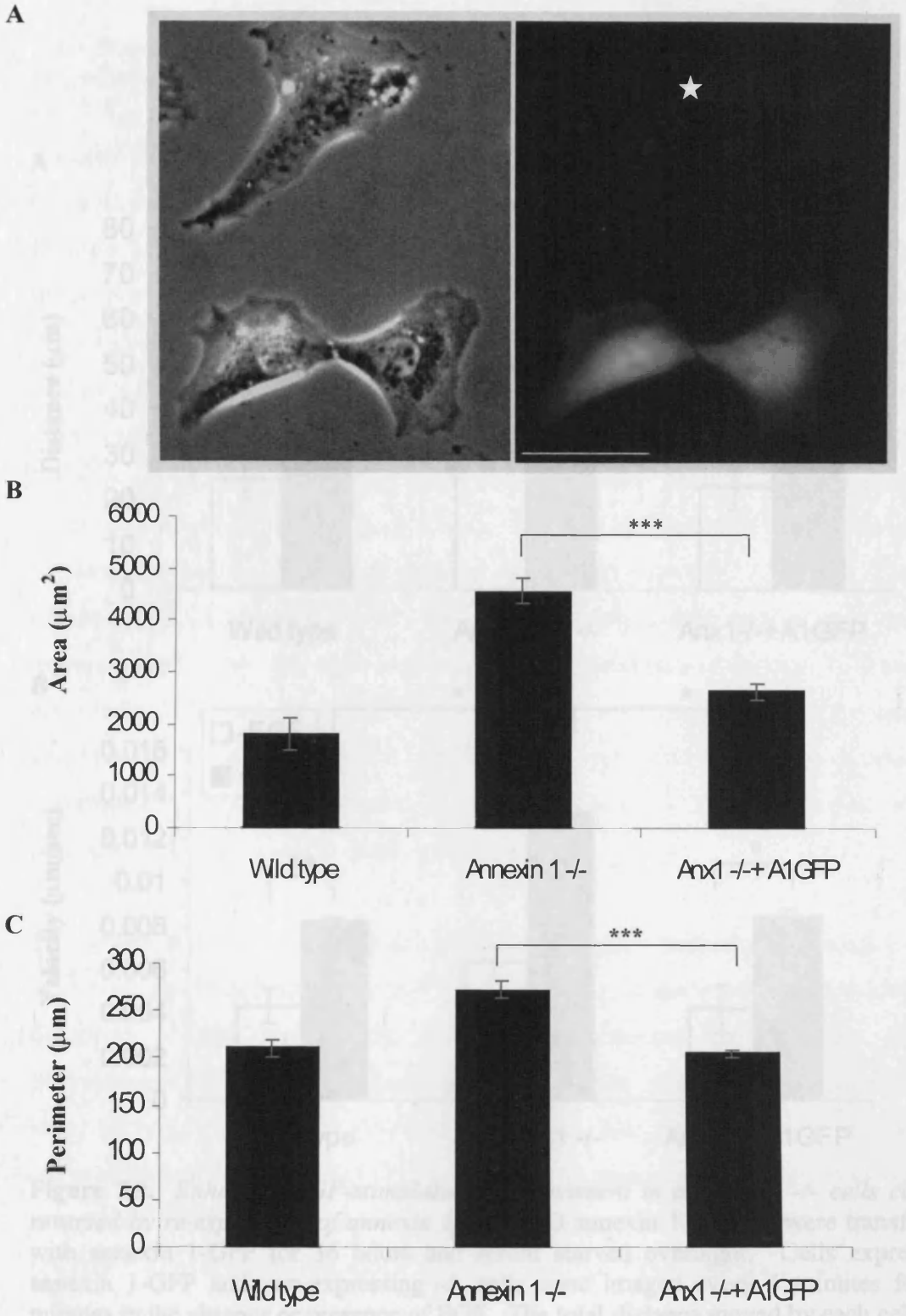

Figure 7.8. *Re-expression of annexin 1 reverses increased cell area.* JACRO annexin 1 -/- cells were nucleofected with annexin 1-GFP for 36 hours and serum starved overnight. Images of annexin 1-GFP expressing and non-expressing cells (*) were taken (A). The area and perimeter of each cell was measured (B, C). Wild type data from previous experiment is included for comparison. Cells expressing annexin 1-GFP were significantly smaller than non-expressing annexin 1 -/- cells. Graphs show the mean ± SEM of three independent experiments. *** $p<0.005$. Bar = 50μm

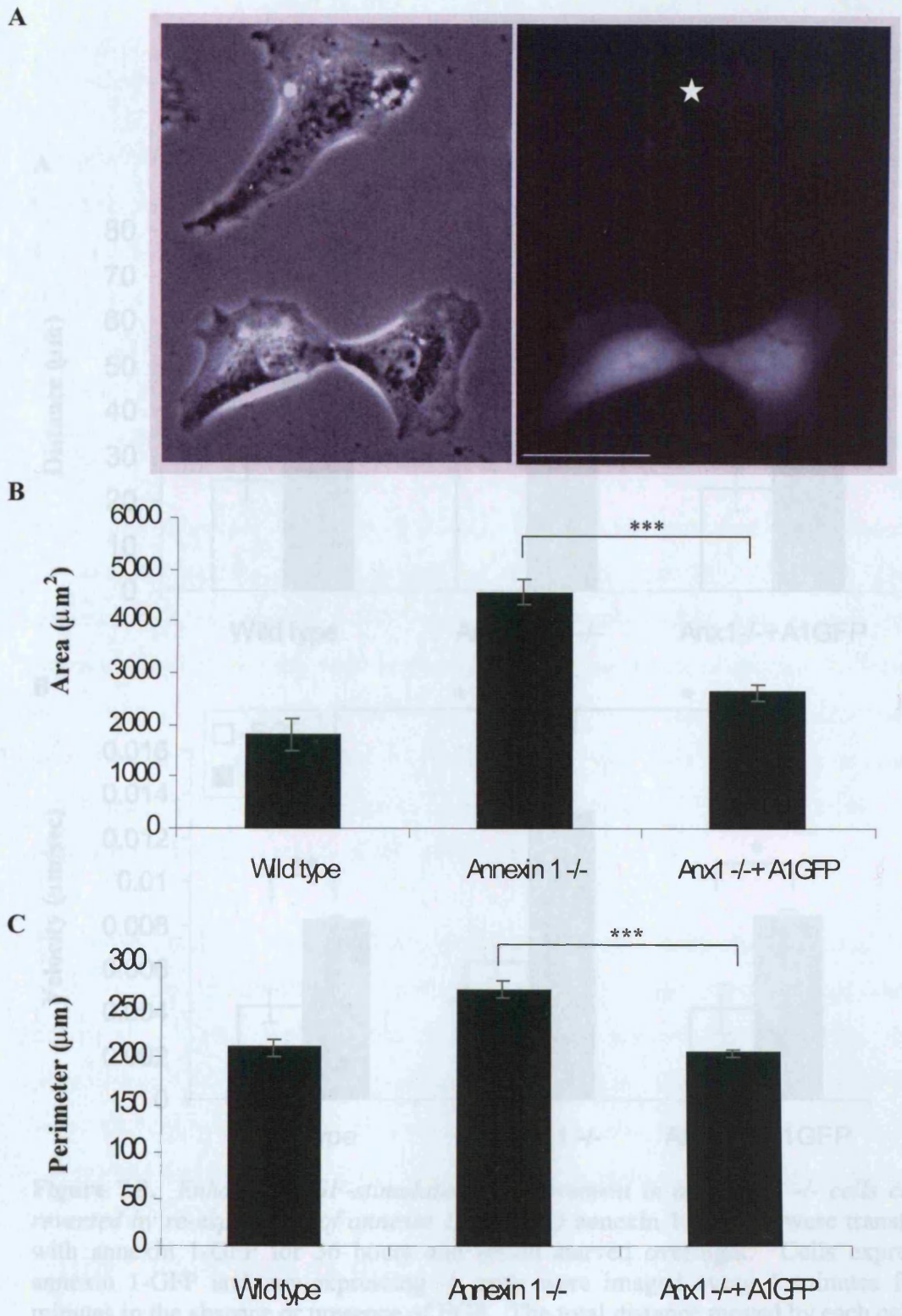

Figure 7.8. *Re-expression of annexin 1 reverses increased cell area.* JACRO annexin 1 -/- cells were nucleofected with annexin 1-GFP for 36 hours and serum starved overnight. Images of annexin 1-GFP expressing and non-expressing cells (*) were taken (A). The area and perimeter of each cell was measured (B, C). Wild type data from previous experiment is included for comparison. Cells expressing annexin 1-GFP were significantly smaller than non-expressing annexin 1 -/- cells. Graphs show the mean ± SEM of three independent experiments. *** $p<0.005$. Bar = 50μm

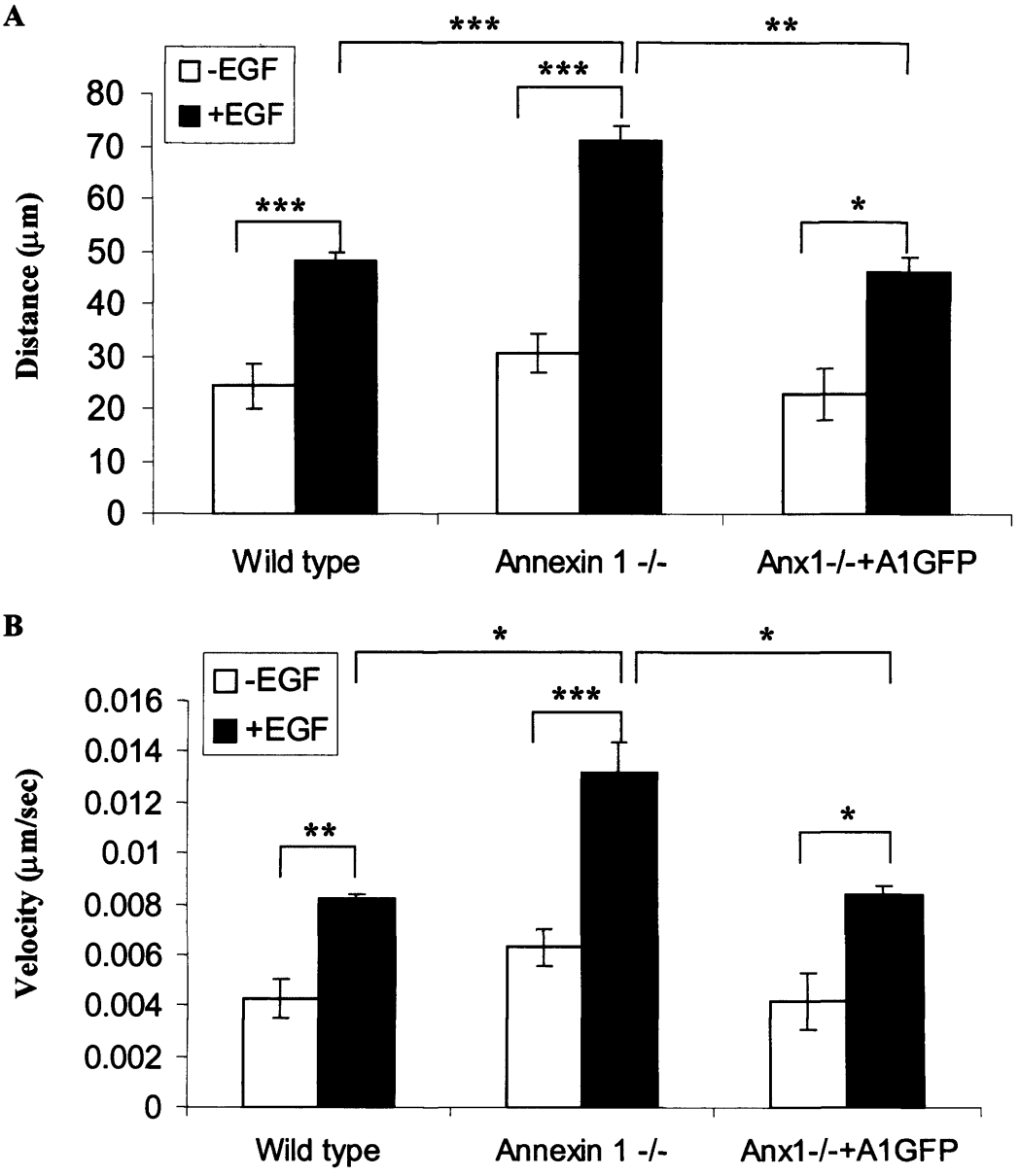

Figure 7.9. *Enhanced EGF-stimulated cell movement in annexin 1 -/- cells can be reversed by re-expression of annexin 1.* JACRO annexin 1 -/- cells were transfected with annexin 1-GFP for 36 hours and serum starved overnight. Cells expressing annexin 1-GFP and non-expressing -/- cells were imaged every 5 minutes for 90 minutes in the absence or presence of EGF. The total distance moved by each cell was recorded and the mean per experiment calculated (A). The mean velocity of each cell was also determined (B). Wild type cell data from the previous experiment is included for comparison. The movement of cells expressing annexin 1-GFP was reduced compared to non-expressing annexin 1 -/- cells. Graphs show the mean ± SEM of three independent experiments. * $p<0.05$, ** $p<0.01$, *** $p<0.005$.

7.2.5 EGF-stimulated phosphorylation of annexin 1 is not required for reversal of the cell size phenotype

Re-expression of annexin 1-GFP in annexin 1 -/- cells reversed both the increased cell area and the enhanced EGF-stimulated cell motility phenotypes. To investigate whether EGF-stimulated phosphorylation of annexin 1 was required for annexin 1 to function in these phenotypes, JACRO annexin 1 -/- cells were transfected with a mutant (Y21F) annexin 1-GFP chimera, lacking the EGFR phosphorylation site, for 36 hours and serum starved. To observe the effect on cell area, several fields of cells were imaged for each experiment. Similar to cells expressing wild type annexin 1-GFP, cells expressing Y21F annexin 1-GFP were smaller than non-expressing annexin 1 -/- cells (Fig. 7.11a). The area and perimeter were measured for each cell and the mean calculated for each experiment (Fig. 7.11b&c). Cells expressing Y21F annexin 1-GFP were approximately 2-fold smaller than non-expressing cells from the same experiments. The mean area of annexin 1 -/- cells expressing Y21F annexin 1-GFP was consistent with that of cells expressing annexin 1-GFP, and also that of JACRO wild type cells (data from previous experiment is included in Figure 7.11 for comparison). The same effect was observed on the mean length of cell perimeters.

To confirm that this reversal of cell size was annexin 1 dependent, annexin 1 -/- cells were also transfected with pGFP-N1, using the same methods as previously described. Cells were serum starved and measured the following day. Measurement of cell area and perimeter revealed that cells expressing pGFP-N1 were slightly smaller than non-expressing cells, but this difference was not statistically significant (Fig. 7.11). Importantly, the mean area of annexin 1 -/- cells expressing pGFP-N1 was significantly larger than JACRO wild type cells or annexin 1 -/- cells expressing either annexin 1-GFP or Y21F annexin 1-GFP.

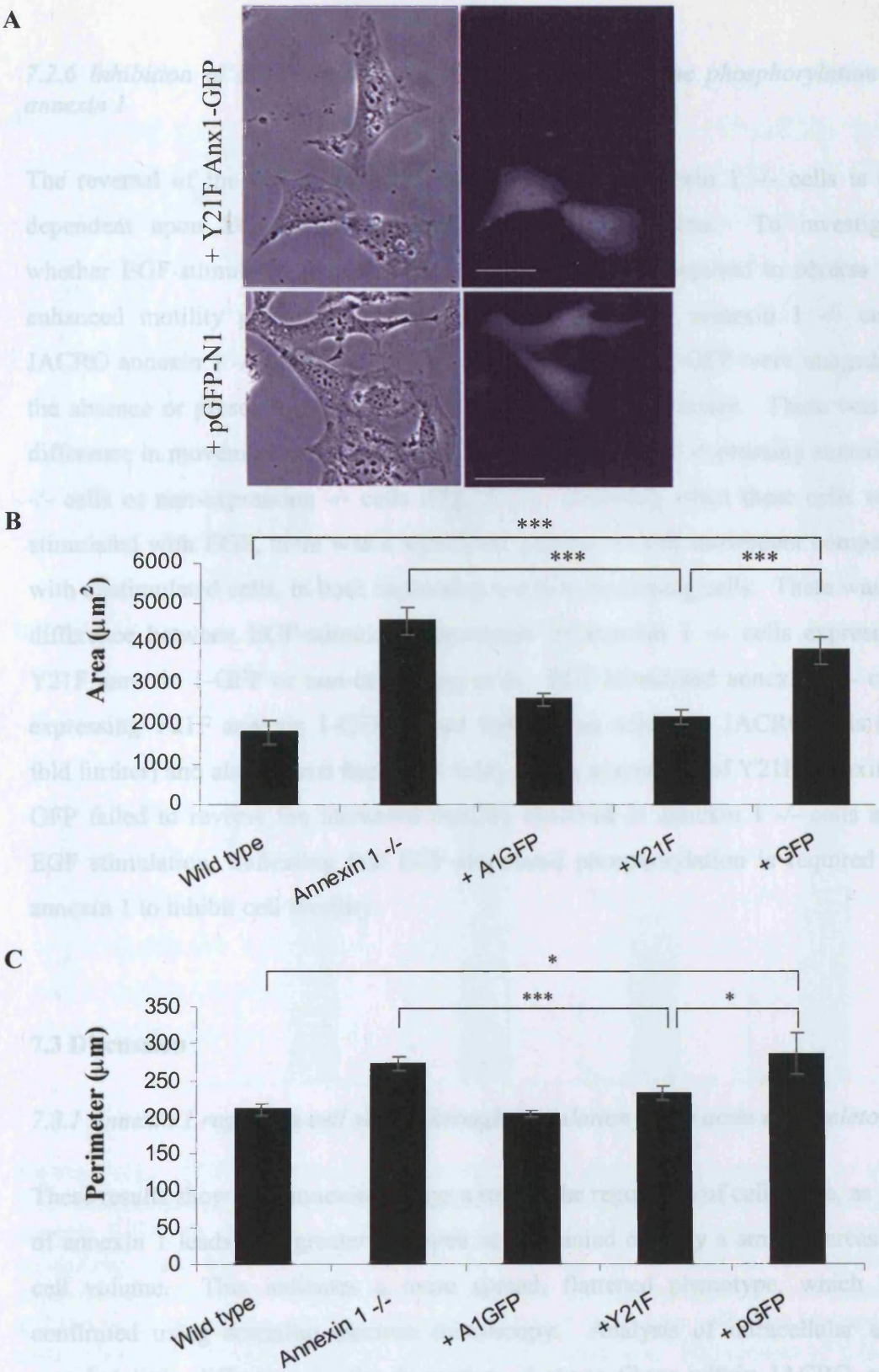

Figure 7.10. *EGF-stimulated phosphorylation of annexin 1 is not required to reverse the increase in cell area.* JACRO annexin 1 -/- cells were nucleofected with Y21F annexin 1-GFP or pGFP-N1 for 36 hours and serum starved overnight. Images of cells expressing annexin 1-GFP, pGFP or non-expressing cells were taken (A). The area (B) and perimeter (C) of all cells was measured and the mean per experiment recorded. Data from wild type cells and annexin 1 -/- cells expressing annexin 1-GFP have been included for comparison. Expression of Y21F, but not pGFP, reduced the mean cell area and perimeter. Graphs show the mean ± SEM of three independent experiments. * $p<0.05$, *** $p<0.005$.

7.2.6 Inhibition of EGF-stimulated motility requires tyrosine phosphorylation of annexin 1

The reversal of the cell shape phenotype observed in annexin 1 -/- cells is not dependent upon EGF-stimulated annexin 1 phosphorylation. To investigate whether EGF-stimulated phosphorylation of annexin 1 is required to reverse the enhanced motility phenotype observed in EGF-stimulated annexin 1 -/- cells, JACRO annexin 1 -/- cells transfected with Y21F annexin 1-GFP were imaged, in the absence or presence of EGF, every 5 minutes for 90 minutes. There was no difference in movement of unstimulated Y21F annexin 1-GFP expressing annexin 1 -/- cells or non-expressing -/- cells (Fig. 7.12). However, when these cells were stimulated with EGF, there was a significant increase in cell movement compared with unstimulated cells, in both expressing and non-expressing cells. There was no difference between EGF-stimulated movement of annexin 1 -/- cells expressing Y21F annexin 1-GFP or non-expressing cells. EGF stimulated annexin 1-/- cells expressing Y21F annexin 1-GFP moved further than wild type JACRO cells (1.5 fold further) and also moved faster (1.8 fold). Thus, expression of Y21F annexin 1-GFP failed to reverse the increased motility observed in annexin 1 -/- cells after EGF stimulation, indicating that EGF-stimulated phosphorylation is required for annexin 1 to inhibit cell motility.

7.3 Discussion

7.3.1 Annexin 1 regulates cell shape through modulation of the actin cytoskeleton

These results show that annexin 1 plays a role in the regulation of cell shape, as loss of annexin 1 leads to a greater cell area accompanied only by a small increase in cell volume. This indicates a more spread, flattened phenotype, which was confirmed using scanning electron microscopy. Analysis of intracellular actin revealed little difference in the formation of stress fibres within JACRO cells. However, annexin 1 -/- cells showed a significant loss of cortical actin when compared with wild type cells. This loss of cortical actin is the likely cause of the difference in cell shape. Increased cell spreading can be induced by increased stress fibre formation and/or enhanced numbers of focal adhesions to the substrate.

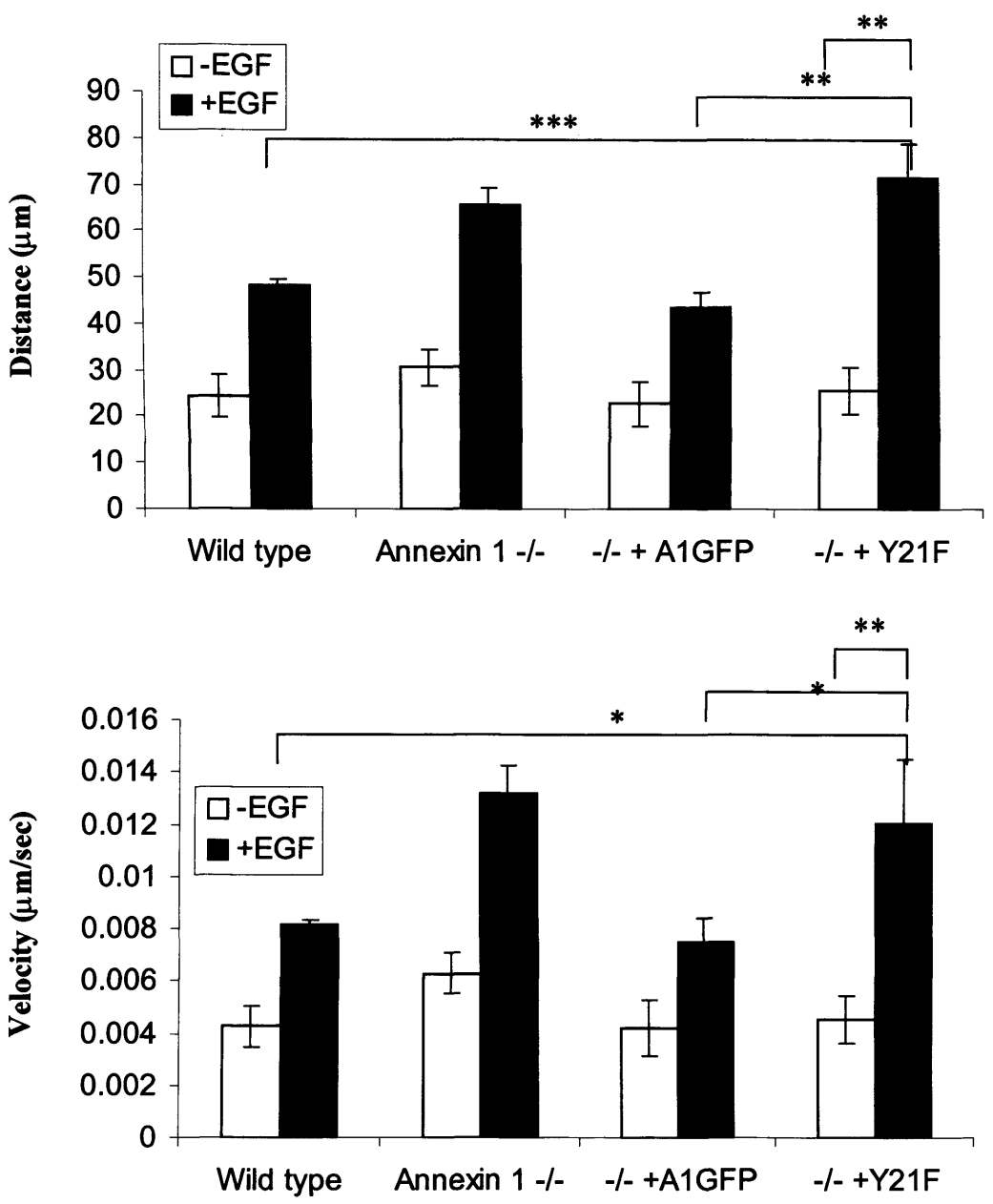

Figure 7.11. *EGF-stimulated phosphorylation of annexin 1 is required to inhibit EGF-stimulated cell motility.* JACRO annexin 1 -/- cells were nucleofected with Y21F annexin 1-GFP for 36 hours and serum starved over night. Y21F-expressing and non-expressing cells were imaged every 5 minutes for 90 minutes in the absence or presence of EGF. The total distance (A) and velocity (B) of each cell was measured, and the mean calculated per experiment. Data from wild type cells and annexin 1 -/- cells expressing annexin 1-GFP are included for comparison. Expression of Y21F did not inhibit the enhanced motility phenotype in annexin 1 -/- cells. * $p<0.05$, ** $p<0.01$, *** $p<0.005$.

These changes would normally result in a decreased level of cell motility, yet in stimulated annexin 1 -/- cells an enhanced level of cell motility was observed. Therefore, it is more likely that the difference in cell shape is mediated through a change in the membrane-cytoskeleton due to the loss of annexin 1.

Annexin 1 binds to negatively charged phospholipids on the inner leaflet of the plasma membrane in a Ca^{2+} dependent manner, where Ca^{2+} ions act as a bridge between the protein and the membrane (Rosengarth *et al.*, 1998). Atomic force microscopy of annexin 1 has indicated that it can self-aggregate on the surface of membranes and form discrete domains (Janshoff *et al.*, 2001). As annexin 1 also binds F-actin, it is likely that these domains are important in the stabilisation/maintenance of the plasma membrane-cytoskeleton. Loss of annexin 1 may alter this stabilisation, thus reducing the rigidity of the plasma membrane resulting in a more flattened phenotype. Annexin 1 modulates the effect of profilin on actin nucleation and so, as well as providing a direct physical link between membrane and actin filaments, annexin 1 may influence cell shape through effects on actin nucleation (Alvarez-Martinez *et al.*, 1996; Alvarez-Martinez *et al.*, 1997). Further evidence that annexin 1 may mediate its effect through profilin is provided by the finding that both annexin 1 and profilin are present in EGF-stimulated actin based cellular protrusions, in ruffles and extending lamellipodia respectively (Campos-Gonzalez *et al.*, 1990; Buss *et al.*, 1992).

7.3.2 Annexin 1 inhibits EGF-stimulated fibroblast motility

The role of annexin 1 in EGF-stimulated cell motility has not been investigated until now, although several groups have reported that extracellular annexins 1 and 2 can inhibit the migration of cells in the inflammatory response (Balch and Dedman, 1997; Perretti *et al.*, 2002). EGF-induced fibroblast migration is a carefully orchestrated sequence of events, triggered by intracellular signalling cascades extending from the activated EGFR, which in turn control actin polymerisation and organisation of the cytoskeleton. EGF stimulation of cells results in the tyrosine phosphorylation of many proteins, including PLCγ1, which localises to the leading edge of EGF-stimulated cells (Goldschmidt-Clermont *et al.*, 1991; Chou *et al.*,

2003). At the leading edge, PLCγ induces PIP_2 hydrolysis, which results in the localised release of gelsolin and its preferential accumulation into actin networks, thus driving cytoskeletal rearrangements and protrusions (Banno *et al.*, 1992; Chen *et al.*, 1996a; Chou *et al.*, 2002). Further evidence to suggest that actin severing activity and motility are linked comes from studies where the overexpression of gelsolin directly increases cell motility (Cunningham *et al.*, 1991). Also, fibroblasts lacking gelsolin show decreased rates of motility accompanied by a decrease in EGF-stimulated ruffling and failure to form lamellipodia (Azuma *et al.*, 1998).

In response to EGF, fibroblasts initially send out actin-based extensions in all directions (ruffles) (Ridley *et al.*, 1992). Moments later, actin-based structures form at the leading edge of the cell, first filopodia then lamellipodia (Nobes and Hall, 1995; Kozma *et al.*, 1995; Chou *et al.*, 2002). Annexin 1 has previously been shown to be recruited to EGF-stimulated ruffles (Campos-Gonzalez *et al.*, 1990). The data presented here suggests that the localised recruitment of annexin 1 to the leading edge of the cell has an inhibitory effect on ruffling/lamellipodia extension. This is somewhat unexpected as, although the roles of annexins in regulating actin remodelling are not entirely understood, existing data suggests that they are more likely to promote actin assembly than to inhibit it. Annexin-actin interactions tend to be associated with localised sites of rapid actin assembly, such as phagosomes, pinosomes and ruffles, and those annexins that bind actin have also been shown to bundle actin in vitro (Ikebuchi and Waisman, 1990; Kusumawati *et al.*, 2000; Merrifield *et al.*, 2001). In addition to gelsolin release at the leading edge, EGF-stimulated hydrolysis of PIP_2, through PLC, also releases profilin (Banno *et al.*, 1992; Chou *et al.*, 2002). Profilin is known to sequester G-actin and is an important protein in accelerating the ADP-ATP exchange on G-actin monomers, thus replenishing the pool of ATP-actin in the cell. Profilin also nucleates the formation of new actin filaments, possibly by increasing nucleotide exchange (Theriot and Mitchison, 1992) and is concentrated at the leading edge of cells, like annexin 1 and PLCγ (Buss *et al.*, 1992). Thus, modulation of profilin activity by locally recruited annexin 1 could be expected to inhibit formation of actin filaments by reducing the pool of ATP-actin in the cytosol.

7.3.3 Possible actin-independent mechanisms for annexin 1 inhibition of motility

The inhibitory effect of annexin 1 on EGF-stimulated motility may not be mediated by direct interaction with actin or actin-binding proteins. Unlike many substrates of the EGFR kinase, annexin 1 does not become phosphorylated until EGFR has become internalised into MVBs. It has previously been suggested that annexin 1 may play a role in the accumulation of EGFR on the internal vesicles of MVBs (Futter *et al.*, 1993) and data presented in Chapter 3 provides evidence to support this hypothesis, showing that annexin 1 is involved in EGF-stimulated inward vesiculation within MVBs. Furthermore, it has been proposed that inward vesiculation within MVBs might play a direct role in attenuating signalling from the EGFR by removing the catalytic domain of the EGFR from the cytoplasm (Futter *et al.*, 2001). Taken together, these hypotheses would predict that loss of annexin 1 would increase numbers of EGFR on the perimeter membrane of MVBs and, thereby, increase signalling from the EGFR kinase. Data presented in Chapter 5 shows that loss of annexin 1 alters the amount or kinetics of EGFR degradation, and this is accompanied by prolonged signalling through the MAPK pathway. Increased signalling from the EGFR kinase could, therefore, induce enhanced motility in response to EGF in annexin 1 -/- cells. Growth factor stimulation leads to disruption of focal contacts to allow movement of the cell. The ERK1/2 MAPK pathway has been proposed to play a role in this process, as it can also be activated by integrins (Klemke *et al.*, 1997). Additionally, EGF-activated MAPK is able to phosphorylate integrins, which would disrupt binding to the extracellular matrix (Hughes *et al.*, 1997). In either case, prolonged MAPK signalling could result in enhanced cell motility.

Other studies of EGF-mediated fibroblast motility have investigated a range of influencing factors, including matrix proteins and growth factor gradients. The data presented here were collected from experiments performed using cells grown on glass. Several groups have shown that the efficient disruption of the interaction between the actin cytoskeleton and the extracellular matrix (ECM) is important in cell motility. EGFR activation and fibronectin were shown to integrate in order to control cell migration (Maheshwari *et al.*, 1999). However, it is not known whether annexin 1 or annexins play a role in this interaction with ECM.

EGF-stimulated cell motility is considered to be an excellent model for many reasons. Firstly, EGFR is ubiquitously expressed on the surface of many mammalian cells and many downstream signalling pathways of EGFR have been well characterized. Secondly, EGFR is closely related to other motility-signalling receptors and activates many of the same downstream molecules. Therefore, information derived from EGF-stimulated motility experiments should also be true for other receptors. Finally, EGFR signalling of motility has been investigated in both physiological (wound healing) and pathological circumstances (tumour invasion) (Chakrabarty *et al.*, 1995; Turner *et al.*, 1996; Turner *et al.*, 1997). Whether annexin 1 plays a role in wound healing is unknown, but the loss of annexin 1, and the closely related annexin 2, have been reported in several types of tumours (Gerke and Moss, 2002).

7.3.4 Summary of findings

In summary, these data provide evidence for a regulatory role for annexin 1 on the shape of fibroblasts, possibly through its interaction with F-actin and profilin. A second novel function for annexin 1 has been described here, in the regulation of EGF-stimulated cell motility. The exact nature of this inhibitory role is undefined, but is dependent upon EGF-stimulated phosphorylation of annexin 1. It seems likely to be mediated either through annexin 1 interaction with profilin and/or the role of annexin 1 in downregulation of EGFR. That annexin 1 plays a role in cell motility has been suggested by various groups investigating monocyte cell migration (Perretti *et al.*, 2002), albeit in a different cellular context. Again the loss of annexin 1 in tumours may lead to enhanced migration of cancerous cells, although this effect has only been reported for annexin 2 (Liu *et al.*, 2003).

Chapter 8 – Conclusions, Perspectives and Future Work

8.1 Conclusions

8.1.1 EGF stimulates MVB formation and inward vesiculation

EGF stimulation is known to induce receptor downregulation by enhancing receptor internalisation (Wiley *et al.*, 1991). The data presented here shows that EGF also stimulates both MVB formation and inward vesiculation, suggesting that EGFR-mediated phosphorylation of downstream molecules is necessary for these processes to occur. Through the discovery of the vps proteins in yeast, and subsequently their mammalian homologues, many proteins have been implicated in MVB formation and/or receptor sorting. Recently Hrs, a protein phosphorylated after EGF stimulation, was proposed to couple the processes of EGFR sorting and formation of internal vesicles (Urbe *et al.*, 2003). However, use of wortmannin, to inhibit PI3K, was shown to uncouple these processes by allowing receptor sorting in the absence of internal vesicle formation (Futter *et al.*, 2001). Aside from Hrs, the EGFR tyrosine kinase has multiple downstream targets, but within MVBs two major substrates were identified; the EGFR itself and annexin 1 (Futter *et al.*, 1993).

8.1.2 Annexin 1 mediates EGF-stimulated inward vesiculation in EGFR-containing MVBs

The membrane binding properties of annexin 1, coupled with the finding that it is a substrate for EGFR tyrosine kinase only within MVBs, led to the proposal that annexin 1 is involved in the formation of internal vesicles within MVBs (Futter *et al.*, 1993). Despite the localisation of annexin 1 to endosomes (Futter *et al.*, 1993; Seemann *et al.*, 1996b; Seemann *et al.*, 1997; Pol *et al.*, 1997; Rescher *et al.*, 2000), little evidence to support this hypothesis had been reported. The data presented here demonstrate that annexin 1 mediates inward vesiculation in response to EGF stimulation, but only in a sub-population of MVBs that contain EGFR. As a small number of internal vesicles containing EGFR form in the absence of annexin 1, it is

clear that annexin 1 is not required for the formation of all internal vesicles. Ultrastructural analysis of EGF-stimulated cells located annexin 1 to EGFR-positive MVBs, both on the perimeter membrane and on internal vesicles with EGFR. However, despite these findings the mechanism of action of annexin 1 in mediating inward vesiculation is unclear.

8.1.3 Annexin 1 is not involved in EGFR sorting

The processes of receptor sorting and inward vesiculation are believed to be linked via Hrs and the ESCRT proteins (Urbe *et al.*, 2003). The data presented here provides evidence that these processes can be uncoupled. Although loss of annexin 1 inhibits the EGF-stimulated formation of internal vesicles, some internal vesicles still form and contain EGFR, indicating that receptor sorting occurs prior to inward vesiculation, and independently of annexin 1. Additionally, in cells lacking annexin 1, no effect was observed on the kinetics of EGF degradation, providing further confirmation that EGF and its receptor are sorted for lysosomal degradation in the absence of annexin 1. However, in annexin 1 -/- cells EGFR degradation was slightly reduced. This small reduction, or delay, in degradation could occur as a direct consequence of the inhibition of inward vesiculation. Additionally, MAPK signalling was prolonged in annexin 1 -/- cells, although whether this occurred as a downstream effect of delayed EGFR degradation, or as a direct effect of loss of annexin 1, is not clear.

8.1.4 Annexin 2 is not required for formation of MVBs or inward vesiculation

Although a recent study reported that annexin 2 is required for the biogenesis of MVBs (Mayran *et al.*, 2003), no evidence to support these claims could be found in the studies presented here, despite detailed quantitative analysis of MVBs in annexin 2 depleted cells. Ultrastructural analysis revealed that annexin 2 is primarily associated with small vesicles, many of which also label for TfR. Roles for annexin 2 in the positioning of early and recycling endosomes (Harder and Gerke, 1993; Zobiack *et al.*, 2003) have previously been reported and it is therefore possible that annexin 2 may be involved in the positioning of MVBs. However, as

no dramatic relocalisation of MVBs was observed here, in cells depleted of annexin 2, it seems unlikely that annexin 2 is essential for positioning of MVBs.

8.1.5 Annexin 1 inhibits EGF-stimulated fibroblast motility

In addition to the effects observed on EGF-stimulated inward vesiculation, mouse lung fibroblasts lacking annexin 1 displayed enhanced levels of cell motility in response to EGF, compared with wild type cells. This phenotype could be reversed by re-expressing wild type annexin 1. However, expression of a phosphorylation mutant annexin 1 construct failed to reverse this enhanced motility, indicating that inhibition of cell motility is mediated through EGF-stimulated tyrosine phosphorylation of annexin 1.

8.1.6 Annexin 1 is involved in regulation of fibroblast cell shape

Loss of annexin 1, in mouse lung fibroblasts, led to an increase in cell area, compared to wild type cells. This difference was not due to a significant increase in cell size, but rather a more flattened phenotype. Annexin 1 is known to interact with actin (Glenney, 1986b; Glenney, Jr. *et al.*, 1987) and cells lacking annexin 1 showed a decrease in the amount of cortical F-actin, which may directly cause the observed change in cell shape.

8.2 Perspectives

8.2.1 Roles for different sub-populations of MVBs

Although EGF stimulates the formation of EGFR-containing MVBs, it is not clear whether all of these MVBs are formed *de novo* or whether some existing MVBs receive endocytosed EGFR. The presence of EGFR-negative MVBs is consistent with unpublished work (White *et al.*, under revision), and published data, showing that EGFR are only present in certain MVBs and that at least one other population of LBPA-containing MVBs exists (Bright *et al.*, 2001; Petiot *et al.*, 2003).

Additionally, both populations of morphologically similar organelles labelled for CD63 and, from this work, it can be concluded that this would be a more accurate marker for MVBs than either EGFR or LBPA, which have commonly been used (White *et al.*, under revision).

The discovery that separate populations of MVBs exist raises the question of what purpose multiple populations of MVB might serve. It is interesting to speculate that a MVB containing active EGFR could be used as a "signalling MVB" operating in a mobile, yet strictly controlled environment that is spatially separated from the plasma membrane. Annexin 1-mediated formation of internal vesicles, in response to EGF stimulation, may represent a method of signal attenuation, by removing the active receptor tyrosine kinase domain away from other signalling proteins in the cytoplasm. EGF-stimulated cells lacking annexin 1 exhibit prolonged signalling through the MAPK pathway in response to EGF. Although it is unclear whether this prolonged signalling occurs as a direct consequence of altered EGFR degradation, this finding supports the proposal that annexin 1 may be involved in downregulation of EGFR signalling. Several members of the MAPK signalling pathway have been localised to endosomes (Di Guglielmo *et al.*, 1994; Pol *et al.*, 1998; Rizzo *et al.*, 2000; Howe *et al.*, 2001; Luttrell *et al.*, 2001) and removal of EGFR onto internal vesicles, as the endosome matures, would limit the number of downstream signalling molecules available to the activated EGFR (Futter *et al.*, 2001). In addition to mediating EGFR signal downregulation, annexin 1 could be involved in formation of specific scaffolding complexes e.g. those containing p14/MP1 for MAPK signalling. Thus, annexin 1 could function to (i) limit the signalling potential of EGFR and (ii) increase the specificity of signalling. However, the nature of the role of annexin 1 in signalling appears to be inhibitory, as indicated by the competitive binding with Grb2 for EGFR (Croxtall *et al.*, 2000).

8.2.2 Annexin 2 and endosomal membranes

Despite detailed analysis of MVB formation and inward vesiculation, no evidence was found to suggest that annexin 2 plays a role within MVBs, or is present within

these structures. Annexin 2 is recruited to membrane sites of actin assembly, both at the plasma membrane and on endosomes (Merrifield *et al.*, 2001; Zobiack *et al.*, 2002). Recently, it was shown that annexin 2 specifically binds PIP_2 at these sites (Hayes *et al.*, 2004; Rescher *et al.*, 2004). In addition to serving as signalling precursors phosphoinositides, including PIP_2, participate in a number of fundamental cellular processes, such as vesicular trafficking and cell motility (Cullen *et al.*, 2001; Martin, 2001). PIP_2 is necessary for the early stages of endocytosis, coat assembly and release of endocytic vesicles and a number of proteins involved in these process are able to bind PIP_2, including AP-2 and dynamin (Jost *et al.*, 1998). Additionally, the formation of PIP_2-rich microdomains is dependent on cholesterol (Pike and Miller, 1998), and these domains were shown to be preferential sites of membrane-linked, PIP_2-mediated actin assembly, such as that occurring during the formation of actin comet tails behind raft-enriched vesicles (Rozelle *et al.*, 2000). It is possible that the absence of annexin 2 from MVBs is due to the lack of PIP_2 enriched microdomains and/or cholesterol in later endocytic structures. Consistent with this hypothesis was the finding that intracellular receptor trafficking compartments contained little detectable PIP_2 (Haugh and Meyer, 2002). However, the ability of annexin 2 to bind to PIP_2 and cholesterol enriched microdomains on membranes, coupled with its actin binding property, makes it an ideal candidate for mediating membrane-cytoskeleton contacts.

Interestingly, in these studies annexin 2 was found associated with TfR-containing CCVs, whereas annexin 1 only co-labelled TfR positive endosomes, and was absent from CCPs or CCVs. This observation is consistent with that of Turpin *et al.* (1996), who reported that annexins 2 and 6 were attached to CCVs, independently of clathrin (Turpin *et al.*, 1998). This indicates that annexin 2, which interacts with the endosomal membrane and the clathrin coat, could be involved in the formation of a microdomain necessary for clathrin coat function.

8.2.3 Additional effects of loss of annexin 1

In addition to mediating formation of internal vesicles within a sub-population of MVBs, annexin 1 was also shown to inhibit EGF-stimulated cell motility. For efficient EGF-stimulated cell motility, EGFR tyrosine kinase activity and receptor autophosphorylation are essential (Chen *et al.*, 1994a). Therefore, if EGFR signalling is dysregulated i.e. prolonged, as observed in EGF-stimulated annexin 1 -/- cells, this may result in enhanced motility. Signalling through the MAPK pathway was prolonged in annexin 1 -/- cells in response to EGF stimulation, however MAPK signalling primarily induces a mitogenic rather than motogenic response (Chen *et al.*, 1994b). Nevertheless, prolonged EGF-stimulated MAPK signalling in annexin 1 -/- cells could serve as an indication that signalling through other pathways is altered, and the activation of these pathways could lead to the observed enhanced cell motility. Therefore, the effect of loss of annexin 1 on membrane trafficking could directly induce enhanced motility.

The actin-binding properties of annexins have been identified but their exact functions are not known. The ability of annexin 1 to bind both actin and profilin indicates that annexin 1 is likely involved in some aspect of cytoskeleton arrangement (Glenney, Jr. *et al.*, 1987; Welsh *et al.*, 1991; Alvarez-Martinez *et al.*, 1996). In response to EGF stimulation, cells form actin-based membrane ruffles, as a precursor to cell movement, and localisation of annexin 1 to these structures provides evidence that annexin 1 is involved in this process (Campos-Gonzalez *et al.*, 1990). The data presented here show that annexin 1 has an inhibitory effect on cell motility, as observed by enhanced EGF-stimulated cell motility in the absence of annexin 1. This could be due to a disruption in cytoskeleton formation, as observed by a loss of cortical actin in annexin 1 -/- cells, which might directly alter the ability of cells to migrate, by reducing their contact to the substratum. Alternatively, cytoskeletal rearrangements could have an indirect effect on cell motility, by altering the stability or localisation of intracellular compartments, including those involved in signalling.

8.2.4 Annexins and cancer

The studies reported here have concentrated primarily on the effects of loss of annexins 1 and 2 on membrane trafficking, specifically of EGFR. Cells lacking annexin 1 demonstrated enhanced levels of EGF-stimulated motility and prolonged signalling through the MAPK pathway. Increased receptor tyrosine kinase signalling is often observed in cancer and is caused by a variety of factors, including gene amplification, increased transcription, increased translation or mutations that promote ligand-independent autophosphorylation (Bache *et al.*, 2004b). Enhanced signalling can also be due to a failure of efficient receptor downregulation and/or deactivation and this has been shown to cause neoplastic growth (Dikic and Giordano, 2003). Therefore, alterations in the expression of proteins involved in receptor downregulation could result in aberrant receptor signalling. Both annexins 1 and 2 are downregulated in a number of cancers, including prostate cancer (Paweletz *et al.*, 2000; Liu *et al.*, 2003; Xin *et al.*, 2003; Smitherman *et al.*, 2004) and human oesophageal squamous cell carcinomas (Paweletz *et al.*, 2000; Zhi *et al.*, 2003; Fang *et al.*, 2004; Luo *et al.*, 2004). Similarly annexin 1 expression is inhibited in B-cell non-Hodgkins lymphoma, giving rise to the proposal that annexin 1 possesses tumour suppressor activity (Vishwanatha *et al.*, 2004). Liu *et al.* (2003) reported that annexins 1 and 2 may be endogenous suppressors of prostate cancer cell migration and that their reduced or lost expression may contribute to prostate cancer development and progression (Liu *et al.*, 2003). The data presented in Chapter 7, investigating the effect of loss of annexin 1 on EGF-stimulated cell motility, provides further evidence in support of this theory, especially as re-expression of annexin 1 reversed the enhanced motility phenotype observed.

However, the roles of annexins 1 and 2 may be tissue or cell type specific, as in other forms of cancer their expression is upregulated. In human hepatocellular carcinoma annexin 1 is overexpressed, is localised mainly in the cytoplasm of cells and is tyrosine phosphorylated (Masaki *et al.*, 1996). Recently, annexin 1 was identified as differentially expressed on the surface of lung endothelial tumour cells in rats (Oh *et al.*, 2004). In this rat model, radiolabelled monoclonal anti-annexin 1

antibodies were used to determine whether annexin 1 expression was tumour specific. The antibodies specifically labelled the tumour, with little labelling observed elsewhere. Additionally, the survival rate of rats injected with ^{125}I-labelled anti-annexin 1 antibodies was increased, compared to that of control rats, indicating that this method allowed antibody-directed delivery of low levels of radionuclides to tumours, resulting ultimately in their destruction (Oh *et al.*, 2004). As annexin 1 is also selectively detected in certain types of human solid tumours, it may act as a target for novel therapies.

8.2.5 Annexin 1 and inflammation

Annexin 1 has been extensively investigated with respect to its role in inflammation. The anti-inflammatory action of the glucocorticoid family is mediated through the induction of annexin 1, which has been shown to inhibit PLA_2 and thus arachidonic acid release (Croxtall *et al.*, 1996; Croxtall *et al.*, 1998). The annexin 1 -/- mouse has been used to investigate the effect of annexin 1 on glucocorticoid action (Hannon *et al.*, 2002). Although viable, these mice exhibited enhanced expression of the pro-inflammatory proteins, COX2 and $cPLA_2$. While dexamethasone treatment of wild type mice inhibited the first phase of oedema, which is PMN (polymorphonuclear leukocyte) dependent, no inhibition was observed in annexin 1 -/- cells. Further evidence for a role for annexin 1 in glucocorticoid action has come from investigations using the annexin 1 -/- cell line, derived from the annexin 1 knockout mouse (Croxtall *et al.*, 2003). Expression of COX2, $cPLA_2$ and several annexins were shown to be upregulated in annexin 1 -/- cells, a similar profile to that observed in the mouse model. These findings indicate that although annexin 2 is upregulated, it is unable to functionally compensate for the loss of annexin 1 in glucocorticoid action (Croxtall *et al.*, 2003).

8.3 Future work

The work described here has provided functional evidence for the roles of annexin 1 in EGF-stimulated inward vesiculation, EGFR-mediated signalling, and control of EGF-stimulated cell motility. Additionally, the role of EGF stimulation in MVB formation has been explored. The data collected during investigations of annexin 2 have ruled out the possibility that annexins 1 and 2 perform the same functions, and have shown that annexin 2 is not involved in MVB formation or inward vesiculation. Despite answering some of the questions relating to annexin 1 function, further work is required to address the specific mechanisms by which annexin 1 mediates its effects.

8.3.1 Ubiquitin and annexin 1

Ubiquitination of EGFR is believed to be a major sorting signal into the lysosomal degradation pathway and away from the recycling pathway. Data presented here showed that annexin 1 is delivered to the lysosome, raising the question of whether annexin 1 is also ubiquitinated. If annexin 1 is ubiquitinated, this would also enable it to interact with UIM-containing proteins, including Hrs and Tsg101. To investigate whether annexin 1 is ubiquitinated, immunoprecipitations should be performed using either anti-annexin 1 or anti-ubiquitin antibodies, followed by western blotting with the other antibody. In addition, the effect of EGF could be investigated on the ubiquitination of annexin 1. Although annexin 1 was observed in MVBs from unstimulated cells, none was observed in lysosomes from these cells, indicating that EGF-stimulation induces annexin 1 delivery to the lysosome.

8.3.2 Does annexin 1 interact with the ESCRT complexes?

It is unknown whether annexin 1 upregulates the existing ESCRT-mediated process of inward vesiculation, or whether it is involved in the generation of new internal vesicles via a different mechanism. In the absence of annexin 1, a small number of

internal vesicles containing EGFR still form. A similar phenotype is seen in MVBs from cells depleted of Hrs (Raiborg *et al.*, 2002) or Tsg101 (Aghakhani *et al.*, under revision). As receptor sorting occurs in the absence of annexin 1, this indicates that annexin 1 functions downstream of Hrs, which is known to mediate sorting of ubiquitinated EGFR (Raiborg *et al.*, 2002). Therefore, it is possible that the formation of internal vesicles observed in the absence of either annexin 1 or ESCRT proteins is mediated by the presence of the remaining protein (either ESCRTs or annexin 1, respectively). To further investigate whether annexin 1-mediated inward vesiculation is dependent upon ESCRT function, RNAi technology could be used to deplete cells of both annexin 1 and a component of ESCRT, such as Tsg101, and observe the effect on EGF-stimulated inward vesiculation. If annexin 1 and ESCRTs mediate internal vesicle formation via independent mechanisms, inhibiting the function of both would be predicted to result in a complete inhibition of inward vesiculation.

The ESCRT complexes are known to assemble on endosomal membranes and function to sort ubiquitinated receptors to the degradative pathway (Babst *et al.*, 2000; Babst *et al.*, 2002a; Babst *et al.*, 2002b). It has not been investigated whether ESCRT complexes are involved in the formation of all MVBs or just in a specific sub-population. Regardless of the ubiquitination status of annexin 1, it is possible that annexin 1 interacts with one or more components of the ESCRT complexes. However, no evidence exists to link annexin 1 and ESCRT proteins. Therefore, to investigate whether annexin 1 interacts with ESCRT proteins, EGF-stimulated cell lysates should be immunoprecipitated with anti-annexin 1 antibodies and then blotted with antibodies against members of the ESCRT complexes.

8.3.3 Investigating the mechanism of annexin 1 action

The models of annexin 1 mediated, EGF-stimulated inward vesiculation, described in Chapter 3, are based on the formation of the annexin 1-S100A11 heterotetramer. Although both annexin 1 and S100A11 have been localised to endosomal membranes, this complex has proved elusive during standard isolation protocols. Unlike the formation of the annexin 2-S100A10 complex, S100A11 requires Ca^{2+}

to bind annexin 1 and this Ca^{2+} dependency could explain the difficulty in isolation of the complex. Having established that annexin 1 is required for the formation of internal vesicles within MVBs of EGF-stimulated cells, it would be interesting to investigate whether this process is affected by RNAi-induced depletion of S100A11. Additionally, the effect of loss, or depletion, of annexin 1 on S100A11 levels should be investigated, as RNAi-induced annexin 2 depletion simultaneously decreased expression of S100A10 (Zobiack *et al.*, 2003). This could be further explored using a mutant annexin 1, lacking S100A11 binding sites.

The role of Ca^{2+} in annexin 1 membrane binding is still somewhat controversial. Futter *et al.* (1993) showed that annexin 1 associates with the plasma membrane and MVBs in a Ca^{2+} independent manner and that EGFR phosphorylation of annexin 1 converts it into a Ca^{2+} dependent species (Futter *et al.*, 1993). In contrast, Seemann *et al.* (1996) used conventional fractionation techniques but found no evidence of a pool of annexin 1 associated with endosomes in the absence of Ca^{2+} (Seemann *et al.*, 1996b). Rescher *et al.* (2000) reported that a specific Ca^{2+} binding site in the second annexin repeat of annexin 1 is required for membrane binding (Rescher *et al.*, 2000). However, it is possible that mutation of this site also changes the conformation of the protein, which would itself alter membrane binding. Therefore, further work is required to address the Ca^{2+} dependency of annexin 1 during endocytosis and specifically during inward vesiculation. To investigate whether annexin 1 requires Ca^{2+} for EGF-stimulated internal vesicle formation, a mutant annexin 1 construct lacking the Ca^{2+} binding site (Rescher *et al.*, 2000) could be expressed in annexin 1 -/- cells, and the effect on inward vesiculation observed. As expression of wild type annexin 1 partially relieved the inhibition on internal vesicle formation, it would be interesting to observe whether this is also true of the Ca^{2+} binding site mutant. BAPTA, a Ca^{2+} chelating agent, is often used to decrease intracellular levels of Ca^{2+}. To observe whether Ca^{2+} is required for EGF-stimulated inward vesiculation, cells could be treated first with BAPTA, then with EGF and finally the morphology of MVBs observed. BAPTA-treated cells could be used for immuno-localisation of annexin 1 and EGFR, to observe whether they still localise to MVBs.

EGF-stimulated phosphorylation of annexin 1 is believed to induce N-terminal proteolysis, although the exact mechanism by which this occurs *in vivo* has not been fully investigated (Haigler *et al.*, 1987; Chuah and Pallen, 1989; Ando *et al.*, 1989). N-terminally truncated annexin 1 has been shown to localise to late endosomes in unstimulated cells (Seemann *et al.*, 1996b; Rescher *et al.*, 2000). Therefore, it would be interesting to observe where N-terminal proteolysis occurs intracellularly. To do so would require the use of specific annexin 1 antibodies, one to the core domain and the other to the N-terminal domain that is cleaved. Double labelling, using these antibodies, would reveal any differences between the localisation of full length annexin 1 and the truncated version. These studies would provide further clues to the exact mechanism of annexin 1 in EGF-stimulated inward vesiculation. From the current model proposed by Gerke and Moss (2002), full length annexin 1 would localise to endosomes and the perimeter membrane of MVBs, while the cleaved version would be present on the EGFR-containing internal vesicles (Gerke and Moss, 2002). Alternatively, an N-terminally truncated annexin 1-GFP construct could be generated and used in fluorescence experiments, to investigate the intracellular localisation of this construct.

8.3.4 Is EGF-stimulated tyrosine phosphorylation of annexin 1 required for inward vesiculation?

Although EGFR tyrosine phosphorylation of annexin 1 was shown to be necessary for its inhibitory role in EGF-stimulated cell motility, the studies into internal vesicle formation and EGFR trafficking were less informative, and further investigation into the role of EGFR-mediated phosphorylation is required. Transfection of annexin 1 -/- cells with the phosphorylation mutant annexin 1-GFP construct could be utilised in two ways: (i) to observe whether a reversion of the inhibition of EGF-stimulated internal vesicles formation can be observed, and (ii) use of cryo-immuno EM to determine the exact location of this construct. From studies shown here, it is predicted that annexin 1 unable to be phosphorylated by EGFR would remain on the perimeter membrane after EGF-stimulation and would be unable to reverse the inhibition on inward vesiculation. Additionally, an anti-phospho annexin 1 antibody could be used both to localise phosphorylated annexin

1 and compare its localisation with the non-phosphorylated form. This would provide further insight as to whether phosphorylated annexin 1 is inside MVBs, or whether phosphorylation induces annexin 1 to fall off the perimeter membrane and only non-phosphorylated annexin 1 is internalised onto internal vesicles with the EGFR.

8.3.5 Is annexin 1-mediated inward vesiculation specific to EGFR or general to all tyrosine kinase receptors?

The work described in these studies has focussed on the roles of annexins 1 and 2 in EGF-stimulated events, although TfR has also been used as a marker of constitutive endocytosis and recycling in unstimulated cells. EGFR is one of several receptor tyrosine kinases in mammalian cells and so it would be interesting to investigate whether annexin 1, or possibly annexin 2, plays a similar role in the processing of other receptors. From the data presented here, it seems likely that the role of annexin 1 would be EGF-specific, taking into account its role in formation of internal vesicles within EGFR-containing MVBs. EGF-mediated phosphorylation appears to act as a switch for activity of annexin 1. However, annexin 1 is also phosphorylated in response to HGF (Skouteris and Schroder, 1996). To investigate whether other growth factors influence annexin 1 function, cells could be treated with FGF, HGF, insulin or PDGF, and the effects observed on MVB formation, internal vesicle formation and also on cell motility.

Annexin 2 was originally identified as a substrate for c-src and phosphorylation decreases the affinity of annexin 2 for phospholipid membranes (Hubaishy *et al.*, 1995). Although annexin 2 is a poor substrate for EGFR, it is phosphorylated by internalised insulin receptors (IR). Therefore, in a cell type where IR are expressed, annexin 2 could be involved in MVB formation and/or IR sorting.

8.3.6 Final Summary

Annexins 1 and 2 were discovered over 20 years ago and implicated in membrane trafficking, due to their actin and membrane-binding properties. The studies

performed here provide, for the first time, functional evidence for a role for annexin 1 in EGF-stimulated inward vesiculation, although the exact mechanism of action remains unclear. However, through the use of modern technologies, such as gene knockout and RNAi, it will be possible to investigate in detail how annexin 1 mediates its effect on inward vesiculation, using the experiments outlined above.

References

Alldridge,L.C., Harris,H.J., Plevin,R., Hannon,R., and Bryant,C.E. (1999) The annexin protein lipocortin 1 regulates the MAPK/ERK pathway. *J.Biol.Chem.* **274,** 37620-37628.

Alldridge,L.C.,and Bryant,C.E. (2003) Annexin 1 regulates cell proliferation by disruption of cell morphology and inhibition of cyclin D1 expression through sustained activation of the ERK1/2 MAPK signal. *Exp.Cell Res.* **290,** 93-107.

Alvarez-Martinez,M.T., Mani,J.-C., Porte,F., Faivre-Sarrailh,C., Liautard,J.P., and Sri,W.J. (1996) Characterisation of the interaction between annexin 1 and profilin. *Eur.J.Biochem.* **238,** 777-784.

Alvarez-Martinez,M.T., Porte,F., Liautard,J.P., and Sri,W.J. (1997) Effects of profilin-annexin I association on some properties of both profilin and annexin I: modification of the inhibitory activity of profilin on actin polymerization and inhibition of the self-association of annexin I and its interactions with liposomes. *Biochim.Biophys.Acta* **1339,** 331-340.

Ando,Y., Imamura,S., Hong,Y.M., Owada,M.K., Kakunaga,T., and Kannagi,R. (1989) Enhancement of calcium sensitivity of lipocortin I in phospholipid binding induced by limited proteolysis and phosphorylation at the amino terminus as analyzed by phospholipid affinity column chromatography. *J.Biol.Chem.* **264,** 6948-6955.

Aniento,F., Emans,N., Griffiths,G., and Gruenberg,J. (1993) Cytoplasmic dynein-dependent vesicular transport from early to late endosomes. *J.Cell Biol.* **123,** 1373-1387.

Azuma,T., Witke,W., Stossel,T.P., Hartwig,J.H., and Kwiatkowski,D.J. (1998) Gelsolin is a downstream effector of rac for fibroblast motility. *EMBO J.* **17,** 1362-1370.

Babiychuk,E.B. and Draeger,A. (2000) Annexins in cell membrane dynamics: Ca(2+)-regulated association of lipid microdomains. *J.Cell Biol.* **150,** 1113-1124.

Babiychuk,E.B., Palstra,R.J., Schaller,J., Kampfer,U., and Draeger,A. (1999) Annexin VI participates in the formation of a reversible, membrane-cytoskeleton complex in smooth muscle cells. *J.Biol.Chem.* **274,** 35191-35195.

Babst,M., Wendland,B., Estepa,E.J., and Emr,S.D. (1998) The Vps4p AAA ATPase regulates membrane association of a Vps protein complex required for normal endosome function. *EMBO J.* **17,** 2982-2993.

Babst,M., Odorizzi,G., Estepa,E.J., and Emr,S.D. (2000) Mammalian tumor susceptibility gene 101 (TSG101) and the yeast homologue, Vps23p, both function in late endosomal trafficking. *Traffic.* **1,** 248-258.

Babst,M., Katzmann,D.J., Estepa-Sabal,E.J., Meerloo,T., and Emr,S.D. (2002a) Escrt-III: an endosome-associated heterooligomeric protein complex required for mvb sorting. *Dev.Cell* **3,** 271-282.

Babst,M., Katzmann,D.J., Snyder,W.B., Wendland,B., and Emr,S.D. (2002b) Endosome-associated complex, ESCRT-II, recruits transport machinery for protein sorting at the multivesicular body. *Dev.Cell* **3,** 283-289.

Bache,K.G., Raiborg,C., Mehlum,A., Madshus,I.H., and Stenmark,H. (2002) Phosphorylation of Hrs downstream of the epidermal growth factor receptor. *Eur.J.Biochem.* **269,** 3881-3887.

Bache,K.G., Brech,A., Mehlum,A., and Stenmark,H. (2003a) Hrs regulates multivesicular body formation via ESCRT recruitment to endosomes. *J.Cell Biol.* **162,** 435-442.

Bache,K.G., Raiborg,C., Mehlum,A., and Stenmark,H. (2003b) STAM and Hrs are subunits of a multivalent Ubiquitin-binding complex on early endosomes. *J.Biol.Chem.* ..

Bache,K.G., Slagsvold,T., Cabezas,A., Rosendal,K.R., Raiborg,C., and Stenmark,H. (2004) The growth-regulatory protein HCRP1/hVps37A is a subunit of mammalian ESCRT-I and mediates receptor down-regulation. *Mol.Biol.Cell* **15,** 4337-4346.

Bache,K.G., Slagsvold,T., and Stenmark,H. (2004b) Defective downregulation of receptor tyrosine kinases in cancer. *EMBO J.* 1-6.

Balch,C. and Dedman,J.R. (1997) Annexins II and V inhibit cell migration. *Exp.Cell Res.* **237,** 259-263.

Banno,Y., Nakashima,T., Kumada,T., Ebisawa,K., Nonomura,Y., and Nozawa,Y. (1992) Effects of gelsolin on human platelet cytosolic phosphoinositide-phospholipase C isozymes. *J.Biol.Chem.* **267,** 6488-6494.

Barbieri,M.A., Roberts,R.L., Gumusboga,A., Highfield,H., Alvarez-Dominguez,C., Wells,A., and Stahl,P.D. (2000) Epidermal growth factor and membrane trafficking. EGF receptor activation of endocytosis requires Rab5a. *J.Cell Biol.* **151,** 539-550.

Barbieri,M.A., Heath,C.M., Peters,E.M., Wells,A., Davis,J.N., and Stahl,P.D. (2001) Phosphatidylinositol-4-phosphate 5-kinase-1beta is essential for epidermal growth factor receptor-mediated endocytosis. *J.Biol.Chem.* **276,** 47212-47216.

Barois,N., Forquet,F., and Davoust,J. (1998) Actin microfilaments control the MHC class II antigen presentation pathway in B cells. *J.Cell Sci.* **111 (Pt 13),** 1791-1800.

Beattie,E.C., Howe,C.L., Wilde,A., Brodsky,F.M., and Mobley,W.C. (2000) NGF signals through TrkA to increase clathrin at the plasma membrane and enhance clathrin-mediated membrane trafficking. *J.Neurosci.* **20,** 7325-7333.

Bellot,F., Moolenaar,W., Kris,R., Mirakhur,B., Verlaan,I., Ullrich,A., Schlessinger,J., and Felder,S. (1990) High-affinity epidermal growth factor binding is specifically reduced by a monoclonal antibody, and appears necessary for early responses. *J.Cell Biol.* **110,** 491-502.

Benaud,C., Gentil,B.J., Assard,N., Court,M., Garin,J., Delphin,C., and Baudier,J. (2004) AHNAK interaction with the annexin 2/S100A10 complex regulates cell membrane cytoarchitecture. *J.Cell Biol.* **164,** 133-144.

Benmerah,A., Gagnon,J., Begue,B., Megarbane,B., Dautry-Varsat,A., and Cerf-Bensussan,N. (1995) The tyrosine kinase substrate eps15 is constitutively associated with the plasma membrane adaptor AP-2. *J.Cell Biol.* **131,** 1831-1838.

Biener,Y., Feinstein,R., Mayak,M., Kaburagi,Y., Kadowaki,T., and Zick,Y. (1996) Annexin II is a novel player in insulin signal transduction. *J.Biol.Chem.* **271,** 29489-29496.

Bishop,N., Horman,A., and Woodman,P. (2002) Mammalian class E vps proteins recognize ubiquitin and act in the removal of endosomal protein-ubiquitin conjugates. *J.Cell Biol.* **157,** 91-101.

Blackwood,R.A. and Ernst,J.D. (1990) Characterization of Ca2(+)-dependent phospholipid binding, vesicle aggregation and membrane fusion by annexins. *Biochem.J.* **266,** 195-200.

Bowers,K., Lottridge,J., Helliwell,S.B., Goldthwaite,L.M., Luzio,J.P., and Stevens,T.H. (2004) Protein-protein interactions of ESCRT complexes in the yeast Saccharomyces cerevisiae. *Traffic.* **5,** 194-210.

Brachvogel,B., Dikschas,J., Moch,H., Welzel,H., von der,M.K., Hofmann,C., and Poschl,E. (2003) Annexin A5 is not essential for skeletal development. *Mol.Cell Biol.* **23,** 2907-2913.

Bram,R.J. and Crabtree,G.R. (1994) Calcium signalling in T cells stimulated by a cyclophilin B-binding protein. *Nature* **371,** 355-358.

Bright,N.A., Reaves,B.J., Mullock,B.M., and Luzio,J.P. (1997) Dense core lysosomes can fuse with late endosomes and are re-formed from the resultant hybrid organelles. *J.Cell Sci.* **110 (Pt 17),** 2027-2040.

Bright,N.A., Lindsay,M.R., Stewart,A., and Luzio,J.P. (2001) The relationship between lumenal and limiting membranes in swollen late endocytic compartments formed after wortmannin treatment or sucrose accumulation. *Traffic.* **2,** 631-642.

Brugge,J.S. (1986) The p35/p36 substrates of protein-tyrosine kinases as inhibitors of phospholipase A2. *Cell* **46,** 149-150.

Bucci,C., Parton,R.G., Mather,I.H., Stunnenberg,H., Simons,K., Hoflack,B., and Zerial,M. (1992) The small GTPase rab5 functions as a regulatory factor in the early endocytic pathway. *Cell* **70,** 715-728.

Bucci,C., Thomsen,P., Nicoziani,P., McCarthy,J., and van Deurs,B. (2000) Rab7: a key to lysosome biogenesis. *Mol.Biol.Cell* **11,** 467-480.

Burke,P., Schooler,K., and Wiley,H.S. (2001) Regulation of epidermal growth factor receptor signaling by endocytosis and intracellular trafficking. *Mol.Biol.Cell* **12,** 1897-1910.

Buss,F., Temm-Grove,C., Henning,S., and Jockusch,B.M. (1992) Distribution of profilin in fibroblasts correlates with the presence of highly dynamic actin filaments. *Cell Motil.Cytoskeleton* **22,** 51-61.

Cadena,D.L., Chan,C.L., and Gill,G.N. (1994) The intracellular tyrosine kinase domain of the epidermal growth factor receptor undergoes a conformational change upon autophosphorylation. *J.Biol.Chem.* **269,** 260-265.

Campos-Gonzalez,R., Kanemitsu,M., and Boynton,A.L. (1990) Epidermal growth factor induces the accumulation of calpactin II on the cell surface during membrane ruffling. *Cell Motil.Cytoskeleton* **15,** 34-40.

Casciola-Rosen,L.A. and Hubbard,A.L. (1991) Hydrolases in intracellular compartments of rat liver cells. Evidence for selective activation and/or delivery. *J.Biol.Chem.* **266,** 4341-4347.

Ceresa,B.P., Kao,A.W., Santeler,S.R., and Pessin,J.E. (1998) Inhibition of clathrin-mediated endocytosis selectively attenuates specific insulin receptor signal transduction pathways. *Mol.Cell Biol.* **18,** 3862-3870.

Chakrabarty,S., Rajagopal,S., and Huang,S. (1995) Expression of antisense epidermal growth factor receptor RNA downmodulates the malignant behavior of human colon cancer cells. *Clin.Exp.Metastasis* **13,** 191-195.

Chang,C.P., Kao,J.P., Lazar,C.S., Walsh,B.J., Wells,A., Wiley,H.S., Gill,G.N., and Rosenfeld,M.G. (1991) Ligand-induced internalization and increased cell calcium

are mediated via distinct structural elements in the carboxyl terminus of the epidermal growth factor receptor. *J.Biol.Chem.* **266,** 23467-23470.

Chang,C.P., Lazar,C.S., Walsh,B.J., Komuro,M., Collawn,J.F., Kuhn,L.A., Tainer,J.A., Trowbridge,I.S., Farquhar,M.G., Rosenfeld,M.G., and . (1993) Ligand-induced internalization of the epidermal growth factor receptor is mediated by multiple endocytic codes analogous to the tyrosine motif found in constitutively internalized receptors. *J.Biol.Chem.* **268,** 19312-19320.

Chavrier,P., Parton,R.G., Hauri,H.P., Simons,K., and Zerial,M. (1990) Localization of low molecular weight GTP binding proteins to exocytic and endocytic compartments. *Cell* **62,** 317-329.

Chen,W.S., Lazar,C.S., Lund,K.A., Welsh,J.B., Chang,C.P., Walton,G.M., Der,C.J., Wiley,H.S., Gill,G.N., and Rosenfeld,M.G. (1989) Functional independence of the epidermal growth factor receptor from the domain required for ligand-induced internalization and calcium regulation. *Cell* **59,** 33-43.

Chen,P., Gupta,K., and Wells,A. (1994a) Cell movement elicited by epidermal growth factor receptor requires kinase and autophosphorylation but is separable from mitogenesis. *J.Cell Biol.* **124,** 547-555.

Chen,P., Xie,H., Sekar,M.C., Gupta,K., and Wells,A. (1994b) Epidermal growth factor receptor-mediated cell motility: phospholipase C activity is required, but mitogen-activated protein kinase activity is not sufficient for induced cell movement. *J.Cell Biol.* **127,** 847-857.

Chen,P., Murphy-Ullrich,J.E., and Wells,A. (1996a) A role for gelsolin in actuating epidermal growth factor receptor-mediated cell motility. *J.Cell Biol.* **134,** 689-698.

Chen,X. and Wang,Z. (2001) Regulation of intracellular trafficking of the EGF receptor by Rab5 in the absence of phosphatidylinositol 3-kinase activity. *EMBO Rep.* **2,** 68-74.

Chin,L.S., Raynor,M.C., Wei,X., Chen,H.Q., and Li,L. (2001) Hrs interacts with sorting nexin 1 and regulates degradation of epidermal growth factor receptor. *J.Biol.Chem.* **276,** 7069-7078.

Choi,J.H., Hong,W.P., Kim,M.J., Kim,J.H., Ryu,S.H., and Suh,P.G. (2004) Sorting nexin 16 regulates EGF receptor trafficking by phosphatidylinositol-3-phosphate interaction with the Phox domain. *J.Cell Sci.* **Pt.**

Chou,J., Stolz,D.B., Burke,N.A., Watkins,S.C., and Wells,A. (2002) Distribution of gelsolin and phosphoinositol 4,5-bisphosphate in lamellipodia during EGF-induced motility. *Int.J.Biochem.Cell Biol.* **34,** 776-790.

Chou,J., Burke,N.A., Iwabu,A., Watkins,S.C., and Wells,A. (2003) Directional motility induced by epidermal growth factor requires Cdc42. *Exp.Cell Res.* **287,** 47-56.

Christoforidis,S., McBride,H.M., Burgoyne,R.D., and Zerial,M. (1999) The Rab5 effector EEA1 is a core component of endosome docking. *Nature* **397,** 621-625.

Chuah,S.Y. and Pallen,C.J. (1989) Calcium-dependent and phosphorylation-stimulated proteolysis of lipocortin I by an endogenous A431 cell membrane protease. *J.Biol.Chem.* **264,** 21160-21166.

Clague,M.J. (2002) Membrane transport: a coat for ubiquitin. *Curr.Biol.* **12,** R529-R531.

Confalonieri,S., Salcini,A.E., Puri,C., Tacchetti,C., and Di Fiore,P.P. (2000) Tyrosine phosphorylation of Eps15 is required for ligand-regulated, but not constitutive, endocytosis. *J.Cell Biol.* **150,** 905-912.

Conner,S.D. and Schmid,S.L. (2003) Differential requirements for AP-2 in clathrin-mediated endocytosis. *J.Cell Biol.* **162,** 773-780.

Connolly,J.L., Green,S.A., and Green,L.A. (1984) Comparison of rapid changes in surface morphology and coated pit formation of PC12 cells in response to nnerve growth factor, epidermal growth factor, and dibutyryl cyclic AMP. *J.Cell Biol.* **98,** 457-465.

Cozier,G.E., Carlton,J., McGregor,A.H., Gleeson,P.A., Teasdale,R.D., Mellor,H., and Cullen,P.J. (2002) The phox homology (PX) domain-dependent, 3-phosphoinositide-mediated association of sorting nexin-1 with an early sorting

endosomal compartment is required for its ability to regulate epidermal growth factor receptor degradation. *J.Biol.Chem.* **277,** 48730-48736.

Creutz,C.E., Pazoles,C.J., and Pollard,H.B. (1978) Identification and purification of an adrenal medullary protein (synexin) that causes calcium-dependent aggregation of isolated chromaffin granules. *J.Biol.Chem.* **253,** 2858-2866.

Creutz,C.E., Zaks,W.J., Hamman,H.C., Crane,S., Martin,W.H., Gould,K.L., Oddie,K.M., and Parsons,S.J. (1987) Identification of chromaffin granule-binding proteins. Relationship of the chromobindins to calelectrin, synhibin, and the tyrosine kinase substrates p35 and p36. *J.Biol.Chem.* **262,** 1860-1868.

Croxtall,J.D., Choudhury,Q., Newman,S., and Flower,R.J. (1996) Lipocortin 1 and the control of cPLA2 activity in A549 cells. Glucocorticoids block EGF stimulation of cPLA2 phosphorylation. *Biochem.Pharmacol.* **52,** 351-356.

Croxtall,J.D., Choudhury,Q., and Flower,R.J. (2000) Glucocorticoids act within minutes to inhibit recruitment of signalling factors to activated EGF receptors through a receptor-dependent, transcription-independent mechanism. *Br.J.Pharmacol.* **130,** 289-298.

Croxtall,J.D., Gilroy,D.W., Solito,E., Choudhury,Q., Ward,B.J., Buckingham,J.C., and Flower,R.J. (2003) Attenuation of glucocorticoid functions in an Anx-A1-/- cell line. *Biochem.J.* **371,** 927-935.

Crumpton,M.J. and Dedman,J.R. (1990) Protein terminology tangle. *Nature* **345,** 212.

Cullen,P.J., Cozier,G.E., Banting,G., and Mellor,H. (2001) Modular phosphoinositide-binding domains--their role in signalling and membrane trafficking. *Curr.Biol.* **11,** R882-R893.

Cunningham,C.C., Stossel,T.P., and Kwiatkowski,D.J. (1991) Enhanced motility in NIH 3T3 fibroblasts that overexpress gelsolin. *Science* **251,** 1233-1236.

Cupers,P., Jadhav,A.P., and Kirchhausen,T. (1998) Assembly of clathrin coats disrupts the association between Eps15 and AP-2 adaptors. *J.Biol.Chem.* **273,** 1847-1850.

Damke,H., Baba,T., Warnock,D.E., and Schmid,S.L. (1994) Induction of mutant dynamin specifically blocks endocytic coated vesicle formation. *J.Cell Biol.* **127,** 915-934.

de Melker,A.A., van der,H.G., Calafat,J., Jansen,H., and Borst,J. (2001) c-Cbl ubiquitinates the EGF receptor at the plasma membrane and remains receptor associated throughout the endocytic route. *J.Cell Sci.* **114,** 2167-2178.

de Melker,A.A., van der,H.G., and Borst,J. (2004) c-Cbl directs EGF receptors into an endocytic pathway that involves the ubiquitin-interacting motif of Eps15. *J.Cell Sci.* **Pt.**

Delouche,B., Pradel,L.A., and Henry,J.P. (1997) Phosphorylation by protein kinase C of annexin 2 in chromaffin cells stimulated by nicotine. *J.Neurosci.* **68,** 1720-1727.

Denzer,K., Kleijmeer,M.J., Heijnen,H.F., Stoorvogel,W., and Geuze,H.J. (2000) Exosome: from internal vesicle of the multivesicular body to intercellular signaling device. *J.Cell Sci.* **113 Pt 19,** 3365-3374.

Desjardins,M., Celis,J.E., van Meer,G., Dieplinger,H., Jahraus,A., Griffiths,G., and Huber,L.A. (1994) Molecular characterization of phagosomes. *J.Biol.Chem.* **269,** 32194-32200.

Di Fiore,P.P. and Gill,G.N. (1999) Endocytosis and mitogenic signaling. *Curr.Opin.Cell Biol.* **11,** 483-488.

Di Guglielmo,G.M., Baass,P.C., Ou,W.J., Posner,B.I., and Bergeron,J.J. (1994) Compartmentalization of SHC, GRB2 and mSOS, and hyperphosphorylation of Raf-1 by EGF but not insulin in liver parenchyma. *EMBO J.* **13,** 4269-4277.

Diakonova,M., Gerke,V., Ernst,J., Liautard,J.P., van,d., V, and Griffiths,G. (1997) Localization of five annexins in J774 macrophages and on isolated phagosomes. *J.Cell Sci.* **110 (Pt 10),** 1199-1213.

Dikic,I. and Giordano,S. (2003) Negative receptor signalling. *Curr.Opin.Cell Biol.* **15,** 128-135.

Ding,Q., Gladson,C.L., Guidry,C.R., Santoro,S.A., Dickeson,S.K., Shin,J.T., and Thompson,J.A. (2000) Extracellular FGF-1 inhibits cytoskeletal organization and promotes fibroblast motility. *Growth Factors* **18,** 93-107.

Donovan,J.A., Ota,Y., Langdon,W.Y., and Samelson,L.E. (1996) Regulation of the association of p120cbl with Grb2 in Jurkat T cells. *J.Biol.Chem.* **271,** 26369-26374.

Duan,L., Miura,Y., Dimri,M., Majumder,B., Dodge,I.L., Lakku,R.A., Ghosh,A.K., Fernandes,N., Zhou,P., Mullane-Robinson,K., Rao,N., Donoghue,S., Rogers,R.A., Bowtell,D., Naramura,M., Gu,H., Band,V., and Band,H. (2003) Cbl-mediated ubiquitinylation is required for lysosomal sorting of EGF receptor but is dispensable for endocytosis. *J.Biol.Chem.* ..

Durrbach,A., Louvard,D., and Coudrier,E. (1996) Actin filaments facilitate two steps of endocytosis. *J.Cell Sci.* **109 (Pt 2),** 457-465.

Egan,S.E., Giddings,B.W., Brooks,M.W., Buday,L., Sizeland,A.M., and Weinberg,R.A. (1993) Association of Sos Ras exchange protein with Grb2 is implicated in tyrosine kinase signal transduction and transformation. *Nature* **363,** 45-51.

Elbashir,S.M., Harborth,J., Lendeckel,W., Yalcin,A., Weber,K., and Tuschl,T. (2001) Duplexes of 21-nucleotide RNAs mediate RNA interference in cultured mammalian cells. *Nature* **411,** 494-498.

Emans,N., Gorvel,J.P., Walter,C., Gerke,V., Kellner,R., Griffiths,G., and Gruenberg,J. (1993) Annexin II is a major component of fusogenic endosomal vesicles. *J.Cell Biol.* **120,** 1357-1369.

Erikson,E., Cook,R., Miller,G.J., and Erikson,R.L. (1981) The same normal cell protein is phosphorylated after transformation by avian sarcoma viruses with unrelated transforming genes. *Mol.Cell Biol.* **1,** 43-50.

Ernst,S., Lange,C., Wilbers,A., Goebeler,V., Gerke,V., and Rescher,U. (2004) An annexin 1 N-terminal peptide activates leukocytes by triggering different members of the formyl peptide receptor family. *J.Immunol.* **172,** 7669-7676.

Fang,M.Z., Liu,C., Song,Y., Yang,G.Y., Nie,Y., Liao,J., Zhao,X., Shimada,Y., Wang,L.D., and Yang,C.S. (2004) Over-expression of gastrin-releasing peptide in human esophageal squamous cell carcinomas. *Carcinogenesis* **25,** 865-871.

Felder,S., Miller,K., Moehren,G., Ullrich,A., Schlessinger,J., and Hopkins,C.R. (1990) Kinase activity controls the sorting of the epidermal growth factor receptor within the multivesicular body. *Cell* **61,** 623-634.

Felder,S., LaVin,J., Ullrich,A., and Schlessinger,J. (1992) Kinetics of binding, endocytosis, and recycling of EGF receptor mutants. *J.Cell Biol.* **117,** 203-212.

Fernandez-Borja,M., Wubbolts,R., Calafat,J., Janssen,H., Divecha,N., Dusseljee,S., and Neefjes,J. (1999) Multivesicular body morphogenesis requires phosphatidyl-inositol 3-kinase activity. *Curr.Biol.* **9,** 55-58.

Filipenko,N.R. and Waisman,D.M. (2001) The C terminus of annexin II mediates binding to F-actin. *J.Biol.Chem.* **276,** 5310-5315.

Flower,R.J. (1986) Background and discovery of lipocortins. *Agents Actions* **17,** 255-262.

Fukazawa,T., Miyake,S., Band,V., and Band,H. (1996) Tyrosine phosphorylation of Cbl upon epidermal growth factor (EGF) stimulation and its association with EGF receptor and downstream signalling pathways. *J.Biol.Chem.* **271,** 14554-14559.

Futter,C.E. and Hopkins,C.R. (1989) Subfractionation of the endocytic pathway: isolation of compartments involved in the processing of internalised epidermal growth factor-receptor complexes. *J.Cell Sci.* **94,** 685-694.

Futter,C.E., Felder,S., Schlessinger,J., Ullrich,A., and Hopkins,C.R. (1993) Annexin I is phosphorylated in the multivesicular body during the processing of the epidermal growth factor receptor. *J.Cell Biol.* **120,** 77-83.

Futter,C.E., Connolly,C.N., Cutler,D.F., and Hopkins,C.R. (1995) Newly synthesized transferrin receptors can be detected in the endosome before they appear on the cell surface. *J.Biol.Chem.* **270,** 10999-11003.

Futter,C.E., Pearse,A., Hewlett,L.J., and Hopkins,C.R. (1996) Multivesicular endosomes containing internalized EGF-EGF receptor complexes mature and then fuse directly with lysosomes. *J.Cell Biol.* **132,** 1011-1023.

Futter,C.E., Collinson,L.M., Backer,J.M., and Hopkins,C.R. (2001) Human VPS34 is required for internal vesicle formation within multivesicular endosomes. *J.Cell Biol.* **155,** 1251-1264.

Gan,Y., McGraw,T.E., and Rodriguez-Boulan,E. (2002) The epithelial-specific adaptor AP1B mediates post-endocytic recycling to the basolateral membrane. *Nat.Cell Biol.* **4,** 605-609.

Garrus,J.E., von Schwedler,U.K., Pornillos,O.W., Morham,S.G., Zavitz,K.H., Wang,H.E., Wettstein,D.A., Stray,K.M., Cote,M., Rich,R.L., Myszka,D.G., and Sundquist,W.I. (2001) Tsg101 and the vacuolar protein sorting pathway are essential for HIV-1 budding. *Cell* **107,** 55-65.

Gary,J.D., Wurmser,A.E., Bonangelino,C.J., Weisman,L.S., and Emr,S.D. (1998) Fab1p is essential for PtdIns(3)P 5-kinase activity and the maintenance of vacuolar size and membrane homeostasis. *J.Cell Biol.* **143,** 65-79.

Gasman,S., Kalaidzidis,Y., and Zerial,M. (2003) RhoD regulates endosome dynamics through Diaphanous-related Formin and Src tyrosine kinase. *Nat.Cell Biol.* **5,** 195-204.

Gerke,V. and Weber,K. (1984) Identity of p36K phosphorylated upon Rous sarcoma virus transformation with a protein purified from brush borders; calcium-dependent binding to non-erythroid spectrin and F-actin. *EMBO J.* **3,** 227-233.

Gerke,V. and Weber,K. (1985) The regulatory chain in the p36-kd substrate complex of viral tyrosine-specific protein kinases is related in sequence to the S-100 protein of glial cells. *EMBO J.* **4,** 2917-2920.

Gerke,V. and Moss,S.E. (2002) Annexins: from structure to function. *Physiol Rev.* **82,** 331-371.

Gillooly,D.J., Morrow,I.C., Lindsay,M., Gould,R., Bryant,N.J., Gaullier,J.M., Parton,R.G., and Stenmark,H. (2000) Localization of phosphatidylinositol 3-phosphate in yeast and mammalian cells. *EMBO J.* **19,** 4577-4588.

Glenney,J.R., Jr. (1985) Phosphorylation of p36 in vitro with pp60src. Regulation by Ca2+ and phospholipid. *FEBS Lett.* **192,** 79-82.

Glenney,J. (1986a) Phospholipid-dependent Ca2+ binding by the 36-kDa tyrosine kinase substrate (calpactin) and its 33-kDa core. *J.Biol.Chem.* **261,** 7247-7252.

Glenney,J. (1986b) Two related but distinct forms of the Mr 36,000 tyrosine kinase substrate (calpactin) that interact with phospholipid and actin in a Ca2+-dependent manner. *Proc.Natl.Acad.Sci.U.S.A* **83,** 4258-4262.

Glenney,J.R., Jr., Tack,B., and Powell,M.A. (1987) Calpactins: two distinct Ca++-regulated phospholipid- and actin-binding proteins isolated from lung and placenta. *J.Cell Biol.* **104,** 503-511.

Glenney,J.R., Jr., Chen,W.S., Lazar,C.S., Walton,G.M., Zokas,L.M., Rosenfeld,M.G., and Gill,G.N. (1988) Ligand-induced endocytosis of the EGF receptor is blocked by mutational inactivation and by microinjection of anti-phosphotyrosine antibodies. *Cell* **52,** 675-684.

Goldschmidt-Clermont,P.J., Kim,J.W., Machesky,L.M., Rhee,S.G., and Pollard,T.D. (1991) Regulation of phospholipase C-gamma 1 by profilin and tyrosine phosphorylation. *Science* **251,** 1231-1233.

Gorvel,J.P., Chavrier,P., Zerial,M., and Gruenberg,J. (1991) Rab5 controls early endosome fusion in vitro. *Cell* **64,** 915-925.

Govers,R., ten Broeke,T., Van Kerkhof,P., Schwartz,A.L., and Strous,G.J. (1999) Identification of a novel ubiquitin conjugation motif, required for ligand-induced internalization of the growth hormone receptor. *EMBO J.* **18,** 28-36.

Green,E.G., Ramm,E., Riley,N.M., Spiro,D.J., Goldenring,J.R., and Wessling-Resnick,M. (1997) Rab11 is associated with transferrin-containing recycling compartments in K562 cells. *Biochem.Biophys.Res.Commun.* **239,** 612-616.

Gruenberg,J. and Stenmark,H. (2004) The biogenesis of multivesicular endosomes. *Nat.Rev.Mol.Cell Biol.* **5,** 317-323.

Guarnieri,F.G., Aterburn,L.M., Penno,M.B., Cha,Y., and August,J.T. (1995) The motif Tyr-X-X-hydrophobic residue mediates lysosomal membrane targeting of lysosome-associated membrane protein. *J.Biol.Chem.* **268,** 1941-1946.

Haft,C.R., de la Luz,S.M., Barr,V.A., Haft,D.H., and Taylor,S.I. (1998) Identification of a family of sorting nexin molecules and characterization of their association with receptors. *Mol.Cell Biol.* **18,** 7278-7287.

Haglund,K., Shimokawa,N., Szymkiewicz,I., and Dikic,I. (2002) Cbl-directed monoubiquitination of CIN85 is involved in regulation of ligand-induced degradation of EGF receptors. *Proc.Natl.Acad.Sci.U.S.A* ..

Haigler,H.T., McKanna,J.A., and Cohen,S. (1979) Direct visualization of the binding and internalization of a ferritin conjugate of epidermal growth factor in human carcinoma cells A-431. *J.Cell Biol.* **81,** 382-395.

Haigler,H.T., Schlaepfer,D.D., and Burgess,W.H. (1987) Characterization of lipocortin I and an immunologically unrelated 33-kDa protein as epidermal growth factor receptor/kinase substrates and phospholipase A2 inhibitors. *J.Biol.Chem.* **262,** 6921-6930.

Haigler,H.T. and Schlaepfer,D.D. (1990) Expression of lipocortin 1 and endonexin II as a function of cellular growth state. *Prog.Clin.Biol.Res.* **349,** 91-98.

Hannon,R., Croxtall,J.D., Getting,S.J., Roviezzo,F., Yona,S., Paul-Clark,M.J., Gavins,F.N., Perretti,M., Morris,J.F., Buckingham,J.C., and Flower,R.J. (2002)

Aberrant inflammation and resistance to glucocorticoids in Annexin 1-/- Mouse. *FASEB J.* 253-255.

Hanover,J.A., Beguinot,L., Willingham,M.C., and Pastan,I.H. (1985) Transit of receptors for epidermal growth factor and transferrin through clathrin-coated pits. Analysis of the kinetics of receptor entry. *J.Biol.Chem.* **260,** 15938-15945.

Harder,T. and Gerke,V. (1993) The subcellular distribution of early endosomes is affected by the annexin II2p11(2) complex. *J.Cell Biol.* **123,** 1119-1132.

Harder,T. and Gerke,V. (1994) The annexin II(2)p11(2) complex is the major component of the Triton X-100 insoluble low-density fraction prepared from MDCK cells in the presence of Ca(2+). *Biochim.Biophys.Acta* **1223,** 375-382.

Harder,T., Kellner,R., Parton,R.G., and Gruenberg,J. (1997) Specific release of membrane-bound annexin II and cortical cytoskeletal elements by sequestration of membrane cholesterol. *Mol.Biol.Cell* **8,** 533-545.

Haugh,J.M. and Meyer,T. (2002) Active EGF receptors have limited access to PtdIns(4,5)P(2) in endosomes: implications for phospholipase C and PI 3-kinase signaling. *J.Cell Sci.* **115,** 303-310.

Hawkins,T.E., Das,D., Young,B., and Moss,S.E. (2002) DT40 cells lacking the Ca2+-binding protein annexin 5 are resistant to Ca2+-dependent apoptosis. *Proc.Natl.Acad.Sci.U.S.A* **99,** 8054-8059.

Hayes,M.J., Merrifield,C.J., Shao,D., Ayala-Sanmartin,J., Schorey,C.D., Levine,T.P., Proust,J., Curran,J., Bailly,M., and Moss,S.E. (2004) Annexin 2 binding to phosphatidylinositol 4,5-bisphosphate on endocytic vesicles is regulated by the stress response pathway. *J.Biol.Chem.* **279,** 14157-14164.

Herbst,J.J., Opresko,L.K., Walsh,B.J., Lauffenburger,D.A., and Wiley,H.S. (1994) Regulation of postendocytic trafficking of the epidermal growth factor receptor through endosomal retention. *J.Biol.Chem.* **269,** 12865-12873.

Herr,C., Smyth,N., Ullrich,S., Yun,F., Sasse,P., Hescheler,J., Fleischmann,B., Lasek,K., Brixius,K., Schwinger,R.H., Fassler,R., Schroder,R., and Noegel,A.A.

(2001) Loss of annexin A7 leads to alterations in frequency-induced shortening of isolated murine cardiomyocytes. *Mol.Cell Biol.* **21,** 4119-4128.

Herr,C., Clemen,C.S., Lehnert,G., Kutschkow,R., Picker,S.M., Gathof,B.S., Zamparelli,C., Schleicher,M., and Noegel,A.A. (2003) Function, expression and localization of annexin A7 in platelets and red blood cells: insights derived from an annexin A7 mutant mouse. *BMC.Biochem.* **4,** 8.

Hicke,L. and Riezman,H. (1996) Ubiquitination of a yeast plasma membrane receptor signals its ligand-stimulated endocytosis. *Cell* **84,** 277-287.

Hierro,A., Sun,J., Rusnak,A.S., Kim,J., Prag,G., Emr,S.D., and Hurley,J.H. (2004) Structure of the ESCRT-II endosomal trafficking complex. *Nature.*

Hill,E., van Der,K.J., Downes,C.P., and Smythe,E. (2001) The role of dynamin and its binding partners in coated pit invagination and scission. *J.Cell Biol.* **152,** 309-323.

Holloway,M.P. and Bram,R.J. (1998) Co-localisation of Calcium-modulating Cyclophilin Ligand with intracellular calcium pools. *J.Biol.Chem.* **273,** 16346-16350.

Honegger,A.M., Dull,T.J., Felder,S., Van Obberghen,E., Bellot,F., Szapary,D., Schmidt,A., Ullrich,A., and Schlessinger,J. (1987) Point mutation at the ATP binding site of EGF receptor abolishes protein-tyrosine kinase activity and alters cellular routing. *Cell* **51,** 199-209.

Hopkins,C.R., Gibson,A., Shipman,M., and Miller,K. (1990) Movement of internalized ligand-receptor complexes along a continuous endosomal reticulum. *Nature* **346,** 335-339.

Howe,C.L., Valletta,J.S., Rusnak,A.S., and Mobley,W.C. (2001) NGF signaling from clathrin-coated vesicles: evidence that signaling endosomes serve as a platform for the Ras-MAPK pathway. *Neuron* **32,** 801-814.

Huang,F., Khvorova,A., Marshall,W., and Sorkin,A. (2004) Analysis of clathrin-mediated endocytosis of epidermal growth factor receptor by RNA interference. *J.Biol.Chem.* **279,** 16657-16661.

Huang,K.S., Wallner,B.P., Mattaliano,R.J., Tizard,R., Burne,C., Frey,A., Hession,C., McGray,P., Sinclair,L.K., Chow,E.P., and . (1986) Two human 35 kd inhibitors of phospholipase A2 are related to substrates of pp60v-src and of the epidermal growth factor receptor/kinase. *Cell* **46,** 191-199.

Hubaishy,I., Jones,P.G., Bjorge,J., Bellagamba,C., Fitzpatrick,S., Fujita,D.J., and Waisman,D.M. (1995) Modulation of annexin II tetramer by tyrosine phosphorylation. *Biochemistry* **34,** 14527-14534.

Hughes,P.E., Renshaw,M.W., Pfaff,M., Forsyth,J., Keivens,V.M., Schwartz,M.A., and Ginsberg,M.H. (1997) Suppression of integrin activation: a novel function of a Ras/Raf-initiated MAP kinase pathway. *Cell* **88,** 521-530.

Ikebuchi,N.W. and Waisman,D.M. (1990) Calcium-dependent regulation of actin filament bundling by lipocortin-85. *J.Biol.Chem.* **265,** 3392-3400.

Ikonomov,O.C., Sbrissa,D., and Shisheva,A. (2001) Mammalian cell morphology and endocytic membrane homeostasis require enzymatically active phosphoinositide 5-kinase PIKfyve. *J.Biol.Chem.* **276,** 26141-26147.

Isacke,C.M., Lindberg,R.A., and Hunter,T. (1989) Synthesis of p36 and p35 is increased when U-937 cells differentiate in culture but expression is not inducible by glucocorticoids. *Mol.Cell Biol.* **9,** 232-240.

Jackle,S., Runquist,E.A., Miranda-Brady,S., and Havel,R.J. (1991) Trafficking of the epidermal growth factor receptor and transferrin in three hepatocytic endosomal fractions. *J.Biol.Chem.* **266,** 1396-1402.

Jackle,S., Beisiegel,U., Rinninger,F., Buck,F., Grigoleit,A., Block,A., Groger,I., Greten,H., and Windler,E. (1994) Annexin VI, a marker protein of hepatocytic endosomes. *J.Biol.Chem.* **269,** 1026-1032.

Appendix 1 – Supplementary Data

Annexin 1

```
   1 agtgtgaaat cttcagagaa gaatttctct ttagttcttt gcaagaaggt agagataaag
                                                5'caagaagCt Cgagataaag
  61 acacttttc aaaa[redacted]gca atggtatcag aattcctcaa gcaggcctgg tttattgaaa
     acac-3'
 121 atgaagagca ggaatatgtt caaactgtga agtcatccaa aggtggtccc ggatcagcgg
 181 tgagccccta tcctaccttc aatccatcct cggatgtcgc tgccttgcat aaggccataa
 241 tggttaaagg tgtggatgaa gcaaccatca ttgacattct aactaagcga aacaatgcac
 301 agcgtcaaca gatcaaagca gcatatctcc aggaaacagg aaagcccctg gatgaaacac
 361 ttaagaaagc ccttacaggt caccttgagg aggttgtttt agctctgcta aaaactccag
 421 cgcaatttga tgctgatgaa cttcgtgctg ccatgaaggg ccttggaact gatgaagata
 481 ctctaattga gattttggca tcaagaacta acaaagaaat cagagacatt aacagggtct
 541 acagagagga actgaagaga gatctggcca aagacataac ctcagacaca tctggagatt
 601 ttcggaacgc tttgctttct cttgctaagg gtgaccgatc tgaggacttt ggtgtgaatg
 661 aagacttggc tgattcagat gccagggcct tgtatgaagc aggagaaagg agaaagggga
 721 cagacgtaaa cgtgttcaat accatcctta ccaccagaag ctatccacaa cttcgcagag
 781 tgtttcagaa atacaccaag tacagtaagc atgacatgaa caaagttctg gacctggagt
 841 tgaaaggtga cattgagaaa tgcctcacag ctatcgtgaa gtgcgccaca agcaaaccag
 901 ctttctttgc agagaagctt catcaagcca tgaaaggtgt tggaactcgc cataaggcat
 961 tgatcaggat tatggtttcc cgttctgaaa ttgacatgaa tgatatcaaa gcattctatc
1021 agaagatgta tggtatctcc ctttgccaag ccatcctgga tgaaaccaaa ggagattatg
1081 agaaaatcct ggtggctctt tgtggaggaa ac--[redacted]aca ttcccttgatgg
tctcaagcta
                          3'-ggaggaa acCGGGatCC ccttg-5'
1141 tgatcagaag actttaatta tatattttca tcctataagc ttaaatagga aagtttcttc
1201 aacaggatta cagtgtagct acctacatgc tgaaaaatat agcctttaaa tcatttttat
1261 attataactc tgtataatag agataagtcc atttttaaa aatgttttcc ccaaaccata
1321 aaaccctata caagttgttc tagtaacaat acatgagaaa gatgtctatg tagctgaaaa
1381 taaaatgacg tcacaagac
```

Figure S.1. *Human annexin 1 sequence and primers.* Human annexin 1 sequence was used to design primers to amplify annexin 1 using PCR from an I.M.A.G.E. Consortium [LLNL] cDNA clone ID3459615. Start and stop codons are highlighted in blue. Primers were designed to contain Xho1 (forward primer, pink) and BamH1 (reverse primer, blue) restriction sites (underlined sequences). Bases in capital letters indicate base changes or additions.

Annexin 1

```
   1 agtgtgaaatcttcagagaaagaatttctc
  31 tttagttctttgcaagaaggtagagataaagacacttttttcaaaa
  75 atggcaatggtatcagaattcctcaagcaggcctggtttattgaa
     M  A  M  V  S  E  F  L  K  Q  A  W  F  I  E
 120 aatgaagagcaggaatatgttcaaactgtgaagtcatccaaaggt
     N  E  E  Q  E  Y  V  Q  T  V  K  S  S  K  G
           5'-gaatTtgttcaaactgtgaagtc-3'
     3'-cttctcgtgcttaAacaagtttgacacttcag-5'
                    F
 165 ggtcccggatcagcggtgagcccctatcctaccttcaatccatcc
     G  P  G  S  A  V  S  P  Y  P  T  F  N  P  S
 210 tcggatgtcgctgccttgcataaggccataatggttaaaggtgtg
 255 gatgaagcaaccatcattgacattctaactaagcgaaacaatgca
 300 cagcgtcaacagatcaaagcagcatatctccaggaaacaggaaag
 345 cccctggatgaaacacttaagaaagcccttacaggtcaccttgag
 390 gaggttgttttagctctgctaaaaactccagcgcaatttgatgct
 435 gatgaacttcgtgctgccatgaagggccttggaactgatgaagat
 480 actctaattgagattttggcatcaagaactaacaaagaaatcaga
 525 gacattaacagggtctacagagaggaactgaagagagatctggcc
 570 aaagacataacctcagacacatctggagattttcggaacgctttg
 615 ctttctcttgctaagggtgaccgatctgaggactttggtgtgaat
 660 gaagacttggctgattcagatgccagggccttgtatgaagcagga
 705 gaaaggagaaaggggacagacgtaaacgtgttcaataccatcctt
 750 accaccagaagctatccacaacttcgcagagtgtttcagaaatac
 795 accaagtacagtaagcatgacatgaacaaagttctggacctggag
 840 ttgaaaggtgacattgagaaatgcctcacagctatcgtgaagtgc
 885 gccacaagcaaaccagctttctttgcagagaagcttcatcaagcc
 930 atgaaaggtgttggaactcgccataaggcattgatcaggattatg
 975 gtttcccgttctgaaattgacatgaatgatatcaaagcattctat
1020 cagaagatgtatggtatctccctttgccaagccatcctggatgaa
1065 accaaaggagattatgagaaaatcctggtggctctttgtggagga
1110 aactaaacattcccttgatggtctcaagctatgatcagaagactt
```

Figure S.2. *Human annexin 1 sequence and point mutation.* Annexin 1 is phosphorylated by EGFR on tyrosine 21. To create a mutant construct lacking this site, primers were designed to create a point mutation at position 62 (A to T), which would result in an amino acid substitution (tyrosine (Y) to phenylalanine (F)). Start and stop codons are highlighted in blue. Amino acids are shown for the first part of annexin 1 sequence to show where the mutation occurs.

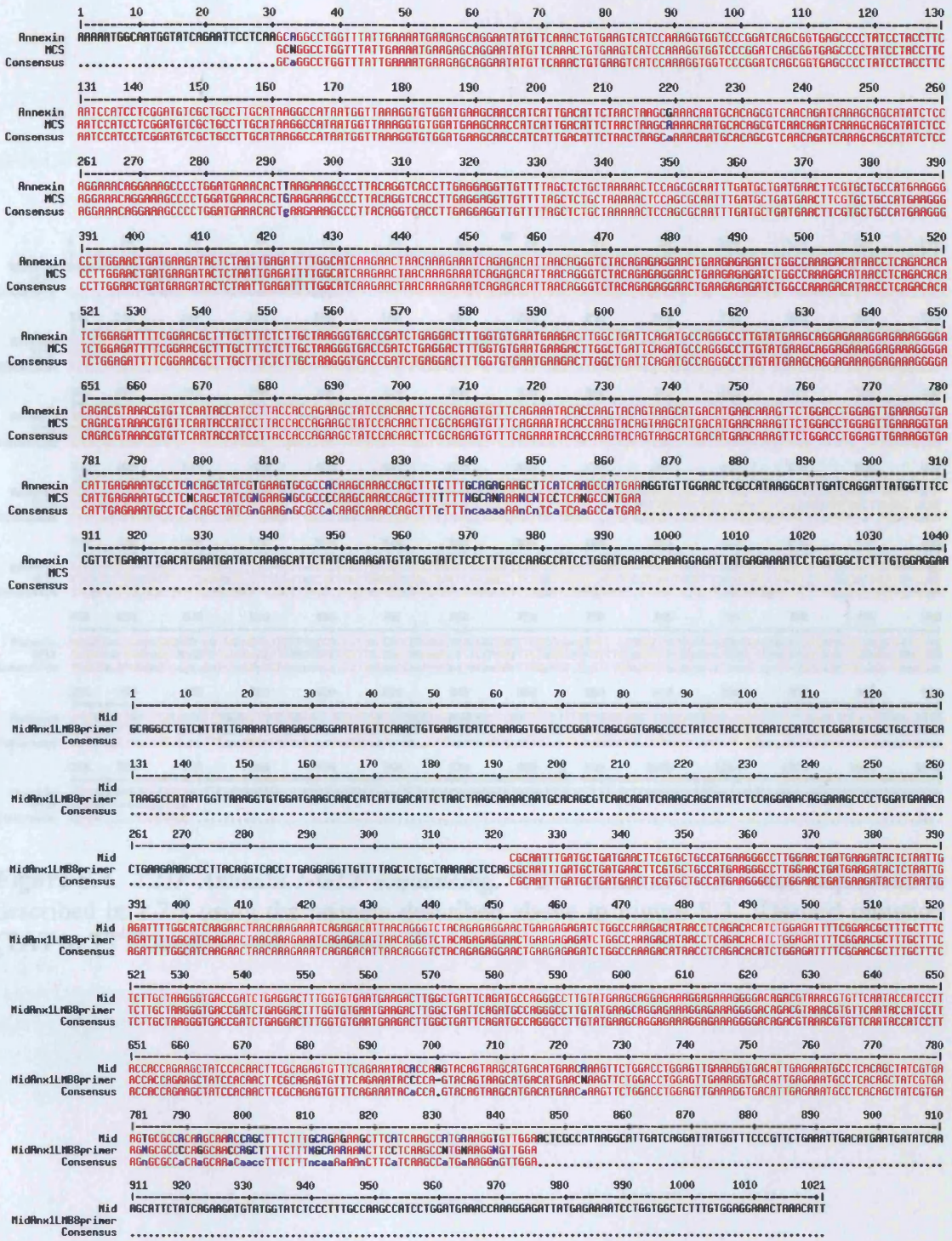

Figure S.3. *Annexin 1-GFP sequencing.* Annexin 1-GFP construct was sequenced as described in 2.2.3. Primers were designed to sequence annexin 1-GFP from the multiple cloning site (MCS) of pGFP-N1 (top) and from midway through annexin 1 (bottom).
Primer 1 (From MCS) 5'-CTAGCGCTACCGGACTCAGAT-3'
Primer 2 (From middle) 5'- TGCTGATGAACTTCGTGCTG-3'

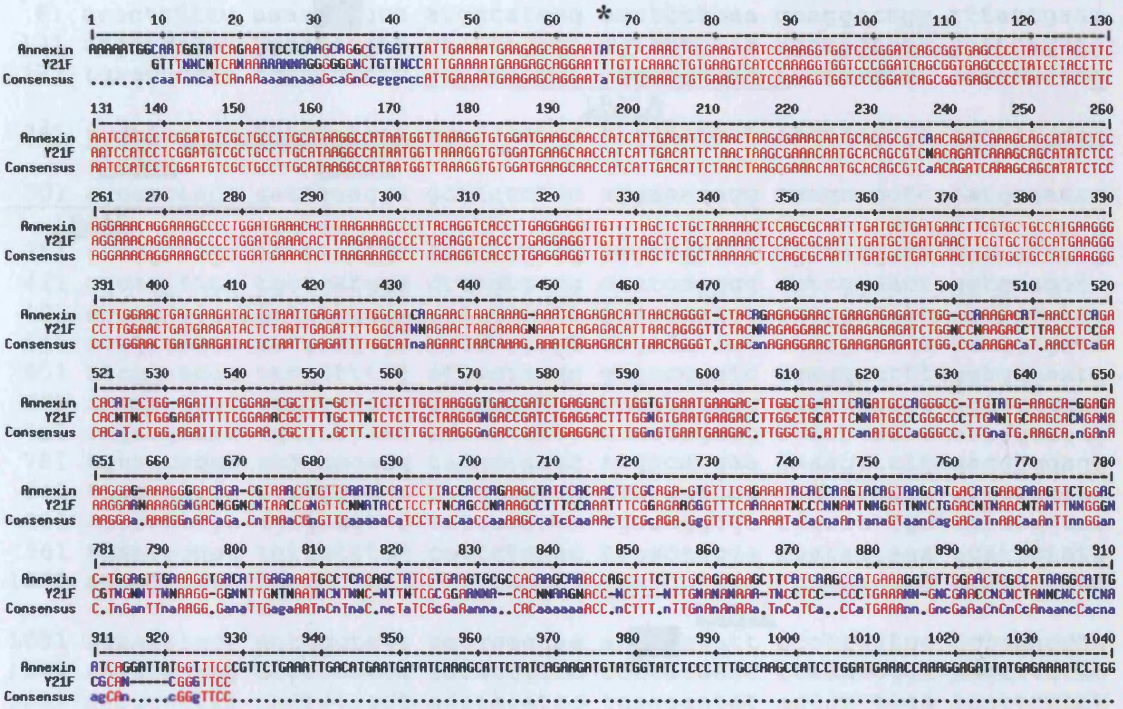

Figure S.4. *Y21F Annexin 1-GFP sequencing.* Y21F annexin 1-GFP was sequenced as described in 2.2.3 using the primers described above in Figure S.3. Desired mutation (TAT to TTT) marked with an asterix (*).

Annexin 1

```
   1 agtgtgaaat cttcagagaa gaatttctct ttagttcttt gcaagaaggt agagataaag
  61 acacttttc aaaa[redacted]gca atggtatcag aattcctcaa gcaggcctgg tttattgaaa
 121 atgaagagca ggaatatgtt caaactgtga agtcatccaa aggtggtccc ggatcagcgg
 181 tgagccccta tcctaccttc aatccatcct cggatgtcgc tgccttgcat aaggccataa
                                    LBA1A
 241 tggttaaagg tgtggatgaa gcaaccatca ttgacattct aactaagcga aacaatgcac
      LBA1X          LBA1C
 301 agcgtcaaca gatcaaagca gcatatctcc aggaaacagg aaagcccctg gatgaaacac
   LBA1B
 361 ttaagaaagc ccttacaggt caccttgagg aggttgtttt agctctgcta aaaactccag
 421 cgcaatttga tgctgatgaa cttcgtgctg ccatgaaggg ccttggaact gatgaagata
 481 ctctaattga gattttggca tcaagaacta acaaagaaat cagagacatt aacagggtct
 541 acagagagga actgaagaga gatctggcca aagacataac ctcagacaca tctggagatt
 601 ttcggaacgc tttgctttct cttgctaagg gtgaccgatc tgaggacttt ggtgtgaatg
 661 aagacttggc tgattcagat gccagggcct tgtatgaagc aggagaaagg agaaagggga
 721 cagacgtaaa cgtgttcaat accatcctta ccaccagaag ctatccacaa cttcgcagag
 781 tgtttcagaa atacaccaag tacagtaagc atgacatgaa caaagttctg gacctggagt
 841 tgaaaggtga cattgagaaa tgcctcacag ctatcgtgaa gtgcgccaca agcaaaccag
 901 ctttctttgc agagaagctt catcaagcca tgaaaggtgt tggaactcgc cataaggcat
 961 tgatcaggat tatggtttcc cgttctgaaa ttgacatgaa tgatatcaaa gcattctatc
1021 agaagatgta tggtatctcc ctttgccaag ccatcctgga tgaaaccaaa ggagattatg
                                        LBA1D
1081 agaaaatcct ggtggctctt tgtggaggaa ac[redacted]acatt cccttgatgg tctcaagcta
1141 tgatcagaag actttaatta tatattttca tcctataagc ttaaatagga aagtttcttc
1201 aacaggatta cagtgtagct acctacatgc tgaaaaatat agcctttaaa tcatttttat
1261 attataactc tgtataatag agataagtcc atttttaaa aatgttttcc ccaaaccata
1321 aaaccctata caagttgttc tagtaacaat acatgagaaa gatgtctatg tagctgaaaa
1381 taaaatgacg tcacaagac
```

Figure S.5. *Human annexin 1 sequence and RNAi sequences.* RNAi oligonucleotides were designed against human annexin 1 according to Qiagen protocol. Sequences for each oligonucleotide are underlined (LBA1A, B, C, D, X). Sequences for LBA1X and LBA1C overlap (double underlined shows overlapping bases). Start and stop codons are highlighted in blue.

Annexin 2

```
1    atttggggac gctctcagct ctcggcgcac ggcccagctt ccttcaaagt gtctactgtt
61   cacgaaatcc tgtgcaagct cagcttggag ggtgatcact ctacaccccc aagtgcatat
                                                          A2RNAi1
121  gggtctgtca aagcctatac taactttgat gctgagcggg atgctttgaa cattgaaaca
     A2RNAi1
181  gccatcaaga ccaaaggtgt ggatgaggtc accattgtca acattttgac caaccgcagc
241  aatgcacaga gacaggatat tgccttcgcc taccagagaa ggaccaaaaa ggaacttgca
301  tcagcactga agtcagcctt atctggccac ctggagacgg tgattttggg cctattgaag
361  acacctgctc agtatgacgc ttctgagcta aaagcttcca tgaaggggct gggaaccgac
421  gaggactctc tcattgagat catctgctcc agaaccaacc aggagctgca ggaaattaac
481  agagtctaca aggaaatgta caagactgat ctggagaagg acattatttc ggacacatct
541  ggtgacttcc gcaagctgat ggttgccctg gcaaagggta gaagagcaga ggatggctct
601  gtcattgatt atgaactgat tgaccaagat gctcgggatc tctatgacgc tggagtgaag
661  aggaaaggaa ctgatgttcc caagtggatc agcatcatga ccgagcggag cgtgccccac
721  ctccagaaag tatttgatag gtacaagagt tacagccctt atgacatgtt ggaaagcatc
781  aggaaagagg ttaaaggaga cctggaaaat gctttcctga acctggttca gtgcattcag
                                                          A2RNAi2
841  aacaagcccc tgtattttgc tgatcggctg tatgactcca tgaagggcaa ggggacgcga
901  gataaggtcc tgatcagaat catggtctcc cgcagtgaag tggacatgtt gaaaattagg
961  tctgaattca agagaaagta cggcaagtcc ctgtactatt atatccagca agacactaag
1021 ggcgactacc agaaagcgct gctgtacctg tgtggtggag atgactgaag cccgacacgg
1081 cctgagcgtc cagaaatggt gctcaccatg cttccagcta acaggtctag aaaaccagct
1141 tgcgaatgac agtccccgtg gccatccctg tgagggtgac gttagcatta cccccaacct
1201 cattttagtt gcctaagcat tgcctggcct tcctgtctag tctctcctgt aagccaaaga
1261 aatgaacatt ccaaggagtt ggaagtgaag tctatgatgt gaaacacttt gcctcctgtg
1321 tactgtgtca taaacagatg aataaactga atttgtactt taaaaaaaaa aaaaaa
```

Figure S.6. *Human annexin 2 sequence and RNAi sequences.* RNAi oligonucleotides were designed against human annexin 2 according to Qiagen protocol. Sequences for each oligonucleotide are underlined (A2RNAi1 and 2). Start and stop codons are highlighted in blue.

Chicken Annexin 2

```
1    cccgccgcca gagcagcctt gcccgccccg gccagcattc tgccaacatg tctactgtcc
61   atgaaatttt aagcaagctc agtctggaag gagatcattc tctccctcca agtgcatatg
121  ccacagttaa ggcttactca aactttgatg ctgaccggga tgctgcagcc ctggaagcag
        5'-ttaa ggcttactca aactttgatg ctgaccg-3'
181  ccatcaagac caaaggtgtg gatgaagtta ccatcatcaa catcctgaca aaccgcagca
241  atgaacagag gcaggatatt gcctttgcct atcagaggag aaccaaaaag gaactttctg
301  cagcacttaa gtctgctctg tcaggtcatt tagaggcagt gatcttgggc ttgctgaaga
                                        3'-tca ctagaacccg aacgacttct
361  caccatcaca gtatgatgcg tctgaactga aagctgccat gaagggcctg ggaactgatg
     gtggt-5'
421  aagacacact tatcgaaatc atttgctcac ggacaaatca ggagcttaat gaaattaata
481  gagtctatag ggaaatgtac aaaacagaac tggaaaagga cattatatca gacacatctg
541  gtgacttccg caagctaatg gttgccctgg ccaagggcaa aaggtgtgaa gatacttctg
601  tgattgacta tgaactgatt gaccaagacg ctagggagct ctatgatgct ggtgtcaaga
661  gaaagggaac agatgttccc aagtggatca acattatgac tgaaagaagt gttccacatc
721  tgcagaaagt gtttgaaagg tacaagagct acagcccata tgatatgttg gagagcatca
781  agaaggaagt taagggagat ctggagaatg ccttccttaa tcttgttcag tgcattcaga
841  acaagcagct atactttgca gacagactct atgattccat gaagggcaag ggaacccgtg
901  acaaggtcct gattaggatt atggtctccc gctgtgaggt tgacatgctg aaaattaaga
961  gtgaattcaa gaggaaatac ggaaaatccc tctattattt catccagcaa gacacaaaag
1021 gtgattacca gagggcgctg ctgaacctgt gtggtggaga ggactgaaag ctgtgatgtg
1081 ggaaatggaa acgcagagac atgcctatct gctcttcgtt ttactccaac ccccgacaaa
1141 atcgagccgc catgcaaacc cttccctgcc ccaatacctg ccacaccacc gacgccgtgt
1201 gcttctggtg ctgcctgcac ttctcagcag cagcgctctg cttggttctg ccaaacttcc
1261 taacagcgta aagccagaga aactaacatt ccccagagat aaaggttaaa cgtgcttgtt
1321 gaggatgcct ccttgtgtaa tgtttctaat aaaacataaa taaaacag
```

Figure S.7. *Chicken annexin 2 sequence.* Chicken annexin 2 cDNA sequence showing primers used for RT-PCR (see 2.6), to confirm DT40 annexin 2 -/- cells were not expressing annexin 2. Primers are shown in pink (forward) and blue (reverse).